EXPERIMENTAL STUDY OF THE AROMATICS PRODUCTION FROM THE PYROLYSIS OF SCRAP TIRE RUBBER USING HETEROPOLYACIDS-BASED CATALYSTS

Doctoral thesis presented to:

Universidad Industrial de Santander

and

L'Université de Lille 1 Sciences et Technologies

As a requirement to obtain the double degree:

Doctor in Chemical Engineering

and

Doctor in Chemistry - Specialty: Science of matter, radiation and the environment

By

CLAUDIA PATRICIA TAVERA RUIZ

Thesis Directors:

PhD. Maria Paola Gauthier Maradei - Universidad Industrial de Santander

PhD. Mickael Capron - Université de Lille 1 Sciences et Technologies

Bucaramanga, Colombia.

October 2017

EXPERIMENTAL STUDY OF THE AROMATICS PRODUCTION FROM THE PYROLYSIS OF SCRAP TIRES RUBBER USING HETEROPOLYACIDS-BASED CATALYSTS

Doctoral thesis presented to:

Universidad Industrial de Santander

and

L'Université de Lille 1 Sciences et Technologies

As a requirement to obtain the double degree:

Doctor in Chemical Engineering

and

Doctor in Chemistry - Specialty: Science of matter, radiation and the environment

By

CLAUDIA PATRICIA TAVERA RUIZ

Dissertation on October 13 of 2017 in Bucaramanga Colombia, in front of the examination committee:

Jury

Dr. Fernando Viejo Abrante –Universidad Industrial de Santander

Dr. Julio Andrés Pedraza Avellaneda-Universidad Industrial de Santander

Dra. Dorothée Laurenti – IRCELYON Université Lyon 1

Dr. Pascal Fongarland – Université Claude Bernard Lyon 1

Dr. Pascal Roussel – Université de Lille 1 Sciences and Technologies.

Thesis Directors:

PhD. Maria Paola Gauthier Maradei - Universidad Industrial de Santander

PhD. Mickael Capron - Université de Lille 1 Sciences et Technologies.

ACKNOWLEDGMENTS

I would like to express my gratitude and appreciation to each person and entities who supported me during the 5 years of my PhD, with which successful completion would not have been possible:

To my director Dr. Maria Paola Maradei, for the trust placed in me, the opportunity offered with the topic of thesis, her support, guidance and inspiration, and for each teaching given at a professional and personal level.

To my director Mickael Capron, for the opportunity given with the cotutele, for all his support, learning, good reception and patience during my stay in France.

To Colciencias for the financial support with the scholarship of the call 567, and to Colfuturo who administered fully and properly the resources during the 5 years.

To the Vicerrectoría de Investigación y Extensión from Universidad Industrial de Santander for the financial support through the project No. 1843 and the program of doctoral support project No. 1858.

To my research group INTERFASE, for the availability of its facilities and equipment, the collaboration, support, friendship and good moments during these 5 years.

To the Chemical Engineering School of the Universidad Industrial de Santander for the financial support for the completion of my internship and for the facilitation of the equipment and the analysis services provided.

To my sons, my students: Diego Villamizar, Yenny Sanchez, Luis Enrique Bohórquez, Catalina Carmargo, Diana Parra, Alejandro Lemus, Deyanira Ferreira, Cristian Palencia and Iván Luna, for their hard work and their extensive collaboration during the experimental tests.

To UCCS and its staff for the reception, financing, training and services provided in the performance of analysis. I want to especially thank to Cyril Pirez, Benjamin Katryniok, Olivier Gardoll and Jean Charles Morin, for all their help, guidance and collaboration.

To the jury: Dr. Fernando Viejo Abrante, Dr. Julio Andrés Pedraza, Dra. Dorothée Laurenti, Dr. Pascal Fongarland and Dr. Pascal Roussel for accepting the role of examiners and evaluators of my thesis.

To my family, my inspiration, they are all in my life, thanks for believing in me and always support me.

To my friends Sebastián, Mónica, Liliana, Lilou, Said and Jesús for their support and always listen to me in difficult and sad moments of my thesis.

And finally, to each of those people who were in my life and heart during these 5 years, each one left something special and great teachings in me.

TABLE OF CONTENTS

LIST OF FIGURES

LIST OF TABLES

LIST OF ANNEXES

ABSTRACT

TITLE: EXPERIMENTAL STUDY OF THE AROMATICS PRODUCTION FROM THE PYROLYSIS OF SCRAP TIRES RUBBER USING HETEROPOLYACIDS-BASED CATALYSTS.[*]

AUTHOR: Claudia Patricia Tavera Ruiz [**§]

KEYWORDS: Waste tires, supported HPA based catalysts, cymenes production, single ring aromatics.

DESCRIPTION:

Scrap tire are waste that produces one of the largest annual production all over the world. Because its non-biodegradable composition, its end of life and treatment is difficult, causing environmental and public health problems, due to the accumulation and implementation of inappropriate treatment techniques. Based on this problem it is conceivable to seek to valorise these wastes through processes such as pyrolysis.
The main objective of this work was to evaluate experimentally the pyrolysis of scrap tire rubber (STR) in order to improve single ring aromatic compounds, which have a higher industrial value in the oil of STR pyrolysis. To this end, an experimental study of pyrolysis of STR without catalyst was carried out and the most favorable temperature and nitrogen conditions were determined. The transformation of D, L limonene present in the oil into aromatics using different heteropolyacid / carrier combinations was evaluated, in order to select the most selective towards the aromatics. The results showed a conversion of limonene to p-cymene, monoterpenes and menthenes, and it was found that the production of p-cymene was promoted by Lewis acidity. Since the catalysts are more selective in the transformation of limonene, have been validated in the pyrolysis of STR. The results show that the yield of aromatics has increased (from 8.05%) to a maximum of 15.06% p and the concentration about 37%p, using a molybdenum catalyst in which the acid sites of Lewis are the predominant.

---

[*] **Doctoral Thesis.**

[**] **Universidad Industrial de Santander. Faculty of Physicochemical Engineering. School of Chemical Engineering. Director: PhD. Maria Paola Maradei García.**

[§] **Université de Lille 1 Sciences et Technologies. Doctoral School of Science of Matter, Radiation and Environment. Director: PhD. Mickael Capron**.

RÉSUMÉ

TITRE: ÉTUDE EXPÉRIMENTALE DE LA PRODUCTION D'AROMATIQUES À PARTIR DE LA PYROLYSE DES PNEUS DE CAOUTCHOUC AVEC L'USE DE CATALYSEURS HETEROPOLYACIDES.[*]

AUTEUR: Claudia Patricia Tavera Ruiz [**§]

MOTS CLEFS: Pneus de déchet , catalyseurs HPA supportés, production de cymènes, les aromatiques à simple anneau.

DESCRIPTION:

Les pneus de caoutchouc usagés sont l'une des plus grandes productions annuelles de déchets dans le monde entier. Ceci est dû à leur composition non biodégradable, leur durée de vie et leur traitement difficile, ce qui provoque des problèmes environnementaux et de santé publique, en raison de son accumulation et de la mise en œuvre de techniques de traitement inappropriées. En tenant compte de ce problème, il est envisageable de chercher à valoriser ces déchets grâce à des procédés comme la pyrolyse.
L'objectif principal de ce travail était d'évaluer expérimentalement la pyrolyse de pneus du caoutchouc (STR) dans le but de produire des composés aromatiques monocycliques. Pour cela, une étude expérimentale de pyrolyse de STR sans catalyseur a été réalisée et les conditions les plus favorables de température et de débit d'azote ont été déterminées. La transformation du D,L limonène présent dans l'huile en aromatiques en utilisant différentes combinaisons hétéropolyacide/support ont été évaluées, afin de sélectionner les plus sélectives vers les aromatiques. Les résultats ont montré une conversion du limonène en p-cymène, monoterpènes et menthènes, et on a constaté que la production de p-cymène est promu par l'acidité de Lewis. Depuis, les catalyseurs étant plus sélectifs dans la transformation du limonène, ont été validés dans la pyrolyse de STR. Les résultats montrent que le rendement en aromatiques a augmenté (de 8,05%) à un maximum de 15,06 %p et la concentration a abouti environ 37%, en utilisant un catalyseur à base de molybdène dans lequel les sites d'acide de Lewis sont les prédominants.

---

[*] **Thèse de doctorat.**

[**] **Universidad Industrial de Santander. Faculté de génie physicochimique. École de génie chimique. Directeur: PhD. Maria Paola Maradei García.**

[§] **Université de Lille 1 Sciences et Technologies. École doctorale des sciences de la matière, du rayonnement et de l'environnement. Directeur: PhD. Mickael Capron.**

RESUMEN

TÍTULO: ESTUDIO EXPERIMENTAL DE LA PRODUCCIÓN DE AROMÁTICOS A PARTIR DE LA PIRÓLISIS DE CAUCHO DE LLANTAS USADAS UTILIZANDO CATALIZADORES HETEROPOLIÁCIDOS SOPORTADOS .

AUTOR: Claudia Patricia Tavera Ruiz [1** §]

PALABRAS CLAVES: Llantas de desecho, catalizadores HPA soportados, producción de cimenos, aromáticos de anillo simple.

DESCRIPTION:

Uno de los desechos que tiene la mayor producción anual casi en todas partes del mundo, son las llantas usadas. Debido a su composición no biodegradable, su tratamiento al final de su vida es difícil, causando problemas ambientales y de salud pública, debido a la acumulación e implementación de técnicas de tratamiento inapropiadas, como el almacenamiento en pozos abiertos o vertederos e incendios incontrolados. A partir de esta problemática, se propone la valorización de este residuo a través del proceso de pirólisis.

El objetivo principal de este trabajo fue evaluar experimentalmente la pirólisis del caucho de llantas usadas (STR) para mejorar los compuestos aromáticos de anillo simple, que son los compuestos con mayor valor industrial en el aceite obtenido en la pirólisis de STR. Para este propósito, se realizó un estudio experimental de pirólisis de STR sin catalizador y se determinaron las condiciones más favorables de temperatura y flujo de nitrógeno. Además, se evaluó la transformación de D-L limoneno en compuestos aromáticos utilizando diferentes combinaciones heteropoliácido/soporte en diferentes condiciones y se seleccionaron las más selectivas hacia aromáticos. Los resultados mostraron una conversión de limoneno en p-cimeno, monoterpenos y mentenos principalmente, y se constató que la producción de p-cimeno es favorecida por la acidez de Lewis.

Finalmente, los catalizadores encontrados como más selectivos en la transformación del D,L limoneno, fueron validados en la pirólisis de STR. Los resultados muestran que el rendimiento de compuestos aromáticos aumentó desde 8,05 %p hasta un máximo de15,06 %, y la concentración alcanzó un máximo de 37 %p, utilizando el catalizador a base de molibdeno, donde predominan los sitios ácidos de Lewis.

---

[1] **Tesis de doctorado.**

[**] **Universidad Industrial de Santander. Facultad de Ingenierías Fisicoquímicas. Escuela de Ingeniería Química. Director: PhD. María Paola Maradei García.**

[§] **Université de Lille 1 Sciences et Technologies. Escuela Doctoral de Ciencia de la Materia, Radiación y Medio Ambiente. Director: PhD. Mickael Capron.**

Chapter 1

Generalities

1.1. GENERAL INTRODUCTION

In modern life, cars have become a necessity, as they are indispensable for the transportation of raw materials, food, people, among others. The use of cars every day is higher, leading to an increase in demand for tires. Unfortunately, because they are manufactured mostly from non-biodegradable and synthetic materials, their treatment on end of life is tough (more than 100 years), causing their uncontrolled accumulation.

Currently in Colombia, according to the Ministry of the Environment, five thousand units of scrap tires rubber (STR) are produced per year [1], a number that increases each year. Among these, only approximately 30% are reused or recycled; a very low quantity compared to European countries where approximately 60% of the scrap tires are recycled [2,3]. The other 70% are treated improperly *e.g*. by uncontrolled incineration, disposition in open pits or sanitary landfills, or simply those are abandoned on roads, fields or rivers causing serious environmental (contamination of the soil, water and landscapes) and public health problems [2,4]. Specifically, in tropical countries like Colombia, their inappropriate deposit could become a serious public health problem because their exposure to rain allow creating deposits of water

that are focus of mosquitoes transmitters of deadly diseases like dengue and chikungunya [1,4,5].

On the other hand, the uncontrolled incineration of STR and their use as fuel in productive processes, cause high air pollution levels, since their combustion generates toxic and carcinogenic gases such as dioxide and monoxide carbon, sulfur compounds, type SO_x and H_2S, polyaromatic compounds, furans, nitrogen and chlorine compounds, among others. These compounds productions modify the atmospheric balance causing the so-called greenhouse effect and producing climate change worldwide, with the consequences already known [6–8]. Due to this problem, the Colombian government has created environmental programs and laws for their management and recovery. As a result of these environmental programs, some techniques have been implemented to reuse this waste (*i.e*. STR). As example, they can be added to the so-called “modified bitumens” for road asphalt mixtures, they can be used for the manufacture and the maintenance of the sports fields, playground flooring and synthetic grass. It can also contribute to the manufacture of different decorative crafts, among others [4,9,10]. Regarding the legal part, norms and laws have been established in which tire producers are obliged to establish collection centers for scrap tires and to make a periodic collection and subsequent treatment [1,11,12]. Despite the efforts made to date by the government, the alternative set of their management and recovery are not enough to solve the environmental problems associated to this waste, and they do not cover the entire current offer of STR produced annually in the country [2,4,13].

One alternative that could really increase the reuse effort of this waste and lead to decrease the environmental impact and its non-controlled growth rate, is its valorization as fuel owing to its high calorific value (32 MJ/kg) [14,15]. There are various technical processes using thermochemical mechanisms among which the pyrolysis is the most promising technology because the toxic gases production as

CO_x, NO_x and SO_x are reduced in comparison with those produced in the traditional incineration due mainly to the use of an oxygen-free atmosphere.

The pyrolysis process allows the breaking down of hydrocarbon chains using high temperature from 300 to 900°C. This process generates gases, oil and char products, the oil being the product with the highest energy value. The pyrolytic oil obtained from the pyrolysis of STR is a mixture of aromatic hydrocarbons (simple ring and polyaromatic), olefin, paraffin, sulfur and nitrogen compounds. The pyrolytic oil has high heating value (HHV), about 40-44MJ/kg [15,16], being higher than coal and similar than commercial diesel; this property provides its great potential as a fuel. However, previous studies show the limitations to its use as fuel due to presence of sulfur compounds [17–19].

Among the compounds present in the oil, those with highest commercial value are simple ring aromatics such as BTX type (benzene, toluene and xylenes) and p-cymene, and partially saturated cyclic compounds such as D, L limonene. BTX aromatics are widely used industrially, mainly in applications such as the chemical synthesis of plastics, synthetic rubber, paints, pigments, explosives, pesticides, detergents and solvents. p-cymene is used as solvent in inks and paints, as a flavoring agent in foods and as raw material in manufacture of p-cresol, resins and fragrances [20–22]. D,L limonene, on the other hand, is widely used in the manufacture of fragrances, degreasers and cleaning products [22–24].

Due to their commercial value and that they are highly used at industrial level, the production of aromatics from STR pyrolysis has begun to be studied. Recent advances have focused on the use of catalysts as zeolites or bifunctional catalysts (metals supported on zeolites or silica), in order to increase the aromatics concentration in pyrolytic oil [25–32]. The effect of Si/Al ratio, has been studied to elucidated the mechanisms understanding to promote the production of aromatic

compounds using acid. It is well known that zeolite catalysts have mainly Brønsted acid sites and that the acid strength could be modified with the ratio between Si and the trivalent T-atom in the framework or by changing the nature of this aforementioned atom. However, the research studies reported in literature use exclusively the Al atom as trivalent T-atom to improve the production of aromatics. This fact allows to check the effect of acid strength but not the nature of the acid site (*i.e.* Brønsted or Lewis) what could be possible changing the T-atom nature. In addition, the influence of other types of characteristics on the selectivity towards aromatics such as the type of support and the pore size have not been studied yet.
It should be noted that, despite the high aromatics concentration reported in the liquid phase, the results of these investigations also demonstrate an increase in the gases amount produced through cracking reactions. This suggests that the composition of the pyrolytic oil is favored towards the aromatic compounds if acid catalysts is used, however, it still remains to the increase their production.

This study proposes the use of a new catalyst alternative: the heteropolyacids (HPAs) supported on mesoporous silicas, which have not been studied until now in the pyrolysis of STR. HPAs are well known owing to their acidic and redox properties and are also as superacids, because they have an acidity higher than strong mineral acids or zeolites [33]. HPA catalysts have been studied in different types of reaction, such as oxidation, isomerization, dehydrogenation/hydrogenation, dehydration, alkylation, among others [16,34,35]. In addition, these type of catalysts have been studied previously in UCCS, therefore, there are already established protocols of synthesis and characterization [36].

The main objective of this work is to evaluate experimentally the STR pyrolysis to produce the simple ring aromatic compounds through the optimization of thermal decomposition of STR followed by a subsequent catalytic stage to reforming the vapors produced during pyrolysis using supported HPA based catalyst.

In order to comply with the proposed objective, the work was divided in three parts: a first focus to an experimental study of STR pyrolysis without catalyst was performed in which the most influential operating conditions were studied: temperature and nitrogen flow, and an optimization was subsequently performed to find the most favorable operating conditions. The characterization of raw material is presented in Chapter 2 and the results of the STR pyrolysis are shown in Chapter 3.

Once the most favorable conditions were obtained, the pyrolytic unit was modified to include a catalytic stage to reforming the vapors produced during pyrolysis. This second part was subdivided in three sub-parts: 1) the preparation and characterization of supported HPA based catalysts to be used in the catalytic stage (Chapter 4) developed in the University of Lille 1 in France, 2) the experimental study using D,L limonene as model molecule to evaluate the best combination HPA/support leading to the maximum of simple ring aromatic compounds. In this part, the influence of the main catalysts characteristics such as acidity strength, acid site types (*i.e.* Lewis and/or Brønsted) and support characteristics on this production were studied (Chapter 5), and 3) the experimental study using the best combinations HPA/support on the STR pyrolysis including the determination of yields of simple ring aromatic compounds is presented in the Chapter 6.

1.2. THEORETICAL FRAMEWORK

1.2.1 Pyrolysis Process. Pyrolysis is a process of thermal degradation of a material or biomass in an inert (oxygen-free) atmosphere (nitrogen, helium or argon is used). This process is endothermic, therefore requiring a heating to be carried out, normally using direct conduction heating. The operating temperature depends on the raw material, usually ranging between 350-700°C [29,37–39].

Since this process is carried out in an inert atmosphere, this allows the breakdown of long chains of hydrocarbons into smaller ones and gases such as CO_2 and H_2 being of the great interest in the study of polymer and solid wastes, and biomass treatment. In this process three types of products are obtained: solid (char), gases and pyrolytic oil. The char has been studied as potential fuel in industrial processes or as raw material to produce activated carbon. The gas produced could be used for the generation of mechanical and thermal energy, and in some cases, depending on the raw material, it is synthesized to produce other chemical products. The pyrolytic oil has been the most studied so far, finding that it has a great potential as a fuel and in the generation of mechanical and thermal energy [38,40].

Depending of the heating rate, pyrolysis can be classified into four principal types: slow, intermediate, fast and flash pyrolysis. Table 1 summarizes the conditions applicable for each type of pyrolysis and the main products in each one, according with the literature [38,41,42]. Slow pyrolysis produces primarily char and it has been the most used for many years. This pyrolysis type is normally applied for different types of biomass and solid waste [37,40,43]. Fast pyrolysis began to be studied in order to decrease char formation and increase oil production. To obtain a high oil yield with this type of pyrolysis the reaction temperature should not be higher than 650 ºC because at a higher temperature gas production is favored [40,44]. Intermediate pyrolysis is characterized by producing high-quality oil and char. The oil obtained has a higher calorific value and higher viscosity than those obtained by fast pyrolysis [45]. Finally, in the flash pyrolysis, the raw material is heated as fast as possible. Due to the high heating ramps and short residence times, this pyrolysis type allows to decrease considerably the secondary reactions, and consequently it is possible to obtain mostly oil and gas [40,46].

Table 1. *Operating conditions for different types of pyrolysis according to the literature [40,46].*

Process	Heating rate (ºc/min)	Main products
Slow pyrolysis	1-7	Char
Intermediate pyrolysis	20-100	Oil and char
Fast pyrolysis	300 - 500	Oil and gas
Flash pyrolysis	1000	Oil and gas

The pyrolysis process can be performed on different types of reactors.

Figure ***1*** shows the configurations of the main reactors used according to the literature [29,46].

Figure ***2*** shows the product lumps in different types of reactors at different temperatures, using STR as raw material. In accordance with the figure, the higher oil yields are obtained with fixed bed reactor and CSBR.

Figure 1. *Several types of reactors used in pyrolysis process: (a) Stirred tank – (b) Fluidized bed reactor – (c) Fixed bed reactor – (d) Auge reactor – (e) CSBR – (f) Rotatory Kiln.*

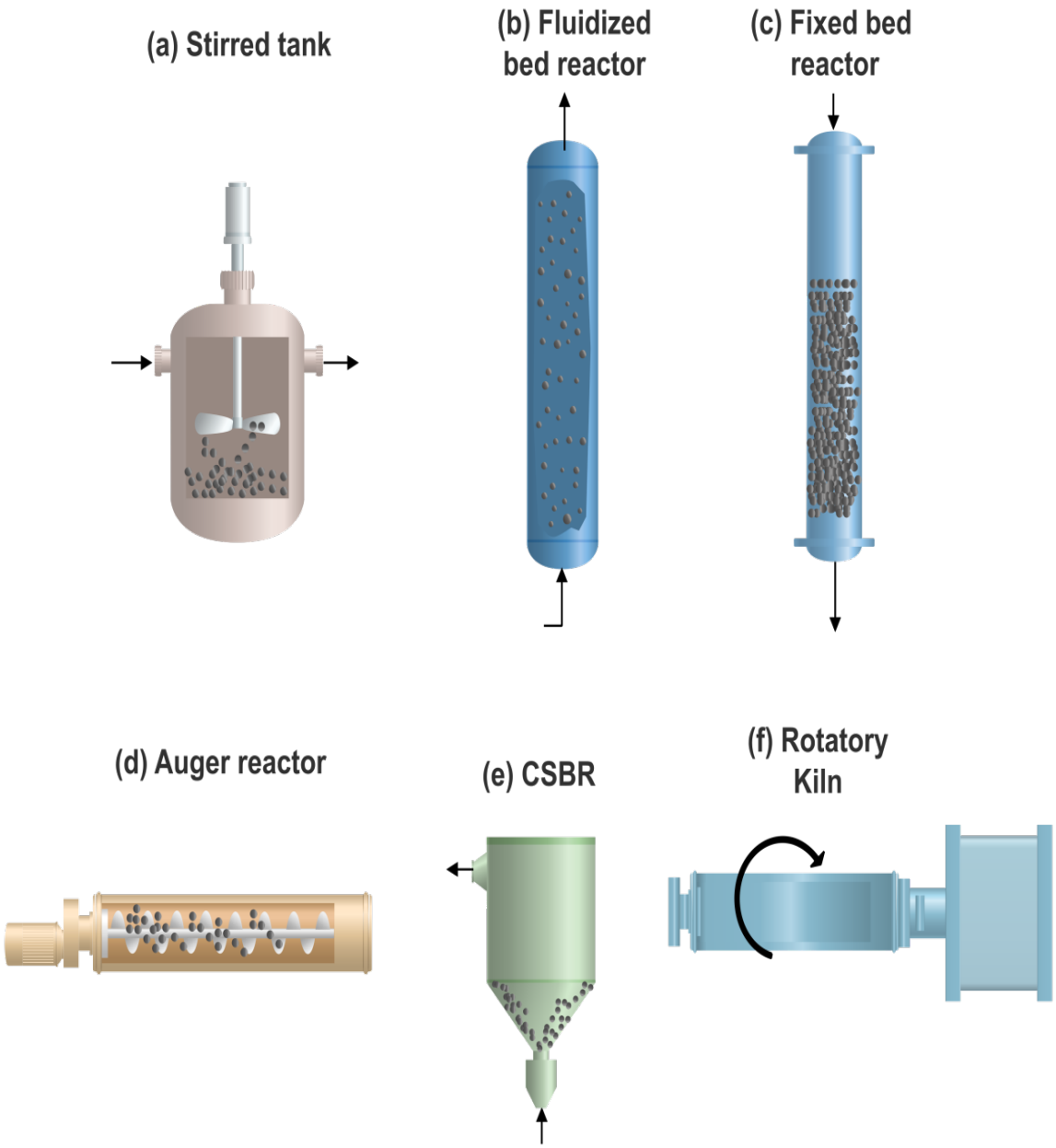

Figure 2. *Distribution of product lumps (wt%) for different types of reactors, taken from Hita et al. [29].*

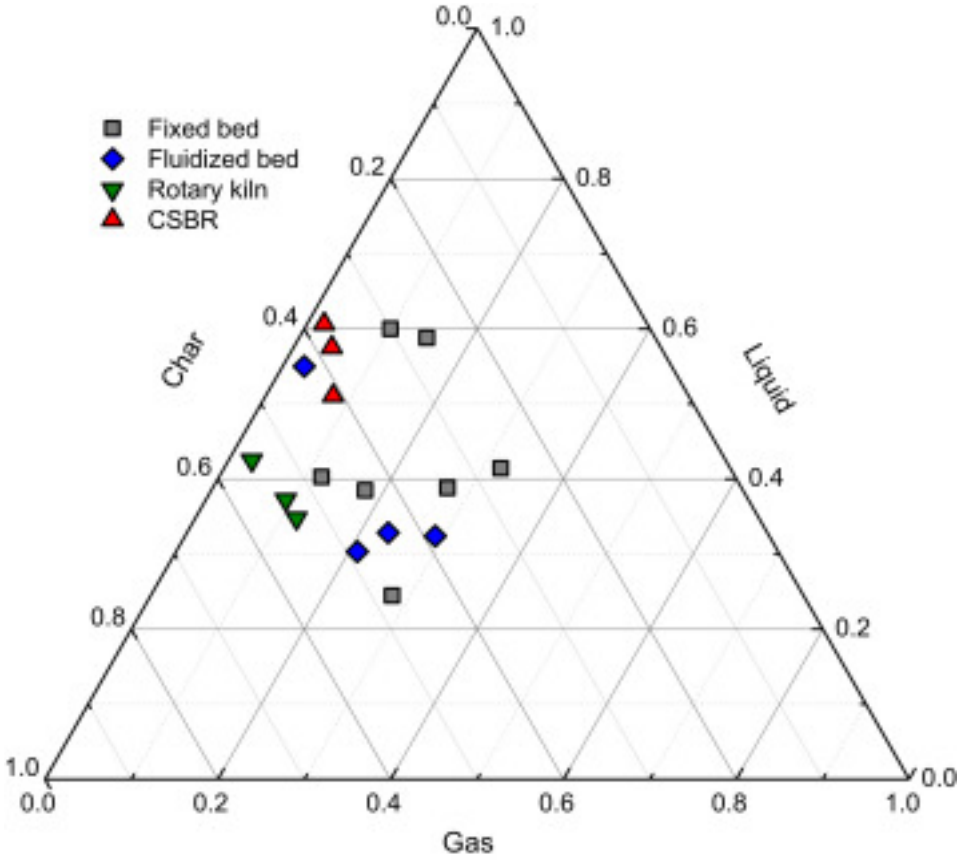

1.2.2 Heteropolyacids. The heteropolyacids (HPA) are polyprotonic mixed oxides, which were discovered in 1826 by Berzelius. A HPA is composed of oxygen atoms, a metal (M) such as Tungsten, Molybdenum or Vanadium named the metallic atom, a central atom or heteroatom (X) which is generally a cation having a +3 to +5 oxidation state, and bound by Hydrogen [47–49]. Table 2 summarizes the most common types of heteropolyacids and their structures.

Table 2. *Structure and chemical formula for the main types of heteropolyacids taken from Viswanathan [47] and modified by the author.*

Structure	Formula	Possible atoms X^{n+}
Keggin	$XM_{12}O_{40}$	P^{5+}, As^{5+}, Si^{4+}, Ge^{4+}
Silverton	$XM_{12}O_{42}$	Ce^{4+}, Th^{4+}
Dawson	$X_2M_{18}O_{62}$	P^{5+}, As^{5+}
Waugh	XM_9O_{32}	Mn^{4+}, Ni^{5+}
Anderson (type A)	XM_6O_{24}	Te^{6+}, I^{7+}

HPA are useful in heterogeneous and homogeneous catalysis, being the most used those with a Keggin or Dawson structure [33,47,49]. As the HPA with a Keggin structure are used in the present study, this section will focus exclusively on this type which is shown in Figure 3. This have a central atom or hereoatom, which is surrounded by 4 oxygens atoms. This central structure is surrounded by 12 MO_6, in which a metallic atom is located in the center of the octahedron while oxygen atoms are located at their vertices [49–52]. The oxygen atoms constituting the heteropolyanion are classified into four classes, and have equivalent symmetry [50]:

- Central oxygen attached to the central tetrahedron with the 4 octahedron triads of MO_6 (Oa).

- Bridging Oxygen that connects the M_3O_{13} groups through the vertices and that binds the octahedrons through the edges to form the triads (Oc and Ob).

- Terminal Oxygen (Ot).

Figure 3. *Keggin Structure from database code ICSD 31897*.

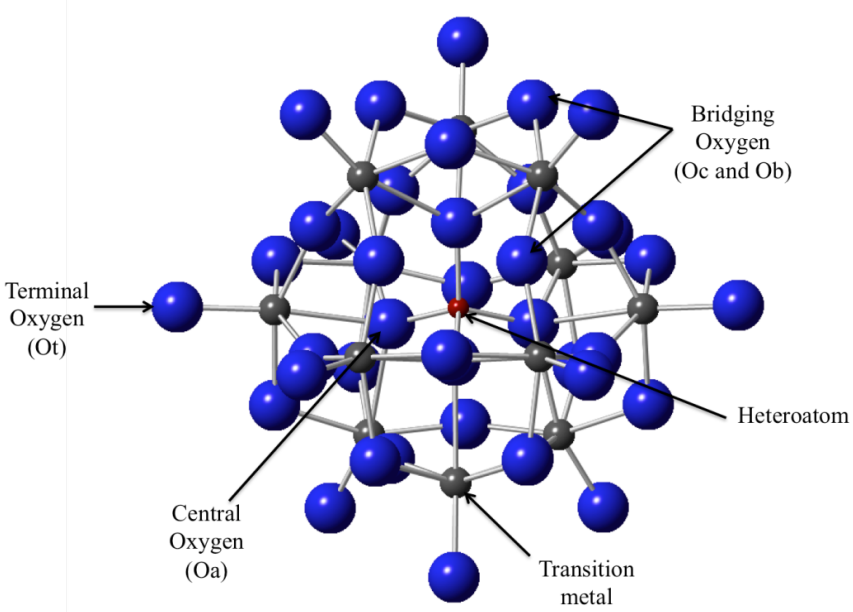

One of the main disadvantages of HPA is its low thermal stability, which depends on its composition. For example, generally those containing tungsten are more stable than those containing molybdenum. Table 3 summarizes the decomposition temperatures of the most used Keggin HPA [49].

Table 3. *Decomposition temperatures of the main Keggin HPA [49].*

HPA	Decomposition temperature (ºC)
$H_3PW_{12}O_{40}$	610
$H_4SiW_{12}O_{40}$	540
$H_3PMo_{12}O_{40}$	495
$H_4SiMo_{12}O_{40}$	375

HPAs are well known for their acidic and redox properties. Its strong acidity in the solid state, as well as in solution, is associated to Lewis and Brønsted acid sites. The Lewis acid sites exhibit weak acid strength whereas the Brønsted acid sites have a strong acid strength. Their acidity is much stronger than solid acid catalysts such as silica, alumina and zeolites, and than mineral acids such as H_2SO_4, HCl and HNO_3 [33]. This is due to the low density of negative charge distributed among many oxygen atoms of polyanion; for example, for $PW_{12}O_{40}$ and $PMo_{12}O_{40}$ the negative charge is delocalized over 40 oxygen atoms.

Because of this delocalization of the charge, the heteropolyanion has a relatively high Brönsted acidity [33,51–53]. In accordance with literature, the acid strength (normally from the Brønsted acidity) decrease as [53]:

$$H_3PW_{12}O_{40} > H_4SiW_{12}O_{40} > H_3PMo_{12}O_{40} > H_4PMo_{11}VO_{40} > H_4SiMo_{12}O_{40}$$

However, although HPA containing tungsten have higher Brønsted acidity, the literature reports that HPA with molybdenum content have higher Lewis acidity [48]. There are five possible mechanisms or ways for the acid sites formation for HPA [47,53]:

- Acidic protons in the acid form or acidic salts.
- Lewis acidity of metal ions.
- Dissociation of coordinated water.
- Protons formed by the reduction of metal ions.
- Partial hydrolysis during the synthesis and after treatment.

In addition to their high acidity, HPAs have generally a second property (*i.e.* redox) owing to the transition metal present in the structure. Because of this fact, HPAs are very useful as catalysts for different reactions of both acid and redox type [49]. Most HPAs have high reduction potentials due to the delocalization of electrons over many atoms in the polyanion. Reversible reductions of one and two electrons are usually produced which produce colored mixed-valence heteropoly anions named heteropoly blues. The reduction potential is usually provided by the metal and the hetero atom (central atom), and is in the order of V > Mo > W and P > Si >B, respectively. For polyanions with mixed metallic atoms, it is indicated that the reduction potential is in the order: $PMo_{10}V_2O_{40}^{5-}$> $PMo_{11}VO_{40}^{4-}$>$PMo_{12}O_{40}^{3-}$ >$PMo_6W_6O_{40}^{3-}$. Normally HPA that contain Molybdenum are stronger oxidants than those containing Tungsten [53,54].

As solid catalysts, HPA present three different types of catalysis [53]:

1) Surface-type: The catalytic reactions take place on the catalyst surface.

2) Bulk-type I (pseudoliquid): The reactions proceed in the three-dimensional volume called "pseudo-liquid". Therefore, there is only acid catalysis for this type.

3) Bulk-type II: Only for redox reactions.

The bulk type reaction does not depend on the specific surface, but it is determined by the mass of the catalyst. On the contrary, the surface type is proportional to the specific surface.

HPA compounds are active catalysts for several reactions such as dehydration, hydrolysis, esterification, conversion of methanol and dimethyl ether to

hydrocarbons, esterification and ester decomposition, alkylation and dealkylation, Diels–Alder reaction, oligomerization of alkenes, isomerization of alkanes, etc. HPA are used as oxidation catalysts in liquid and vapor phases. In the vapor phase, they are effective catalysts for the dehydrogenation [48,53].

As a disadvantage, in addition to present a low thermal stability, HPA has a low specific surface area (SSA : 1-10m^2/g) [55]. To increase SSA and improve catalytic activity, HPA have been supported on different materials such as SiO_2, activated carbon, Al_2O_3, acidic ion exchange resins and different mesoporous materials with organized structure, among others. The HPA are usually deposited on the support by the wet impregnation technique dissolving it in a solvent [33,55].
In this study, different mesoporous materials, both commercial and lab made have been used as substrates. For this reason, the following section will be focused on this type of materials.

1.2.3 Mesoporous materials. The International Union of Pure and Applied Chemistry (IUPAC) defines mesoporous materials as those having a pore size between 2-50 nm. The first attempt to synthesize mesoporous materials was made in 1969, but this was not well defined and recognized, and it was in 1992 that the first material with a high order structure was synthesized. This material was first prepared by Mobil Corporation and was named MCM-41 (Mobil Composition of Matter) [56,57]. Mobil studied and created other new structured mesoporous materials to which they named as M41S family, identifying within these three main structures: hexagonal, cubic and laminar designated as MCM-41, MCM-48 and MCM-50, respectively [58]. MCM-41 has hexagonal structure and parallel two-dimensional channels, which do not connect to each other. Figure 4 presents the structure for the mesoporous materials of M41S family.

The use of mesoporous materials has been of great interest since the 1990s, so the researches focused on these materials have increased year after year, finding so far more than 20 materials developed, which have different sizes of pore, channels and structures [56,58]. These materials have several advantages over other porous materials: their perfectly ordered channels, the ease of synthesis, the possibility of controlling the pore size, their high thermal stability, but above all their high SSA and large pore volume [58].

For the synthesis of these materials, three fundamental components are necessary:

- An inorganic species for the formation of walls.

- A surfactant which is necessary to create the template. It might be cationic or anionic.

- A solvent which serves as the reaction medium.

Although the structural and textural parameters can be modified during the synthesis, MCM-41 is characterized by its high SSA (greater than 1000 m^2/g). The surfactant normally used for its synthesis is an ammonium salt [36,58].

Other typical mesoporous material is SBA-15 (Santa Barbara Amorphous) which was discovered by Zhao and coworkers (See Figure 5). It has also hexagonal structure, but unlike MCM-41, its channels have interconnections between each other by some small channels. SBA-15 has larger wall-thickness than MCM-41, which results in an enhanced steam tolerance. The SSA of this material is about 700-1000 m^2/g, and this characteristic can be modified by the synthesis conditions [36,60].

Figure 4. *Structure of MCM-41 and other M41S family taken from Grecco et al. [59].*

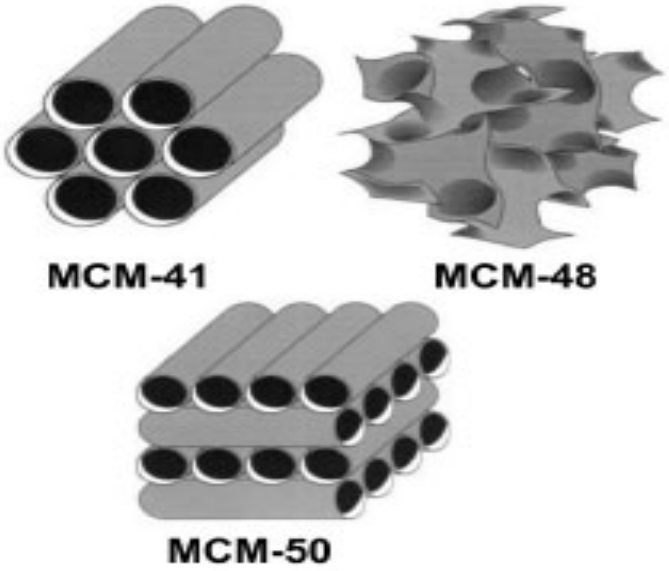

Figure 5. *SBA-15 Structure taken from Yue et al. and Database of Material Center of Technische Universitat Dresden [60,61].*

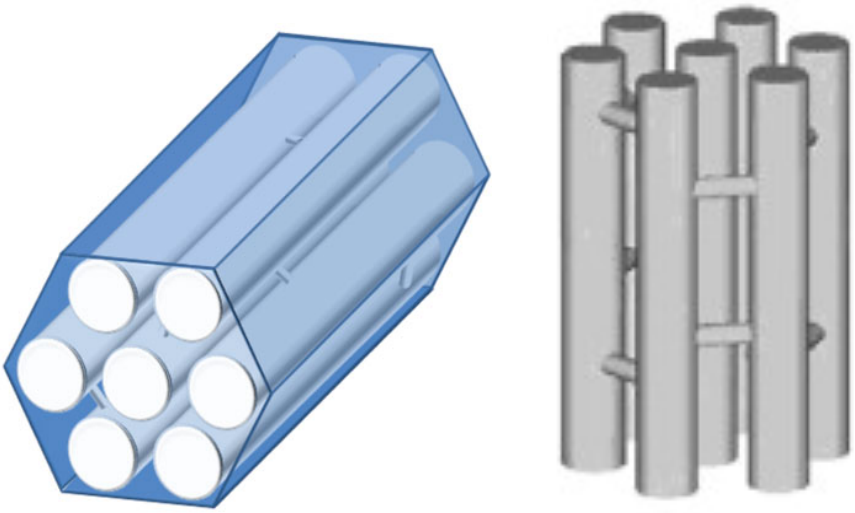

Finally, the third mesoporous material used in this study is named KIT-6 which was made the first time by Ryoo group in 2003. Its synthesis uses triblock copolymer (Pluronic P123) and butanol. The structure of KIT-6, is cubic (space group Ia3d). The average SSA of this material is 800 m^2/g. The structure of KIT-6 is shown in Figure 6.

Figure 6. *KIT-6 Structure taken from Ye et al. [62].*

1.3. REFERENCES OF THIS CHAPTER

[1] COLOMBIA. MINISTRY OF ENVIRONMENT. Resolution 1457 of July 29 of 2010 by mean which separate collection systems and environmental management of used tires are established and other provisions are adopted. 2010.

[2] PNUD COLOMBIA, *et al*. Diagnóstico ambiental sobre el manejo actual de llantas y neumáticos usados generados por el parque automotor de Santa Fe de Bogotá.

[3] MARTÍNEZ, Gonzalo, *et al.* Materiales sustentables y reciclados en la construcción. Omnia Science Editors. 2015. ISBN 8494341804.

[4] ALCALDÍA MAYOR DE BOGOTÁ. Boletín Técnico No3 Mejoras mecánicas de las mezclas asfálticas con grano de caucho reciclado GCR. 2015.

[5] AQUINO, John. Waste age and recycling times: Recycling hanbook. CRC Press. 1995. ISBN 9781566700689.

[6] LEE, Sunggyu; SPEIGHT, James G. and LOYALKA Sudarshan. Handbook of Alternative Fuel Technologies. CRC Press. 2014. ISBN 146659456X.

[7] NIESSEN, Walter. Combustion and Incineration Processes: Applications in Environmental Engineering. CRC Press. 2010. ISBN 9781439875582.

[8] CÁMARA DE COMERCIO DE BOGOTÁ; DEPARTAMENTO TÉCNICO ADMINISTRATIVO DEL MEDIO AMBIENTE. Guía para el manejo de llantas usadas: Un sector transporte con operación más limpia. Kimpres Ltd. 2006.

[9] ALCALDÍA MAYOR DE BOGOTÁ. Decree 442 of 2015: By means of which the Program of utilization and/or valorization of scrap tires in the Capital District is created and other dispositions are adopted. 2015.

[10] CARDONA GÓMEZ, Laura and SÁNCHEZ MONTOYA Laura María. Aprovechamiento de llantas usadas para la fabricación de pisos decorativos. Specialization monograph in PML, Universidad de Medellín. 2011.

[11] ALCALDÍA MAYOR DE BOGOTÁ. Decree 265 of 2016: Which District Decree 442 of 2015 is modified and other layout are adopted. 2016.

[12] PARQUE AMBIENTAL MUNDO LIMPIO S.A. Reciclaje de llanta [online]. 2015 [Consulted 2015-03-27]. Available from: www.mundolimpio.com.co/productos.

[13] DE MARCO RODRIGUEZ, Isabel, *et al.* Pyrolysis of scrap tyres. In: Fuel Processing Technology [online]. 2001, 72(1), p.9–22.

[14] ACOSTA, Rolando, *et al.* Production of Oil and Char by Intermediate Pyrolysis of Scrap Tyres: Influence on Yield and Product Characteristics. In: International Journal of Chemical Reactor Engineering [online]. 2015, 13(2), p. 189–200.

[15] ISLAM, Rofiqul M., *et al*. Liquid fuels and chemicals from pyrolysis of motorcycle tire waste: Product yields, compositions and related properties. In: Fuel [online]. 2008, 87(13–14), p. 3112–3122.

[16] GIRODS, P., *et al*. Low-temperature pyrolysis of wood waste containing urea-formaldehyde resin. In: Renewable Energy [online]. 2008, 33(4), p. 648–654.

[17] MAYER, Ludwig. Métodos de la industria química: en esquemas de flujo en colores. Parte 2a, Orgánica. Reverté. 1987. ISBN 8429179623.

[18] BEYER, Hans and Wolfgang WALTER. Manual de química orgánica. Reverté. 1987. ISBN 8429170669.

[19] OPDYKE, D. L. J. Monographs on Fragrance Raw Materials: A Collection of Monographs Originally Appearing in Food and Cosmetics Toxicology. Chapter 196: p-Cymene. Elsevier. 2013, p. 291. ISBN 1483147975.

[20] BURDOCK, Gerorge A. Fenaroli's Handbook of Flavor Ingredients. Fifth Edition. CRC Press. 2004. ISBN 1420037870.

[21] RAUTER, Amelia, *et al*. Natural Products in the New Millennium: Prospects and Industrial Application. Springer Science & Business Media. 2013. ISBN 9401598762.

[22] MOHAMMAD, Ali and INAMUDDIN, Dr. Green Solvents I: Properties and Applications in Chemistry. Chapter 5: Limonene as green solvent for extraction of natural products. Springer science & business media. 2012, p. 176. ISBN 9400717113.

[23] KERTON, Francesca M. Alternative solvents for green chemistry. Chapter 5. Renewable Solvents. Royal society of chemistry. 2009, p. 97–166. ISBN 085404163X.

[24] DŨNG, Nguyễn Anh, *et al*. Light olefins and light oil production from catalytic pyrolysis of waste tire. In: Journal of Analytical and Applied Pyrolysis [online]. 2009, 86(2), p. 281–286.

[25] DŨNG, Nguyễn Anh, *et al*. Roles of ruthenium on catalytic pyrolysis of waste tire and the changes of its activity upon the rate of calcination. In: Journal of Analytical and Applied Pyrolysis [online]. 2010, 87(2), p. 256–262.

[26] DŨNG, Nguyễn Anh, WONGKASEMJIT Sujitra and JITKARNKA Sirirat. Effects of pyrolysis temperature and Pt-loaded catalysts on polar-aromatic content in tire-derived oil. In: Applied Catalysis B: Environmental [online]. 2009, 91(1–2), p. 300–307.

[27] HITA, Idoia, *et al*. Phosphorus-containing activated carbon as acid support in a bifunctional Pt-Pd catalyst for tire oil hydrocracking. In: Catalysis Communications [online]. 2016, 78, p. 48–51.

[28] HITA, Idoia, *et al*. Opportunities and barriers for producing high quality fuels from the pyrolysis of scrap tires. In: Renewable and Sustainable Energy Reviews [online]. 2016, 56, p. 745–759.

[29] WILLIAMS, Paul T. and BRINDLE, Alexander J.. Aromatic chemicals from the catalytic pyrolysis of scrap tyres. In: Journal of Analytical and Applied Pyrolysis [online]. 2003, 67(1), p. 143–164.

[30] ARABIOURRUTIA, M., *et al*. Product distribution obtained in the pyrolysis of tyres in a conical spouted bed reactor. In: Chemical Engineering Science [online]. 2007, 62(18–20), p. 5271–5275.

[31] OLAZAR, Martin, *et al*. Catalyst effect on the composition of tire pyrolysis products. In: Energy and Fuels [online]. 2008, 22(5), p. 2909–2916.

[32] SILVA, Manuel and HENRIQUEZ, Miguel Angel. Preparación de catalizadores superácidos del tipo heteropoliacido soportados para el estudio de la

reacción de alquilación de tolueno con 1-dodeceno. Thesis in Chemical Engineering. Caracas: Universidad Central de Venezuela. 2003.

[33] WILLIAMS, Paul T. and BOTTRILL, Richard. Sulfur-polycyclic tyre pyrolysis oil. In: Fuel. 1995, 74(5), p. 736–742.

[34] CUNLIFFE, Adrian M. and WILLIAMS, Paul T. Composition of oils derived from the batch pyrolysis of tyres. In: Journal of Analytical and Applied Pyrolysis [online]. 1998, 44(2), p. 131–152.

[35] KATRYNIOK, Benjamin. Nouvelle voie de synthese d'acroleine a partir de biomasse. Doctoral Thesis. Lille France: Université des Sciences et Technologies de Lille. Ecole doctoral de Science de la matière, du rayonnement et de l'environnement, 2010.

[36] WANG, Shurong and LUO, Zhongyang. Pyrolysis of Biomass. Walter de Gruyter GmbH & Co. 2017. ISBN 311036963X, 9783110369632.

[37] CASTELLS, Xavier Elías. Reciclaje y tratamiento de residuos diversos: Reciclaje de residuos industriales. Ediciones Díaz de Santos. 2012. ISBN 8499693741.

[38] YOUNG, Gary C. Municipal Solid Waste to Energy Conversion Processes: Economic, Technical, and Renewable Comparisons. John Wiley & Sons. 2010. ISBN 1118029275, 9781118029275.

[39] BASU, Prabir. Biomass Gasification, Pyrolysis and Torrefaction: Practical Design and Theory. Second Edition. Academic Press. 2013. ISBN 0123965438, 9780123965431.

[40] CAPAREDA, Sergio. Introduction to Biomass Energy Conversions. Ilustrated Edition. CRC Press. 2013. ISBN 1466513349, 9781466513341.

[41] PANDEY, Ashok. Handbook of plant-based biofuels. CRC Press. 2008. ISBN 0789038749.

[42] DAHLQUIST, Erik. Technologies for Converting Biomass to Useful Energy: Combustion, Gasification, Pyrolysis, Torrefaction and Fermentation. CRC Press. 2013. ISBN 0203120264, 9780203120262.

[43] SUIB, Steven L. New and Future Developments in Catalysis: Catalytic Biomass Conversion. Newnes Editors. 2013. ISBN 0444538798, 9780444538796.

[44] SINGH, Lalit Kumar and CHAUDHARY, Gaurav. Advances in Biofeedstocks and Biofuels, Volume One: Biofeedstocks and Their Processing. John Wiley & Sons. 2016. ISBN 1119117275, 9781119117278.

[45] ANTONIOU, N. and ZABANIOTOU, A. Features of an efficient and environmentally attractive used tyres pyrolysis with energy and material recovery. In: Renewable and Sustainable Energy Reviews [online]. 2013, 20, p. 539–558.

[46] VISWANATHAN, B. Catalysis: Principles and Applications. CRC Press, 2002. ISBN 0849324246, 9780849324246.

[47] AUGUSTINE, Robert L. Heterogeneous Catalysis for the Synthetic Chemist. Illustrated Edition. CRC Press. 1995. ISBN 0824790219, 9780824790219.

[48] MATLACK, Albert. Introduction to Green Chemistry. Second Edition. CRC Press. 2010. ISBN 1439882118, 9781439882115.

[49] PALERMO, Valeria; ROMANELLI, Gustavo P. and VÁZQUEZ, Patricia G.. Mo-based Keggin heteropolyacids as catalysts in the green and selective oxidation of diphenyl sulfide. In: Journal of Molecular Catalysis A: Chemical [online]. 2013, 373, p. 142–150.

[50] PALERMO, Valeria. Síntesis y caracterización de heteropoliácidos. Doctoral Thesis. Universidad de la Plata. Faculty of exact sciences. Department of chemistry. 2012, 305 p.

[51] MOSER, William R. Advanced Catalysts and Nanostructured Materials: Modern Synthetic Methods. Academic Press.1996. ISBN 0080526551, 9780080526553.

[52] MISONO, M. Chapter 4 – Catalysis of Heteropoly Compounds (Polyoxometalates) [online]. First Edition. Elsevier. 2013. ISBN 9780444538338.

[53] BORRÁS-ALMENAR, Juan J., *et al*. Polyoxometalate Molecular Science. Volumen 98 de Nato Science Series II. Ilustrated Edition. Springer Science & Business Media. 2012. ISBN 9401000913, 9789401000918.

[54] TOUFAILY, J., *et al*. Synthesis and characterization of new catalysts formed by direct incorporation of heteropolyacids into organized mesoporous silica. In: Colloids and Surfaces A: Physicochemical and Engineering Aspects [online]. 2008, 316(1–3), p. 285–291.

[55] SHARMA, Sanjay K. and SANGHI, Rashmi. Advances in Water Treatment and Pollution Prevention. Chapter 6: Mesoporous-Assembled Nanocrystal Photocatalysts for degradation of Azo Dyes. Springer science & businnes media. Ilustrated Edition. 2012. ISBN 9400742045, 9789400742048.

[56] BAERNS, Manfred. Basic Principles in Applied Catalysis. Springer Science & Business Media. 2013. ISBN 3662059819, 9783662059814.

[57] VALTCHEV, Valentin; MINTOVA, Svetlana and TSAPATSIS, Michael. Ordered Porous Solids: Recent Advances and Prospects. Elsevier. 2011. ISBN 0080932452, 9780080932453.

[58] GRECCO, Saulo de Tarso and RANGEL Maria do Carmo. Zeólitas Hierarquicamente Estruturadas. In: Quim. Nova. 2013, 36(1), p. 131–142.

[59] YUE, Wenbo and ZHOU Wuzong. Crystalline mesoporous metal oxide. In: Progress in Natural Science [online]. 2008, 18, p. 1329–1338.

[60] MATERIALS CENTER OF TECHNISCHE UNIVERSITAT DRESDEN. Chemical Data of SBA-15 Hexagonal mesoporous SiO2. Dresden: Technische Universitat Dresden. 1998.

[61] YE, Youngjin, *et al*. Functional mesoporous materials for energy applications: solar cells, fuel cells, and batteries. In: Nanoscale [online]. 2013.

1.4. BIBLIOGRAPHY OF THIS CHAPTER

ACOSTA, Rolando, *et al.* Production of Oil and Char by Intermediate Pyrolysis of Scrap Tyres: Influence on Yield and Product Characteristics. In: International Journal of Chemical Reactor Engineering [online]. 2015, 13(2), p. 189–200.

ALCALDÍA MAYOR DE BOGOTÁ. Boletín Técnico No3 Mejoras mecánicas de las mezclas asfálticas con grano de caucho reciclado GCR. 2015.

ALCALDÍA MAYOR DE BOGOTÁ. Decree 265 of 2016: Which District Decree 442 of 2015 is modified and others layout are adopted. 2016.

ALCALDÍA MAYOR DE BOGOTÁ. Decree 442 of 2015: By means of which the Program of utilization and/or valorization of scrap tires in the Capital District is created and other dispositions are adopted. 2015.

ANTONIOU, N. and ZABANIOTOU, A. Features of an efficient and environmentally attractive used tyres pyrolysis with energy and material recovery. In: Renewable and Sustainable Energy Reviews [online]. 2013, 20, p. 539–558.

AQUINO, John. Waste age and recycling times: Recycling hanbook. CRC Press. 1995. ISBN 9781566700689.

ARABIOURRUTIA, M., *et al*. Product distribution obtained in the pyrolysis of tyres in a conical spouted bed reactor. In: Chemical Engineering Science [online]. 2007, 62(18–20), p. 5271–5275.

AUGUSTINE, Robert L. Heterogeneous Catalysis for the Synthetic Chemist. Illustrated Edition. CRC Press. 1995. ISBN 0824790219, 9780824790219.

BAERNS, Manfred. Basic Principles in Applied Catalysis. Springer Science & Business Media. 2013. ISBN 3662059819, 9783662059814.

BASU, Prabir. Biomass Gasification, Pyrolysis and Torrefaction: Practical Design and Theory. Second Edition. Academic Press. 2013. ISBN 0123965438, 9780123965431.

BEYER, Hans and Wolfgang WALTER. Manual de química orgánica. Reverté. 1987. ISBN 8429170669.

BORRÁS-ALMENAR, Juan J., *et al*. Polyoxometalate Molecular Science. Volumen 98 de Nato Science Series II. Ilustrated Edition. Springer Science & Business Media. 2012. ISBN 9401000913, 9789401000918.

BURDOCK, Gerorge A. Fenaroli's Handbook of Flavor Ingredients. Fifth Edition. CRC Press. 2004. ISBN 1420037870.

CÁMARA DE COMERCIO DE BOGOTÁ; DEPARTAMENTO TÉCNICO ADMINISTRATIVO DEL MEDIO AMBIENTE. Guía para el manejo de llantas usadas: Un sector transporte con operación más limpia. Kimpres Ltd. 2006

CAPAREDA, Sergio. Introduction to Biomass Energy Conversions. Ilustrated Edition. CRC Press. 2013. ISBN 1466513349, 9781466513341.

CARDONA GÓMEZ, Laura and SÁNCHEZ MONTOYA Laura María. Aprovechamiento de llantas usadas para la fabricación de pisos decorativos. Specialization monograph in PML, Universidad de Medellín. 2011.

CASTELLS, Xavier Elías. Reciclaje y tratamiento de residuos diversos: Reciclaje de residuos industriales. Ediciones Díaz de Santos. 2012. ISBN 8499693741.

COLOMBIA. MINISTRY OF ENVIRONMENT. Resolution 1457 of July 29 of 2010 by mean which separate collection systems and environmental management of used tires are established and other provisions are adopted. 2010.

CUNLIFFE, Adrian M. and WILLIAMS, Paul T. Composition of oils derived from the batch pyrolysis of tyres. In: Journal of Analytical and Applied Pyrolysis [online]. 1998, 44(2), p. 131–152.

DAHLQUIST, Erik. Technologies for Converting Biomass to Useful Energy: Combustion, Gasification, Pyrolysis, Torrefaction and Fermentation. CRC Press. 2013. ISBN 0203120264, 9780203120262.

DE MARCO RODRIGUEZ, Isabel, *et al.* Pyrolysis of scrap tyres. In: Fuel Processing Technology [online]. 2001, 72(1), p.9–22.

DŨNG, Nguyễn Anh, *et al*. Light olefins and light oil production from catalytic pyrolysis of waste tire. In: Journal of Analytical and Applied Pyrolysis [online]. 2009, 86(2), p. 281–286.

DŨNG, Nguyễn Anh, *et al*. Roles of ruthenium on catalytic pyrolysis of waste tire and the changes of its activity upon the rate of calcination. In: Journal of Analytical and Applied Pyrolysis [online]. 2010, 87(2), p. 256–262.

DŨNG, Nguyễn Anh, WONGKASEMJIT Sujitra and JITKARNKA Sirirat. Effects of pyrolysis temperature and Pt-loaded catalysts on polar-aromatic content in tire-derived oil. In: Applied Catalysis B: Environmental [online]. 2009, 91(1–2), p. 300–307.

GIRODS, P., *et al*. Low-temperature pyrolysis of wood waste containing urea-formaldehyde resin. In: Renewable Energy [online]. 2008, 33(4), p. 648–654.

GRECCO, Saulo de Tarso and RANGEL Maria do Carmo. Zeólitas Hierarquicamente Estruturadas. In: Quim. Nova. 2013, 36(1), p. 131–142.

HITA, Idoia, *et al*. Phosphorus-containing activated carbon as acid support in a bifunctional Pt-Pd catalyst for tire oil hydrocracking. In: Catalysis Communications [online]. 2016, 78, p. 48–51.

HITA, Idoia, *et al*. Opportunities and barriers for producing high quality fuels from the pyrolysis of scrap tires. In: Renewable and Sustainable Energy Reviews [online]. 2016, 56, p. 745–759.

ISLAM, Rofiqul M., *et al*. Liquid fuels and chemicals from pyrolysis of motorcycle tire waste: Product yields, compositions and related properties. In: Fuel [online]. 2008, 87(13–14), p. 3112–3122.

KATRYNIOK, Benjamin. Nouvelle voie de synthese d'acroleine a partir de biomasse. Doctoral Thesis. Lille France: Université des Sciences et Technologies de Lille. Ecole doctoral de Science de la matière, du rayonnement et de l'environnement, 2010.

KERTON, Francesca M. Alternative solvents for green chemistry. Chapter 5. Renewable Solvents. Royal society of chemistry. 2009, p. 97–166. ISBN 085404163X.

LEE, Sunggyu; SPEIGHT, James G. and LOYALKA Sudarshan. Handbook of Alternative Fuel Technologies. CRC Press. 2014. ISBN 146659456X.

MARTÍNEZ, Gonzalo, *et al.* Materiales sustentables y reciclados en la construcción. Omnia Science Editors. 2015. ISBN 8494341804.

MATERIALS CENTER OF TECHNISCHE UNIVERSITAT DRESDEN. Chemical Data of SBA-15 Hexagonal mesoporous SiO2. Dresden: Technische Universitat Dresden. 1998.

MATLACK, Albert. Introduction to Green Chemistry. Second Edition. CRC Press. 2010. ISBN 1439882118, 9781439882115.

MAYER, Ludwig. Métodos de la industria química: en esquemas de flujo en colores. Parte 2a, Orgánica. Reverté. 1987. ISBN 8429179623.

MOHAMMAD, Ali and INAMUDDIN, Dr. Green Solvents I: Properties and Applications in Chemistry. Chapter 5: Limonene as green solvent for extraction of natural products. Springer science & business media. 2012, p. 176. ISBN 9400717113.

MOSER, William R. Advanced Catalysts and Nanostructured Materials: Modern Synthetic Methods. Academic Press.1996. ISBN 0080526551, 9780080526553.
MISONO, M. Chapter 4 – Catalysis of Heteropoly Compounds (Polyoxometalates) [online]. First Edition. Elsevier. 2013. ISBN 9780444538338.

NIESSEN, Walter. Combustion and Incineration Processes: Applications in Environmental Engineering. CRC Press. 2010. ISBN 9781439875582.

OPDYKE, D. L. J. Monographs on Fragrance Raw Materials: A Collection of Monographs Originally Appearing in Food and Cosmetics Toxicology. Chapter 196: p-Cymene. Elsevier. 2013, p. 291. ISBN 1483147975.

OLAZAR, Martin, *et al*. Catalyst effect on the composition of tire pyrolysis products. In: Energy and Fuels [online]. 2008, 22(5), p. 2909–2916.

PALERMO, Valeria. Síntesis y caracterización de heteropoliácidos. Doctoral Thesis. Universidad de la Plata. Faculty of exact sciences. Department of chemistry. 2012, 305 p.

PALERMO, Valeria; ROMANELLI, Gustavo P. and VÁZQUEZ, Patricia G.. Mo-based Keggin heteropolyacids as catalysts in the green and selective oxidation of diphenyl sulfide. In: Journal of Molecular Catalysis A: Chemical [online]. 2013, 373, p. 142–150.

PARQUE AMBIENTAL MUNDO LIMPIO S.A. Reciclaje de llanta [online]. 2015 [Consulted 2015-03-27]. Available from: www.mundolimpio.com.co/productos.

PNUD COLOMBIA, *et al.* Diagnóstico ambiental sobre el manejo actual de llantas y neumáticos usados generados por el parque automotor de Santa Fe de Bogotá.
PANDEY, Ashok. Handbook of plant-based biofuels. CRC Press. 2008. ISBN 0789038749.

RAUTER, Amelia, *et al*. Natural Products in the New Millennium: Prospects and Industrial Application. Springer Science & Business Media. 2013. ISBN 9401598762.

SHARMA, Sanjay K. and SANGHI, Rashmi. Advances in Water Treatment and Pollution Prevention. Chapter 6: Mesoporous-Assembled Nanocrystal Photocatalysts for degradation of Azo Dyes. Springer science & businnes media. Ilustrated Edition. 2012. ISBN 9400742045, 9789400742048.

SILVA, Manuel and HENRIQUEZ, Miguel Angel. Preparación de catalizadores superácidos del tipo heteropoliacido soportados para el estudio de la reacción de alquilación de tolueno con 1-dodeceno. Thesis in Chemical Engineering. Caracas: Universidad Central de Venezuela. 2003.

SINGH, Lalit Kumar and CHAUDHARY, Gaurav. Advances in Biofeedstocks and Biofuels, Volume One: Biofeedstocks and Their Processing. John Wiley & Sons. 2016. ISBN 1119117275, 9781119117278.

SUIB, Steven L. New and Future Developments in Catalysis: Catalytic Biomass Conversion. Newnes Editors. 2013. ISBN 0444538798, 9780444538796.

TOUFAILY, J., *et al*. Synthesis and characterization of new catalysts formed by direct incorporation of heteropolyacids into organized mesoporous silica. In: Colloids and Surfaces A: Physicochemical and Engineering Aspects [online]. 2008, 316(1–3), p. 285–291.

VALTCHEV, Valentin; MINTOVA, Svetlana and TSAPATSIS, Michael. Ordered Porous Solids: Recent Advances and Prospects. Elsevier. 2011. ISBN 0080932452, 9780080932453.

VISWANATHAN, B. Catalysis: Principles and Applications. CRC Press, 2002. ISBN 0849324246, 9780849324246.

WANG, Shurong and LUO, Zhongyang. Pyrolysis of Biomass. Walter de Gruyter GmbH & Co. 2017. ISBN 311036963X, 9783110369632.

WILLIAMS, Paul T. and BOTTRILL, Richard. Sulfur-polycyclic tyre pyrolysis oil. In: Fuel. 1995, 74(5), p. 736–742.

WILLIAMS, Paul T. and BRINDLE, Alexander J.. Aromatic chemicals from the catalytic pyrolysis of scrap tyres. In: Journal of Analytical and Applied Pyrolysis [online]. 2003, 67(1), p. 143–164.

YE, Youngjin, *et al.* Functional mesoporous materials for energy applications: solar cells, fuel cells, and batteries. In: Nanoscale [online]. 2013.

YOUNG, Gary C. Municipal Solid Waste to Energy Conversion Processes: Economic, Technical, and Renewable Comparisons. John Wiley & Sons. 2010. ISBN 1118029275, 9781118029275.

YUE, Wenbo and ZHOU Wuzong. Crystalline mesoporous metal oxide. In: Progress in Natural Science [online]. 2008, 18, p. 1329–1338.

Chapter 2

Characterization of raw material

Part of this chapter is published in International Journal of Chemical Reactor Engineering:

R. Acosta, C. Tavera, P. Gauthier-Maradei, D. Nabarlatz. (2015). Production of oil and char by intermediate pyrolysis of scrap tires: influence on yield and product characteristics. Int. J. Chem. React. Eng; 13:189–200.

2.1 INTRODUCTION

The tires are an indispensable element in the vehicles to support the weight, the braking and also to cushion the irregularities of the road. For this reason, the use of tires has become a necessity for the human because it is a key component of the different existing means of transport, which are necessary for the mobility of raw materials, products or people. The first existing tires were made of wood and metals such as iron and steel, which date from the discovery of the wheel in prehistory. In the XVIII century, the rough and heavy tires were replaced by bands of natural rubber, which is obtained from the *Hevea Brasiliensis* tree [1]. In 1888, the first pneumatic tire (inflated with air) was invented by the Scottish John Boyd Dunlop, who replaced the solid rubber wheels with rubber bands inflated with air, which is

used today [2]. Later the tire began to be made of a mixture of natural and synthetic rubber, and a metallic reinforcement was added [3, 4].

Over time, arose the necessity to make tires more resistant to friction, heating and the hydrocarbon compounds that could dissolve it. In this way, was created by Goodyear the process known as vulcanization, which consists of adding additives to the rubber (usually sulfur, carbon black, zinc oxide and plasticizers) at a temperature of 140 °C [5–7].

Thus, the tires are composed of a mixture of natural and synthetic rubber, additives and a metallic reinforcement. The concentrations of each component are variable according to the brand and the application, being different for cars, trucks and passenger cars. Considering that this is necessary to define the specific characteristics of the scrap tires to be used in the experimental tests of this study, this chapter refers to the characterization of the sample of scrap tire rubber (STR) acquired, in order to determine its composition, type (vehicles, trucks or buses) and density.

The raw material used in this study is pulverized STR with a particle size less than 1mm, obtained from a crushing plant in the city of Medellín - Colombia. This material is normally used for the maintenance of synthetic fields and consists in the polymeric part without metallic reinforcement. The diameter was selected according to the results obtained in a study carried out in the same research group by Acosta *et al.* [8]. They found that although there was no significant variation of the oil yield when the particle size was changed in the range of 0.85 to 2.10 mm, the higher oil yield obtained was with particle size less than 1 mm.

2.2 METHODOLOGY

2.2.1 Elemental and Proximate analysis. Elemental analysis of STR sample was performed in join with Acosta *et al.* [9]. This analysis was carried out in an elemental analyzer (LECO, model TruSpec Micro) following the ASTM D-5373-08 standard. The mass composition of carbon, hydrogen and sulfur was determined in a single step, while the oxygen content was determined by using another column inside the instrument.

The proximate analysis for STR, NR, SBR and BR samples were taken from Cely [10]. The analysis was performed in a thermogravimetric analyzer (ATG 2050, TA Instruments), following the ASTM D-7582 standard.

2.2.2 Real and Bulk densities. The real and bulk densities were measured. To determine the bulk density, the weight of a standard volume in a volumetric test piece was measured by triplicate. For the real density measurements, each sample was separately ground and dried. About 2 g of the STR sample was weighed and introduced into a pycnometer, which finally was filled with deionized water and weighed. Finally, the pycnometer was emptied and washed, filled with only deionized water and weighed again. The real density was expressed as the ratio of the mass of the ground dry specimen and the volume of liquid displaced by this mass. The tests were measured by duplicate, and the analysis was also performed with a volumetric flask (100 mL) to confirm.

2.2.3 Quantification of the polymer compounds. The methodology used for the development of this technique is shown in Figure 7. Likewise, the quantification of the main polymer compounds in the STR sample as natural rubber (NR), styrene–butadiene rubber (SBR) and butadiene rubber (BR) was performed using a pyroprobe coupled to GC/FID. This technique has been reported by several authors

for the identification and quantification of polymers [11–15]. They suggest that the area of the principal compound(s) produced during pyrolysis of each polymer (NR, BR and SBR) can be correlated with the weight percent composition of each polymer.

Figure 7. *Methodology for quantification of polymers in the tire using Py-GC/FID.*

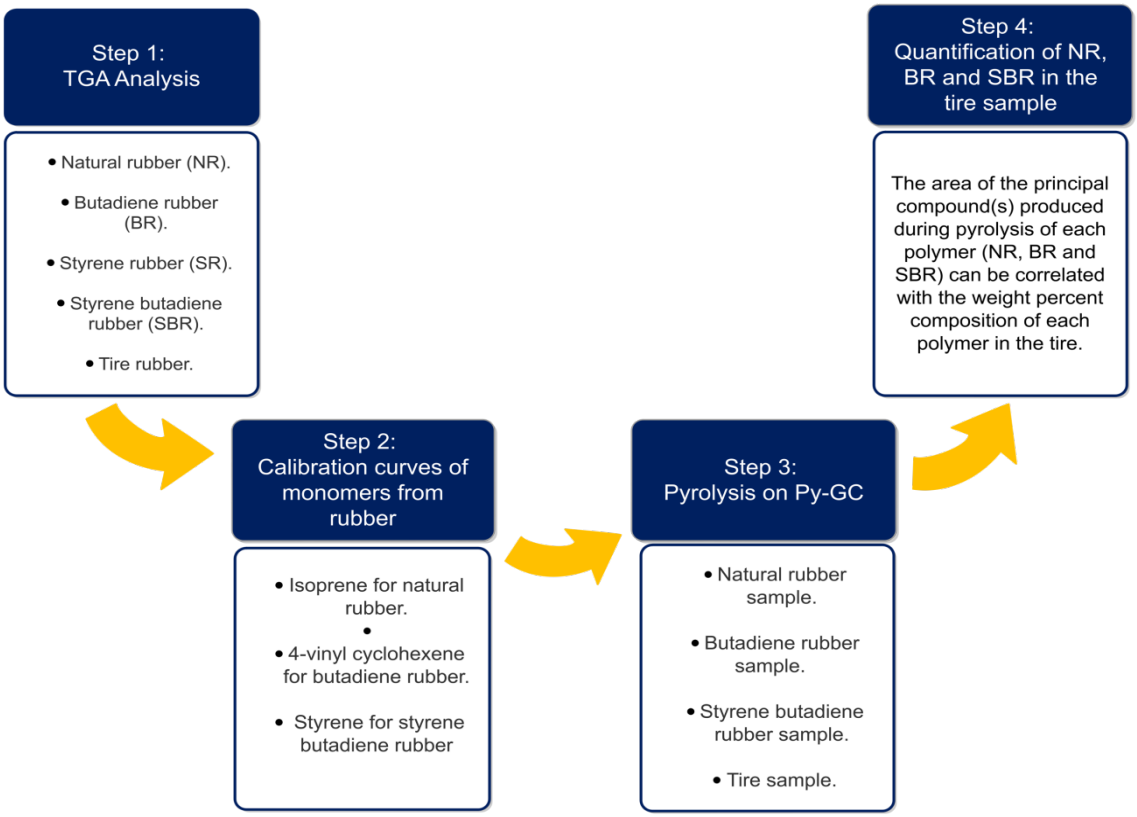

A pyroprobe CDS 5150 coupled to a Gas Chromatography with Flame Ionization Detector (py-GC/FID) chromatograph (Figure 8), and a capillary column HP-5 30m x 0.320mm x 0.25 µm was used. The pyroprobe was programmed at initial temperature of 300 °C for 1 s, with a rate of 10 °C/ms, until reaching a final temperature of 550 °C, at which it remains constant for 10 s. The interface was programmed at initial temperature of 50 ºC, with a rate of 0ºC/min (Immediate

heating), and a final temperature of 250 ºC, remaining constant during 1 min. The transfer line and the valve oven was programmed at 280 ºC.

Figure 8. *Unit Pyroprobe coupled to a GC/FID chromatograph.*

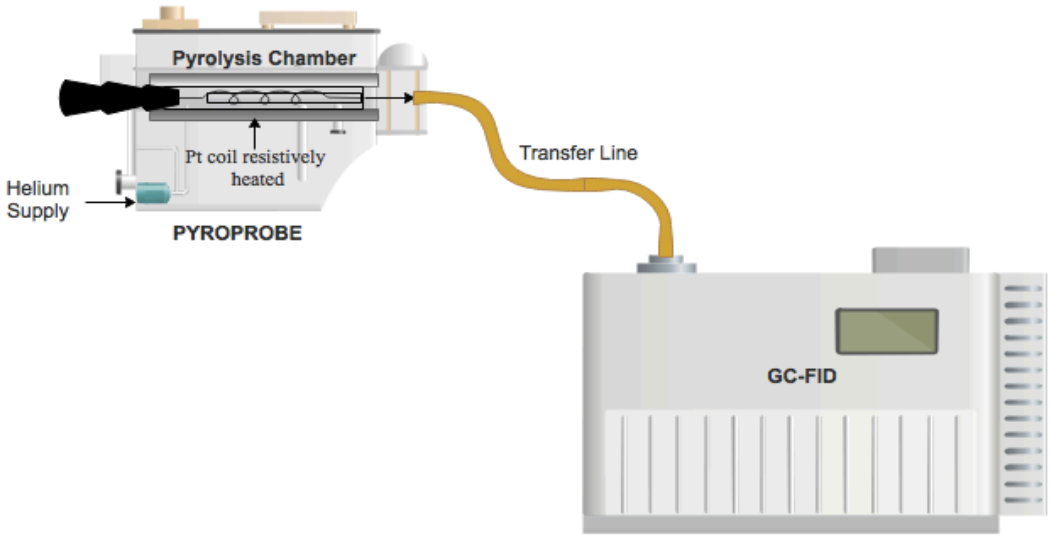

0.1 mg of each sample (NR, SBR, SR, BR, and scrap tire rubber) were weighed and placed in the pyroprobe according to the method reported by Lee *et al.* [11]. NR sample was supplied by Procauchos S.A. (Bucaramanga, Colombia), SBR and BR samples were supplied by Mil Cauchos Industries (Bucaramanga, Colombia) and SR sample was supplied by Metalcril (Bucaramanga, Colombia). The calibration curves for GC/FID analysis were performed using standards of the main components obtained after thermal degradation of each polymer (NR and SBR): isoprene, 4-vinylcyclohexene and styrene (Dr Ehrenstorfer GmbH, 99% certified standards), respectively.

2.3 RESULTS AND DISCUSSION

The real density obtained for the particle size <1mm was 511.86 ± 0.06 kg/m^3 and the bulk density was 347.70 ± 0.01 kg / m^3.

The results of the elemental analysis are compare with those found in other studies in Table 4. It can be observed that the STR sample is composed mainly of carbon and it is in agree with other authors [16–21]. However, the carbon content obtained by Islam *et al.* [18] is lower than the others authors. They mention that the study was performed with a motorcycle tire and the carbon content of this type of tire is lower than passenger or truck tires, this mainly because of the difference in composition of rubbers and additives added to each type of tire.

Table 4. *The elementary analysis for STR samples. Comparison between the sample used in this study and that reported by literature. (Dry basis).*

	wt%				
	This study [9]	**Martínez *et al.*** [16]	**Murillo *et al.*** [17]	**Islam *et al.*** [18]	**Zhang *et al.*** [19]
Tire type	Trucks	Mixture of trucks, tractors, and cars tires	Not specified	Motorcycle	Not specified
Nitrogen	1.68	0.30	0.43	0.81	0.78
Carbon	86.00	87.90	88.64	75.50	83.92
Hydrogen	7.55	7.40	8.26	6.75	6.83
Sulfur	1.60	1.10	1.43	1.44	0.92

On the other hand, Ucar *et al.* [21] evaluated two types of tires: passenger and truck tires. They found that truck tires have higher carbon content and lower sulfur content than passenger tires. In conclusion, based on reported by these authors, the carbon content varies according with the type of tire in this way: trucks > passenger > motorcycles. Moreover, nitrogen and sulfur content measured in this study on STR sample is higher than the authors. The sulfur content present varies according with the amount of sulfur compounds added to each type and brand of tire during the vulcanization process.

The results of the proximate analysis for the STR, NR, SBR, BR and SR samples were taken from Cely [10]. The proximate analysis for the STR sample is shown in Table 5. The analysis for NR, SBR, BR and SR samples are reported in ANNEX A. It is observed that the STR sample has a high content of volatile matter, a value that is in agreement with the other authors, except for Islam *et al*. [18], which has a lower content. Murillo *et al*. [17] mention that the volatile matter has direct relation to the polymeric materials present in the tire, therefore, this also varies depending on the brand and type of tire. This is complemented by Ucar *et al*. [21] who found that the volatile matter content is higher for truck tires than that for passenger tires.

A difference in the ash content measured in this study on STR sample is observed with the other authors [18, 22]. According to they, the ash variation is mainly due to the variation of the contents of inorganic materials of the additives used during the manufacture of the tires such as zinc and titanium oxides, clay, silica, among others, which vary as a function of the manufacturer and type of vehicle. For the fixed carbon content, several authors relate it to the content of carbon black added in the manufacture of the tires, which also varies according with the brand and type of vehicle [17, 18, 22].

Table 5. *Proximate Analysis for STR samples. Comparison between the sample used in this study and that reported by literature.*

	Wt%				
	Cely [10] (This study)	**Martínez *et al.* [16]**	**Murillo *et al.* [17]**	**Islam *et al.* [18]**	**Zhang *et al.* [19]**
Moisture	1.20	0.80	0.94	1.53	0.75
Volatile matter*	65.41	63.60	64.09	57.50	64.97
Fixed carbon	27.31	31.80	31.14	20.85	30.08
Ash	6.08	3.80	3.83	20.12	4.16

* Dry basis

For the identification and quantification of the composition of STR sample was used a Py-GC/FID beforementioned. The analysis was based on the technique reported by several authors [11–15]. Figure 9 shows the main monomers from the pyrolysis for each polymer: for the NR are isoprene and dipentene, for the SBR are styrene and 4-vinylcyclohexene, and for the BR is 4-vinylcyclohexene.

For this study, the calculation of NR and SBR concentrations in STR sample, isoprene and styrene were taken as the main monomers, respectively. BR concentration was calculated by difference due to difficulty to dissociated the area done by GC/FID for 4-vinylcyclohexene that is associated to degradation of BR and SBR. The calibration and the chromatography curves for those compounds as well as the details of method used are presented in ANNEX B.

Figure 9. *Main monomers produced by pyrolysis for each polymer present in the STR sample: (a) NR, (b) BR and (c) SBR.*

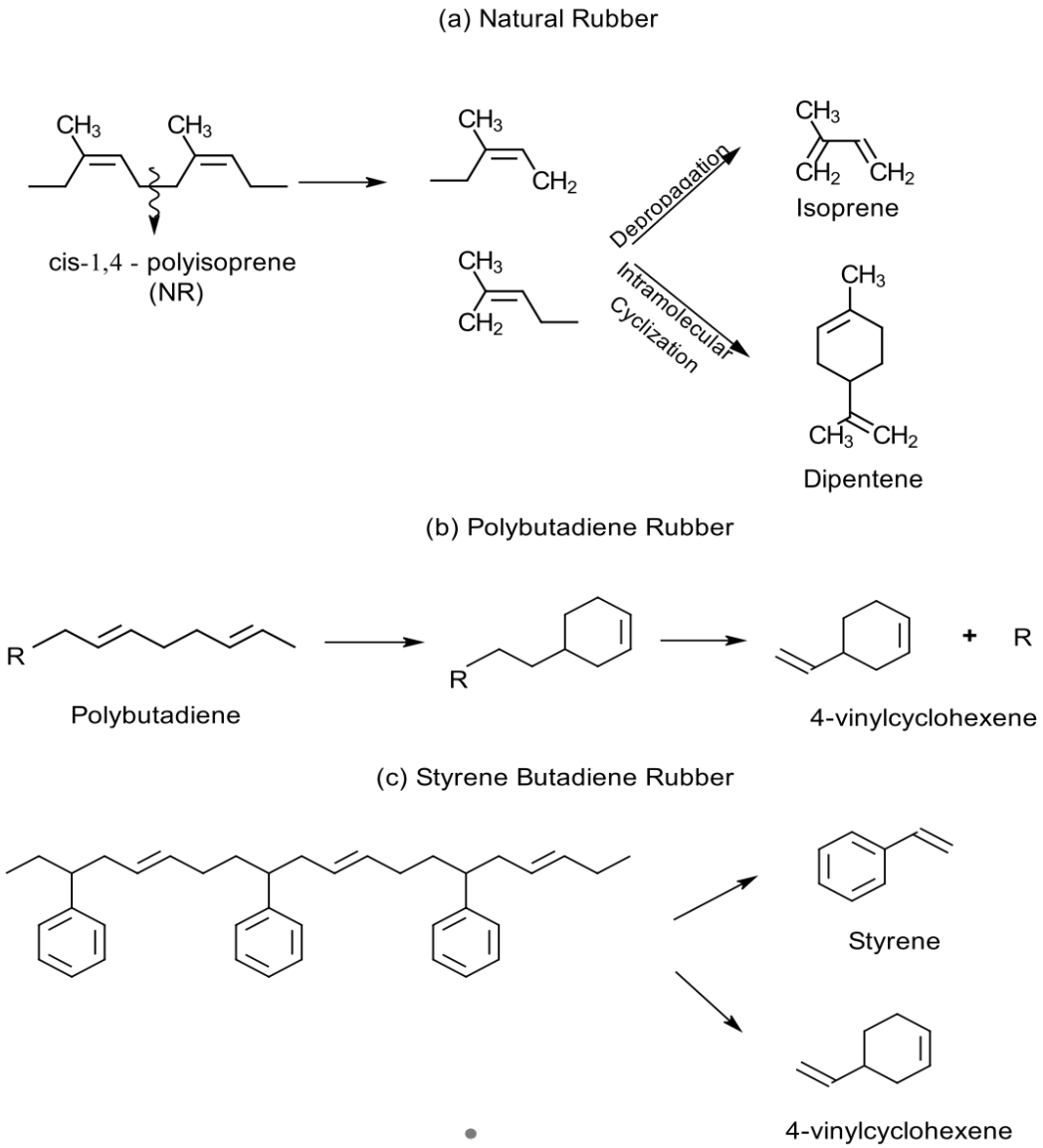

Table 6 shows the results obtained in the determination of the composition of the STR sample. The measurements were performed by duplicate. On the table, the quantification of the carbon black and additives (silica and zinc oxide using during tire vulcanization) were taken the value determined by thermogravimetric analyze

(TGA) performed by Cely [10], which correspond to the same batch of raw material used in the study. The TGA are presented in ANNEX C. In accordance with Cely [10], carbon black and additives could be associated with fixed carbon and ash content, respectively, determined by the proximate analysis (see Table 5)

Table 6. *Mass composition of STR sample as a function of its main rubber compounds.*

Compound	Concentration (wt%)*
NR	50.05 ± 2.07
SBR	1.44 ± 0.13
BR**	14.72 ± 2.20
Black carbon + additives	33.79

* Dry basis

** Determined by difference

According to the literature, the amount of NR in truck tires is higher than that in car tires, passengers or motorcycles. For passenger and truck tires the ratio of NR and synthetic rubber (SBR + BR) is 1: 2 and 2: 1, respectively [21, 23, 24]. In the same way, Ucar *et al*. [21] determined the composition of the rubbers present in the scrap tires, and they found that the truck tire is composed of approximately 50% NR, while the passenger tire is composed only of 35% NR. Therefore, considering the results presented before in this study, it is possible to conclude that the STR sample to be used in the study corresponds to a truck tires.

2.4 CONCLUSIONS

- From the elementary analysis, it can be concluded that the tire is composed mainly of carbon (86 wt%), which is according with previous research.

- From the proximate analysis, it is concluded that the STR sample has a high content of volatile matter (65.41 wt%) and fixed carbon (27.31 wt%). The volatile matter is directly related to the content of rubbers, and the carbon fixed with the content of carbon black.

- The STR sample of this study is composed of 50.05 wt% of NR, 14.72 wt% of BR and 1.44 wt% SBR, which accordint to literature, corresponds to a truck tire, in which the content of NR is higher than that in synthetic rubbers (SBR + BR).

2.5 REFERENCES OF THIS CHAPTER

[1] MARTÍNEZ, Gonzalo, *et al*. Materiales sustentables y reciclados en la construcción. Omnia Science Editors. 2015. ISBN 8494341804.

[2] LUQUE, Pablo. Investigación de accidentes de tráfico. Publicaciones Universidad de Oviedo. 2003. ISBN 8483173484.

[3] CALVO, Jesús. Mecánica del automóvil actual. Reverté. 1997. ISBN 8492134941.

[4] CASTELLS, Xavier Elías. Reciclaje de residuos industriales: Residuos sólidos urbanos y fangos de depuradora. Ediciones Díaz de Santos. 2012. ISBN 8499693660.

[5] GROOVER, Mikell. Fundamentos de manufactura moderna: materiales, procesos y sistemas. Chapter 10. Pearson Education. 1997. ISBN 9688808466.

[6] BILLMEYER, Fred. Ciencia de los polímeros. Reimpresa. 1975. ISBN 8429170480.

[7] MARK, James; ERMAN, Burak and ROLAND, Mike. The science and Technology of Rubber. Academic Press. 2013. ISBN 0123948320.

[8] ACOSTA, Rolando*, et al*. Estudio preliminar de la producción de aceite y carbón mediante pirólisis intermedia de caucho de llantas usadas. In: Revista de Investigaciones Universidad del Quindío. 2013, 24(1), p. 139–145.

[9] ACOSTA, Rolando, *et al.* Production of Oil and Char by Intermediate Pyrolysis of Scrap Tyres: Influence on Yield and Product Characteristics. In:

International Journal of Chemical Reactor Engineering [online]. 2015, 13(2), p. 189–200.

[10] CELY, Yeniffer. Modelo matmático de la pirólisis intermedia de caucho de llantas en un reactor a lecho fijo. Thesis of Master in Chemical Engineering, Bucaramanga, Colombia: Universidad Industrial de Santander. Faculty of physicochemical engineering. School of Chemical Engineering. 2015.

[11] LEE, Youn Suk, *et al.* Quantitative analysis of unknown compositions in ternary polymer blends: A model study on NR / SBR / BR system. In: Journal of Analytical and Applied Pyrolysis [online]. 2007, 78, p. 85–94.

[12] IRWIN, W.J. Analytical Pyrolysis- An overview. In: Journal of Analytical and Applied Pyrolysis. 1979, 1, p. 89–122.

[13] MA, Xiao-Ming; LU, Rong and MIYAKOSHI, Tetsuo. Application of Pyrolysis Gas Chromatography/Mass Spectrometry in Lacquer Research: A Review [online]. In: Polymers. 2014, p. 132–144.

[14] SHIELD, Stephanie; GHEBREMESKEL, Ghebrehiwet and HENDRIX, Cebron. Pyrolysis-GC/MS and TGA as tools for characterizing blends of SBR and NBR. In: Rubber Chemistry and Technology. 74, p. 803-813.

[15] TSUGE, Shin; OHTANI, Hajima and WATANABE Chuichi. In: Pyrolysis - GC/MS Data Book of Synthetic Polymers: Pyrograms, Thermograms [online]. Elsevier. 2011. ISBN 9780444538925.

[16] MARTÍNEZ, Juan Daniel*, et al.* Fuel properties of tire pyrolysis liquid and its blends with diesel fuel. In: Energy and Fuels [online]. 2013, 27(6), p. 3296–3305.

[17] MURILLO, R*., et al*. The application of thermal processes to valorise waste tyre. In: Fuel Processing Technology [online]. 2006, 87(2), p. 143–147.

[18] ISLAM Rofiqul, *et al.* Liquid fuels and chemicals from pyrolysis of motorcycle tire waste: Product yields, compositions and related properties. In: Fuel [online]. 2008, 87(13–14), p. 3112–3122.

[19] ZHANG, Xinghua, *et al.* Vacuum pyrolysis of waste tires with basic additives. In: Waste Management [online]. 2008, 28(11), p. 2301–2310.

[20] ANTONIOU, N. and ZABANIOTOU A. Features of an efficient and environmentally attractive used tyres pyrolysis with energy and material recovery. In: Renewable and Sustainable Energy Reviews [online]. 2013, 20, p. 539–558.

[21] UCAR, Suat, *et al.* Evaluation of two different scrap tires as hydrocarbon source by pyrolysis. In: Fuel [online]. 2005, 84(14–15), p. 1884–1892.

[22] GONZÁLEZ, Juan F., *et al.* Pyrolysis of automobile tyre waste. Influence of operating variables and kinetics study. In: Journal of Analytical and Applied Pyrolysis [online]. 2001, 58–59, p. 667–683.

[23] LOPEZ, Roberto A. Progress in Sustainable Development Research. Nova Publishers. 2008. ISBN 1600218474.

[24] MUKESH, C; LIMBACHIYA J. and ROBERTS J. Used/post-consumer Tyres. In: Conference Proceedings of International Conference Organised by the Concrete and Masonry Research Group and Held at Kingston. 2004, p. 3.

2.6 BIBLIOGRAPHY OF THIS CHAPTER

ACOSTA, Rolando*, et al*. Estudio preliminar de la producción de aceite y carbón mediante pirólisis intermedia de caucho de llantas usadas. In: Revista de Investigaciones Universidad del Quindío. 2013, 24(1), p. 139–145.

ACOSTA, Rolando, *et al.* Production of Oil and Char by Intermediate Pyrolysis of Scrap Tyres: Influence on Yield and Product Characteristics. In: International Journal of Chemical Reactor Engineering [online]. 2015, 13(2), p. 189–200.

ANTONIOU, N. and ZABANIOTOU A. Features of an efficient and environmentally attractive used tyres pyrolysis with energy and material recovery. In: Renewable and Sustainable Energy Reviews [online]. 2013, 20, p. 539–558.

BILLMEYER, Fred. Ciencia de los polímeros. Reimpresa. 1975. ISBN 8429170480.

CALVO, Jesús. Mecánica del automóvil actual. Reverté. 1997. ISBN 8492134941.

CASTELLS, Xavier Elías. Reciclaje de residuos industriales: Residuos sólidos urbanos y fangos de depuradora. Ediciones Díaz de Santos. 2012. ISBN 8499693660.

CELY, Yeniffer. Modelo matmático de la pirólisis intermedia de caucho de llantas en un reactor a lecho fijo. Thesis of Master in Chemical Engineering, Bucaramanga, Colombia: Universidad Industrial de Santander. Faculty of physicochemical engineering. School of Chemical Engineering. 2015.

MARTÍNEZ, Gonzalo, *et al*. Materiales sustentables y reciclados en la construcción. Omnia Science Editors. 2015. ISBN 8494341804.

GONZÁLEZ, Juan F., *et al.* Pyrolysis of automobile tyre waste. Influence of operating variables and kinetics study. In: Journal of Analytical and Applied Pyrolysis [online]. 2001, 58–59, p. 667–683.

GROOVER, Mikell. Fundamentos de manufactura moderna: materiales, procesos y sistemas. Chapter 10. Pearson Education. 1997. ISBN 9688808466.

IRWIN, W.J. Analytical Pyrolysis- An overview. In: Journal of Analytical and Applied Pyrolysis. 1979, 1, p. 89–122.

ISLAM Rofiqul, *et al.* Liquid fuels and chemicals from pyrolysis of motorcycle tire waste: Product yields, compositions and related properties. In: Fuel [online]. 2008, 87(13–14), p. 3112–3122.

LEE, Youn Suk, *et al.* Quantitative analysis of unknown compositions in ternary polymer blends: A model study on NR / SBR / BR system. In: Journal of Analytical and Applied Pyrolysis [online]. 2007, 78, p. 85–94.

LOPEZ, Roberto A. Progress in Sustainable Development Research. Nova Publishers. 2008. ISBN 1600218474.

LUQUE, Pablo. Investigación de accidentes de tráfico. Publicaciones Universidad de Oviedo. 2003. ISBN 8483173484.

MA, Xiao-Ming; LU, Rong and MIYAKOSHI, Tetsuo. Application of Pyrolysis Gas Chromatography/Mass Spectrometry in Lacquer Research: A Review [online]. In: Polymers. 2014, p. 132–144.

MARK, James; ERMAN, Burak and ROLAND, Mike. The science and Technology of Rubber. Academic Press. 2013. ISBN 0123948320.

MARTÍNEZ, Juan Daniel*, et al.* Fuel properties of tire pyrolysis liquid and its blends with diesel fuel. In: Energy and Fuels [online]. 2013, 27(6), p. 3296–3305.

MUKESH, C; LIMBACHIYA J. and ROBERTS J. Used/post-consumer Tyres. In: Conference Proceedings of International Conference Organized by the Concrete and Masonry Research Group and Held at Kingston. 2004, p. 3.

MURILLO, R*., et al*. The application of thermal processes to valorise waste tyre. In: Fuel Processing Technology [online]. 2006, 87(2), p. 143–147.

SHIELD, Stephanie; GHEBREMESKEL, Ghebrehiwet and HENDRIX, Cebron. Pyrolysis-GC/MS and TGA as tools for characterizing blends of SBR and NBR. In: Rubber Chemistry and Technology. 74, p. 803-813.

TSUGE, Shin; OHTANI, Hajima and WATANABE Chuichi. In: Pyrolysis - GC/MS Data Book of Synthetic Polymers: Pyrograms, Thermograms [online]. Elsevier. 2011. ISBN 9780444538925.

UCAR, Suat, *et al.* Evaluation of two different scrap tires as hydrocarbon source by pyrolysis. In: Fuel [online]. 2005, 84(14–15), p. 1884–1892.

ZHANG, Xinghua, *et al.* Vacuum pyrolysis of waste tires with basic additives. In: Waste Management [online]. 2008, 28(11), p. 2301–2310.

Chapter 3

Experimental study of the pyrolytic oil and aromatic compounds production from pyrolysis of scrap tires rubber

Part of this chapter is published in International Journal of Chemical Reactor Engineering:
R. Acosta, C. Tavera, P. Gauthier-Maradei, D. Nabarlatz. (2015). Production of oil and char by intermediate pyrolysis of scrap tires: influence on yield and product characteristics. Int. J. Chem. React. Eng; 13:189–200.

3.1 INTRODUCTION

The pyrolysis process consists of tire rubber breaking down using a heating system at adequate temperatures ranging between 300 and 700°C. This process is carried out in the absence of oxygen using an inert gas (commonly Nitrogen or Helium) as carrier gas to pull out of reactor, the condensates and gases produced during

reaction [1–3]. Three kinds of products could be obtained: gases, liquids (pyrolytic oil) and solids (char), the mass distribution between these fractions depend on the operating conditions of the pyrolysis, the reactor type and the tire composition [4–7].

Since the 1990s, different operating variables have been studied that can influence mainly the pyrolytic oil production during the pyrolysis of STR such as pressure, temperature, heating rate, particle size, gas volumetric flow and reaction time. In all these studies, it has been established that temperature is the most influential variable, however, the experimental results have shown that it exists a huge variability in term of pyrolytic oil yield even at the optimal temperature depending of the reactor type used [3, 8]. On the other hand, other variables as pressure, heating rate and particle size do not have an important effect on the pyrolytic oil production [9–13]. It is important to highlight that gas volumetric flow has not been studied in depth, in spite of its direct influence on the gas residence time produced in a fixed bed reactor.

The pyrolytic oil obtained from the pyrolysis of STR is a mixture of aromatic hydrocarbons, olefin and paraffin, sulfur and Nitrogen compounds [4, 14]. The high heating value (HHV) has been measured and was in the range 40-44MJ/kg, approximately [14–16], being higher than mineral carbon and similar than commercial diesel. This property provides its great potential as a fuel. However, to make this possible, it is necessary to decrease the number of undesirable compounds as paraffin, sulfur and nitrogen species. The paraffin can crystallize and cause clogging in the fuel filter, sulfur compounds can oxidize and cause corrosion in the engine, and the nitrogen compounds can oxidize and generate toxic emissions [17–19].

Among the compounds present in the pyrolytic oil, those with the higher additional value are the aromatics as BTX (*i.e.* benzene, toluene, xylenes) and unsaturated

cyclic hydrocarbons as dipentene or limonene. The firsts due to their uses at industrial level in applications as plastics chemical synthesis, synthetic rubbers, paints, pigments, explosives, pesticides, detergents and perfumes and as solvents; and the last ones due to their uses in the manufacture of flavors, fragrances, cleaning agents, degreasing agents and they are used as solvent and in a variety of household applications [20, 21].

Currently, the BTX production is exclusively done to catalytic processes from coal or petroleum. These processes are mainly dominated by the petroleum refineries which produce more than 95 million metric tons per year to supply the petrochemical market in the world [22–24].

The STR pyrolysis has been studied since 1990s [5, 25–28], however, these studies were focused mainly on pyrolytic oil production or activated carbon and very few of them aimed to the production of BTX. The results of these previous researches on STR pyrolysis show a maximum concentration of benzene, toluene and xylenes in pyrolytic oil of 1, 1 and 4 wt% , respectively [5, 29–31]. This chapter is focused on the determination the optimal operating conditions to obtain the maximum yield of pyrolysis oil and aromatic compounds in the oil. The experimental study was divided into two sections: the first one, a design of experiments (DOE) 4x3 was performed with two variables: temperature and Nitrogen volumetric flow, using as carrier gas**.** This part of the study aims to establish the better conditions of temperature and nitrogen volumetric flow to maximize the pyrolytic oil production and aromatic compounds concentration. Once these best conditions were found, the second section of this study was performed applying different residence times.

3.2 STATE OF THE ART

For the STR pyrolysis, different reactors types have been studied in laboratory and pilot scales: autoclaves, rotary kilns, auger, fixed beds, fluidized beds, rotary cone reactors, vortex reactors, plasma reactors, among others [3, 7, 8, 32]. These research works have allowed defining the technical advantages and disadvantages of each one and their influence on the product distribution.

Diéz *et al.* [33] carried out a comparison of the yields of three products (gas, liquid and solid) using two scales: laboratory and a pilot plant. They found that at the large scales, the pyrolytic oil is not obtained, due mainly to the length of the reactor favoring the higher residence time of the volatiles and allowing the secondary reactions as cracking and polymerization. As a result of these conditions, the production of gas and char increases whereas the one of pyrolytic oil decreases. These observations were also confirmed by Roy *et al*. [34], who compared three reactors of different size and capacity: laboratory batch reactor, pilot plant (30 kg/h) and a demonstration plant (3 ton/h). They found that a higher pyrolytic oil yield was obtained when the laboratory reactor was used suggesting that a small reactor and a low residence time is required for pyrolytic oil production.

Aylon E. *et al*. [32] carried out an experimental study of STR pyrolysis in two types of reactor: fixed bed and fluidized bed reactor, in order to evaluate their influences on conversion and product yields. Pyrolysis in the two types of reactors was carried out at 600 °C under Nitrogen atmosphere (2 NL/min[2]). The authors found that the liquid yield is higher in the fixed bed reactor (approx. 55 wt%) whereas in the fluidized bed reactor, the gas yield is higher (approx. 17 wt%). On the other hand, a

[2] Nml / min corresponds to the volumetric flow at normal conditions of temperature and pressure (298K and relative 1atm pressure).

bibliographic review presented by Hita *et al.* [8] mentions the advantages and disadvantages of each type of reactors. The authors concluded that the most convenient reactors to maximize the liquid yield are the fixed bed reactor and the conical spouted bed reactor. Therefore, considering the research studies presented before, the experimental study in this work was performed in a fixed bed reactor at laboratory scale.

Due to the STR pyrolysis is an endothermic process [35–38], the temperature has an important effect on the distribution and product composition, so it is one of the most studied parameters. Islam *et a*l. [39] reported a research study in a fixed-bed tubular reactor using 750 g of STR, a temperature range between 350 and 575 °C and a reaction time equal to 50 min. The results showed that the liquid yield increases as the temperature increases until obtaining a maximum value at 475 ºC (51 wt%) even if at this temperature, the STR sample is not completely decomposed (pyrolysis is not complete).

Different results were obtained by Fernandez *et al.* [40] who studied three temperatures (400, 550 and 900 °C) in a fixed bed reactor. The yields of products found by these authors are shown in Figure 10. The authors characterized and studied the composition of the three products (gas, pyrolytic oil and solid). It was observed that at 400 °C, the product of higher yield was the solid residue (60-70 wt%). Besides, they found that the solid yield decreases as the temperature increases, whereas the gas and pyrolytic oil yields increase. The maximum pyrolytic oil yield was presented at 550 °C (approx. 55 wt%).

Another study was reported by González *et al.* [41] in 2001. The authors evaluated the effect of temperature between 350 and 700 ºC finding that the maximum pyrolytic oil yield is obtained at 575 ºC (54.5 wt%). Besides, they observed that once the maximum pyrolytic oil yield is reached, this decreases constantly with the

temperature obtaining an pyrolytic oil yield of 36.7 wt% at 700 °C. The temperature reported in this research study is very close to reported by Fernandez *et al.* [40], and higher than this reported by Islam *et al*. [39]; approximately 100 °C above.

Figure 10. *Yields of pyrolysis products at different temperatures by Fernandez et al. [40].*

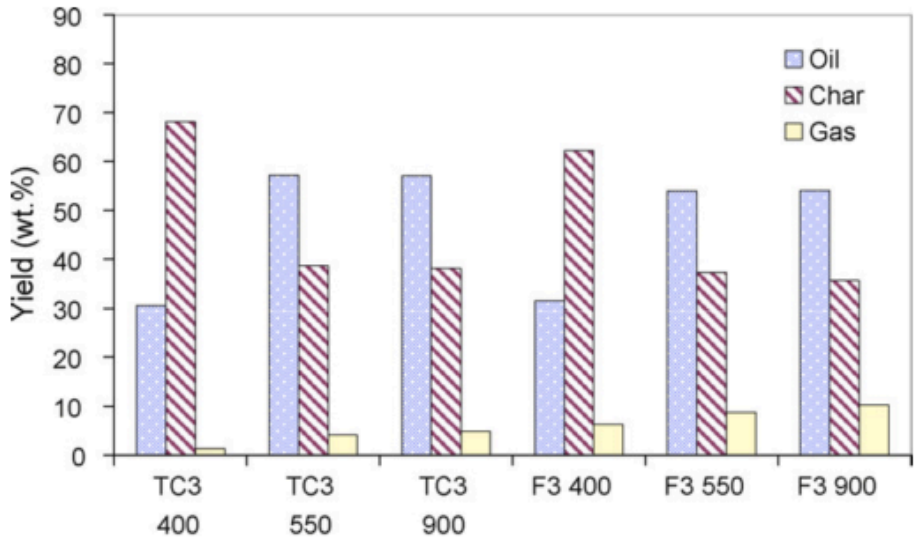

Ucar *et al*. [42] compared the yields of the three pyrolysis products using two kinds of tires: passenger car tire and truck tire, at temperature range between 550 and 800 ºC. They observed that, depending of the tires types, the yields of different products vary at a same temperature meaning that the type of tire and its composition affect the yields of the products. However, they found for both types of tires, a maximum yield of pyrolytic oil at 650 ºC what is slightly different with the optimal temperature found for other authors and mentioned above.

Conesa *et al.* [43] performed a study in a fixed bed reactor using different inert atmospheres (*i.e.* N_2, nitrogen-synthetic air mixture 10 wt% O_2) at three

temperatures: 450, 750 and 1000 ºC. The results are shown in Figure 11, and it can be observed that the higher pyrolytic oil yield (approx. 38%) was obtained in a Nitrogen atmosphere at 450 °C. In addition, it was found that the pyrolytic oil yield decreases when the temperature increases until 1000 ºC; in which the pyrolytic oil production was not observed. The authors mentioned that at this temperature the cracking reactions of the volatile compounds are very important producing no condensable gases and solid carbon polycondensates.

In accordance with the research mentioned before, the experimental study in this work was performed in a temperature range between 400 and 650 C°; operating conditions allowing the maximum pyrolytic oil yield. Besides, it is also observed that the characteristics of STR used, as well as the characteristics of the reactor, can influence the yields of the fractions.

Figure 11. *Yield of the different fractions as a function of temperature by Conesa et al. [43].*

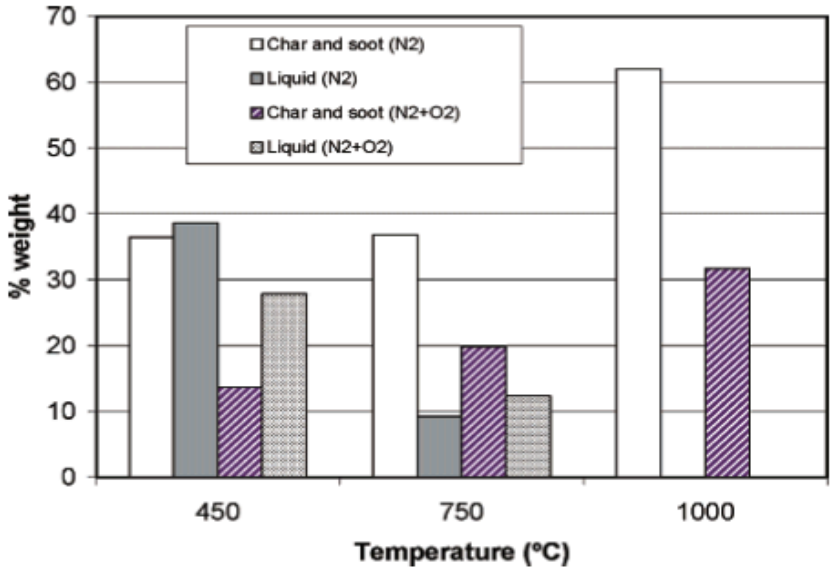

Another variable studied in the STR pyrolysis is the heating rate; its influence is attributed by some authors, to the combined effects of heat transfer and degradation kinetics. According to Senneca *et al.* [44], higher heating rates give rise to more volatile compounds. However, as previously discussed, this could encourage secondary reactions and lead to higher gas yields with rapid heating rates. González *et al.* [41] studied the effect of the heating rate on the gaseous fraction. They used a fixed bed reactor and heating rates between 5 and 20 °C/min. It was observed that as the heating rate increased from 5 to 20 °C/min, the gaseous fraction increased; increasing also the concentration of H_2, CO, CH_4, CO_2, C_2H_4 and C_2H_6.

On the contrary, Murillo *et al*. [45] who also performed a study in a fixed bed reactor and studied heating rate of 25, 100 and 300 ºC/min, did not find a significant influence of the heating rate on the pyrolytic oil yield and its composition obtaining a similar concentration around 70 wt% in the three heating ramps. In this study, the heating rate is not a variable that can be controlled in the system because this is fixed by the electrical oven at 30°C/min. Therefore, considering the research studies presented before it is decided not to carry out an in-depth review of this variable.

Another operating variable that has been studied by several authors is the pressure. Roy *et al.* [46] performed an experimental work on pyrolysis in a batch reactor under vacuum pressure. The total pressure was varied between 0.8 and 28.0 kPa, at a temperature of 500 °C. It was observed that the gas, liquid and solid yields changed slightly with the pressure; at lower pressures, less gas and more liquid were obtained. In the liquid fraction, it was found that the amount of DL-Limonene increases as the pressure decreases. A similar result was reported by Zhang *et al*. [15] who used a fixed-bed reactor under vacuum conditions (3.5-4.0kPa). As a conclusion, they found that the concentration of DL-Limonene in the liquid fraction increases as the pressure decreases confirming that it was reported by Roy *et al*. [46]. The authors also observed that a certain amount of carbonaceous material was

formed in the solid fraction attributing this behavior to the occurrence of secondary reactions of re-polymerization. Thus, even at vacuum pressure, secondary reactions may occur giving rise to the formation of carbonaceous deposits and a higher gas yield.

Lopez *et al.* [47] propose that the vacuum effect improves the diffusion of the volatiles formed due to the generated pressure gradient. Thus, rapid diffusion of the volatiles into the particle reduces the residence time and, consequently, the occurrence of secondary reactions decreases. These authors finally concluded that lower operating pressures may reduce the occurrence of secondary reactions as cracking, re-polymerization and re-condensation, but not completely avoid them. This is directly related to the fact that under vacuum conditions the volatiles are drawn faster from the hot zone of the reactor, which implies a low residence time. Another general advantage of carrying out the pyrolysis process at a low pressure is that the operating temperature can be reduced, thereby decreasing the energy demand of the process.

To reduce and control the occurrence of secondary reactions, the inclusion of an inert gas to drag the volatiles in the pyrolysis process has been studied. This adds a new variable: the gas flow, which has a direct influence on the surface velocity and residence time of the volatiles. Larger flows eliminate the vapors in the reaction zone faster and thus minimize secondary reactions [41].

Islam *et al.* [39] studied the influence of the residence time of volatiles of 5, 10 and 20 s, which corresponds to flows of 8, 4 and 2 NL/min, in a fixed bed reactor. They found that liquid and solid waste yields decline (5 and 2% respectively) whereas gas yields increase as the residence time of the volatiles increases from 5 to 20 s.
Likewise, Martínez *et al.* [3] mentioned that several authors have concluded that high residence times may favor some secondary reactions, such as cracking and

polymerization, which alter the distribution and composition of char, pyrolytic oil and gas. Also, Nkosi *et al.* [1] suggested that this is due to the decomposition of vapor phase pyrolytic oil into secondary permanent gases. The primary vapors that are produced in the STR pyrolysis are then degraded into secondary gases (*i.e.* CH_4 + C_2H_4 + C_3H_6 + ...). For example, heavy hydrocarbons and light hydrocarbons are obtained from the pyrolytic oil in the vapor phase, which leads to less pyrolytic oil and more non-condensable gas product.

Although many authors [1, 3, 14, 41, 48] claimed that the composition of the pyrolytic oil can be affected by the residence time of the volatiles in the reactor but no complete study have been carried out to evaluate this parameter. For this reason, it has been decided to carry out in this work an experimental study of the residence time of the volatile on the yield of both: pyrolytic oil and aromatic compounds.

De Marco Rodríguez *et al.* [49] performed a STR pyrolysis study in a fixed bed reactor at 500 °C and reported the chemical characterization of the pyrolytic oil obtained. The results indicate that this pyrolytic oil is composed of 62.4 wt% aromatic compounds (single ring and polyaromatic), 31.6 wt% aliphatic compounds, 4.2 wt% nitrogenous compounds and 1.8 wt% sulfur compounds. Another similar research study, which is in agreement with these results, was performed by Lie *et al.* [16]. They also reported that the pyrolysis oil is composed mostly of aromatic and aliphatic compound.

A complete characterization performed by Kyari *et al.* [4] on the liquid stream, showed mainly the presence of single ring aromatic compounds and polyaromatics, as well as alkylates, and also alkanes and alkenes. The authors identified compounds such as benzene, toluene, limonene, styrene, ethylbenzene, biphenyl, indene and naphthalene, and among the alkanes were identified pentadecane, heptadecane and octadecane. Besides, they reported the presence of sulfur, nitrogenous and oxygenated compounds, among which 2,7 dimethyl

benzothiophene, 2,4,6 trimethylbenzene amine and dimethylamine were identified. The authors highlighted that within the compounds with significant concentrations are limonene (2-5 wt%), and some polyaromatics such as naphthalene, phenanthrene and pyrene. These results are in agreement with the characterization of pyrolytic oil obtained by Bajus *et al*. [50]. The authors measured higher concentrations of benzene (about 4.7 wt%) and limonene (about 9 wt%). Several authors reported the limonene like majority product.

3.3 DESCRIPTION OF THE PILOT UNIT

For the development of this experimental study, the pilot unit was designed by Calderón M. and Torres A. [51]. The system was designed in such a way as to guarantee maximum pyrolytic oil collection. The pilot pyrolysis unit used in the development of the experimental tests is detailed in Figure 12. The system consists of four zones: the gas inlet (1), a heating zone in which the pyrolysis reaction is performed (2), a condensation zone (3) and a gas collection zone (4).

The carrier gas (Nitrogen UAP grade 5.0, Cryogas) (1) is fed to the reactor (2) at constant volumetric flow controlled by a Cole-Parmer flow meter (range 0-1240 Nml/min). The reactor of heating zone (2) is a vertical tubular reactor made of 316L stainless steel, the STR is placed inside it. The tubular reactor has two grids, one inlet and one outlet to prevent the entrainment of solid material. This was heated by a tubular furnace equipped with an electric resistance with a maximum power of 2400W to 220V which allows a heating rate of approximately 30 °C/min. The tubular furnace has a thermocouple that measures the reactor wall temperature.

Two reactor sizes were used during experimental tests; one first with a length of 50 cm and a diameter of 4 cm, and a second with length of 30,5 cm and a diameter of

1.8. This choice was supported by the need to obtain a larger range of gas residence time in the reactor zone.

Figure 12. *The pilot pyrolysis unit used for the experimental test.*

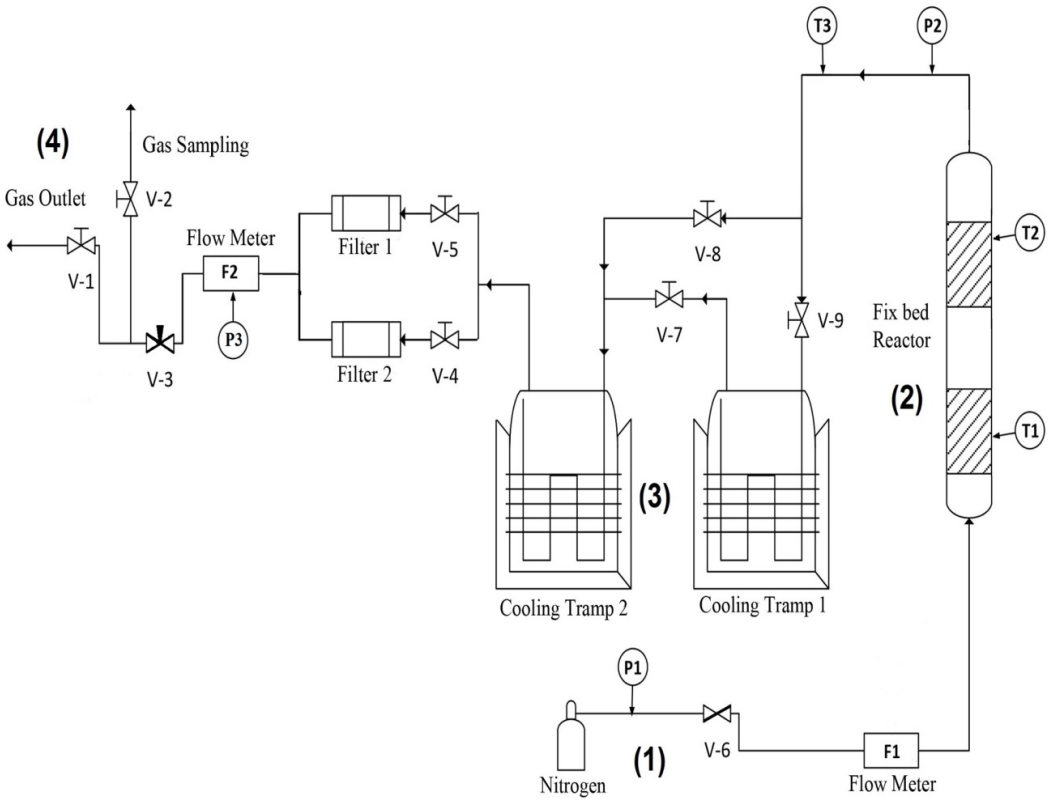

The gases produced during the pyrolysis process exit by the top of the reactor toward a cooling zone (3), this zone has a heating cord which avoids the condensation in the tubing and their return to the reactor. Subsequently, they are directed to the gas cooling system, composed of two cooling traps made of stainless steel, hermetically sealed. The first trap is cooled with dry ice and the second with ice. In the cooling traps, the pyrolytic oil is recovered from the condensation of the volatiles generated. The non-condensable gases pass through a mass flowmeter before being

evacuated into the atmosphere (4). The gas flowmeter (Cole-Parmer, range 0-1280 Nml/min) at the outlet was regulated to assure a relative pressure of 100 kPa in the system.

The reactor was charged before pyrolysis tests as shown in Figure 13, using glass wool in the lower zone, and STR in the highest zone. This configuration was chosen to minimize the residence time of the volatiles compounds produced during the reaction in the hot zone and ensure their condensation only in the cooling trap.

Figure 13. *Loading scheme to fill the reactor*

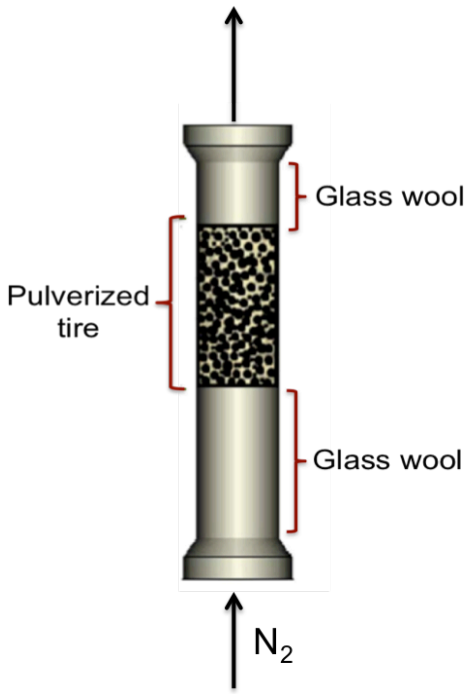

Inside the reactor, a fixed bed containing crushed tire rubber (particle diameter <1 mm) was used. The mass of STR was calculated according with the bulk density of the material, depending on particle size used in the experiments, to obtain the length of the fixed bed. A tire fixed bed of 20 cm was used for the first reactor (length =50 cm) while for the second reactor (length =30.5 cm), 10cm of tire bed was used.

3.4 METHODOLOGY

3.4.1 Preliminary tests. To carry out the experimental test, the protocols for loading, leakage test, start, stop and discharge of the reactor were studied. These protocols can be observed in detail in ANNEX D.

Prior to initiating the development of the experimental test, a series of preliminary tests were performed in duplicate (*i.e*. perform twice the same reaction) under the same conditions of temperature, nitrogen flow and bed height in order to check the reproducibility of the results, ensure a mass balance greater than 90% and avoid errors due to ignorance of the pilot unit's operating protocols.

3.4.2 Study of the temperature and nitrogen flow influence on pyrolytic oil yield and aromatic concentration. The set of tests in this section considered a range of operating conditions according to the experimental studies performed by other authors aforementioned in state of the art (Section 3.2) indicated as good conditions to produce liquid through a pyrolysis process.

To maximize the pyrolytic oil production, two multifactorial design of experiment (DoE) (4x3) was performed using as response variables: the pyrolytic oil yield and the aromatics concentration in the pyrolytic oil. In this DoE, we considered as independent variables; temperature (4 levels) and nitrogen volumetric flow (3 levels). The range of operating conditions used in this work is presented in Table 7. A total of twelve tests for each experimental plan were performed with their respective duplicates. The tests were carried out at a constant pressure of 1 barg and a reaction time of 2h [11]. During each test, the volumetric flow, pressure and temperature of reaction mixing and synthesis gases were recorded each 2 min.

Table 7. *Range of operating conditions used in two multifactorial designs of emperiments 4x3 performed in this study.*

Variable 1: Temperature (ºC)	Variable 2: Nitrogen volumetric flow (Nml/min)	Response variable 1	Response variable 2
400	116	Pyrolytic oil yield (wt %)	Aromatic compounds yield (wt%)
466	155		
533	223		
600			

For each test, the initial and final weight of the solid sample, wool and traps plates of cooling zone of reactor (zone 3 in Figure 12) were recorded in order to calculated the products yields. The pyrolytic oil, gas and char yield were determined as Equation 1. The mass of the gas and its yield were determined by closing the mass balance due to instability in the measurement of the outflow which did not allow the quantification of the amount of gas produced during the reaction.

$$\textbf{Yield of product } [\textbf{wt}\%] = \frac{\text{Weight of product}}{\text{Weight initial of tire}} * 100 \qquad \text{Equation 1}$$

An ANOVA was performed to determine the significance and influence of the variables in the pyrolytic oil yield and aromatic concentration in pyrolytic oil using Statgraphics Centurion Software. ANOVA is a statistical technique that is intended to analyze variability in data by statistical models used to distinguish between an observed variance in a particular variable and its component parts. The Two-Way ANOVA determines the differences and possible interactions when variables are presented from the perspective of two or more categories [52].

On the other hand, according to the review of the state of the art, it was found that the major concentration of STR in the pyrolytic oil is limonene, therefore it is decided to quantify this compound as well. The yields of of both aromatics compounds and limonene were calculated, based on the concentration of them in the pyrolytic oil, and also the pyrolytic oil yield obtained at each operating condition, according with Equation 2. [53].

$$\textbf{Yield of compound}\ [\textbf{wt}\%] = \text{Compound Concentration} * \left(\frac{\textbf{Oil Yield}}{\textbf{100}}\right) \quad \text{Equation 2}$$

3.4.3 Study of the gas residence time influence on the pyrolytic oil and aromatic compounds production. Taking into account that the gas residence time is influenced by the nitrogen volumetric flow according with literature (see Section 3.2), additional experiments were performed using a second reactor described in Section 3.3 (i.e. the 30.5 cm length), to reach smaller gas residence times (less than 10s). The gas residence time was calculated following Equation 3.

$$\mathbf{t_R} = \left(1\text{-}P_p\right)\left(\frac{TA_{reactor}{}^{*}h}{Q_{N_2}}\right)\frac{\left(\frac{P_{reactor}}{T_{std}}\right)}{\left(\frac{T_{reactor}}{P_{std}}\right)}{}^{*}60 \qquad \text{Equation 3}$$

Where:

t_R = Residence Time [s]

P_p = Porosity of fixed bed

$TA_{reactor}$ = Total reactor area [cm^2]

h = Bed height[cm]

Q_{N_2} = Nitrogen volumetric Flow[Nml/min]

$P_{reactor}$ = Reactor pressure = 2 [bar]

P_{std} = Standard pressure = 1 [bar]

$T_{reactor}$ = Reactor Temperature

T_{std} = Standard Temperature = 298 [K].

The operating conditions used in these additional experimental tests are specified in Table 8.

Table 8. *The operating conditions of the experimental plan.*

Temperature constant (ºC)	**Variable 1: Residence time (s)**	**Response variable 1**	**Response variable 2**
466	1.80 2.80 3.70 12.8 19.2 25.7	Pyrolytic oil Yield (wt%)	Aromatic compounds yield (wt %)
600	1.58 2.38 3.17 10.8 16.3 21.8		

To study the influence of gas residence time on the pyrolytic oil yield, three points (gas residence time between 1 and 4s) were performed with their respective duplicates and only at two temperatures chosen in accordance with operating conditions observed in the aforementioned tests to maximize pyrolytic oil yield and aromatic concentration in the pyrolytic oil. These tests were carried out at the same operating conditions of pressure and reaction time that the study explained in section 3.4.2 (gas residence times between 10 and 25s) and presented also in Table 8.

3.4.4 Experimental study of the reaction time influence on the aromatic compounds production. The reaction time was evaluated at favorable conditions of temperature and nitrogen flow, determined in previous section (*i.e.* 466 °C and 155 Nml/min). Two reaction times were evaluated: 1 and 2 hours. At each reaction time, yields of oil, gas and char were determined, as was done in section 3.4.2 (Equation 1).

3.4.5 Characterization of pyrolytic oil. The pyrolytic oil was characterized by determination of HHV, real density and acidity. The HHV determination was done in a calorimetric pump Parr 6200 following the ASTM D-4809 and ASTM D-5865 standards [54, 55]. The real density was determined by gravimetry using a pycnometer of 1 mL. The acidity was measured by an acid-base titration with sodium hydroxide according with the standard UNE-EN ISO 660 [56].

The chemical characterization of the pyrolytic oil was firstly performed by Gas Chromatography– Mass Spectrometry (GC/MS). The compounds that could not be identified by GC-MS were identified by GC-FID using standards. In both cases, an HP-5 column (30 m x 0.320 mm with 0.25 microns diameter) was used. The method was programmed as follow: the oven was first programmed from an initial temperature of 50°C (during 2 min) and increases up to 290°C at 5°C/min, this temperature is then maintained at 290°C for 2 min. The injector and detector temperatures were 250 and 280°C, respectively. The injection split ratio was fixed at 1:100.

For the aromatic compounds quantification, an external standard technique was used employing n-heptane. The relative response factors (RRFs) of the aromatic compounds (benzene, toluene, ethylbenzene, xylenes) were taken from Katritzky *et al*. [57]. In the case of limonene, the RRF was calculated according with the method

and expression reported by this author obtaining an RRF of 0.98. The RRF are shown in ANNEX E.

Chromatography samples were prepared diluting the oil obtained in each test in n-pentane to obtain a 20 wt% solution.

3.5 RESULTS AND DISCUSSION

3.5.1 Experimental study of the temperature and nitrogen volumetric flow influence on pyrolytic oil yield. The results of the product yields (pyrolytic oil, gas and char) of the STR pyrolysis obtained in the experimental tests detailed in Table 7 are shown in Figure 14. It is observed that the highest pyrolytic oil yield (42.60 wt%) were obtained at 600 °C using a flow equal to 233 Nml/min. In addition, it can be observed that for the pyrolytic oil, char and gas yield, there not significant differences when the nitrogen volumetric flow is varied. On the contrary, differences can be observed for whole yields when the temperature is increased. Specifically, it was found that the pyrolytic oil and gas yields increase as the temperature increases, while the char yield decreases.

According with Figure 14, it is evident that the increase in temperature allows an increase in the pyrolytic oil yield, due to the decomposition of the natural rubber, butadiene rubber and styrene-butadiene rubber in lower molecular weight compounds, which is favored when the temperature increases [31].

Regarding Figure 14 (a), It can be noticed that the lower pyrolytic oil yield is obtained in most of the tests performed at lowest nitrogen volumetric flow. According to Islam *et al.* [14] a lower nitrogen volumetric flow (inert gas) means a longer residence time of the volatiles in the hot zone, favoring the secondary cracking reactions, in which

the condensable volatiles are converted to secondary gases, and causing a decrease of the pyrolytic oil and an increase in the gas fraction.

Figure 14. *Yields at different conditions of temperatures and nitrogen volumetric flow: (a) Pyrolytic oil yield, (b) Char yield and (c) Gas yield.*

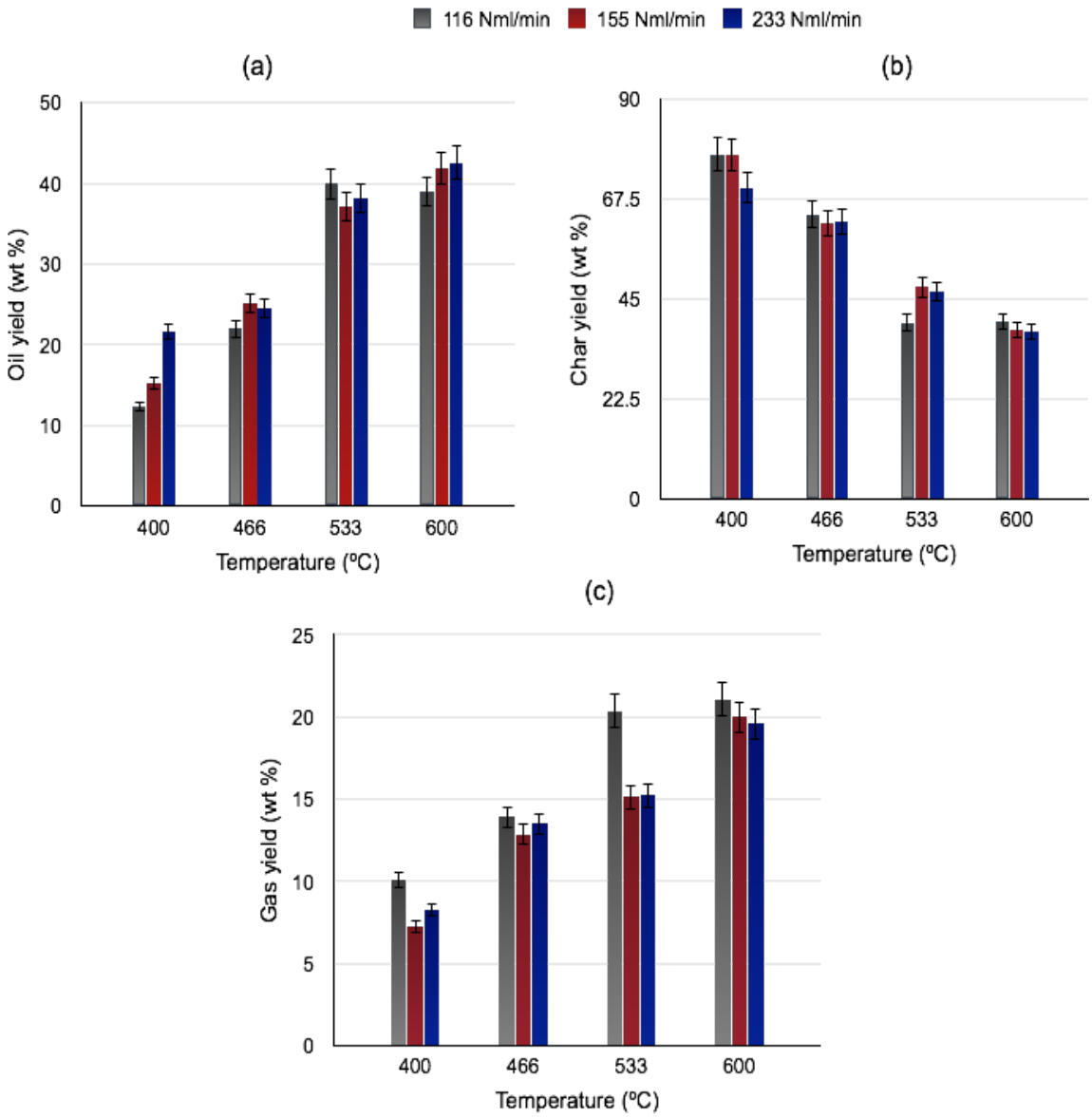

This trend is also found in this study (see Figure 14 (c)), in which at a maximum temperature (600 ° C) and minimum nitrogen volumetric flow (116 Nml/min), the lowest pyrolytic oil yields and higher gas yields are obtained whereas, at a maximum nitrogen volumetric flow (minimum gas residence time), the maximum pyrolytic oil yield and minimum gas yield were obtained. This allows to suppose that not only the gas residence time has an influence on the increase of the secondary reactions, but also the high temperature can participate, being more notorious the effect of secondary reactions at higher temperatures.

According to Martínez *et al*. [3], there are three kinds of behavior of the pyrolysis products as a function of temperature. Following this classification, the products obtained in this study have a behavior of *Type I*, in which the liquid and gas increase with increasing temperature, whereas the char decreases until reaching a constant value. In agreement with these authors, this type of behavior represents a normal pyrolysis in which there are not secondary reactions. This may explain why there are no marked differences in the yields obtained at different nitrogen volumetric flows.

The pyrolytic oil yield obtained by some authors in a fix bed reactor and at similar operational conditions in pyrolysis of scrap tires are shown in Table 9. The pyrolytic oil yield obtained in this study (*i.e.* 42.60 wt%) is one of the best amoung the one presented in the literature (except for Islam *et al*. [14]). Comparing with the study done by Berrueco *et al*. [58], where the pyrolytic oil yield obtained is very close to the one of this study, it was obtained at a lower temperature (100 °C less), which means an energy saving.

It should be made clear that the maximum pyrolytic oil yield presented in Table 9, which was obtained by different authors at similar temperatures, could be influenced

by other variables, non-analyzed in this study, which could promote (or not) the secondary reactions as it is aforementioned in the state of art (Section 3.2). This is the case of the tire type, its composition, its particle size and the reactor dimensions.

Table 9. *Pyrolytic oil yield obtained in different studies reported in literature.*

Authors	**Operating Conditions: temperature range (ºC)**	**Maximum oil yield (wt%)**
Aydin and Ilkilic (2012) [59]	400 - 700	40.26 % at 500 ºC
Banar *et al.* (2012) [60]	350 – 600	38.8 % at 400 ºC
Islam *et al.* (2008) [14]	375- 475	49.13% at 475 ºC
Berrueco *et al.* (2005) [58]	400 - 700	42.8 % at 700 ºC
Díez *et al.* (2005) [33]	Constant temperature at 500-600	38%
De Marco Rodriguez *et al.* (2001) [49]	300-700	38.50 at 700 ºC
This Study	400-600	42.60 at 600

To determine the significance and influence of each variable in the pyrolytic oil yield an ANOVA was performed using Statgraphics Centurion software. For the analysis, the dependent variables and their possible interactions were considered. Table 10 presents the summary of ANOVA with a confidence level to 95% using a multiple linear regression models to fit the experimental data. According with the analysis, the model has a good fitted with a R-squared statistic explaining near to 91% of the variation in the responses. Besides, the standard error of the estimate shows that the standard deviation of the residuals is approx. 3.5; the value can be used to construct prediction limits for new observations.

Table 10. *ANOVA; Sum of squares type III for pyrolytic oil yield with all factors and their interactions.*

Source	Sum of squares	DF	Middle Square	F-Value	p-Value
A:Temperature	90.0938	1	90.0938	7.04	0.0162
B: Nitrogen Flow	13.2439	1	13.2439	1.03	0.3226
A*B	24.2664	1	24.2664	1.90	0.1855
A*A	33.5121	1	33.5121	2.62	0.1231
B*B	0.828008	1	0.828008	0.06	0.8021
Residue	230.455	18	12.8031		
Total (corrected)	2706.61	23			

R-square = 91.4855 %

R-square (ajusted by DF) = 89.1203 %

Standard error of estimate = 3.57814

Absolute mean error = 2.28756

Durbin-Watson statistic = 2.71009 (P=0.8823)

Furthermore, it is observed that the most influential variable is the temperature (p-value of 0.0162) whereas the change on the nitrogen volumetric flow and the interactions between this operating variable and the temperature are not significant on pyrolytic oil yield. This result is in agreement with various previous investigations, which concluded that the temperature is the most important parameter having an influence on the yield and composition of pyrolytic oil due to the endothermic reactions involved in STR pyrolysis process [10, 16, 31, 43, 53, 61]. On the other hand, the general trend observed for pyrolysis oil yield at different volumetric gas

flow rates agreed with the results observed in other studies using waste biomass as feed- stock [62].

The R-Squared statistic indicates the adjustment of the model that explains the variability of Oil yield. The adjusted R-Squared statistic compares models with a different number of independent variables. The standard error of the estimate shows the standard deviation of the residuals, and this value can be used to construct prediction limits for new observations. The absolute mean error (MAE) is the average value of the residuals. The Durbin-Watson (DW) statistic tests the residuals to determine if there is any significant correlation.

To improve the fitting of experimental data and predict pyrolytic oil yield as a function of temperature and nitrogen volumetric flow, a mathematical model adjustment was necessary eliminating the effects that are less significant on the response. All treatment of data is presented in ANNEX F. The model thus obtained to described the oil yield as a function of temperature (T) and nitrogen volumetric flow (Q) is presented in Equation 4.

$$\textbf{Oil yield}\ (\textbf{WT}\%) = 0.3909*\mathrm{T} + 0.0000495*\mathrm{T}*\mathrm{Q} - 0.000266*\mathrm{T}^2 - 101.71 \quad \text{Equation 4}$$

Using the experimental results and the proposed model (Equation 4), the contour plot were elaborated (Figure 15). These show the combined influence of the two variables (temperature and nitrogen volumetric flow) on the pyrolytic oil yield. According with Figure 15, the highest pyrolytic oil yields are obtained at temperatures between 530 – 600 ºC.

Figure 15. *Contour plot of the effect of temperature and nitrogen volumetric flow on the pyrolytic oil yield.*

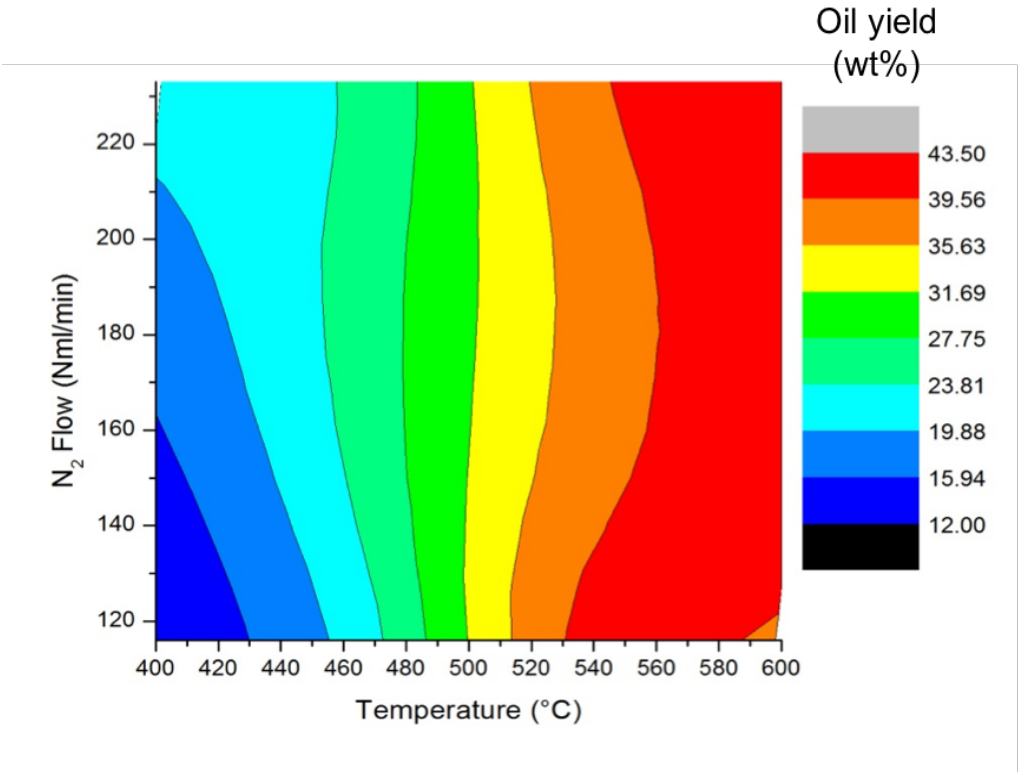

Furthermore, it is observed that the pyrolytic oil yield changes considerably with the temperature, being this variable the most influential as aforementioned. On the contrary, the nitrogen volumetric flow has a higher influence at lower temperature than at higher temperature, in which the effect on pyrolytic oil yield is slight. In other works, at lower and higher temperatures, the pyrolytic oil yield increases when the volumetric gas flow rate increases too (indicating that it decreases with gas residence time). This phenomenon can be explained by the presence of cracking reactions that are favored at higher gas residence times [33, 58, 63, 64]. In this study, the volumetric gas flow rate range studied corresponds to a gas residence time range varying between 10 and 28 s according to Equation 3.

3.5.2 Characterization of pyrolytic oil. The pyrolysis oil obtained has a brown color, which becomes darker at high temperatures. The pyrolysis oil comprises two phases, the lighter phase corresponding to about 90 wt% of the pyrolysis oil, which presents a darker color than the heavier phase.

The pyrolytic oils densities obtained in each test in the experimental plan are shown in Figure 16. The measures of density show that the changes in temperature and nitrogen volumetric flow do not cause significant variations in the density of the pyrolytic oil. The average pyrolytic oil density was 0.85 ± 0.01 g/ml, the value that is in agreement with those reported by some authors [59]. On the other hand, the density of this pyrolytic oil is close to the commercial diesel fuel range (about 0.845 g/ml) [59, 60, 65], and a slightly higher than gasoline (about 0.7 g/ml) [60, 66].

The pyrolytic oil acidity as a function of temperature and nitrogen volumetric flow is presented in Figure 17. The pyrolytic oil presents an acidity between 0.39 and 1.57 mg KOH/g. Only the values of acidity for the pyrolytic oil obtained at 466°C are closed to the permissible limit for fuel oils (0.3 mg KOH/g) [67, 68]. According to Benallal *et al.* [69] in the pyrolysis reaction at low temperatures, the olefins and diolefinic hydrocarbons are the predominant compounds in the pyrolysis oil, which may be the cause of its high acidity. The reactions such as aromatic cyclization and dehydrogenation of olefins and diolefins in the reactor can also decrease the acidity [69].

Figure 16. *The density of pyrolytic oil measured at each operating conditions of the experimental plan.*

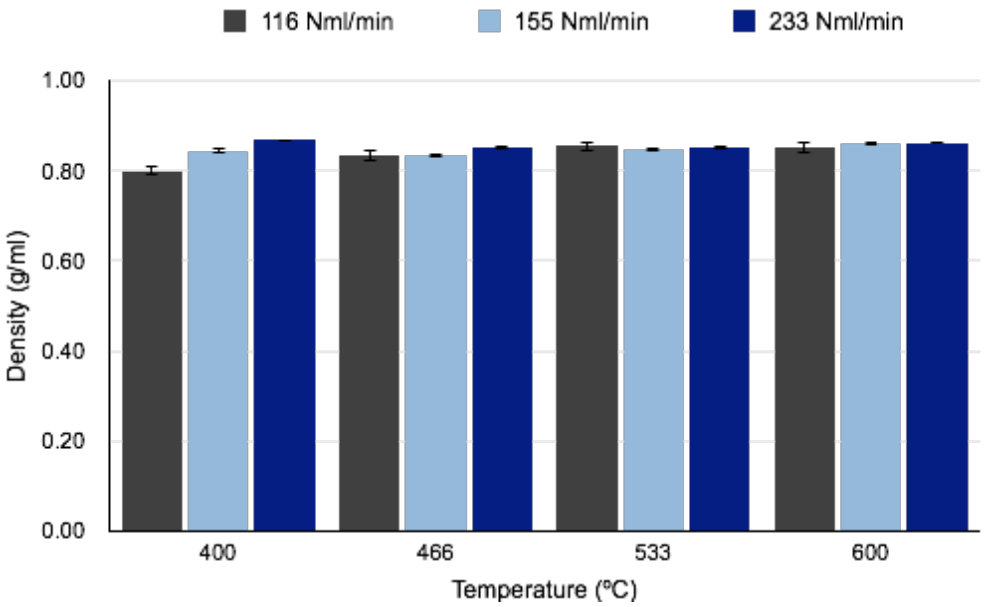

Figure 17. *Acidity of pyrolytic oil as function of temperature and volumetric gas flow.*

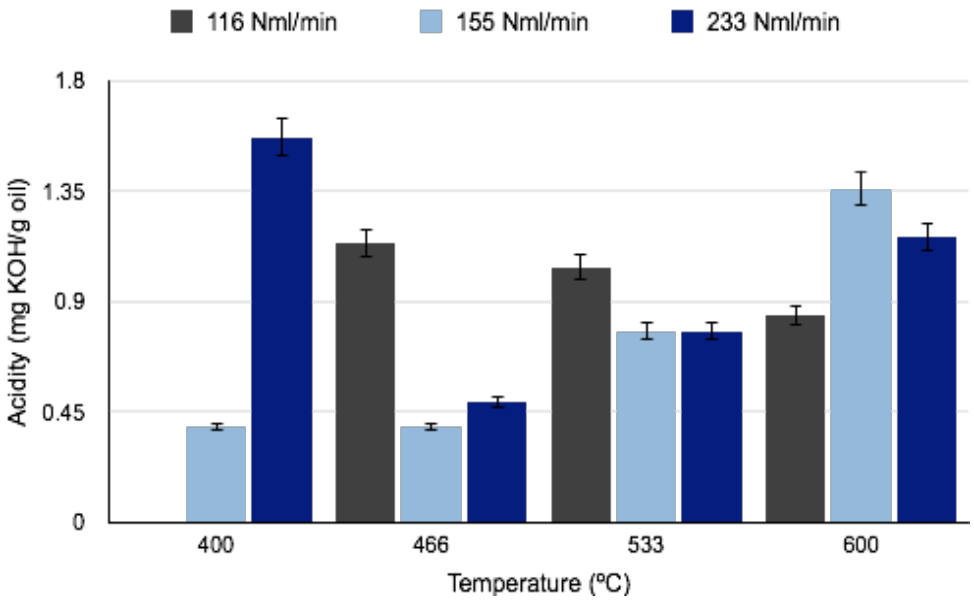

The results for the HHV are presented in Figure 18. It can be seen that the variation in operating conditions does not produce a significant difference in the values found for HHV. The average value of HHV obtained was 42.12 ± 1.20 MJ/kg, value agrees with other authors [14–16, 59]. This value is slightly lower than the one of the commercial diesel (43-46 MJ/kg) and close to the one of the commercial gasoline (42-44 MJ/kg). However, it is higher than that observed for coal (29-36.8 MJ/kg) and for oil obtained from different biomasses (25-32 MJ/kg) [9, 59, 62]. This HHV represents the energy potential for the use of this type of pyrolytic oil as a substitute for fuels. In the present work, the energy yield (MJ/kg) of pyrolysis oil yield (wt%/100), was 22.72 (MJ/kg of the tire) [70], representing the amount of energy that can be obtained per scrap tire mass unit used in the process.

Figure 18. *HHV obtained at different operating conditions.*

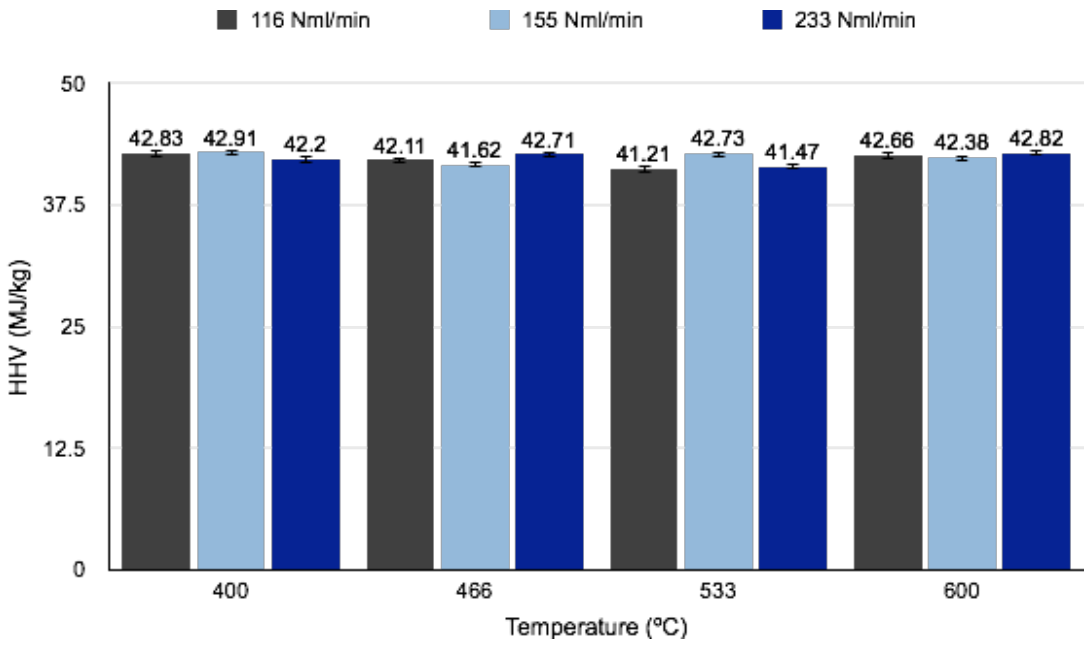

The concentration of single ring aromatic compounds (BTX, alkyl benzenes and cymene) and limonene in pyrolytic oil is shown in Figure 19 for each operating condition studied. The compound found in the highest proportion in all samples analyzed in this study was limonene (10 – 50 wt%) whereas the aromatic compounds are in few proportions (11 – 25 wt%). The maximum aromatic concentration is observed at 466 °C using a nitrogen flow equal to 155 Nml/min, indicating that the production of aromatics does not follow the same trend observed for pyrolysis oil, and, therefore, it is not possible to obtain the highest pyrolysis oil yield having the highest aromatics concentration. Likewise, the volumetric gas flow rate seems to have a significant influence on the aromatic yield; in an opposite way to that observed for pyrolysis oil yield, in which at higher nitrogen volumetric flow (low residence time) the production of aromatic compounds and limonene are not favored.

Figure 19. *Concentration of aromatics compounds and limonene on pyrolytic oil at each operating condition.*

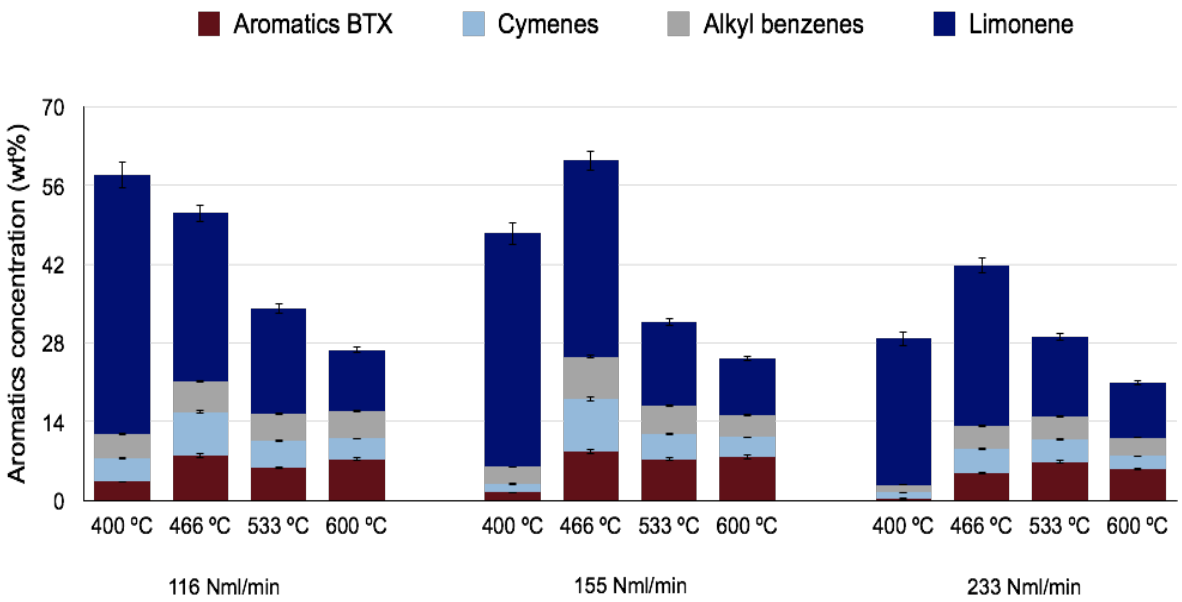

It can also be observed that at all flows, the total concentration of aromatics has a maximum at medium temperatures. Some authors indicate that the influence of temperature on the aromatic yield can be explained by the occurrence of other reaction types like as dealkylation, dearomatization or cracking reactions, which are more important at higher temperatures and higher residence times thus favoring the production of lighter condensable compounds [29, 69, 71].

The high concentration of limonene is due to the presence of natural rubber (cis-1,4-polyisoprene) in the STR samples. Some authors suggest its transformation by two competitive reactions: 1) by the cracking of the allylic radicals with respect to the double bond present in the polyisoprene chain and their intramolecular cyclization to obtain D-L Limonene, and 2) by the depropagation of allylic radicals to isoprene monomer initially formed by a dimer (Figure 20) [25, 53, 72, 73], and after it is aromatized. This may explain the high limonene concentration at low temperature, however, once the temperature increases, its concentration decreases.

In the 1990s, one of the first authors who study aromatic compounds from STR pyrolysis was Pakdel *et al.* [25, 73] and Cunliffe *et al* [5]. These authors attribute the formation of aromatics to the decomposition of limonene to aromatic products, mainly benzene, xylene, toluene, methylbenzene, styrene and methylstyrene, which is more important at temperatures closed 500 °C, and at temperatures above 560 °C. The simple ring aromatic compounds obtained with the decomposition of Limonene decrease and the formation of polyaromatic compounds increases.

Further, Cypres *et al.* [74] suggest another way of producing aromatics during STR pyrolysis through the Diels Alder reaction from aliphatic compounds to produce principally benzene, toluene and xylenes. These authors agree with the results found

in this study, in which toluene and xylenes are the aromatic compounds found in the highest concentrations followed by trimethylbenzene, propylbenzene and styrene.

Figure 20. *Polyisoprene (cis-1,4-polyisoprene) transformation to isoprene and limonene by two competitive reactions.*

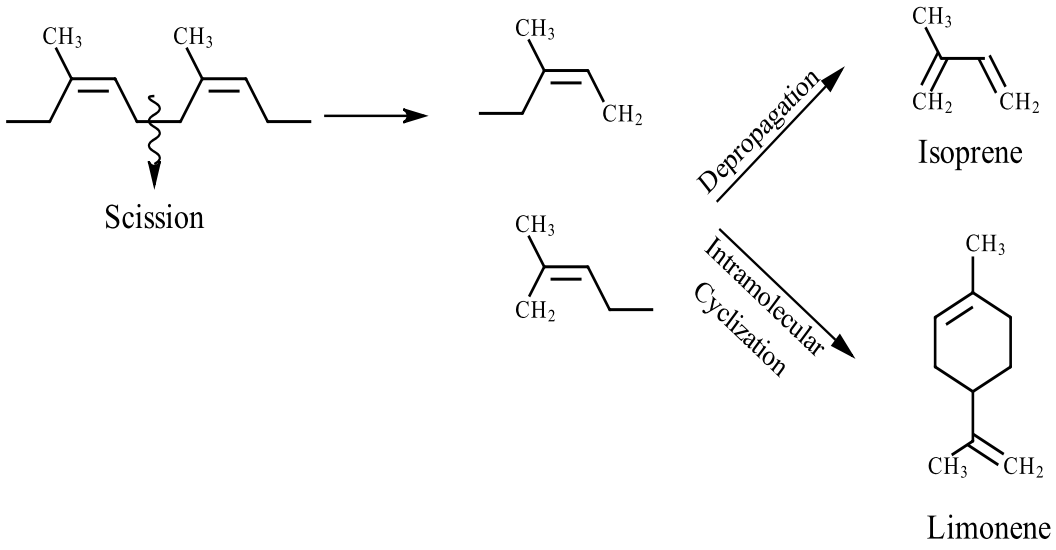

3.5.3 Experimental study of the temperature and nitrogen volumetric flow influence on aromatic yield. The results obtained for the aromatic and limonene yields are shown in Figure 21. Comparing Figure 14 (a) and Figure 21, even if the oil yield increases as the temperature increases, the aromatic yield (including BTX compounds) seems to rise a maximum at 466 °C and remains constant at higher temperatures. An exception is observed for a nitrogen volumetric flow of 233 Nml/min, in which the maximum is reached at 533 °C followed by a decrease at higher temperatures.

The experimental data show that the highest yield of both, total aromatics and limonene, was obtained at 466 °C and 155 Nml/min. This behavior can be explained according to the aforementioned studies performed by Pakdel *et al.* [25, 73] and Cunliffe *et al* [5] about the formation of aromatic compounds from limonene and the presence of other reactions as cracking or polymerization favored at higher temperature and nitrogen volumetric flow conditions.

Figure 21. *Aromatics and limonene yields at each operating condition.*

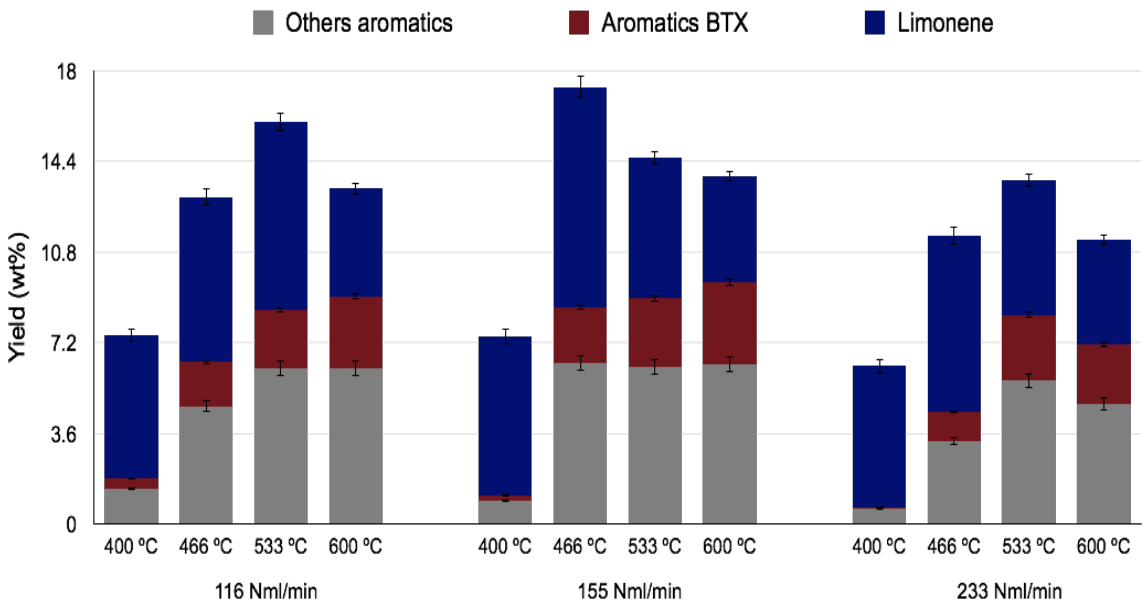

A multiple regression was performed to establish the effect of each variable and their possible interactions on the aromatics yield. Table 11 shows the results of fitting a multiple linear regression models to describe the aromatics yield. All data treatments are presented in ANNEX F.

Table 11. *Multiple linear regression for aromatics yield with all factors and their interactions.*

Parameter	Estimate	Standard Error	T Statistical	P-Value
Constant	-66,2919	9,94624	-6,66502	0,0000
A: Temperature	0,244898	0,0359946	6,80375	0,0000
B: Nitrogen Flow	0,0676975	0,045022	1,50365	0,1500
A*A	-0,000221624	0,000035194	-6,29709	0,0000
A*B	0,0000040245	0,000043144	0,0932809	0,9267
B*B	-0,000222578	0,000111081	-2,00374	0,0604

Residue= 10.57
Total (corrected)= 117.51
R-Square = 91.005
R-Square (ajusted by DF) = 88.597
Standar Error of estimate = 0.766
Absolute mean error = 0.553
Durbin-Watson statistic = 2.773 (P=0.9110)

The final model selected to describe the relation between aromatic yield and the variables selected (temperature (T) and nitrogen volumetric flow(Q)) with a statistic significance is shown in Equation 5.

$$\textbf{Aromatic yield } [\textbf{wt}\%] = 0.2456*\mathrm{T}\text{-}0.000221*\mathrm{T}^2\text{-}0.0000273\ \mathrm{Q}^2 \qquad \text{Equation 5}$$

R-Square = 89.4461
R-Square (Ajusted by DF) = 87.863
Standard error of estimate = 0.7875

Absolute mean error = 0.5167

Taking into account the analysis of experimental data presented before, the adjusted model evidences the influence of operating variables as temperature and nitrogen volumetric flow on aromatic yield, differing that the ones found for the pyrolytic oil yield (section 3.5.1).

In order to graphically evaluate the most favorable operating conditions for the maximization of aromatics, the response surface and contour plots (Figure 22) were done using the experimental results and the proposed model (Equation 5).

Figure 22. *Effect of temperature and nitrogen volumetric flow on aromatics yield: (a) Response surface - (b) Contour plot.*

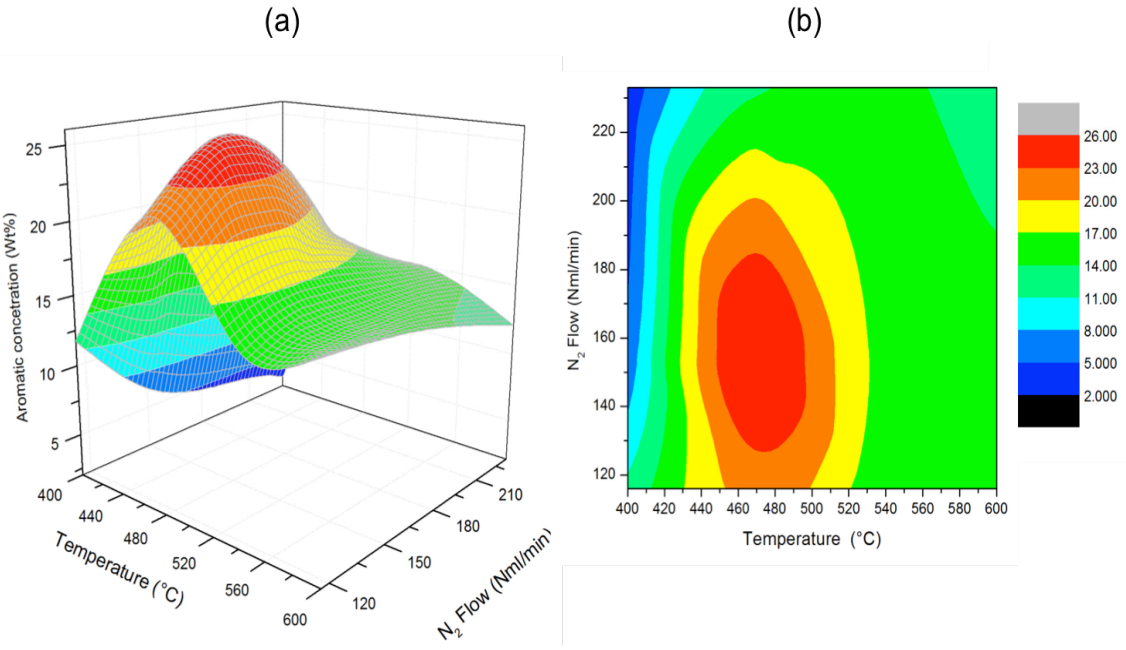

The figures show the combined influence of the two variables (temperature and nitrogen volumetric flow) on the aromatic yield. According with the figures, the most favorable conditions for the maximum yield are: temperatures between 450 - 490 °C and nitrogen volumetric flows between 130 and 180 Nml/min, being the highest point at 466 °C and 155 Nml/min. Note that the temperature is the most influence variable on aromatic oil in the operating range that was analyzed. On the other hand, the nitrogen volumetric flow has a most important effect a lower temperature than a higher temperature, in which it has not an influence on aromatic oil.

3.5.4 Experimental study of the gas residence time influence on pyrolytic oil yield and aromatic concentration. This study was performed considering the operating conditions that promote the oil and aromatic yield and considering the results observed by some authors on the important effect of gas residence time on those yields [2,3].

Figure 23 shows the pyrolytic oil and gas yields as a function of temperature and residence time. Figure 23 (a) shows the pyrolytic oil yields obtained at all residence times (between 1.58 and 3.70 s) at 466 ºC (temperature for maximum aromatic yield, 3.5.3), and Figure 23 (b) the results for all gas residence times (between 10.80 and 25.70 s) at 600°C (temperature for maximum pyrolytic oil yield, section 3.5.1) . Two behaviors are clearly observed function of the gas residence times. In the case of long gas residence times, it can be observed that the temperature is the most influent variable in the pyrolytic oil yield, as aforementioned in section 3.5.1, in which the considerable differences in the pyrolytic oil yield is observed between the two temperatures.

On the other hand at low residence times, the similar yields are obtained for both temperatures (466 and 600 °C); this is of considerable interest concerning the energy consumption because at low residence times it is possible to obtain good

pyrolytic oil yields at a lower temperature, having an energy saving of 134 °C. According to Aylón *et al.* [75], the great decrease in the residence time of gases when the nitrogen flow increases, causes limitation of cracking of the volatiles, which leads to a higher amounts of liquid in the process. This link to the interaction effect between temperature and nitrogen flow can be explain the higher oil yield at lower temperature and lower residence time by reducing of cracking reactions.

Figure 23. *Pyrolytic oil and gas yield at all residence times and at: (a) 466 °C and (b) 600 °C.*

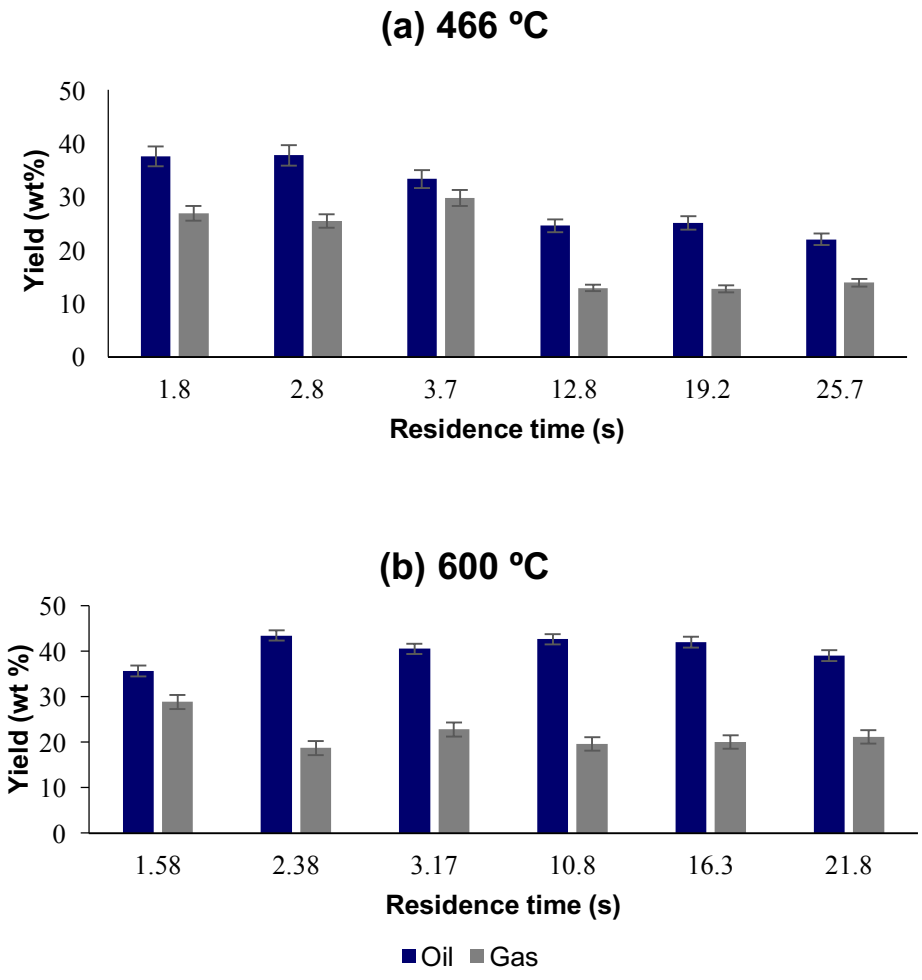

In Figure 23 (a), at 466 °C, lower pyrolytic oil and gas yields are obtained at high gas residence times. On the other hand, the higher liquid fraction obtained at low gas residence times is due to the fact that the vapors leave the hot zone quickly, avoiding the secondary reactions as thermal cracking and polymerization; in agreement with the observations of Martínez *et al.*[48].

Further, at 600 °C, it is observed that the pyrolytic oil yields range from 35.6 to 43.4 wt%, approx. The difference between the different conditions is not significant, compared to the range of yields calculated at 466 °C. It means that when the temperature increases, the gas residence time becomes a less important variable. According to Leung *et al.* [35], high temperatures are the key factor for the cracking of heavy hydrocarbon gases, so the effect of increasing the gas residence time is not so strong at these conditions. According to Aylón *et al.* [75], the reduction of the gas residence time when the nitrogen volumetric flow increases, causes the cracking of the gas fraction to be limited, which leads to the obtaining of higher amounts of pyrolytic oil.

Referring to the pyrolytic oil composition, the aromatics and limonene concentration were quantified, which are the most interesting in this study, and the dependence of the formation of these compounds was analyzed. The concentration of aromatics and limonene at 466 ºC are presented in Figure 24. Higher concentrations of aromatics are obtained at lower gas residence times. Specifically, the most favorable conditions to maximize aromatics production are a temperature of 466 °C and a gas residence time of 2.80 min.

Hita *et al***.** [8] mentioned that the increase in gas residence time results in the increase in the polyaromatic compounds yield (*e.g.* naphthalene, biphenyle). It is possible because of the longer time of the volatiles in the reactor cause that the

single ring aromatic compounds tend to bind to form a long chain. Obviously, this reaction leads to a decrease of the simple ring aromatic compounds, as could be found in this study. Therefore, a long residence time does not favor the maximization of single ring aromatic compounds.

Figure 24. *Aromatics and limonene concentration at 466 ºC function of the gas residence times.*

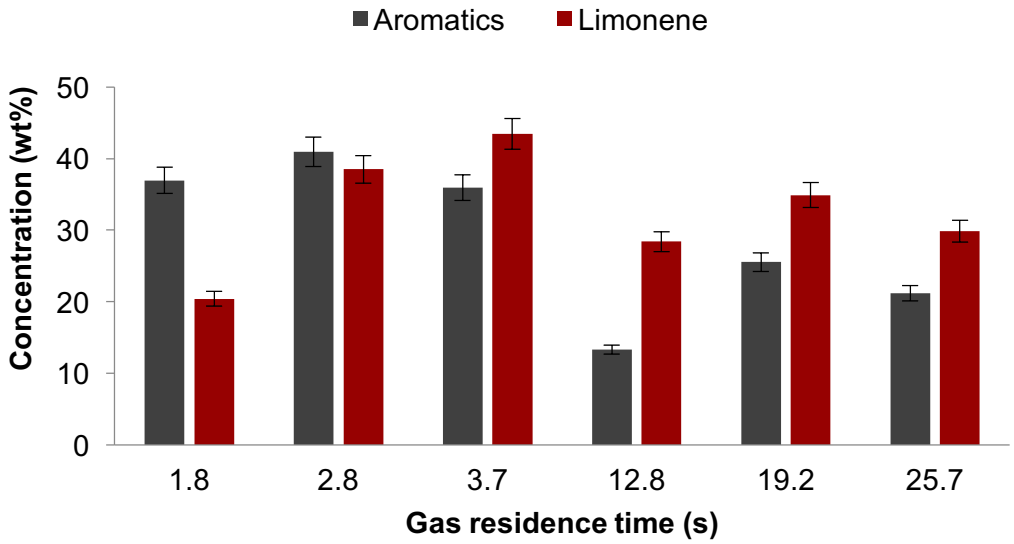

Table 12 presents the comparison of the aromatics and limonene concentration found in this study with those reported by other authors. Although it is not possible to compare the gas residence times studied by the other authors, it can be concluded that in this study a higher aromatic concentration was obtained than the other studies and their production was effectively maximized by the study of temperature and gas residence time.

Additionally, the concentration of limonene is lower than the values reported by others authors. Ucar *et al.* [42] mentioned that the differences found in the concentrations of limonene in different studies are directly related to the tire composition, specifically with the amount of natural rubber (NR), which decomposes directly to limonene. Therefore, a higher concentration of NR can lead to a higher concentration of limonene. On the other hand, Danon *et al.* [72] confirmed that although the tire composition is the main factor that can vary the concentration of limonene, also the pressure and the residence time are important, obtaining greater limonene concentrations when vacuum conditions are used.

Table 12. *Comparison of aromatics and Limonene concentration found by other authors.*

Author	Operating conditions	Aromatics concentration (wt%)	D-L Limonene concentration (wt%)
Olazar *et al.* [76]	500 ºC	20,17 %	26.80 %
Arabiourrutia *et al.* [30]	425 ºC	7,77 %	23.93 %
Qu *et al.* [71]	430 ºC y 30 ml/min de N_2	27,43 %	8.08 %
This study	466 °C y 155 Nml/min de N_2 (2,80 min)	40,92%	19,26%

Considering that the aromatics compounds with higher industrial value are the BTX due to their applications, an individual evaluation was made for each of them:

benzene, toluene and xylenes, to determine the most favorable temperature and gas residence time. Figure 25 shows the BTX concentration at 466 ºC for each residence time. In Figure 25 (a) it is observed that the concentration of toluene increases with the decrease of gas residence time; it can be explained remaining that compounds such as toluene and ethylbenzene are easily formed from partially saturated aromatics such as limonene. According to Cely [77], compounds such as ethylbenzene and toluene are formed in a final step of depolymerization of NR and SBR to cyclic compounds, which are favored at low residence times.

Figure 25. *Concentrations of BTX aromatic compounds at 466 ° C and different residence times: (a) toluene, (b) benzene and (c) xylenes.*

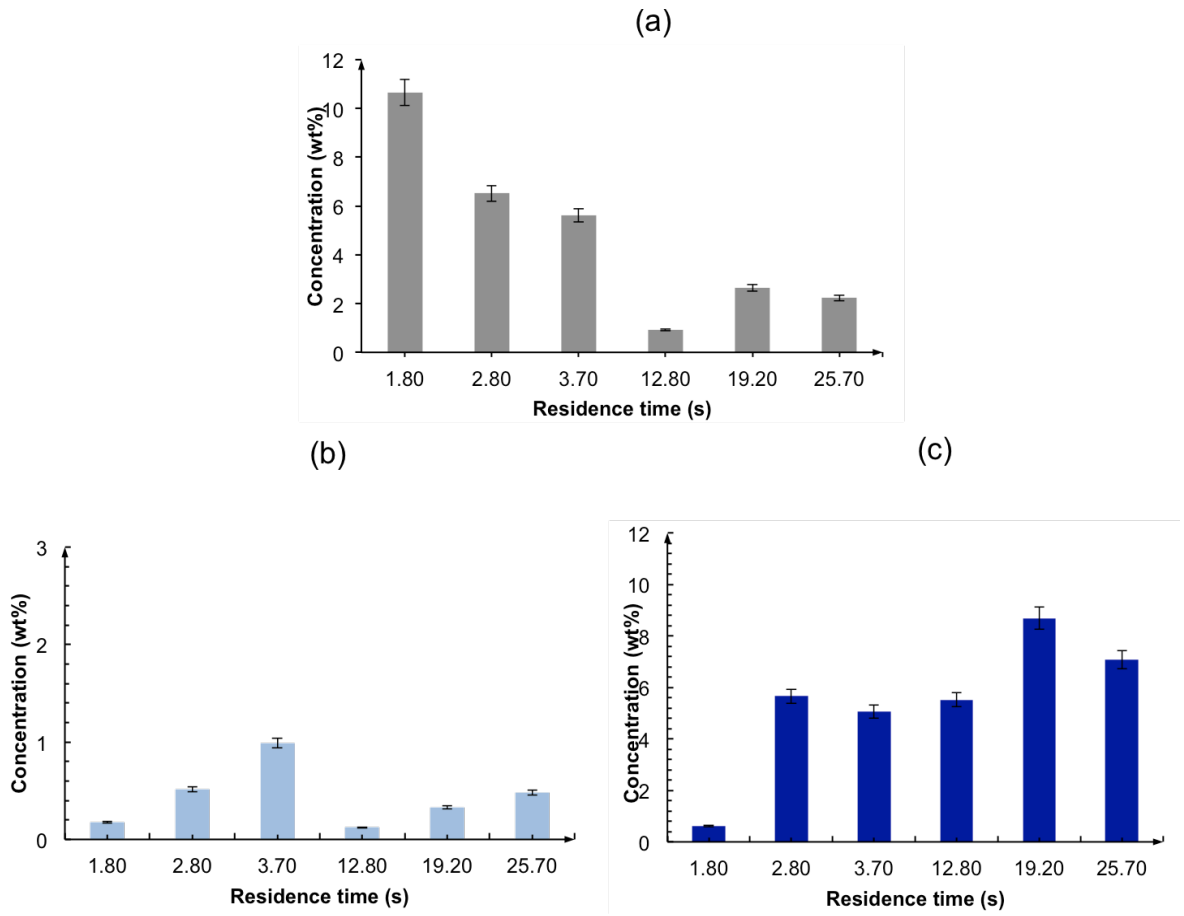

Unlike toluene, xylene concentrations are higher at high residence times. The xylenes are formed in a depolymerization step as well, but longer residence times are required for the formation of them, due to the complexity in the distribution of the ortho-xylene, para-xylene and meta-xylene bonds. The benzene concentrations did not show a trend as a function of gas residence time compared to the other BTX compounds because their concentrations were very low. Benzene is the aromatic in lower concentration, because its formation must undergo thermal degradation of other compounds previously formed with strong molecular structures that prevent the separation of their molecules.

The comparison of BTX obtained by different authors is shown in Table 13.The BTX concentrations were higher in the present study compared to literature data.

Table 13. *Comparison the BTX concentration obtained in this study with those reported by other authors.*

Author	Operating conditions	BTX concentration (wt%)
Bajus *et al.* [50]	450 ºC and 50 ml/min	7,5%
	570 ºC and 50 ml/min	8%
Li *et al.* [16]	600 ºC	11%
Olazar *et al*. [76]	500 ºC	2,74%
This study	466 °C and 155 Nml/min (2,8 min)	17,43%

As observed in this section, temperature and gas residence time play a fundamental role in maximizing the yield of pyrolytic oil, as well as the concentration of aromatics.

Working on these two parameters simultaneously, it is possible to obtain a significant pyrolytic oil yield at lower temperatures (466 °C) and also a considerable concentration of aromatic compounds. It allows to reach the goal saving energy.

3.5.5. Experimental study of the reaction time influence on aromatic concentration. The results of the oil, char and gas yields at the different reaction times are shown in Figure 26. It can be observed that the yields of the products do not vary significantly with the reaction time, finding a slight increase in oil at one hour, compared to two hours.

Figure 26. *Yields of products of STR pyrolysis at different reaction times, and at constant temperature and nitrogen flow (466 ºC and 155 Nml/min).*

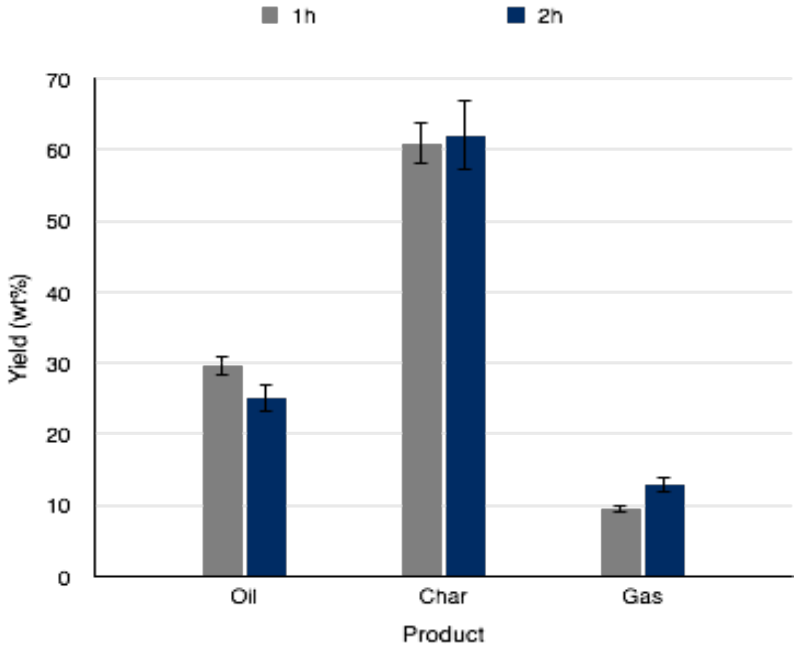

According to Cely [77], the decomposition of the rubber of the tire at 466 ºC, once the temperature is reached, is complete at the 1200 seconds (20 min), which would

indicate that, the products of the pyrolysis do not vary with reaction times longer than this time of decomposition. The fact of obtaining fewer oil at two hours can be linked to a possible volatilization of those compounds with lower volatilization temperature, such as benzene, due to the long time the oil must remain in the cooling trap. On the other hand, although it was found that the yields of products did not vary significantly with the reaction time, the composition of the oil could vary, so it was decided to check the concentration of aromatics at the two reaction times.

Figure 27 shows the concentration of aromatics at one and two hours of reaction, at constant temperature and nitrogen flux (466 ºC and 155 NmL / min). It is observed that the concentration of aromatics is similar at both reactions time, with a slightly greater at one hour of reaction.

Figure 27. *Aromatics concentration at different reaction times, and constant temperature and nitrogen flow (466 ºC and 155 Nml/min).*

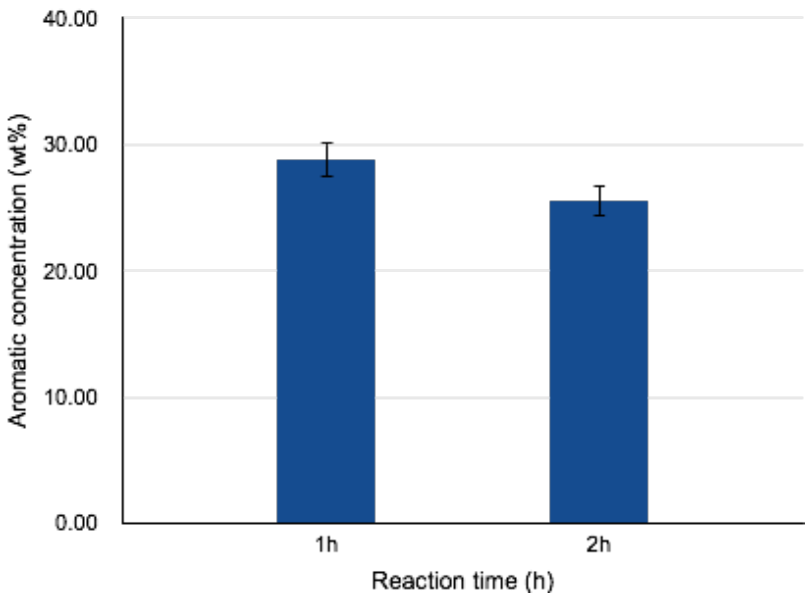

The reduction of aromatics may be linked to a possible volatilization or entrainment of these compounds during the long reaction period of two hours, as was mentioned before. According to the results obtained in these tests, it was decided that a reaction time of one hour is more convenient and favorable, since a similar yield of pyrolysis products is obtained, as well as aromatics concentration in the oil, which can mean an energy saving to obtain equal yields with the reduction of an hour of reaction time.

3.6 CONCLUSIONS

- Based on the results obtained in the statistical analysis, it is observed that the pyrolytic oil yield depends on the operating conditions evaluated (temperature and nitrogen flow), being the temperature the most influential variable.

- From the physicochemical characterization of the pyrolytic oil, it can be stated that both: nitrogen volumetric flow and the temperature do not affect significantly the density or HHV. However, the acidity does vary, this because the acidity depends mainly on the composition of the pyrolytic oil. The lowest acidity was obtained at lower temperaturea (400 and 466 °C) and nitrogen volumetric flow of 155 Nml / min, conditions in which the highest yield of total aromatics was obtained.

- The residence time is an influential variable in the pyrolytic oil yield and formation of aromatic compounds of interest because at low residence times the maximum percentage of pyrolytic oil yield is reached.

- The pyrolytic oil yield is higher at temperature conditions of 600 ° C at high residence times. However, at low residence times, it is possible to obtain similar yields at a lower temperature (466 ° C), which implies lower operating costs, since a lower temperature means also an energy saving.

- The higher BTX concentration was produced at low residence time. The toluene and xylenes are predominant, and a significant concentration percentage is obtained for these compounds of interest.

3.7 REFERENCES OF THIS CHAPTER

[1] NKOSI, Nhlanhla and MUZENDA Edison. A review and discussion of waste tyre pyrolysis and derived products. Proceedings of the World Congress in Engineering. 2014. ISSN 20780958.

[2] BLANCO MACHIN, E.; TRAVIESO PEDROSO, D. and ANDRADE DE CARVALHO, J. Energetic valorization of wate tires. In: Renewable and Sustainable Energy Reviews [online]. 2008, 68, p. 6–11.

[3] MARTÍNEZ, Juan Daniel, *et al*. Waste tyre pyrolysis - A review. Renewable and Sustainable Energy Reviews [online]. 2013, 23, p. 179–213.

[4] KYARI, Mohammed; CUNLIFFE, Adrian and WILLIAMS, Paul T. Characterization of oils, gases, and char in relation to the pyrolysis of different brands of scrap automotive tires. In: Energy and Fuels [online]. 2005, 19(3), p. 1165–1173.

[5] CUNLIFFE, Adrian M. and WILLIAMS, Paul T. Composition of oils derived from the batch pyrolysis of tyres. In: Journal of Analytical and Applied Pyrolysis [online]. 1998, 44(2), p. 131–152.

[6] KUMARAVEL, S.T.; MURUGESAN A. and KUMARAVEL A. Tyre pyrolysis oil as an alternative fuel for diesel engines – A review. In: Renewable and Sustainable Energy Reviews [online]. 2016, 60, p. 1678–1685.

[7] WILLIAMS, Paul T. Pyrolysis of waste tyres: A review. In: Waste Management [online]. 2013, 33(8), p. 1714–1728.

[8] HITA, Idoia, *et al*. Opportunities and barriers for producing high quality fuels from the pyrolysis of scrap tires. In: Renewable and Sustainable Energy Reviews [online]. 2016, 56, p. 745–759.

[9] EDWIN RAJ, R.; ROBERT KENNEDY Z. and PILLAI B.C. Optimization of process parameters in flash pyrolysis of waste tyres to liquid and gaseous fuel in a fluidized bed reactor. In: Energy Conversion and Management [online]. 2013, 67, p. 145–151.

[10] PINTO, Filomena, *et al*. Prediction of liquid yields from the pyrolysis of waste mixtures using response surface methodology. In: Fuel Processing Technology. 2013, 116, p. 271–283.

[11] ACOSTA, Rolando, *et al.* Production of Oil and Char by Intermediate Pyrolysis of Scrap Tyres: Influence on Yield and Product Characteristics. In: International Journal of Chemical Reactor Engineering [online]. 2015, 13(2), p. 189–200.

[12] MASTRAL, A. M, *et al.* Optimisation of scrap automotive tyres recycling into valuable liquid fuels. In: Resources Conservation & recycling. 2000, 29, p. 263–272.

[13] MKHIZE, N. M., *et al.* Condensation of the hot volatiles from waste tyre pyrolysis by quenching. In: Journal of Analytical and Applied Pyrolysis. 2017. p. 1-6.

[14] ISLAM Rofiqul M., et al. Liquid fuels and chemicals from pyrolysis of motorcycle tire waste: Product yields, compositions and related properties. In: Fuel [online]. 2008, 87(13–14), p. 3112–3122.

[15] ZHANG, Xinghua, *et al.* Vacuum pyrolysis of waste tires with basic additives. In: Waste Management [online]. 2008, 28(11), p. 2301–2310.

[16] LI, S.Q., et al. Pilot-Scale Pyrolysis of scrap tires in a continuous rotary kiln reactor. In: Industrial & Engineering Chemistry Research. 2004, (1), p. 5133–5145.

[17] GIRODS, P., *et al*. Low-temperature pyrolysis of wood waste containing urea-formaldehyde resin. In: Renewable Energy [online]. 2008, 33(4), p. 648–654.

[18] MAYER, Ludwig. Métodos de la industria química: en esquemas de flujo en colores. Parte 2a, Orgánica. Reverté. 1987. ISBN 8429179623.

[19] BEYER, Hans a Wolfgang WALTER. Manual de química orgánica. Reverté. 1987. ISBN 8429170669.

[20] MOHAMMAD, Ali and INAMUDDIN Dr. Green Solvents I: Properties and Applications in Chemistry. Chapter 5. Limonene as green solvent for extraction of natural products. Springer science & business media. 2012, p. 176. ISBN 9400717113.

[21] KERTON, Francesca M. Alternative solvents for green chemistry. Chapter 5. Renewable Solvents. Royal society of chemistry. 2009, p. 97–166. ISBN 085404163X, 9780854041633.

[22] MEUWESE, Anne. The sustainability of producing BTX from biomass. Thesis of Master programme Energy and Enviromental Sciences. Groningen, Netherlands: University of Groninfen. 2013. Center for Energy and Environmental Studies.

[23] BAHAMONDE, J M López. La industria petroquímica de los aromáticos en el siglo XXI., p. 99–102.

[24] BENDER, M. Global Aromatics Supply - Today and Tomorrow. Proceeding of DGMK CONFERENCE, ed. New Technologies and Alternative Feedstocks in Petrochemistry and Refining. 2013. ISBN 9783941721326.

[25] PAKDEL, Hooshang, *et al.* Formation of dl-Limonene in Used Tire Vacuum Pyrolysis Oils. In: Enviromental Sciences Technologies. 1991, 25 (9), p. 1646–1649.

[26] WILLIAMS, Paul T and BOTTRILL, P. Sulfur-polycyclic tyre pyrolysis oil. In: Fuel. 1995, 74(5), p. 736–742.

[27] AMARI, Takeshi, *et al*. Resource recovery from used rubber tires. In: Resources Policy. 1999, 25, p. 179–188.

[28] WILLIAMS, Paul T. and BESLER, S. The Influence of temperature and heating rate on the slow pyrolysis of biomass. In: Fuel. 1996, 1481(96), p. 6–7.

[29] WILLIAMS, Paul T. and BRINDLE, Alexander J. Aromatic chemicals from the catalytic pyrolysis of scrap tyres. In: Journal of Analytical and Applied Pyrolysis [online]. 2003, 67(1), p. 143–164.

[30] ARABIOURRUTIA, M., *et al.* Product distribution obtained in the pyrolysis of tyres in a conical spouted bed reactor. In: Chemical Engineering Science [online]. 2007, 62(18–20), p. 5271–5275.

[31] LARESGOITI, M. F., *et al*. Characterization of the liquid products obtained in tyre pyrolysis. In: Journal of Analytical and Applied Pyrolysis [online]. 2004, 71(2), p. 917–934.

[32] AYLÓN, E., *et al.* Waste tire pyrolysis: Comparison between fixed bed reactor and moving bed reactor. In: Industrial and Engineering Chemistry Research [online]. 2008, 47(12), p. 4029–4033.

[33] DÍEZ, C., *et al.* Pyrolysis of tyres : A comparison of the results from a fixed-bed laboratory reactor and a pilot plant (rotatory reactor). In: Journal of Analytical and Applied Pyrolysis [online]. 2005, 74, p. 254–258.

[34] SADHAN K., *et al.* Rubber recycling. Chapter 11: Conversion of Used Tires to Carbon Black and Oil by Pyrolysis. CRC Press. 2005. ISBN 9780203499337.

[35] LEUNG, D Y C, *et al.* Pyrolysis of tire powder : influence of operation variables on the composition and yields of gaseous product. In: Fuel Processing Technology. 2002, 79, p. 141–155.

[36] PUY, Neus, *et al*. Waste tyre pyrolysis – A review. In: Renewable and Sustainable Energy Reviews. 2013, 23, p. 179–213.

[37] ALKHATIB, Radwan, *et al.* Effect of heating power on the scrap tires pyrolysis derived oil. In: Journal of Analytical and Applied Pyrolysis. 2015, 116, p. 10–17.

[38] LAH, B; KLINAR D. and LIKOZAR, B. Pyrolysis of natural, butadiene , styrene – butadiene rubber and tyre components : Modelling kinetics and transport phenomena at different heating rates and formulations. In: Chemical Engineering Science. 2013, 87, p. 1–13.

[39] ISLAM, M Rofiqul, *et al*. Innovation in pyrolysis technology for management of scrap tire: A solution of energy and environment. In: International Journal of Environmental Science and Development. 2010, 1(1), p. 89–96.

[40] FERNÁNDEZ, A. M.; BARRIOCANAL C. and ALVAREZ R. Pyrolysis of a waste from the grinding of scrap tyres. In: Journal of Hazardous Materials [online]. 2012, 204, p. 236–243.

[41] GONZÁLEZ, Juan F., *et al.* Pyrolysis of automobile tyre waste. Influence of operating variables and kinetics study. In: Journal of Analytical and Applied Pyrolysis [online]. 2001, 58–59, p. 667–683.

[42] UCAR, Suat, *et al.* Evaluation of two different scrap tires as hydrocarbon source by pyrolysis. In: Fuel [online]. 2005, 84(14–15), p. 1884–1892.

[43] CONESA, Juan A., *et al.* Complete study of the pyrolysis and gasification of scrap tires in a pilot plant reactor. In: Environmental Science and Technology [online]. 2004, 38(11), p. 3189–3194.

[44] SENNECA, O.; SALATINO, P. and CHIRONE, R. Fast heating-rate thermogravimetric study of the pyrolysis of scrap tyres. In: Fuel [online]. 1999, 78(13), p. 1575–1581.

[45] MURILLO, R., *et al*. The application of thermal processes to valorise waste tyre. In: Fuel Processing Technology [online]. 2006, 87(2), p. 143–147.

[46] ROY, Christian, *et al.* Characterization of naphtha and carbon black obtained by vacuum pyrolysis of polyisoprene rubber. In: Fuel Processing Technology. 1997, 50, p. 87-103.

[47] LOPEZ, Gartzen, *et al*. Influence of Tire Formulation on the Products of Continuous Pyrolysis in a Conical Spouted Bed Reactor in a Conical Spouted Bed Reactor. In: Energy & Fuels [online]. 2009, 23, p. 5423-5431.

[48] MARTÍNEZ, Juan Daniel, *et al.* Demonstration of the waste tire pyrolysis process on pilot scale in a continuous auger reactor. In: Journal of Hazardous Materials [online]. 2013, 261, p. 637–645.

[49] DE MARCO RODRIGUEZ, Isabel, *et al.* Pyrolysis of scrap tyres. In: Fuel Processing Technology [online]. 2001, 72(1), p. 9–22.

[50] BAJUS, Martin and OLAHOVÁ, Natália. Thermal conversion of scrap tyres. In: Petroleum and Coal. 2011, 53(2), p. 98–105.

[51] CALDERÓN, María Fernanda a Astrid Lorena TORRES. Diseño y puesta en marcha del montaje de una planta piloto a escala laboratorio para producción de bio-oil a partir de biomasa mediante pirólisis. Undergraduate Thesis in chemical engineering. Bucaramanga, Colombia: Universidad Industrial de Santander. Faculty of physical chemical engineering. Chemical engineering school. 2012.

[52] MACFARLAND, Thomas W. Two-way Analysis of variance: Statistical Test and Graphics Using R [online]. Springer. 2012. ISBN 9783642179792.

[53] MKHIZE, N. M.,*et al.* Effect of temperature and heating rate on limonene production from waste tyre pyrolysis. In: Journal of Analytical and Applied Pyrolysis [online]. 2016, 120, p. 314–320.

[54] ASTM INTERNATIONAL. ASTM D-4809-13: Standard Test Method for Heat of Combustion of Liquid Hydrocarbon Fuels by Bomb Calorimeter (Precision Method).

[55] ASTM INTERNATIONAL. ASTM D-5865-04: Standard Test Method for Gross Calorific Value of Coal and Coke.

[56] INTERNATIONAL ORGANIZATION FOR STANDARDIZATION ISO. Standard UNE-EN ISO 660: Animal and vegetable fats and oils - Determination of acid value and acidity. 2010

[57] KATRITZKY, Alan R, *et al.* Prediction of gas chromatographic retention times and response factors using a general quantitative structure-property relationship treatment. In: Anal. Chem. 1994, 6(11), p. 1799–1807.

[58] BERRUECO, C., *et al.* Pyrolysis of waste tyres in an atmospheric static-bed batch reactor: Analysis of the gases obtained. In: Journal of Analytical and Applied Pyrolysis [online]. 2005, 74(1–2), p. 245–253.

[59] AYDIN, Hüseyin and ILKILIÇ, Cumali. Optimization of fuel production from waste vehicle tires by pyrolysis and resembling to diesel fuel by various desulfurization methods. In: Fuel [online]. 2012, 102, p. 605–612.

[60] BANAR, Müfide, *et al.* Characterization of pyrolytic oil obtained from pyrolysis of TDF (Tire Derived Fuel). In: Energy Conversion and Management [online]. 2012, 62, p. 22–30.

[61] WILLIAMS, Paul T. and BRINDLE Alexander J.. Temperature selective condensation of tyre pyrolysis oils to maximise the recovery of single ring aromatic compounds. In: Fuel [online]. 2003, 82(9), p. 1023–1031.

[62] VECINO, Sebastián, *et al*. Comparative study of bio-oil production from sugarcane bagasse and palm empty fruit bunch : Yield optimization and bio-oil characterization. In: Journal of Analytical and Applied Pyrolysis. 2014, 108, p. 284–294.

[63] BENALLAL, B, *et al.* Characterization of pyrolytic light naphtha from vacuum pyrolysis of used tyres Comparison with petroleum naphtha. In: Fuel. 1995, 74(11), p. 1589–1594.

[64] NAPOLI A., *et al*. Scrap tyre pyrolysis: Are the effluents valuable products. In: Journal of Analytical and Applied Pyrolysis [online]. 1997, 40–41, p. 373–382.

[65] CHEVRON CORPORATION. Diesel Fuels Technical Review. 2007.

[66] AYANOGLU, Abdulkadir and YUMRUTAS Recep. Production of gasoline and diesel like fuels from waste tire oil by using catalytic pyrolysis. In: Energy. 2016, 103, p. 456–468.

[67] ASTM INTERNATIONAL D396 − 16. Standard Specification for Fuel Oils [online]. 2017.

[68] ASTM INTERNATIONAL D7467 − 15C. Standard Specification for Diesel Fuel Oil , Biodiesel Blend (B6 to B20) [online]. 2017.

[69] SAN MIGUEL, G., *et al.* Thermal and catalytic conversion of used tyre rubber and its polymeric constituents using Py-GC / MS. In: Applied Catalysis B: Environmental [online]. 2006, 64(2006), p. 209–219.

[70] QUEK, Augustine and BALASUBRAMANIAN Rajasekhar. Liquefaction of waste tires by pyrolysis for oil and chemicals - A review. In: Journal of Analytical and Applied Pyrolysis [online]. 2013, 101, p. 1–16.

[71] QU, Wei, *et al*. Pyrolysis of waste tire on ZSM-5 zeolite with enhanced catalytic activities. In: Polymer Degradation and Stability [online]. 2006, 91(10), p. 2389–2395.

[72] DANON, B., *et al*. A review of dipentene (dl-limonene) production from waste tire pyrolysis. In: Journal of Analytical and Applied Pyrolysis [online]. 2015, 112, p. 1–13.

[73] PAKDEL, Hooshang, Dana Magdalena PANTEA and ROY Christian. Production of dl-limonene by vacuum pyrolysis of used tires. In: Journal of Analytical and Applied Pyrolysis [online]. 2001, 57(1), p. 91–107.

[74] CYPRES, R. Aromatics hydrocarbons formation during coal pyrolysis. In: Fuel Processing Technology. 1987, 15, p. 1–15.

[75] AYLÓN, E, *et al*. Valorisation of waste tyre by pyrolysis in a moving bed reactor [online]. 2010, 30, p. 1220–1224.

[76] OLAZAR, Martin, *et al*. Catalyst effect on the composition of tire pyrolysis products. In: Energy and Fuels [online]. 2008, 22(5), p. 2909–2916.

[77] CELY, Yeniffer. Modelo matemático de la pirólisis intermedia de caucho de llantas en un reactor a lecho fijo. Thesis of Master in Chemical Engineering, Bucaramanga, Colombia: Universidad Industrial de Santander. Faculty of physicochemical engineering. School of Chemical Engineering. 2015.

3.8 BIBLIOGRAPHY OF THIS CHAPTER

ACOSTA, Rolando, *et al.* Production of Oil and Char by Intermediate Pyrolysis of Scrap Tyres: Influence on Yield and Product Characteristics. In: International Journal of Chemical Reactor Engineering [online]. 2015, 13(2), p. 189–200.

ALKHATIB, Radwan, *et al.* Effect of heating power on the scrap tires pyrolysis derived oil. In: Journal of Analytical and Applied Pyrolysis. 2015, 116, p. 10–17.
ASTM INTERNATIONAL. ASTM D-4809-13: Standard Test Method for Heat of Combustion of Liquid Hydrocarbon Fuels by Bomb Calorimeter (Precision Method).

AMARI, Takeshi, *et al*. Resource recovery from used rubber tires. In: Resources Policy. 1999, 25, p. 179–188.

ARABIOURRUTIA, M., *et al.* Product distribution obtained in the pyrolysis of tyres in a conical spouted bed reactor. In: Chemical Engineering Science [online]. 2007, 62(18–20), p. 5271–5275.

ASTM INTERNATIONAL D396 − 16. Standard Specification for Fuel Oils [online]. 2017.

ASTM INTERNATIONAL. D-5865-04: Standard Test Method for Gross Calorific Value of Coal and Coke.

ASTM INTERNATIONAL D7467 − 15C. Standard Specification for Diesel Fuel Oil , Biodiesel Blend (B6 to B20) [online]. 2017.

AYANOGLU, Abdulkadir and YUMRUTAS Recep. Production of gasoline and diesel like fuels from waste tire oil by using catalytic pyrolysis. In: Energy. 2016, 103, p. 456–468.

AYDIN, Hüseyin and ILKILIÇ, Cumali. Optimization of fuel production from waste vehicle tires by pyrolysis and resembling to diesel fuel by various desulfurization methods. In: Fuel [online]. 2012, 102, p. 605–612.

AYLÓN, E, *et al*. Valorisation of waste tyre by pyrolysis in a moving bed reactor [online]. 2010, 30, p. 1220–1224.

AYLÓN, E., *et al.* Waste tire pyrolysis: Comparison between fixed bed reactor and moving bed reactor. In: Industrial and Engineering Chemistry Research [online]. 2008, 47(12), p. 4029–4033.

BAHAMONDE, J M López. La industria petroquímica de los aromáticos en el siglo XXI., p. 99–102.

BAJUS, Martin and OLAHOVÁ, Natália. Thermal conversion of scrap tyres. In: Petroleum and Coal. 2011, 53(2), p. 98–105.

BANAR, Müfide, *et al.* Characterization of pyrolytic oil obtained from pyrolysis of TDF (Tire Derived Fuel). In: Energy Conversion and Management [online]. 2012, 62, p. 22–30.

BENALLAL, B, *et al.* Characterization of pyrolytic light naphtha from vacuum pyrolysis of used tyres Comparison with petroleum naphtha. In: Fuel. 1995, 74(11), p. 1589–1594.

BENDER, M. Global Aromatics Supply - Today and Tomorrow. Proceeding of DGMK CONFERENCE, ed. New Technologies and Alternative Feedstocks in Petrochemistry and Refining. 2013. ISBN 9783941721326.

BERRUECO, C., *et al.* Pyrolysis of waste tyres in an atmospheric static-bed batch reactor: Analysis of the gases obtained. In: Journal of Analytical and Applied Pyrolysis [online]. 2005, 74(1–2), p. 245–253.

BEYER, Hans a Wolfgang WALTER. Manual de química orgánica. Reverté. 1987. ISBN 8429170669.

BLANCO MACHIN, E.; TRAVIESO PEDROSO, D. and ANDRADE DE CARVALHO, J. Energetic valorization of wate tires. In: Renewable and Sustainable Energy Reviews [online]. 2008, 68, p. 6–11.

CALDERÓN, María Fernanda a Astrid Lorena TORRES. Diseño y puesta en marcha del montaje de una planta piloto a escala laboratorio para producción de bio-oil a partir de biomasa mediante pirólisis. Undergraduate Thesis in chemical engineering. Bucaramanga, Colombia: Universidad Industrial de Santander. Faculty of physical chemical engineering. Chemical engineering school. 2012.

CELY, Yeniffer. Modelo matemático de la pirólisis intermedia de caucho de llantas en un reactor a lecho fijo. Thesis of Master in Chemical Engineering, Bucaramanga, Colombia: Universidad Industrial de Santander. Faculty of physicochemical engineering. School of Chemical Engineering. 2015.

CHEVRON CORPORATION. Diesel Fuels Technical Review. 2007.

CONESA, Juan A., *et al.* Complete study of the pyrolysis and gasification of scrap tires in a pilot plant reactor. In: Environmental Science and Technology [online]. 2004, 38(11), p. 3189–3194.

CUNLIFFE, Adrian M. and WILLIAMS, Paul T. Composition of oils derived from the batch pyrolysis of tyres. In: Journal of Analytical and Applied Pyrolysis [online]. 1998, 44(2), p. 131–152.

CYPRES, R. Aromatics hydrocarbons formation during coal pyrolysis. In: Fuel Processing Technology. 1987, 15, p. 1–15.

DANON, B., *et al*. A review of dipentene (dl-limonene) production from waste tire pyrolysis. In: Journal of Analytical and Applied Pyrolysis [online]. 2015, 112, p. 1–13.

DE MARCO RODRIGUEZ, Isabel, *et al.* Pyrolysis of scrap tyres. In: Fuel Processing Technology [online]. 2001, 72(1), p. 9–22.

DÍEZ, C., *et al.* Pyrolysis of tyres : A comparison of the results from a fixed-bed laboratory reactor and a pilot plant (rotatory reactor). In: Journal of Analytical and Applied Pyrolysis [online]. 2005, 74, p. 254–258.

EDWIN RAJ, R.; ROBERT KENNEDY Z. and PILLAI B.C. Optimization of process parameters in flash pyrolysis of waste tyres to liquid and gaseous fuel in a fluidized bed reactor. In: Energy Conversion and Management [online]. 2013, 67, p. 145–151.

FERNÁNDEZ, A. M.; BARRIOCANAL C. and ALVAREZ R. Pyrolysis of a waste from the grinding of scrap tyres. In: Journal of Hazardous Materials [online]. 2012, 204, p. 236–243.

GIRODS, P., *et al*. Low-temperature pyrolysis of wood waste containing urea-formaldehyde resin. In: Renewable Energy [online]. 2008, 33(4), p. 648–654.

GONZÁLEZ, Juan F., *et al.* Pyrolysis of automobile tyre waste. Influence of operating variables and kinetics study. In: Journal of Analytical and Applied Pyrolysis [online]. 2001, 58–59, p. 667–683.

HITA, Idoia, *et al*. Opportunities and barriers for producing high quality fuels from the pyrolysis of scrap tires. In: Renewable and Sustainable Energy Reviews [online]. 2016, 56, p. 745–759.

INTERNATIONAL ORGANIZATION FOR STANDARDIZATION ISO. Standard UNE-EN ISO 660: Animal and vegetable fats and oils - Determination of acid value and acidity. 2010.

ISLAM, M Rofiqul, *et al*. Innovation in pyrolysis technology for management of scrap tire: A solution of energy and environment. In: International Journal of Environmental Science and Development. 2010, 1(1), p. 89–96.

ISLAM Rofiqul M., *et al.* Liquid fuels and chemicals from pyrolysis of motorcycle tire waste: Product yields, compositions and related properties. In: Fuel [online]. 2008, 87(13–14), p. 3112–3122.

KATRITZKY, Alan R, *et al.* Prediction of gas chromatographic retention times and response factors using a general quantitative structure-property relationship treatment. In: Anal. Chem. 1994, 6(11), p. 1799–1807.

KERTON, Francesca M. Alternative solvents for green chemistry. Chapter 5. Renewable Solvents. Royal society of chemistry. 2009, p. 97–166. ISBN 085404163X, 9780854041633.

KUMARAVEL, S.T.; MURUGESAN A. and KUMARAVEL A. Tyre pyrolysis oil as an alternative fuel for diesel engines – A review. In: Renewable and Sustainable Energy Reviews [online]. 2016, 60, p. 1678–1685.

KYARI, Mohammed; CUNLIFFE, Adrian and WILLIAMS, Paul T. Characterization of oils, gases, and char in relation to the pyrolysis of different brands of scrap automotive tires. In: Energy and Fuels [online]. 2005, 19(3), p. 1165–1173.

LAH, B; KLINAR D. and LIKOZAR, B. Pyrolysis of natural, butadiene , styrene – butadiene rubber and tyre components : Modelling kinetics and transport phenomena at different heating rates and formulations. In: Chemical Engineering Science. 2013, 87, p. 1–13.

LARESGOITI, M. F., *et al*. Characterization of the liquid products obtained in tyre pyrolysis. In: Journal of Analytical and Applied Pyrolysis [online]. 2004, 71(2), p. 917–934.

LEUNG, D Y C, *et al.* Pyrolysis of tire powder : influence of operation variables on the composition and yields of gaseous product. In: Fuel Processing Technology. 2002, 79, p. 141–155.

LI, S.Q., *et al*. Pilot-Scale Pyrolysis of scrap tires in a continuous rotary kiln reactor. In: Industrial & Engineering Chemistry Research. 2004, (1), p. 5133–5145.

LOPEZ, Gartzen, *et al*. Influence of Tire Formulation on the Products of Continuous Pyrolysis in a Conical Spouted Bed Reactor in a Conical Spouted Bed Reactor. In: Energy & Fuels [online]. 2009, 23, p. 5423-5431.

MACFARLAND, Thomas W. Two-way Analysis of variance: Statistical Test and Graphics Using R [online]. Springer. 2012. ISBN 9783642179792.

MARTÍNEZ, Juan Daniel, *et al.* Demonstration of the waste tire pyrolysis process on pilot scale in a continuous auger reactor. In: Journal of Hazardous Materials [online]. 2013, 261, p. 637–645.

MARTÍNEZ, Juan Daniel, *et al*. Waste tyre pyrolysis - A review. Renewable and Sustainable Energy Reviews [online]. 2013, 23, p. 179–213.

MASTRAL, A. M, *et al.* Optimisation of scrap automotive tyres recycling into valuable liquid fuels. In: Resources Conservation & recycling. 2000, 29, p. 263–272.

MAYER, Ludwig. Métodos de la industria química: en esquemas de flujo en colores. Parte 2a, Orgánica. Reverté. 1987. ISBN 8429179623.

MEUWESE, Anne. The sustainability of producing BTX from biomass. Thesis of Master programme Energy and Enviromental Sciences. Groningen, Netherlands: University of Groninfen. Center for Energy and Environmental Studies. 2013

MKHIZE, N. M., *et al.* Condensation of the hot volatiles from waste tyre pyrolysis by quenching. In: Journal of Analytical and Applied Pyrolysis. 2017. p. 1-6.

MKHIZE, N. M.,*et al.* Effect of temperature and heating rate on limonene production from waste tyre pyrolysis. In: Journal of Analytical and Applied Pyrolysis [online]. 2016, 120, p. 314–320.

MOHAMMAD, Ali and INAMUDDIN Dr. Green Solvents I: Properties and Applications in Chemistry. Chapter 5. Limonene as green solvent for extraction of

natural products. Springer science & business media. 2012, p. 176. ISBN 9400717113.

MURILLO, R., *et al*. The application of thermal processes to valorise waste tyre. In: Fuel Processing Technology [online]. 2006, 87(2), p. 143–147.

NAPOLI A., *et al*. Scrap tyre pyrolysis: Are the effluents valuable products. In: Journal of Analytical and Applied Pyrolysis [online]. 1997, 40–41, p. 373–382.

NKOSI, Nhlanhla and MUZENDA Edison. A review and discussion of waste tyre pyrolysis and derived products. Proceedings of the World Congress in Engineering. 2014. ISSN 20780958.

OLAZAR, Martin, *et al*. Catalyst effect on the composition of tire pyrolysis products. In: Energy and Fuels [online]. 2008, 22(5), p. 2909–2916.

PAKDEL, Hooshang, *et al.* Formation of dl-Limonene in Used Tire Vacuum Pyrolysis Oils. In: Enviromental Sciences Technologies. 1991, 25 (9), p. 1646–1649.

PAKDEL, Hooshang, PANTEA Dana Magdalena and ROY Christian. Production of dl-limonene by vacuum pyrolysis of used tires. In: Journal of Analytical and Applied Pyrolysis [online]. 2001, 57(1), p. 91–107.

PINTO, Filomena, *et al*. Prediction of liquid yields from the pyrolysis of waste mixtures using response surface methodology. In: Fuel Processing Technology. 2013, 116, p. 271–283.

PUY, Neus, *et al*. Waste tyre pyrolysis – A review. In: Renewable and Sustainable Energy Reviews. 2013, 23, p. 179–213.

QU, Wei, *et al*. Pyrolysis of waste tire on ZSM-5 zeolite with enhanced catalytic activities. In: Polymer Degradation and Stability [online]. 2006, 91(10), p. 2389–2395.

QUEK, Augustine and BALASUBRAMANIAN Rajasekhar. Liquefaction of waste tires by pyrolysis for oil and chemicals - A review. In: Journal of Analytical and Applied Pyrolysis [online]. 2013, 101, p. 1–16.

ROY, Christian, *et al.* Characterization of naphtha and carbon black obtained by vacuum pyrolysis of polyisoprene rubber. In: Fuel Processing Technology. 1997, 50, p. 87-103.

SADHAN K., *et al.* Rubber recycling. Chapter 11: Conversion of Used Tires to Carbon Black and Oil by Pyrolysis. CRC Press. 2005. ISBN 9780203499337.

SAN MIGUEL, G., *et al.* Thermal and catalytic conversion of used tyre rubber and its polymeric constituents using Py-GC / MS. In: Applied Catalysis B: Environmental [online]. 2006, 64(2006), p. 209–219.

SENNECA, O.; SALATINO, P. and CHIRONE, R. Fast heating-rate thermogravimetric study of the pyrolysis of scrap tyres. In: Fuel [online]. 1999, 78(13), p. 1575–1581.

UCAR, Suat, *et al.* Evaluation of two different scrap tires as hydrocarbon source by pyrolysis. In: Fuel [online]. 2005, 84(14–15), p. 1884–1892.

VECINO, Sebastián, *et al*. Comparative study of bio-oil production from sugarcane bagasse and palm empty fruit bunch: Yield optimization and bio-oil characterization. In: Journal of Analytical and Applied Pyrolysis. 2014, 108, p. 284–294.

WILLIAMS, Paul T. Pyrolysis of waste tyres: A review. In: Waste Management [online]. 2013, 33(8), p. 1714–1728.

WILLIAMS, Paul T. and BESLER, S. The Influence of temperature and heating rate on the slow pyrolysis of biomass. In: Fuel. 1996, 1481(96), p. 6–7.

WILLIAMS, Paul T and BOTTRILL, P. Sulfur-polycyclic tyre pyrolysis oil. In: Fuel. 1995, 74(5), p. 736–742.

WILLIAMS, Paul T. and BRINDLE, Alexander J. Aromatic chemicals from the catalytic pyrolysis of scrap tyres. In: Journal of Analytical and Applied Pyrolysis [online]. 2003, 67(1), p. 143–164.

WILLIAMS, Paul T. and BRINDLE Alexander J. Temperature selective condensation of tyre pyrolysis oils to maximise the recovery of single ring aromatic compounds. In: Fuel [online]. 2003, 82(9), p. 1023–1031.

ZHANG, Xinghua, *et al.* Vacuum pyrolysis of waste tires with basic additives. In: Waste Management [online]. 2008, 28(11), p. 2301–2310.

Chapter 4

Catalysts synthesis and characterization

Part of this chapter was summited recently in Journal Waste and Biomass Valorization,

C. Tavera, P. Gauthier-Maradei, M. Capron, D. Ferreira, C. Palencia, O. Gardoll, J.C. Morin, B. Katryniok, F. Dumeignil. Improvement of the production of aromatic compounds obtained from the pyrolysis of scrap tires rubber using heteropolyacids-based catalysts.

4.1. INTRODUCTION

The pyrolysis of scrap tires leads to a fraction of gas, char and oil. Among these fractions, the oil one has the highest valorization potential. Its composition regroups aromatics [1–4], aliphatic, olefin and sulfur compounds. In agreement with previous studies, it has been found that the groups of molecules in higher proportion in the oil are aromatics and partially saturated cyclic compounds. These molecules are useful

in many industrial applications such as the synthesis of plastics, paints, explosives, pesticides, detergents, synthetic rubbers, perfumes and others [5, 6].

The aromatics concentrations (*e.g.* toluene, benzene and xylenes) in the pyrolytic oil can reach up to 8 wt% [7–9]. Acosta *et al.* [4] reported that the optimal pyrolysis temperature to obtain high aromatics yields (*i.e.* 12 wt%) in the pyrolytic oil is 466 °C. In order to achieve better yields of aromatic compounds, different studies have used catalysts in the scrap tire rubber (STR) pyrolysis, such as zeolites, bifunctional catalysts (metals supported on zeolites or silica), and pure silica [6, 8, 10–15].

The zeolite catalysts have been the most studied materials, for example, the studies developed by Williams *et al.* [9, 16] Olazar *et al.* [6, 12], Arrabiourrutia *et al.*[11, 17] and Li *et al.*[8], who focus on the catalyst effect on the oil composition and the increase of aromatic concentration. Their conclusions are that the catalysts need to present high acid character to increase the aromatics concentration in the oil (*i.e.* mainly single ring aromatics). Although this type of catalyst allows an improvement in the aromatic concentration, they present a disadvantage due to their high temperatures of work (over 500 ºC). This high temperature of work also leads to a high cracking activity, leading to a decrease of oil yield and an increase of gas yield and some coke formation and so a rapid deactivation of the catalyst [18]. The same disadvantage occurs with metal-containing catalysts, due to their hydrogenation capacity. This property leads to the formation of hydrogenated compounds which can then react through cracking and ring-opening reactions, leading to higher gas yield and lower oil yield. The composition of the oil is also less concentrated in aromatic compounds than when zeolites is used [3, 15, 19, 20].

A new alternative of acid catalysts are the heteropolyacids (HPA) catalysts, which have not been studied until now for this type of reaction. HPAs have acidic and redox functions and are useful in a large variety of reactions, such as oxidation, reduction, condensation, carboxylation, dehydrogenation, among others [21]. Those have

higher acidity than strong mineral acids such as H_2SO_4 and HCl when they are used in non-aqueous medium, and higher than other acid solids such as aluminas, silicas and zeolites. HPA catalysts have been studied in reactions such as alkylation of toluene, esterification of benzoic acid, synthesis of acrolein and oxidation of sulfur compounds in fuel oils, among others, showing good results of their catalytic activity [21, 22].

Noting the HPA potential owing to its high acidity and its possible application in oxidation of sulfur compounds, the present study proposes the use of heteropolyacid catalysts deposited on mesoporous support in order to improve the concentration of aromatic compounds present in the oil obtained from STR pyrolysis.

This chapter shows the techniques used for the catalysts synthesis and characterizations.
Initially, four different active phases (*i.e*. $H_3PW_{12}O_{40}$, $H_3PMo_{12}O_{40}$, $H_4SiW_{12}O_{40}$ and $H_3PMo_{11}VO_{40}$) were deposited on a commercial support (*i.e.* CARiACT Q-10 by Fuji Silysia Chemical LTD), in order to evaluate the influence of active phase on the selectivity toward aromatics. After, three supports were synthesized: SBA-15, MCM-41 and KIT-6, and the best active phase found in the previous catalytic tests was supported on them. Finally, the best active phase was supported on the best support at different concentrations, to evaluate the influence of the amount of active phase. A total of nine catalysts were synthesized and characterized.

The active phases were characterized by RAMAN and XRD. The synthesized mesoporous supports were characterized by N_2 adsorption – desorption, XRD, and TEM. The catalysts (HPA based on support) were characterized by N_2 adsorption - desorption, XRD, NH_3 TPD, FTIR, pyridine adsorption – FTIR. These characterizations allowed to check the correct catalysts synthesis and the determination of the textural and structural properties, the types of acid sites (*i.e.* Brönsted, Lewis), their strength and their number for each catalyst.

4.2 STATE OF THE ART

Some authors have studied the effect of catalysts on the oil yield from STR pyrolysis, finding that the catalysts with high acidity increase the yield of liquids and have high selectivity towards aromatic compounds. Zeolites, such as ZSM-5, USY and HSM-5, H-Beta and HY, which have different acidity, depending on their Si/Al ratio, have been used [6, 9, 11, 13, 16, 18].

Boxiong. *et al.* [13] studied the use of USY catalyst in STR pyrolysis, this zeolite has a Si/Al ratio equal to 5, which represents a high acidity. The pyrolysis is performed in a fixed bed reactor, the vapors and gases produced are passed to a second reactor, where the catalytic bed is located. It was observed that addition of zeolite USY reduced oil production (from 33.6 to 20.1 wt%) and increased gas production (29.8 to 41.6 wt%). In spite of the low liquid performance that was presented with the USY catalyst, the oil composition shows a total concentration of single ring aromatics of 62 wt%, where the compounds with the highest concentration are benzene (1.23 wt%), toluene (9.35 wt%), ethylbenzene (3.68 wt%), xylenes (12.64 wt%) and limonene (1.81 wt%).

In another study, Boxiong *et al.* [18] compared two types of zeolites: USY and ZSM-5, which have a Si/Al ratio of 5 and 37, respectively. The study concluded that the catalyst with a lower Si/Al ratio (higher acidity) allows obtaining a higher concentration of aromatics in the pyrolytic oil. However, the high acidity means a high cracking activity what is prove by the increase of the gas fraction.

These results were supported by Arabiourrutia M. *et al.* [11] who studied the effect of acid catalysts on the composition of gaseous products and pyrolytic liquids. Catalytic pyrolysis was performed using a commercial microreactor (Pyroprobe 2500 from CDS Analytical, Inc.) used in three different reaction configurations : 1) a

thermal pyrolysis, in which the reaction is performed without catalysts, 2) an *in situ* pyrolysis, in which the catalyst is mixing with the STR sample in the pyroprobe and 3) a pyrolysis + reforming step, in which the volatile compounds produced during pyrolysis in the pyroprobe are carried to catalysis chamber to be reforming in aromatic species. Thermal pyrolysis and *in situ* pyrolysis were performed at 723K, and pyrolysis + reforming step was carried out at 723K in the pyroprobe and 673K in the catalytic chamber using two different amounts of catalyst. *In situ* pyrolysis was performed with three acid catalysts: HZSM-5 (Si/Al = 30), HY (Si/Al = 5.2) and HBeta (Si/Al = 75).

Comparing the results obtained by the thermal pyrolysis with those of the pyrolysis + reforming step, it was found that there is a great difference in the yields of gas and non-aromatic C5-C10 compounds. In the case of thermal pyrolysis, the gas yield is about 2 wt% at 723 K, while the pyrolysis + reforming step achieves almost 20 wt%. In the gas obtained with the pyrolysis + reforming step, a remarkable increase of the yields of C2 and C3 compounds was observed while the authors evidenced a decrease of main compounds in thermal pyrolysis, such as isoprene and D-limonene. The yield of benzene and toluene is slightly higher in pyrolysis + reforming step, while the yield of xylenes is very similar between pyrolysis and pyrolysis + reforming step. Furthermore, Arabiourrutia M. *et al.* [11] observed that yield oil is similar, but the composition is different, with a higher concentration of aromatics with zeolite HY. These results show that the aromatics yield is higher with catalysts of high acidity, (*i.e.* with a low Si/Al ratio), which in turn increase gas production considerably.

Otherwise, this behavior had also been observed by Williams *et al.* with another type of zeolites. They used three catalysts; two Y type (CBV-400 and CBV-780) and one ZSM-5, the Si/Al ratio of the three catalysts are 5.4, 40 and 40, respectively. The experimental study was performed using 200g of tire, and different ratios of tire/catalyst were evaluated. The CBV-400, which has the highest acidity, showed a

reduction in oil yield from 55.8 wt% without catalyst to 32 wt%, and the gas yield increase from 14 wt% to 20 wt%, linking to the formation of coke on the catalyst surface. It is due to the acidity of the catalyst, which favors cracking on the condensable fraction. The oil yield for zeolite CBV-780 (33.4 wt%) was lower than the oil yield with ZSM-5 zeolite (35.8 wt%). A decrease of oil yields was found with the three catalysts, as it was explained above, due to the acidity. Nevertheless, the authors report an increase in the aromatic concentrations, obtaining the greater production with the zeolite CBV-400 (lower Si/Al ratio), which agrees with the two authors mentioned above. Besides, the authors report a complete loss of limonene, and they suggest that this decomposition is due to limonene being transformed into some aromatics such as benzene, toluene, xylene and styrene with the presence of a catalyst.

Another type of catalyst studied so far in STR pyrolysis are the bifunctional catalysts. This is the case of Dung *et al.* [14, 20, 23] who used catalysts with Ru and Pt in tire pyrolysis. According to the authors, the use of this type of catalyst showed a strong decrease of polyaromatics, while the single ring aromatics yield increased. These results suggest the conversion of polyaromatic compounds to the single ring aromatic compounds. These authors conclude that metal allows a high aromatic hydrogenation activity, therefore, the polyaromatics can be hydrogenated on the metallic sites causing cracking and ring-opening reactions.

With the research carried out up to now, it has been concluded that high acidity favors the aromatics yield, although there is also a low oil yield due to the increase of gas formation and coke. On the other hand, it can be inferred that, apparently, the increase in the aromatics production is due to the cracking of the polyaromatics compounds and the transformation of limonene, species present in the pyrolysis liquids. With all these studies carried out with a catalyst in STR pyrolysis, the impact of various parameters has been evaluated such as the pyrolysis zone temperature,

the catalytic bed temperature, the total acidity of the catalysts and the catalyst/tire ratio. However, there is no study reporting the type of acidity leading specifically to the production of aromatics. This information would be useful to maximize the production of these high industrial value compounds. In order to reach this goal, it will therefore be necessary to use a catalyst, which, in addition to high acidity, has Lewis and Brønsted acid sites.

Considering this and that a high acidity is required to increase the aromatic concentration in the pyrolysis oil, this study proposes the use of heteropolyacid catalysts. The heteropolyacid catalysts have been previously studied in different types of reactions as esterification, transesterification, alkylation and acylation. These catalysts have been compared with conventional acid catalysts (zeolites: HY, H-Beta) and with acids such as H_2SO_4, finding in most cases better results with HPA, thanks to their high acidity.

HPAs have important disadvantages that make their use difficult, as their thermal instability and low specific surface area. Recent research has studied the use of these catalysts on supports that allow to improve these characteristics. The literature reports their uses deposited on different supports as SiO_2, SiO_2-Al_2O_3 and mesoporous materials like MCM-41 (spherical nanoparticles) and SBA-15 (hexagonal nanoparticles), for reactions such as the esterification of benzoic acid or oleic acid with methanol. From these studies, it was concluded that, in addition to an improvement in the thermal stability of these materials, they also present a greater number of acid sites, greater conversion and greater selectivity towards the desired products than the bulk HPA.

Silva & Henriquez [24] studied the use of heteropolyacid catalysts supported on MCM-41 mesoporous solids, for the alkylation reaction of toluene with 1-dodecene. They obtained supports MCM-41 and MCM-41-Al (Si/Al= 25), which were

impregnated with 20, 40 and 60 wt% of heteropolyacid ($H_3PW_{12}O_{40}$) to obtain the superacid catalysts containing mainly Brönsted sites. The catalytic tests showed that MCM-41 (Si) and MCM-41 (Si/Al = 25) supports do not have the acidic strength needed to catalyze the reaction, so the heteropolyacid is required. A higher conversion was obtained in the case of $H_3PW_{12}O_{40}$/MCM-41 (Si), than in the catalyst $H_3PW_{12}O_{40}$/MCM-41 (Si/Al = 25), increasing this conversion as the amount of heteropolyacid increased, and in turn, as measured that it is increased, greater selectivity towards the monoalkylates is obtained.

Similar results were obtained by Sazo *et al.* [25], who performed the synthesis and characterizations of catalysts based on Al-SBA-15 supporting tungsten heteropolyacid ($H_3PW_{12}O_{40}$ - HPW). The catalysts were tested in the esterification reaction of benzoic acid with methanol. The supports were synthesized with low mineral acid content (HCl), obtaining ordered mesoporous materials with good textural characteristics. They observed that the catalytic activity in the esterification reaction was greater when the HPW was impregnated on the support containing a lower amount of aluminum (Si/Al=60), with a low HPW content (10 wt%), concluding that the dispersion of the heteropolyacid, and not only the amount thereof, is an important factor to be consider in the design of these catalysts. These investigations demonstrate that impregnation with heteropolyacid improves the selectivity of the catalysts in various types of reactions.

Further research studies have shown that in addition to the acidic strength of the catalysts, the type of acid sites also has an important influence on the catalytic yields, independent of the type of reaction. One case is the research study conducted by Chai *et al.* [26, 27] and Tao *et al.*[28], who found that the Brønsted and Lewis acid sites do not follow the same reaction pathway. They obtained lower selectivities, in this case to acrolein, on Lewis acid sites [19]. A more exhaustive study on the different catalytic behaviors of the Brønsted and Lewis acid sites was performed by Alhanash *et al*. [29]. They compared a catalyst with only Brønsted acid sites and a

catalyst with only Lewis acid sites. With this comparison, they were able to find and demonstrate that catalysts with Lewis acid sites require higher reaction temperatures, although they have a higher selectivity to the product, in this case acetol.

Although the influence of the acid site type has not been discerned for STR pyrolysis reaction, these previous investigations indicate that the strength and the type of acid site of the catalysts are of great importance to obtain good catalytic yields, this suggests that for each type of reaction it is required to study the effect of each type of acidity, and the mechanism to be followed However, when supported catalysts are used, new parameters different than acidity must be considered, such as the distribution of the active phase on the support, structure and the pore size.
Chai *et al.* [27] were able to observe that the nature of the catalyst support has a great impact on its thermal stability and on the dispersion of the active Keggin-type phase. These researchers were able to conclude that the density of the active phase on the surface of the support is a key variable for the adjustment of HPA activity and selectivity.

The HPA-based catalysts have been previously studied in UCCS. Katryniok [30] studied the heterogeneous catalysis of glycerol dehydration to acrolein, using different HPA with a Keggin structure, supported on mesoporous materials. He studied the influence of several parameters on the selectivity to acrolein and acetol, such as the acidity and redox properties of the active phases, the reaction temperature and the characteristics of the support. He concluded that a good combination of heteropolyacid-support is the key to obtain good selectivities and conversions.

4.3 METHODOLOGY

The catalysts synthesis and characterization were developed in the UCCS (its acronym in French of Unité de Catalyse et du Chimie de Solide); lab of the University of Lille -1 in France, under the direction of Dr. Mickael Capron.
For the development of the catalytic tests two series of catalysts were synthesized and characterized, which will be named in this chapter as: catalysts series 1 and catalysts series 2. All catalysts consist of a heteropolyacids (active phase) supported on a mesoporous support, and were used in the pyrolysis tests using a model molecule representative of the saturated cyclic compounds (i.e. limonene) produced during the STR pyrolysis, and the pyrolysis tests using STR sample.

4.3.1 Catalysts series 1: Synthesis and characterization: Four active phases supported on a commercial support. With this series of catalysts, the goal is to evaluate the influence of the active phase type on the selectivity towards aromatics. For the catalyst synthesis of this catalyst series, four HPA were used as active phases: $H_3PW_{12}O_{40}$ (HPW - commercial), $H_3PMo_{12}O_{40}$ (HPMo - commercial), $H_4SiW_{12}O_{40}$ (HSiW - commercial) and $H_4PMo_{11}VO_{40}$ (HPMoV - synthesized.

The active phases HPW, HPMo, HWSi were purchased from Sigma Aldrich, all with a purity of 99.99%. $H_4PMo_{11}VO_{40}$ (HPMoV) was synthesized following the method described by Ressler *et al.*[31]. The synthesis protocol is shown graphically in Figure 28. 5.96 g of MoO_3 (Sigma Aldrich) and 0.34 g of V_2O_5 (Sigma Aldrich) were dissolved in 216.6 ml of distilled water. The mixture was heated under reflux at 100 ºC for 1 h. Afterwards, 31 ml of 0.12 molar solution of phosphoric acid was added in drops. The resulting mixture was heated under reflux for 3 h; after this time, the solution was left to stand at room temperature for 12 h until an orange solution was obtained. The solution was filtered and the orange solution was evaporated to obtain

about 15 ml of solution. This final solution was crystallized at room temperature for two weeks.

Figure 28. *HPMoV synthesis protocol*

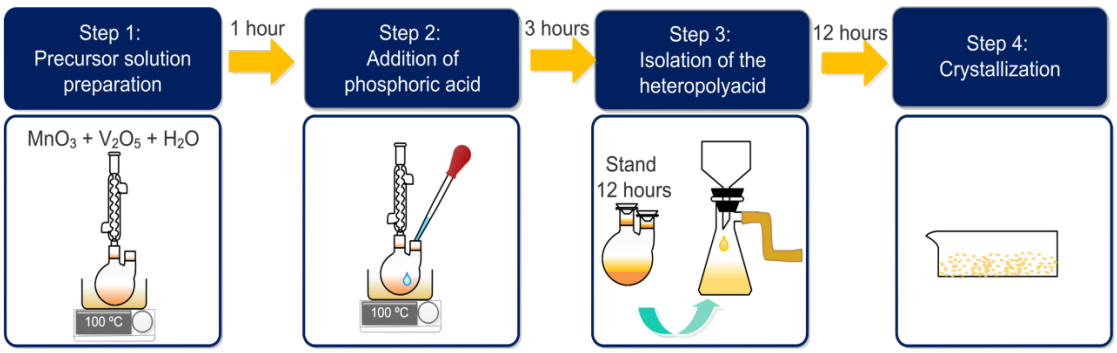

The active phases were deposited to obtain a concentration of 20 wt% on commercial silica CARiACT Q-10 (Fuji Silysia Chemical LTD) and using the wet impregnation method. The impregnation is performed by dissolving the heteropolyacid in distilled water, and then added to the support. The mixture is stirred for 3 hours, then the solvent is evaporated at 70 °C by rotoevaporation. It is immediately dried for 24 hours at 70 ° C. After impregnation, the catalyst was calcinated at 300 ºC (heating rate: 10 ºC/min) during a two-hour period. The concentration value of active phase was chosen in accordance with the previous study in UCCS by Katryniok. [30].

As for characterization, the structure of the commercial active phases has been checked using X-Ray diffraction (XRD). HPMoV synthesized was characterized by XRD and RAMAN spectroscopy to check the purity of the crystalline phase obtained. XRD was done in wide-angle scans, with 2θ range equal to 5-90º, with a step of 0.05° with a count time of 0.5 s. RAMAN test was carried out with a confocal

microscopy with magnification of 100 and an excitation wavelength of 532 nm for 20s.

To verify the presence of the active phase after impregnation, RAMAN spectroscopy was performed on the catalysts, with a confocal microscopy with magnification of 50 and an excitation wavelength of 638 nm for 20s.

The textural characteristics of the catalysts were determined using N_2 adsorption – desorption; Brunauer− Emmett−Teller (BET) surface area, pore volume and pore size were determined, over the P/P0 range 0.01−0.2. The catalysts were outgassed at 150 ºC under vacuum for 4 h. The isotherms were measured at 77.35 K in a Micromeritics Tristar II analyzer.

The total acidity and the strength of the sites were determined by NH_3 TPD using TCD and MS detectors. The tests were performed using 100mg of calcined catalyst. A pre-treatment step was applied at 150ºC for two hours. Afterwards, the adsorption was carried out at room temperature by passing 40mL/min of a mixture of 10vol% of ammonia in high purity helium for 30min. A purge with pure helium flow (5mL/min) was done to remove the physisorbed ammonia. The TPD analysis was carried out from room temperature up to 650°C (heating rate: 10°C/min) under helium flow (30mL/min). The types and the number of acid sites were determined by pyridine adsorption follow by FTIR. For this analysis, pellets of about 10-20mg of catalyst were manufactured. Each pellet was charged in the IR cell and outgassed under vacuum for 10min. Afterwards, cleaning was performed at 350°C for 3h. Pyridine (Py) was adsorbed at 25ºC for 10min (Py equilibrium 0,0016 bar). The Pyridine chemisorbed on the acid sites was followed by thermal treatment at 150, 250 and 350 ºC, under vacuum. IR spectra were recorded at each temperature with an MCT detector and a resolution of 4 cm^{-1}. The identification of acid sites was done using

the 1545 cm^{-1} band for the Brønsted acid sites and the 1455 cm^{-1} band for the Lewis acid sites. The number of both acid sites were calculated using Equation 6.

$$\eta = A * S * \varepsilon * m \qquad \text{Equation 6}$$

Where A is peak area, S is surface of the pellet, ε is extinction molar coefficient and m is the pellet mass. The ε extinction molar coefficient used was the one reported by Tamura *et al.* [32].

4.3.2 Catalysts series 2: Synthesis and characterization: One active phase supported on three supports. With the second series of catalysts, the goal is to evaluate the influence of the characteristics of the support on the selectivity towards aromatics. The active phase HPMoV, therefore the second series of catalysts was prepared with 20 wt% HPMoV on the different supports synthesized: SBA-15, MCM-41 and KIT-6.

All supports were synthesized by the procedure described in Figure 29. For SBA-15 and KIT-6 supports, a solution of Pluronic 123 triblock copolymer and HCl were used as surfactant. For MCM-41, the surfactant solutions were n-hexadecyltrimethylammonium bromide (C_{16}TMABr), ammonia and ethanol. For all supports, tetraethyl orthosilicate (TEOS) was used as the precursor of silica.

The SBA-15 support was synthesized following the protocol reported by Pirez *et al*.[33]. In a polypropylene bottle, 25 g of triblock copolymer P-123 were dissolved in 187.5 ml of distilled water and 625 ml of a 2M HCl solution. The solution was stirred at 35 °C until complete dilution. After, 2.3 ml of TEOS (Sigma Aldrich 99.9%) was added, and the solution stirred at 35 °C for 24 hours. The solution was capped and

baked in oven at 80 °C for 24 hours. The solid resulting was vacuum filtered, and washed three times with distilled water. The solid resulting from the filtration was dried at 60 °C for 12 hours. Finally, it was calcined at 550 °C, with heating rate of 1 °C/min, for 6 hours.

Figure 29. *General procedure for the synthesis of mesoporous silica supports.*

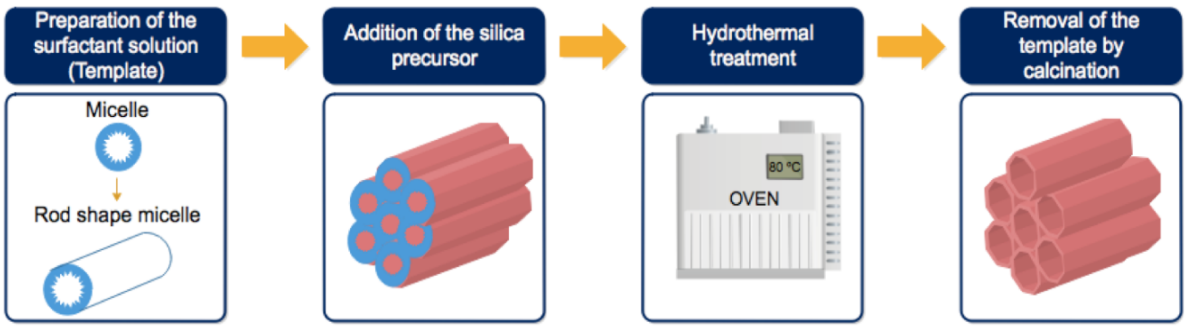

The KIT-6 support was synthesized following the protocol described by Pirez *et al.*[33]. 20 grams of triblock copolymer P-123 were dissolved in 720 ml of distilled water and 37.5 grams of HCl (36 vol%). The solution was stirred at 35 °C until the solution was homogeneous. Then, 20 g of butanol were added and stirred at 35 °C for one hour. 43 g of TEOS were then added and stirred at 35 °C for 24 hours. The solution was capped and placed in the oven at 80 °C for 24 hours. After this time, the solution is vacuum filtered and the resulting solid is dried at 100 °C for 12 hours. Finally, it was calcined at 550 ºC, with a heating rate of 1 ºC/min, for 6 hours.

The MCM-41 synthesis was performed according to the protocol reported by Grün *et al.* [34], for a homogeneous system of spheres. 15 g of C_{16}TMABr were dissolved in 300 mL of distilled water, 112 mL of aqueous ammonia (32 wt%) and 456.27 mL of absolute ethanol. The solution was stirred for 15 min for complete dilution. After 30.2 mL of TEOS were added, the resulting solution was stirred for 4 hours. The

solution was filtered. The resulting solid was washed with 100 mL of distilled water and 100 mL of absolute methanol. It was dried overnight in the oven at 80 °C. Finally, it was calcined at 550 ºC, with a heating rate of 1 ºC/min, for 5 hours.

In order to check the structure of each synthesized supports, low angle XRD and transmission electron microscopy (TEM) were performed. Low angle XRD was performed in the 2θ range 0.3−6° with a step of 0.01º. TEM images were taken in a Phillips CM12 transmission electron microscope operating at 100 kV, and the images were recorded by a SIS MegaView III digital camera.

The textural characteristics were determined for the support before and after the impregnation of the active phase, by the N_2 adsorption-desorption technique. This technique was carried out in the same way as for the catalysts of the series one (section 4.3.1).

The presence of the active phase after impregnation was checked using RAMAN, as previous section.

Total acidity was measured by NH_3TPD. Types of acid sites were determined by Pyridine adsorption-FTIR. These techniques were performed in the same way as in section 4.3.1 of this chapter.

4.4 RESULTS AND DISCUSSION

4.4.1 Catalysts Series 1 characterization.

4.4.1.1 Verification of the purity of synthesized HPMoV. Figure 30 shows the X-Ray diffractogram obtained for HPMoV which it is in agreement with that obtained by Ressler *et al.* [31] and is closed to $H_3Mo_{12}PO_{40}.13H_2O$ (PDF-00-052-1117). The difference between them, which consists only of the substitution of one Molybdenum by one Vanadium, cannot be evident using XRD.

Figure 30. *X-Ray diffractogram of pure HPMoV synthetized. In red, the PDF-00-052-1117 file corresponding to $H_3PMo_{12}O_{40}.13H_2O$.*

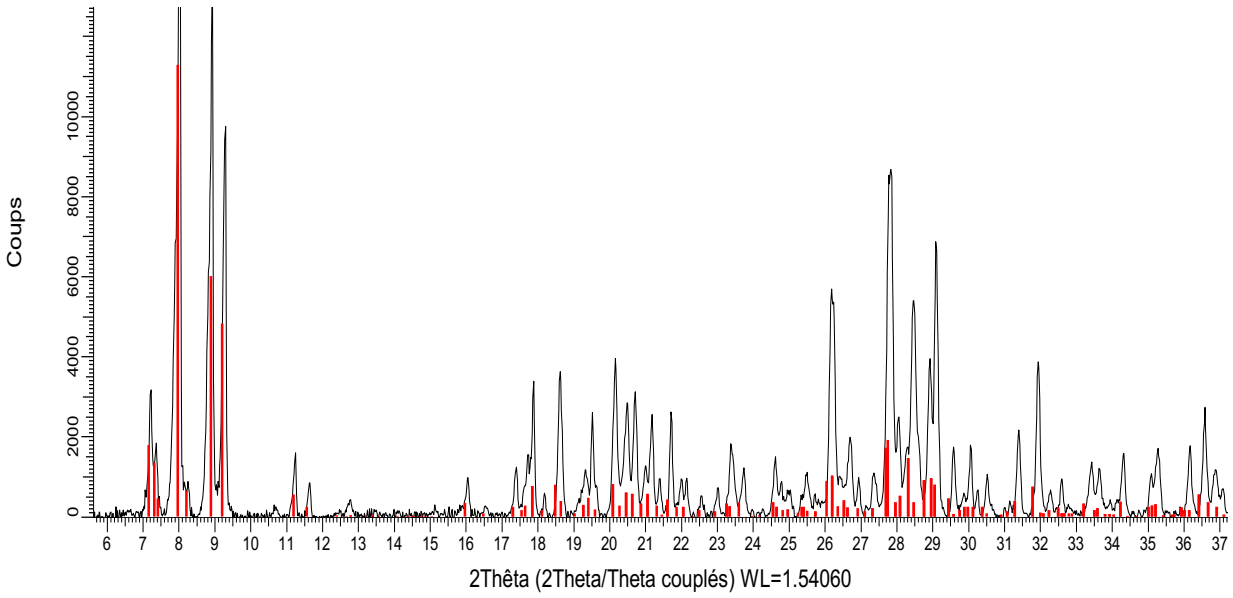

The Raman spectrum of HPMoV is presented Figure 31. It exhibits bands at 291, 670, 820 and 995 cm^{-1}, and it is in agreement with the results published by Viswanadham *et al.* [35]. This author assigned the bands at 1000 cm^{-1} to νs (Mo-

Ot), bands at 840 correspond to *v*as (Mo-Ot), bands at 670 to *v*s (Mo-Oc-Mo) and at 291 to *v*s (Mo-Oa), a characteristic band of Keggin structure (**Figure 3**).

Figure 31. *Raman spectrum of pure HPMoV synthetized.*

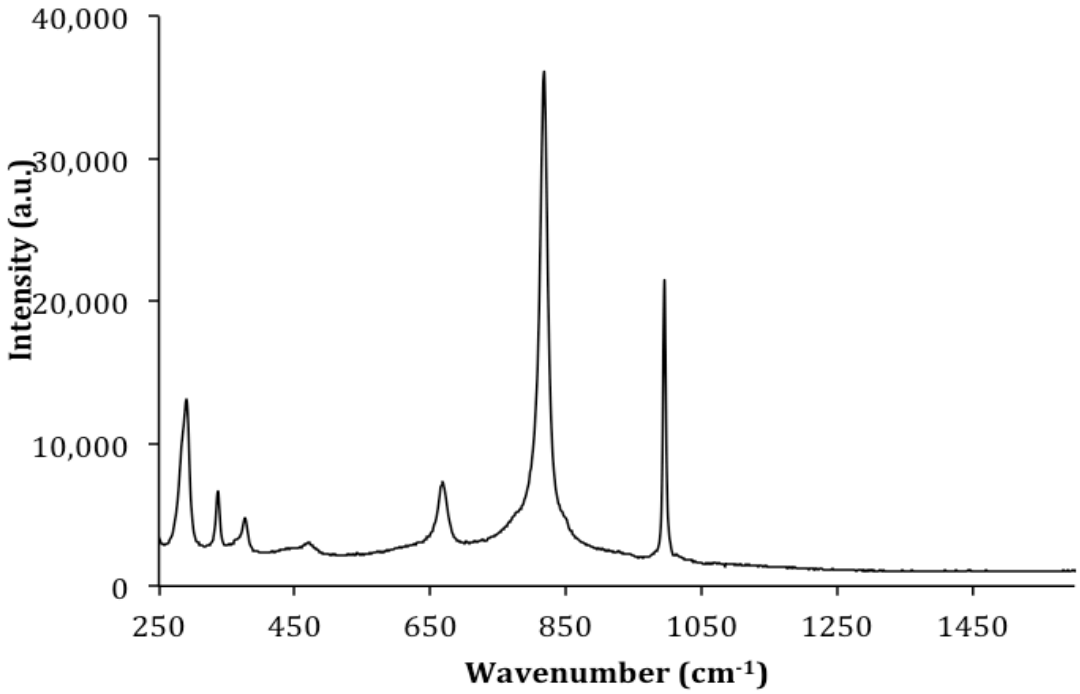

4.4.1.2 Textural Characteristics. Figure 32 shows the N_2 adsorption/desorption isotherms and the pore distribution of the fresh support and after its impregnation with the active phases. The isotherms are type IV indicating the mesoporous character of the materials. In addition, it is possible to observe that after impregnation, the isotherms are preserved, meaning that the support structure was not altered.

Figure 32. *N_2 adsorption/desorption isotherms and the pore distribution for: (a) Support Q-10 without impregnation, (b) HPMo supported on Q-10, (c) HPMoV supported on Q-10, (d) HPW supported on Q-10, (e) HSiW supported on Q-10.*

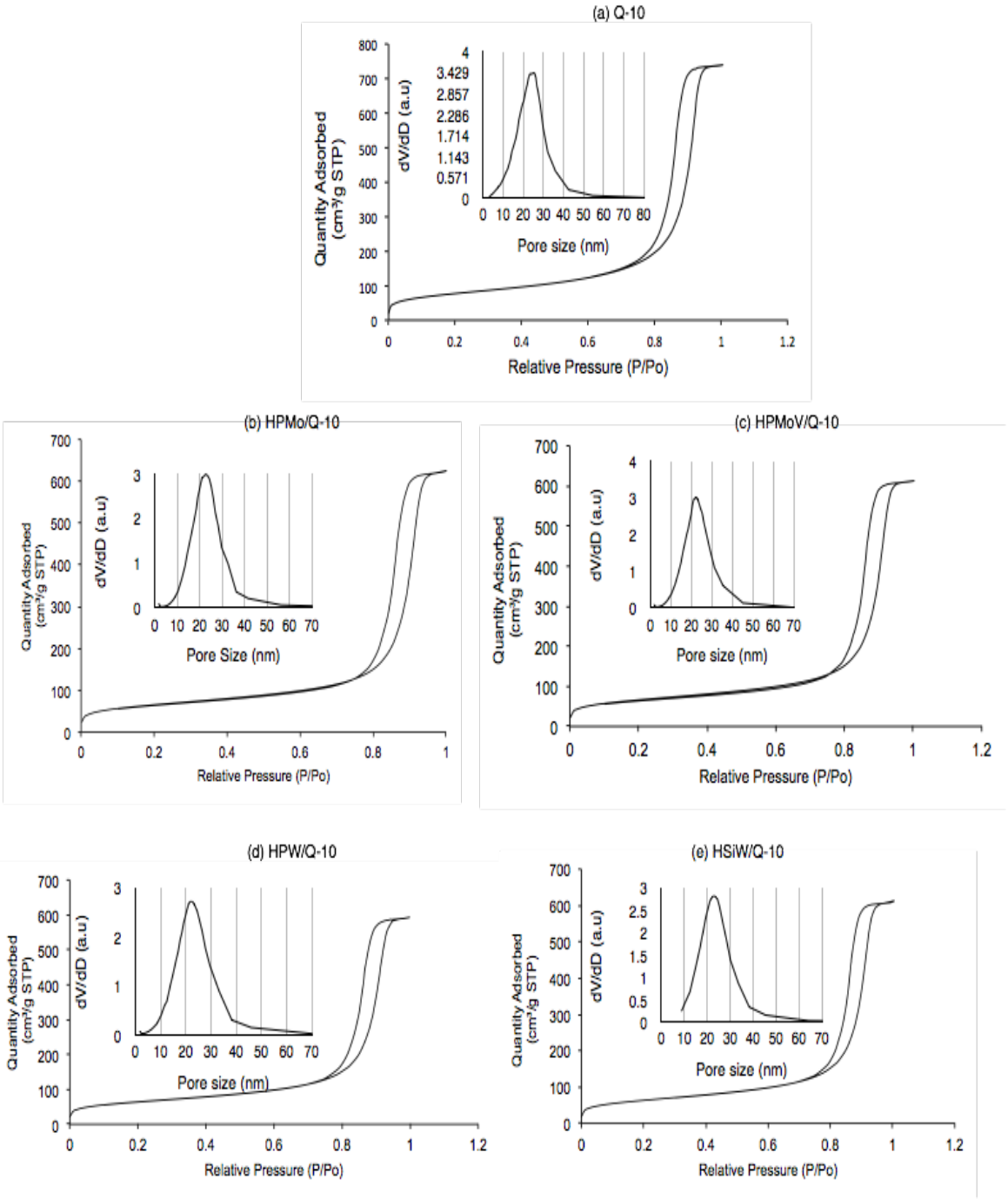

Table 14 shows the textural characteristics for the support before and after impregnation. It is noted that there is a small decrease (~17-20 %) of the specific surface area and the pore volume after impregnation of 20 wt% of the active phase. The impregnation doesn't lead to pore plugging according to Katryniok [30] for Q-10 support, thanks to its large pore diameter.

Table 14. *Textural characteristics for the support before and after impregnation of active phase.*

	BET Surface Area (m^2/g)	**Pore Volume (cm^3/g)**	**Pore Size (nm)**
Q-10	274.2	1.21	13-15.4
HPMo/Q-10	232.2	1.02	13-16.3
HPMoV/Q-10	232.6	1.01	13-16
HPW/Q-10	226.9	0.96	13-15.7
HSiW/Q-10	226.2	0.94	13-15.7

4.4.1.3 Verification of the active phase on the support after impregnation and calcination. Raman spectrums for HPMo, HPMoV, HPW and HSiW supported on Q-10 are shown in Figure 33. All catalysts present a strong band at 1000 cm^{-1} corresponding to us (Mo-Ot), which is mentioned by several authors [35–38] as a significant band of the heteropoly anion of the Keggin structure (us (Mo-Ot)), indicating that the Keggin structure of HPMoV was preserved on the surface. The spectra are in agreement with those reported by several authors [35–38]

***Figure 33**. Raman Spectrum for each catalyst: (a) HPMo/Q-10, (b) HPMoV/Q-10 and (c) HPW/Q-10, (d) HSiW/Q-10.*

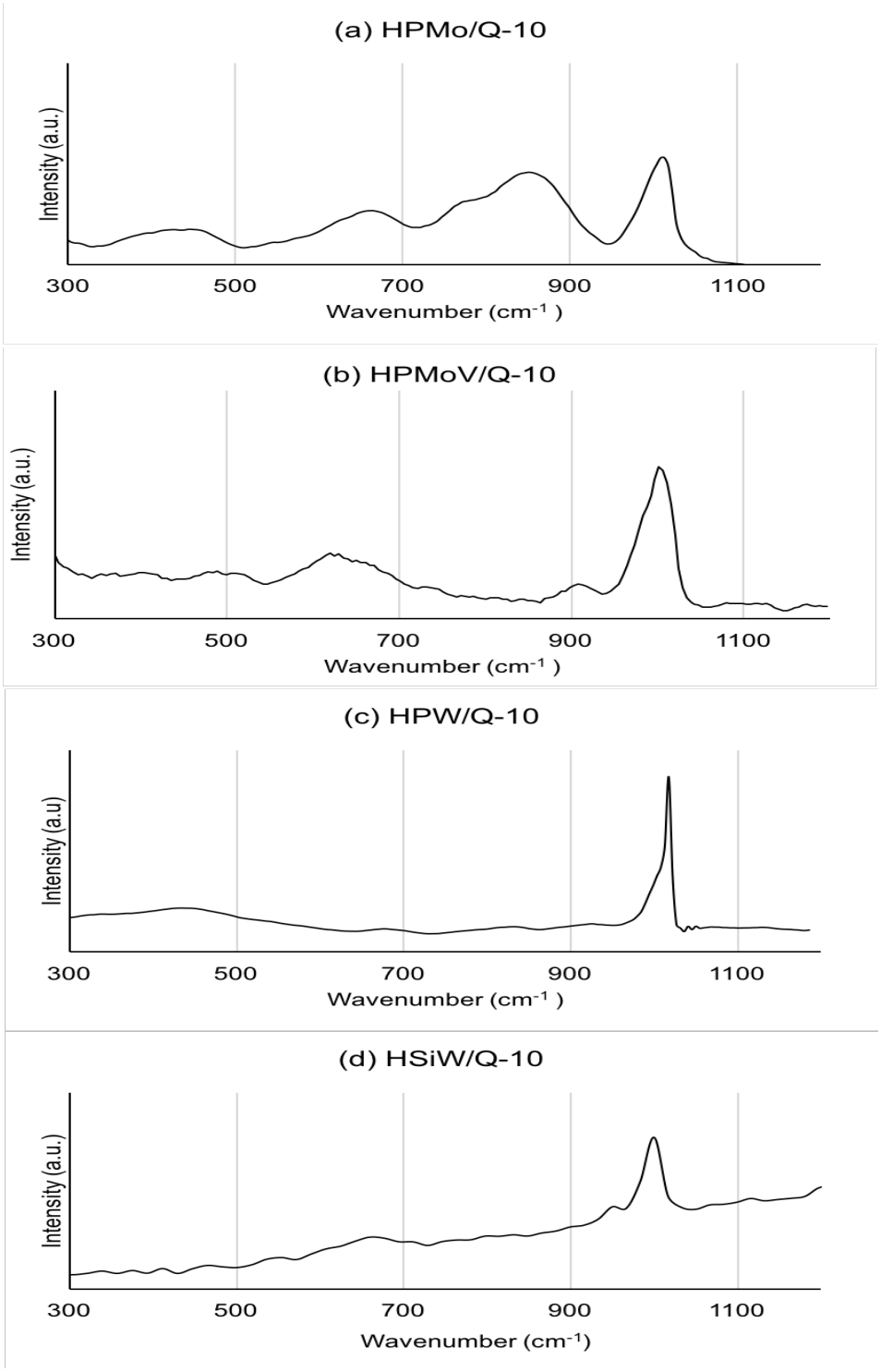

4.4.1.4 Acidity characteristics. The strength of the acid sites was determined regarding the NH_3 desorption temperature. In Figure 34, the evolution of desorbed NH_3 as a function of temperature is depicted for all catalysts. The main NH_3 desorption peak, for all catalysts, is located between 100 and 300°C (characteristic of weak acid sites). The catalysts with the highest number of weak acid sites are HPMoV/Q-10 and HPMo/Q-10 (Table 15). Although the catalyst HPW/Q-10 and HSiW/Q-10 present the lowest number of weak acid sites, and exhibiting strong acid sites characterized by NH_3 desorption peak located at 500°C.

Figure 34. *Total acidity function of temperature determined by NH_3 TPD for catalysts with different active phase on commercial silica.*

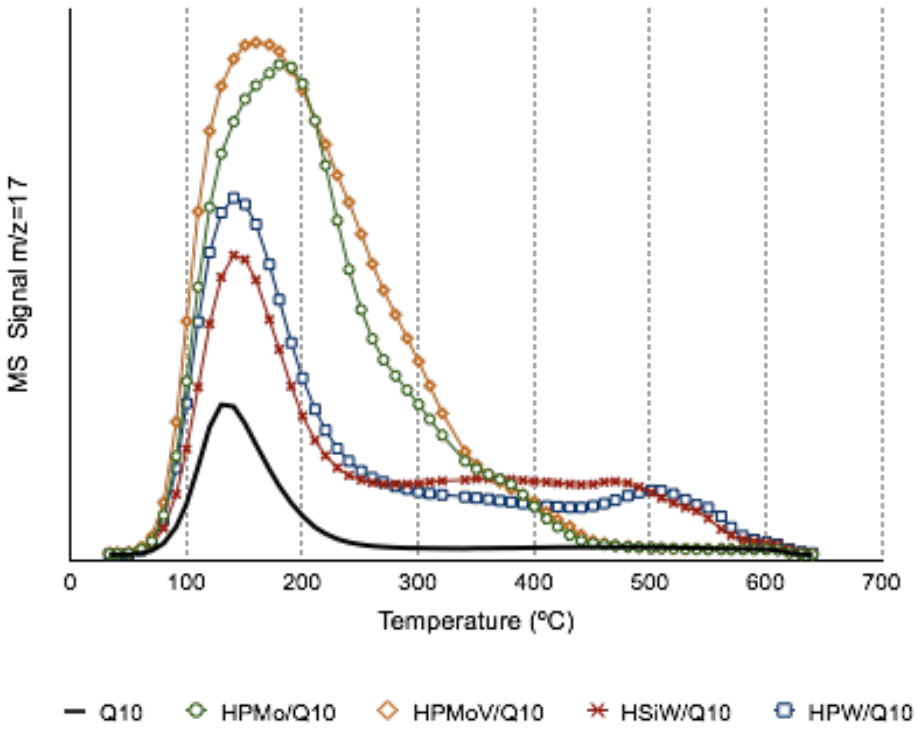

In order to complete this study, were performed pyridine adsorption follow by FTIR. The results are given in Table 15. *Total acidity and determination of Brønsted and*

Lewis acid sites number as a function of temperature for the commercial support before and after impregnation with different active phases. , for a thermal treatment at three temperatures: 150, 250 and 350 ºC, after the physical adsorption. The table shows the number of both types of acid sites (*i.e.* Brønsted and Lewis). As one can see, the scale of the two experiments mentioned above is very different (i.e. mmol/g for NH_3 TPD and µmol/g for pyridine adsorption), which is due to the fact that the pyridine adsorption is a technique that needs low pressure of pyridine to be efficient; in this way, the materials are not exposed to the same dose of probe molecules. Therefore, the NH_3 TPD experiments provide the total number of acid sites and the pyridine adsorption provides a speciation between the different types of acid sites.

Table 15. *Total acidity and determination of Brønsted and Lewis acid sites number as a function of temperature for the commercial support before and after impregnation with different active phases.*

Catalyst	Total Ammonia desorbed (mmol/g) *	Amount of pyridine adsorbed ** (µmol/g)					
		150 ºC		250 ºC		350 ºC	
		Lewis 1455 cm^{-1}	BrØnsted 1545 cm^{-1}	Lewis 1455 cm^{-1}	BrØnsted 1545 cm^{-1}	Lewis 1455 cm^{-1}	BrØnsted 1545 cm^{-1}
Q-10	0.17	0	0	0	0	0	0
HPW/Q-10	0.66	45.5	74.6	25.5	48	2.1	8.4
HPMo/Q-10	1.07	129.6	19.5	6	0	1.8	0
HPMoV/Q-10	1.20	153.9	34.9	11.8	1.5	4.6	0
HSiW/Q-10	0.59	38.9	79.5	10.9	40.3	4.8	8.3

* Determinated by NH_3 TPD.

** Determinated by pyridine adsorption-FTIR.

The HPAs provide Lewis and Brønsted acid sites to Q-10 support. For studied catalysts, the Lewis acid sites (L) are the most predominant in the case of HPMoV/Q-10 and HPMo/Q-10 catalysts, whereas the Brønsted acid sites (B) predominate in HPW/Q-10 and HSiW/Q-10 catalysts. The general evolution is the same for each catalyst; the global number of acid sites decreases with the increase of temperature in the thermal treatment. After treatment at 350°C, only the stronger acid sites remain. The HPW/Q-10 and HSiW/Q10 are the catalysts exhibiting the highest number of strong acid sites in agreement with the NH_3 TPD experiments.

4.4.2 Catalysts series 2 characterization.

4.4.2.1 Synthesized supports characterization. The low angle XRD diffractograms for the synthesized supports are shown in Figure 35.

For SBA-15 (Figure 35-a), peaks in 2θ = 0.94º, 1.62º and 1.83º are clearly identified. According to the literature, these peaks correspond to the reflections of planes 100, 110 and 200, respectively, which are characteristic of ordered hexagonal structure of SBA-15 [33, 39–43].

For MCM-41 (Figure 35-b), a large peak is identified at 2θ = 2.5 º, and two small peaks at 2θ = 4º and 4.5º, which are not clearly visible. These peaks correspond to the planes 100, 110 and 200, respectively, which also are characteristic of a two-dimensional hexagonal mesoporous structure [34, 39, 44].

Finally, for the KIT-6 support (Figure 35-c), peaks at 2θ = 1º, 1.3º and 1.90º corresponding to planes 211, 220 and 420 were identified. These planes are typical of an ordered cubic structure [45–47]. It can be concluded, then, that for the three supports, ordered structures were obtained and are in agreement with the literature [33, 34, 39, 44].

Figure 35. *Low-angle XRD patterns of the synthesized supports: (a) SBA-15, (b) MCM-41 and (c) KIT-6.*

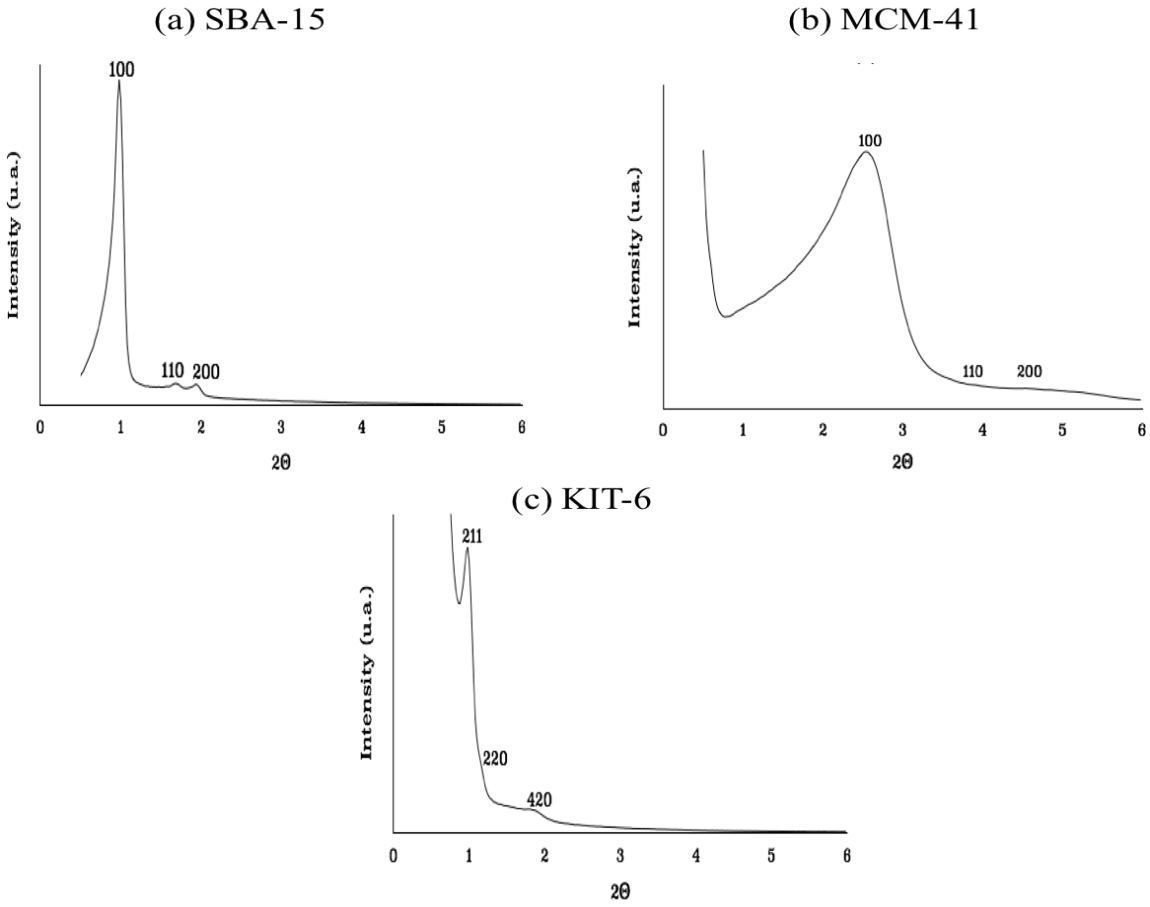

TEM microscopy was performed to corroborate the results obtained by low angle XRD and the orderly structure of each support. The supports TEM images are shown in Figure 36 for SBA-15 (a), MCM-41(b) and KIT-6 (c), respectively. In Figure 36-a, the image on the left shows a top view of the SBA-15 support, in which a very orderly structure what presented an hexagonal form. The image on the right shows a side view, in which the parallel longitudinal channels are observed. These images are characteristic of a well synthesized SBA-15 support [33, 48, 49].

Figure 36. *TEM Images of the synthesized supports: (a) SBA-15, (b) MCM-41 and (c) KIT-6.*

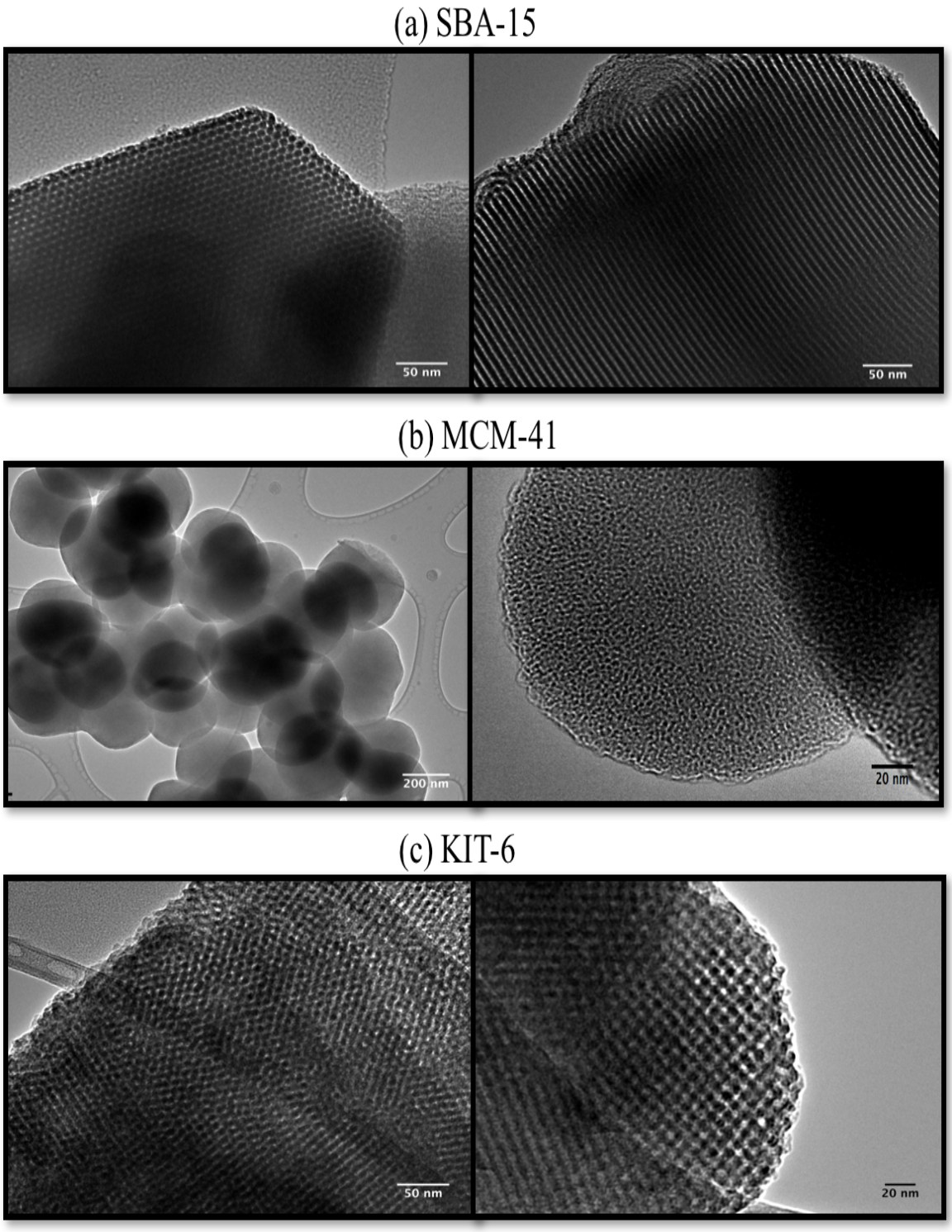

On the other hand, in Figure 36-b, the image on the left shows that spheres were obtained, which is in agreement with Grün *et al.* [34] for MCM-41 support. The figure on the right shows the top focus of a sphere, where it is possible to see the hexagonal arrangement of the channels. And in the last, Figure 36-c shows up (left) and lateral (right) views of KIT-6 support. The images are in agreement with those obtained in previous studies. The top view shows well-organized mesopores and the lateral image shows cubically interconnected channels.

Figure 37 shows the N_2 adsorption/desorption isotherms of each support obtained. The isotherms for all supports are type IV indicating the mesoporous character of the materials.

Figure 37. *N_2 adsorption/desorption isotherms for the supports: (a) Support Q-10 (commercial), (b) SBA-15, (c) MCM-41 and (d) KIT-6.*

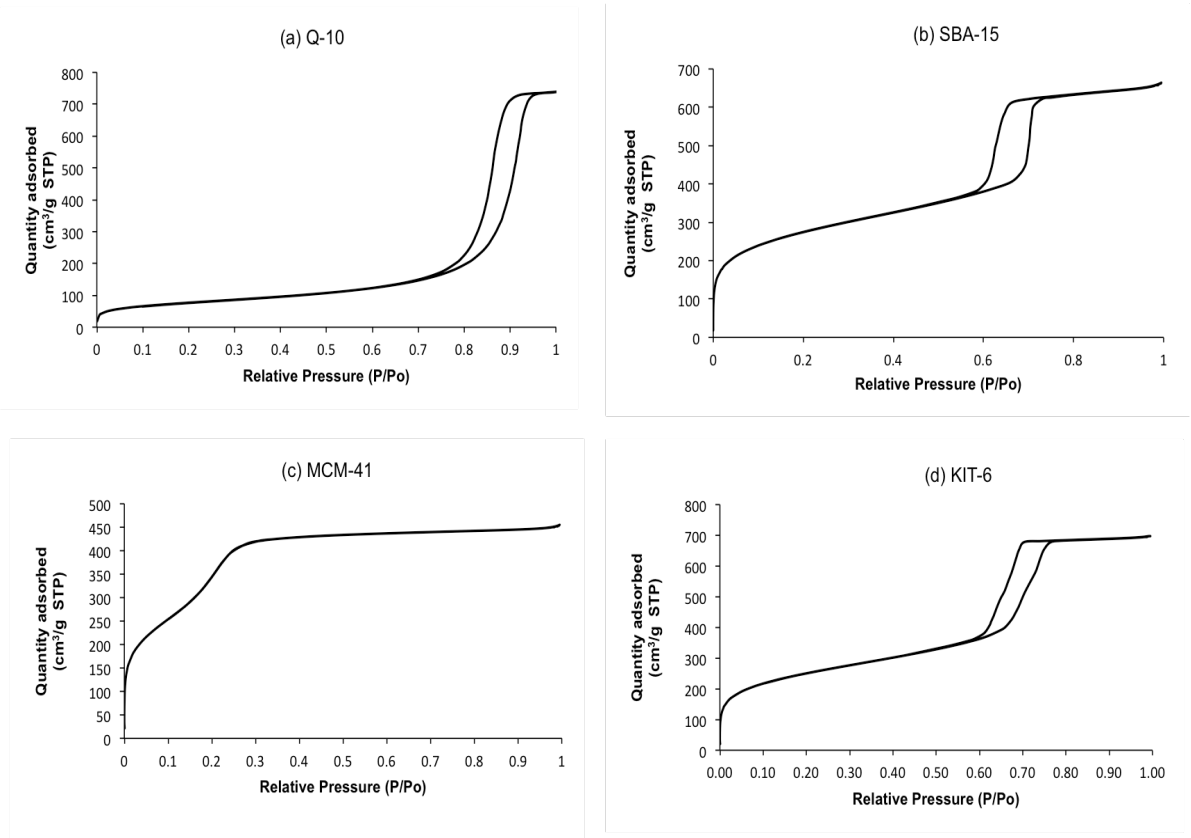

The results obtained determining the surface area, volume and pore size of the supports are presented in Table 16. All supports are mesoporous (pore diameter between 2 and 50 nm) and present great differences between their properties (pore size, surface area and pore volume). These textural characteristics are consistent with those reported in the literature [33, 34, 37, 39].

The support with the lowest surface area is the commercial support Q-10, which has the largest pore size. The support with greater surface area is MCM-41, which has the smaller pore size among all the supports. The SBA-15 and KIT-6 supports have similar characteristics in terms of surface area, pore volume and pore size, their difference is in the structure, which is hexagonal for SBA-15 and cubic for KIT-6

Table 16. *Comparison of the textural characteristics of commercial and synthesized supports.*

	BET Surface Area (m^2/g)	**Pore Volume (cm^3/g)**	**Pore Size (nm)**
Q-10	274.23	1.17	13-15
SBA-15	960.12	1.03	4.7-4.9
MCM-41	1423.90	0.70	2.24-2.36
KIT-6	880.88	1.08	5.1-5.4

4.4.2.2 Catalysts supported characterization. The results obtained in the determination of the surface area, volume and pore size of the supports after impregnation are presented in Table 17. It can be found that all supports after

impregnation exhibit a decrease of the surface area respect to the support without impregnation (Table 16); this decrease is related to the occupation of the active phase in the pores of the support.

Table 17. *Textural characteristics of the catalysts HPMoV on different supports*.

	BET Surface Area (m^2/g)	**Pore Volume (cm^3/g)**	**Pore Size (nm)**
HPMoV/Q-10	232.6	1.01	13.58 - 15.55
HPMoV/SBA-15	465.81	0.63	5.11 - 5.17
HPMoV/MCM-41	1026.91	0.49	2.23 - 2.45
HPMoV/KIT-6	584.75	0.80	5.4-5. 6

A Raman analysis was performed in order to check the presence of active phase on the support after impregnation and calcination of the catalyst. The Raman spectrum is shown in Figure 38.

All catalysts present a strong band at 1000 cm^{-1} corresponding to υs (Mo-Ot), which is mentioned by several authors [35–38] as a significant band of the heteropoly anion of the Keggin structure (υs (Mo-Ot)), indicating that the Keggin structure of HPMoV was preserved on the surface. The spectra are in agreement with those reported by several authors [35–38].

Figure 38. *Raman Spectrum for each catalyst: (a) HPMo/Q-10, (b) HPMoV/Q-10 and (c) HPW/Q-10, (d) HSiW/Q-10.*

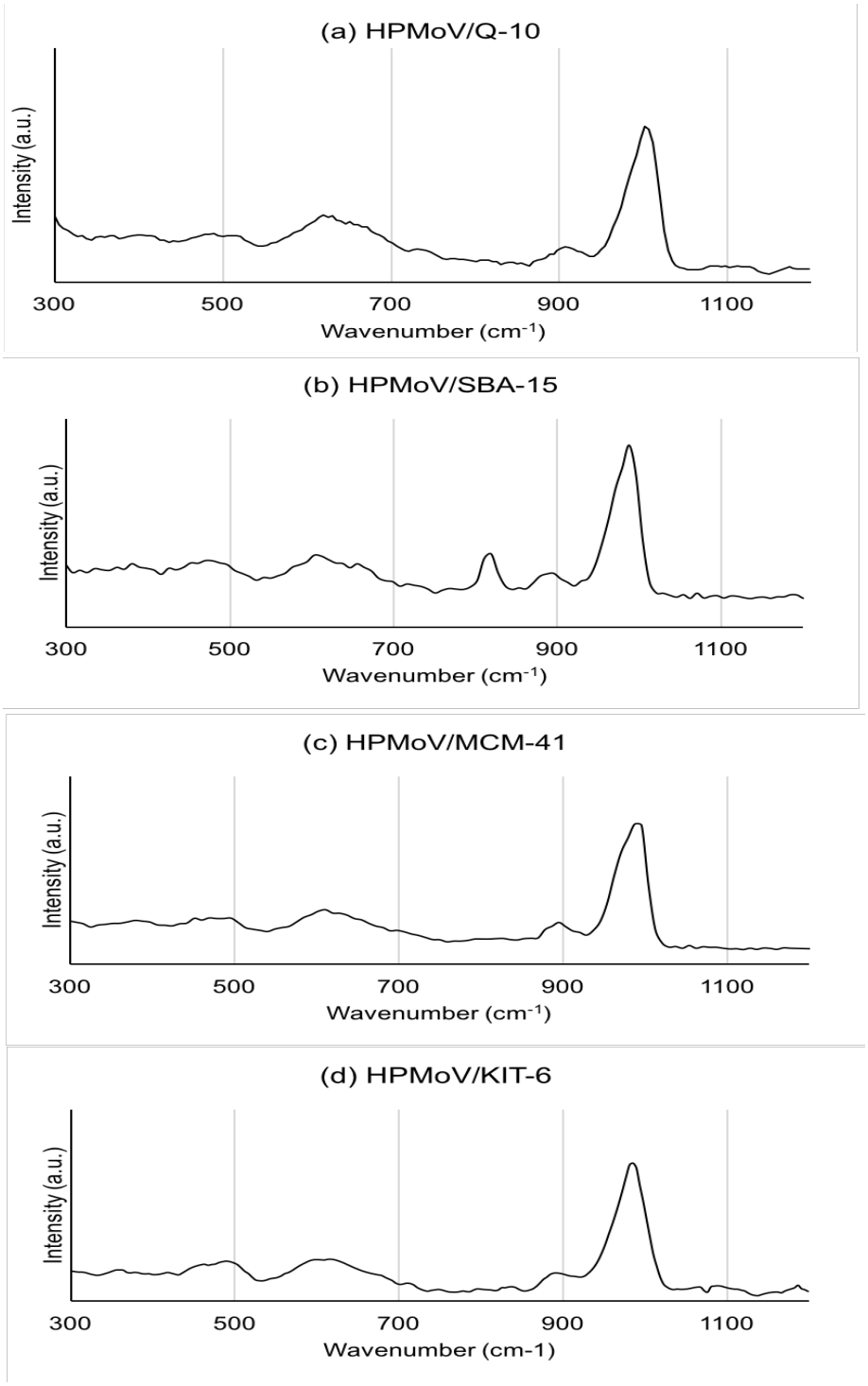

4.4.2.3 Acidity characteristics. Figure 39 shows the results of the total acidity obtained for each support after impregnation. It can be observed that the most acid support is the SBA-15. As presented in Table 18, the supports do not provide a significant acidity; it means that the active phase is mainly responsible for the acidity of the catalysts. In the evaluated temperature range, the highest number of acid sites is between 140 and 170 °C, however, this acidity is not strong and decreases when the temperature increases.

Figure 39. *Total acidity in function of temperature determined by NH_3 TPD for catalysts with one active phase on different supports.*

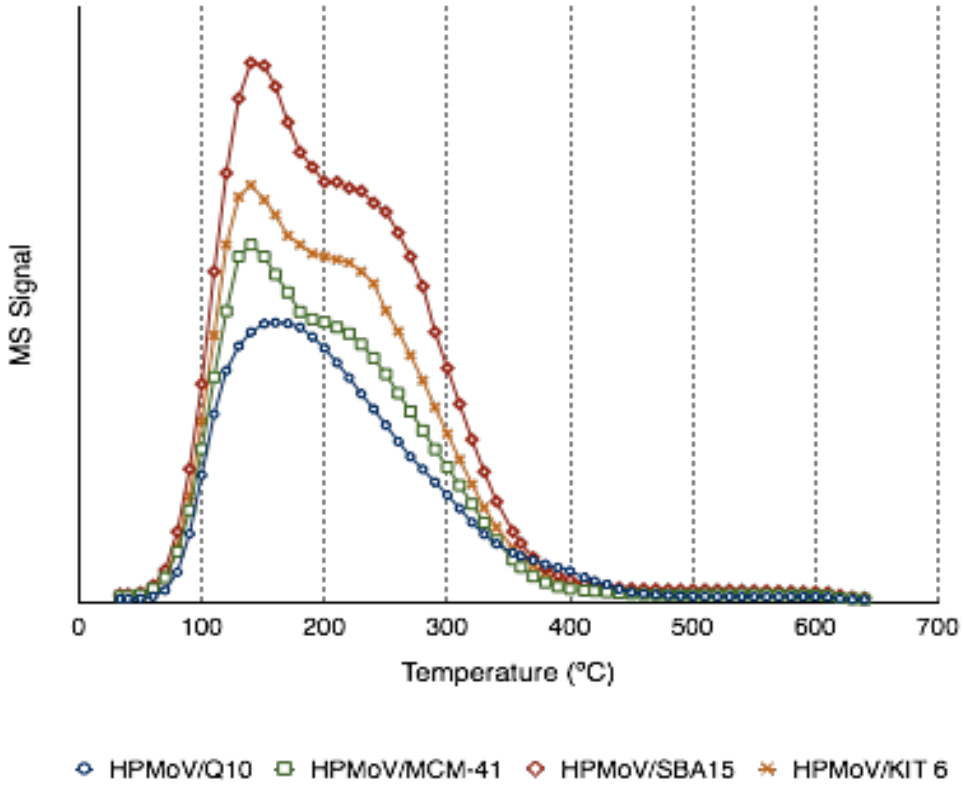

Table 18 shows the total acidity determined by NH_3 TPD and the types of acids sites present in the catalysts identified by pyridine adsorption/FT-IR after three different

thermal treatment. The results report for all catalysts that Lewis sites are predominant and their quantity is more important at low temperatures (around 150 °C).

Table 18. *Total acidity characterized by number of NH_3 desorbed and determination of Brønsted and Lewis acid sites number as a function of temperature for catalysts on different supports.*

Catalyst	Total Ammonia desorbed (mmol/g) *	Amount of pyridine adsorbed ** (μmol/g)					
		150 ºC		250 ºC		350 ºC	
		Lewis 1455 cm^{-1}	BrØnsted 1545 cm^{-1}	Lewis 1455 cm^{-1}	BrØnsted 1545 cm^{-1}	Lewis 1455 cm^{-1}	BrØnsted 1545 cm^{-1}
Q-10	0.17	0.0	0.0	0.0	0.0	0.0	0.0
SBA-15	0.51	1.9	0.3	1.3	0.6	0.6	0.1
MCM-41	0.17	0.0	0.0	0.0	0.0	0.0	0.0
KIT-6	0.10	0.0	0.0	0.0	0.0	0.0	0.0
HPMoV/Q-10	1.20	153.9	34.9	11.8	1.5	4.6	0.0
HPMoV/SBA-15	2.16	182.3	36.1	14.9	0.9	1.8	0.0
HPMoV/MCM-41	1.69	154.7	33.7	19.1	5.8	2.4	6.7
HPMoV/KIT-6	1.67	186.5	28.4	29.0	3.5	3.7	0.0

* Determinated by NH_3 TPD

** Determinated by pyridine adsorption-FTIR

It can be found a similar number of Brønsted acid sites at 150 ºC for the four catalysts studied. Comparing the HPMoV/Q-10, HPMoV/MCM-41 and HPMoV/KIT-6, which have similar acidity (TPD NH_3) in the support, a similar number of Lewis and

Brönsted acid sites was found. The HPMoV/SBA-15 catalyst has a higher number of Lewis acid sites and present the most important total acidity confirming the observed by TPD NH_3 (Figure 39). Its higher acidity can be attributed partially to the additional acidity done by support as aforementioned and shown in Table 18.

4.5 CONCLUSIONS

- The three synthesized supports were obtained with highly ordered mesoporous structure, which was confirmed by XRD, TEM and BET.

- Three different catalysts series were synthesized and characterized to be tested on the reforming of a model molecule representative of the STR rubber pyrolysis and on STR pyrolysis reactions. The different catalysts series will allow the evaluation of the active phase type influence, the textural characteristics and structure of the support and the amount of active phase impregnated in the support, toward the production and selectivity to aromatic compounds from STR pyrolysis

- For each catalysts series, the total acidity and types of acid sites were determined in order to evaluate in the reactions the influence of each type of acid site on the production of aromatics. Molybdenum based catalysts have more Lewis sites than Bronsted ones, while Tungsten catalysts have more Bronsted acid sites than Lewis ones.

- The support does not provide a significant acidity, the active phase being the supplier of the acidity of the catalyst.

.

4.6 REFERENCES OF THIS CHAPTER

[1] KYARI, Mohammed; CUNLIFFE, Adrian and WILLIAMS, Paul T. Characterization of oils, gases, and char in relation to the pyrolysis of different brands of scrap automotive tires. In: Energy and Fuels [online]. 2005, 19(3), p. 1165–1173.

[2] ISLAM Rofiqul M., et al. Liquid fuels and chemicals from pyrolysis of motorcycle tire waste: Product yields, compositions and related properties. In: Fuel [online]. 2008, 87(13–14), p. 3112–3122.

[3] HITA, Idoia, *et al*. Opportunities and barriers for producing high quality fuels from the pyrolysis of scrap tires. In: Renewable and Sustainable Energy Reviews [online]. 2016, 56, p. 745–759.

[4] ACOSTA, Rolando, *et al*. Production of Oil and Char by Intermediate Pyrolysis of Scrap Tyres: Influence on Yield and Product Characteristics. In: International Journal of Chemical Reactor Engineering [online]. 2015, 13(2), p. 189–200.

[5] LI, S.Q., *et al*. Pilot-Scale Pyrolysis of scrap tires in a continuous rotary kiln reactor. In: Industrial & Engineering Chemistry Research. 2004, (1), p. 5133–5145.

[6] OLAZAR, Martín, *et al*. Effect of acid catalysts on scrap tyre pyrolysis under fast heating conditions. In: Journal of Analytical and Applied Pyrolysis [online]. 2008, 82(2), 1p. 99–204.

[7] WILLIAMS, Paul T. Pyrolysis of waste tyres: A review. In: Waste Management [online]. 2013, 33(8), p. 1714–1728.

[8] LI, Wei, *et al*. Derived oil production by catalytic pyrolysis of scrap tires. In: Chinese Journal of Catalysis [online]. 2014, 35(2), p. 108–119.

[9] WILLIAMS, Paul T. and BRINDLE, Alexander J. Aromatic chemicals from the catalytic pyrolysis of scrap tyres. In: Journal of Analytical and Applied Pyrolysis [online]. 2003, 67(1), p. 143–164.

[10] CUNLIFFE, Adrian M. and WILLIAMS, Paul T. Composition of oils derived from the batch pyrolysis of tyres. In: Journal of Analytical and Applied Pyrolysis [online]. 1998, 44(2), p. 131–152.

[11] ARABIOURRUTIA, Miriam, *et al*. Efecto del uso de catalizadores ácidos sobre la distribución de productos en la pirólisis de neumáticos. In: Informacion Tecnologica [online]. 2010, 21(1), p. 33–41.

[12] OLAZAR, Martin, *et al*. Catalyst effect on the composition of tire pyrolysis products. In: Energy and Fuels [online]. 2008, 22(5), p. 2909–2916.

[13] BOXIONG, Shen, *et al*. Pyrolysis of waste tyres: The influence of USY catalyst/tyre ratio on products. In: Journal of Analytical and Applied Pyrolysis [online]. 2007, 78(2), p. 243–249.

[14] DŨNG, Nguyễn Anh, *et al*. Light olefins and light oil production from catalytic pyrolysis of waste tire. In: Journal of Analytical and Applied Pyrolysis [online]. 2009, 86(2), p. 281–286.

[15] NAMCHOT, Witsarut and JITKARNKA Sirirat. Impacts of nickel supported on different zeolites on waste tire-derived oil and formation of some petrochemicals. In: Journal of Analytical and Applied Pyrolysis [online]. 2016, 118, p. 86–97.

[16] WILLIAMS, Paul T. and BRINDLE, Alexander J. Catalytic pyrolysis of tyres: Influence of catalyst temperature. In: Fuel [online]. 2002, 81(18), p. 2425–2434.

[17] ARABIOURRUTIA, M., *et al*. Product distribution obtained in the pyrolysis of tyres in a conical spouted bed reactor. In: Chemical Engineering Science [online]. 2007, 62(18–20), p. 5271–5275.

[18] BOXIONG, Shen, *et al*. Pyrolysis of waste tyres with zeolite USY and ZSM-5 catalysts. In: Applied Catalysis B: Environmental [online]. 2007, 73(1–2), p. 150–157.

[19] QUEK, Augustine and BALASUBRAMANIAN Rajasekhar. Liquefaction of waste tires by pyrolysis for oil and chemicals - A review.In: Journal of Analytical and Applied Pyrolysis [online]. 2013, 101, p. 1–16.

[20] DŨNG, Nguyễn Anh, WONGKASEMJIT Sujitra and JITKARNKA Sirirat. Effects of pyrolysis temperature and Pt-loaded catalysts on polar-aromatic content in tire-derived oil. In: Applied Catalysis B: Environmental [online]. 2009, 91(1–2), p. 300–307.

[21] KNÖZINGER, H. and KOCHLOEFL K. Heterogeneous catalysis and solid catalysts. In: Ullmann's Encyclopedia of Industrial Chemistry [online]. 2009, 1, p. 2–110.

[22] MISONO, M., T. OKUHARA a N. MIZUNO. Catalysis by Heteropoly Compounds. In: Studies in Surface Science and Catalysis [online]. 1989, 44, p. 267–278.

[23] DŨNG, Nguyễn Anh, *et al*. Roles of ruthenium on catalytic pyrolysis of waste tire and the changes of its activity upon the rate of calcination. In: Journal of Analytical and Applied Pyrolysis [online]. 2010, 87(2), p.256–262.

[24] SILVA, Manuel and HENRIQUEZ, Miguel Angel. Preparación de catalizadores superácidos del tipo heteropoliacido soportados para el estudio de la reacción de alquilación de tolueno con 1-dodeceno. Thesis in Chemical Engineering. Caracas: Universidad Central de Venezuela. 2003.

[25] SAZO, Virginia, Carmen M LÓPEZ, Mireya R GOLDWASSER, Jaime FELIU a Pedro PÉREZ. Síntesis y caracterización de catalizadores HPW/AlSBA-15, y su evaluación en la reacción de esterificación del ácido benzoico con metanol. In: Avances en Ciencias e Ingeniería. 2012, 3(3), p. 1–10.

[26] CHAI, Song-hai, *et al*. Sustainable production of acrolein : Catalytic gas-phase dehydration of glycerol over dispersed tungsten oxides on alumina , zirconia and silica. In: Catalysis Today. 2014, 234, p. 215–222.

[27] CHAI, Song-hai, *et al*. General Sustainable production of acrolein : Preparation and characterization of zirconia-supported 12-tungstophosphoric acid catalyst for gas-phase dehydration of glycerol. In: Applied Catalysis A: General [online]. 2009, 353, p. 213–222.

[28] TAO, Li-zhi, *et al*. Sustainable production of acrolein : Acidic binary metal oxide catalysts for gas-phase dehydration of glycerol. In: Catalysis Today [online]. 2010, 158, p. 310–316.

[29] ALHANASH, Abdullah, KOZHEVNIKOVA Elena F. and KOZHEVNIKOV Ivan V. General Gas-phase dehydration of glycerol to acrolein catalysed by caesium heteropoly salt. In: Applied Catalysis A: General [online]. 2010, 378, p. 11–18.

[30] KATRYNIOK, Benjamin. Nouvelle voie de synthese d'acroleine a partir de biomasse. Doctoral Thesis. Lille France: Université des Sciences et Technologies de Lille. Ecole doctoral de Science de la matière, du rayonnement et de l'environnement, 2010.

[31] RESSLER, T., *et al*. Structure and properties of PVMo11O40 heteropolyoxomolybdate supported on silica SBA-15 as selective oxidation catalyst. Journal of Catalysis [online]. 2010, 275(1), p. 1–10.

[32] TAMURA, Masazumi, SHIMIZU Ken-ichi and SATSUMA Atsushi. Comprehensive IR study on acid/base properties of metal oxides. In: Applied Catalysis A: General [online]. 2012, 433–434, p. 135–145.

[33] PIREZ, Cyril, *et al*. Tunable KIT-6 Mesoporous Sulfonic Acid Catalysts for Fatty Acid Esteri fi cation. In: ACS catalysis [online]. 2012, p. 2–7.

[34] GRÜN, Michael, *et al*. Novel pathways for the preparation of mesoporous MCM-41 materials: control of porosity and morphology. In: Microporous and Mesoporous Materials [online]. 1999, 27(2–3), p. 207–216.

[35] VISWANADHAM, Balaga, SRIKANTH Amirineni and CHARY Komandur V. R. Characterization and reactivity of 11-molybdo-1-vanadophosphoric acid catalyst supported on zirconia for dehydration of glycerol to acrolein. In: Journal of Chemical Sciences [online]. 2014, 126(2), p. 445–454.

[36] PREDOEVA, Albena, *et al*. The surface and catalytic properties of titania-supported mixed PMoV heteropoly compounds for total oxidation of chlorobenzene. Applied In: Catalysis A: General [online]. 2007, 319, p. 14–24.

[37] CARRIAZO, Daniel, *et al*. PMo or PW heteropoly acids supported on MCM-41 silica nanoparticles: Characterisation and FT-IR study of the adsorption of 2-butanol. In: Journal of Solid State Chemistry [online]. 2008, 181(8), p. 2046–2057.

[38] JI, Haiyan, *et al*. Deep oxidative desulfurization with a microporous hexagonal boron nitride confining phosphotungstic acid catalyst. In: Journal of Molecular Catalysis A: Chemical [online]. 2016, 423, p. 207–215.

[39] CHEN, Ya, *et al*. Mesoporous solid acid catalysts of 12-tungstosilicic acid anchored to SBA-15: Characterization and catalytic properties for esterification of oleic acid with methanol. In: Journal of the Taiwan Institute of Chemical Engineers [online]. 2015, 51, p. 186–192.

[40] KRUK, M., *et al*. Characterization of the porous structure of SBA-15. In: Chemistry of Materials [online]. 2000, 12(7), p. 1961–1968.

[41] KUMAR, G. Satish, *et al*. SBA-15 supported HPW: Effective catalytic performance in the alkylation of phenol. In: Journal of Molecular Catalysis A: Chemical [online]. 2006, 260(1–2), p. 49–55.

[42] LI, Bing, *et al*. Ordered mesoporous Sn - SBA - 15 as support for Pt catalyst with enhanced performance in propane dehydrogenation. In: Chinese Journal of Catalysis [online]. 2017, 38(4), p. 726–734.

[43] KARIMI, Z. and MAHJOUB A. R. Efficient epoxidation over cyanocobalamine containing SBA-15 organic – inorganic nanohybrids. In: Applied Surface Science [online]. 2010, 256, p. 4473–4479.

[44] SIRIWORARAT, Kritsada; DEERATTRAKUL Varisara and DITTANET Peerapan. Production of methanol from carbon dioxide using palladium-copper- zinc

loaded on MCM-41 : Comparison of catalysts synthesized from fl ame spray pyrolysis and sol-gel method using silica source from rice husk ash. In: Jounal of Cleaner Production 2017, 142, p. 1234–1243.

[45] BENSACIA, Nabila, *et al*. Kinetic and equilibrium studies of lead (II) adsorption from aqueous media by KIT-6 mesoporous silica functionalized with -COOH. In: Comptes Rendus Chimie. 2014, 17, p. 869–880.

[46] SURESH, C., *et al*. Highly active CoMo / Al (10) KIT-6 catalysts for HDS of DBT : Role of structure and aluminum heteroatom in the support matrix. In: Catalysis Today. 2017, (January), p. 4–8.

[47] BALAKRISHNAN, Umesh, *et al*. Microporous and Mesoporous Materials Immobilization of chiral amide derived from (1 R , 2 S) - (À) -norephedrine over 3D nanoporous silica for the enantioselective addition of diethylzinc to aldehydes. Microporous and Mesoporous Materials [online]. 2012, 155, p. 40–46.

[48] RIVOIRA, Lorena, *et al*. Microporous and Mesoporous Materials Vanadium oxide supported on mesoporous SBA-15 modi fi ed with Al and Ga as a highly active catalyst in the ODS of DBT. In: Microporous and Mesoporous Materials. 2017, p. 1–18.

[49] TALEB, Abu, BHARADWAJ Saitanya K and SAIKIA Pranjal. Surfactant free synthesis of gold nanoparticles within meso-channels of non-functionalized SBA-15 for its promising catalytic activity. In: Powder Technology. 2017, 315, p. 147–156.

4.7 BIBLIOGRAPHY OF THIS CHAPTER

ACOSTA, Rolando, *et al.* Production of Oil and Char by Intermediate Pyrolysis of Scrap Tyres: Influence on Yield and Product Characteristics. In: International Journal of Chemical Reactor Engineering [online]. 2015, 13(2), p. 189–200.

ALHANASH, Abdullah, KOZHEVNIKOVA Elena F. and KOZHEVNIKOV Ivan V. General Gas-phase dehydration of glycerol to acrolein catalysed by caesium heteropoly salt. In: Applied Catalysis A: General [online]. 2010, 378, p. 11–18.

ARABIOURRUTIA, M., *et al*. Product distribution obtained in the pyrolysis of tyres in a conical spouted bed reactor. In: Chemical Engineering Science [online]. 2007, 62(18–20), p. 5271–5275.

ARABIOURRUTIA, Miriam, *et al*. Efecto del uso de catalizadores ácidos sobre la distribución de productos en la pirólisis de neumáticos. In: Informacion Tecnologica [online]. 2010, 21(1), p. 33–41.

BALAKRISHNAN, Umesh, *et al*. Microporous and Mesoporous Materials Immobilization of chiral amide derived from (1 R , 2 S) - (À) -norephedrine over 3D nanoporous silica for the enantioselective addition of diethylzinc to aldehydes. *Microporous and Mesoporous Materials* [online]. 2012, 155, p. 40–46.

BENSACIA, Nabila, *et al*. Kinetic and equilibrium studies of lead (II) adsorption from aqueous media by KIT-6 mesoporous silica functionalized with -COOH. In: Comptes Rendus Chimie. 2014, 17, p. 869–880.

BOXIONG, Shen, *et al*. Pyrolysis of waste tyres: The influence of USY catalyst/tyre ratio on products. In: Journal of Analytical and Applied Pyrolysis [online]. 2007, 78(2), p. 243–249.

BOXIONG, Shen, *et al*. Pyrolysis of waste tyres with zeolite USY and ZSM-5 catalysts. In: Applied Catalysis B: Environmental [online]. 2007, 73(1–2), p. 150–157.

CARRIAZO, Daniel, *et al*. PMo or PW heteropoly acids supported on MCM-41 silica nanoparticles: Characterisation and FT-IR study of the adsorption of 2-butanol. In: Journal of Solid State Chemistry [online]. 2008, 181(8), p. 2046–2057.

CHAI, Song-hai, *et al*. Sustainable production of acrolein : Catalytic gas-phase dehydration of glycerol over dispersed tungsten oxides on alumina , zirconia and silica. In: Catalysis Today. 2014, 234, p. 215–222.

CHAI, Song-hai, *et al*. General Sustainable production of acrolein : Preparation and characterization of zirconia-supported 12-tungstophosphoric acid catalyst for gas-phase dehydration of glycerol. In: Applied Catalysis A: General [online]. 2009, 353, p. 213–222.

CHEN, Ya, *et al*. Mesoporous solid acid catalysts of 12-tungstosilicic acid anchored to SBA-15: Characterization and catalytic properties for esterification of oleic acid with methanol. In: Journal of the Taiwan Institute of Chemical Engineers [online]. 2015, 51, p. 186–192.

CUNLIFFE, Adrian M. and WILLIAMS, Paul T. Composition of oils derived from the batch pyrolysis of tyres. In: Journal of Analytical and Applied Pyrolysis [online]. 1998, 44(2), p. 131–152.

DŨNG, Nguyễn Anh, *et al*. Light olefins and light oil production from catalytic pyrolysis of waste tire. In: Journal of Analytical and Applied Pyrolysis [online]. 2009, 86(2), p. 281–286.

DŨNG, Nguyễn Anh, WONGKASEMJIT Sujitra and JITKARNKA Sirirat. Effects of pyrolysis temperature and Pt-loaded catalysts on polar-aromatic content in tire-derived oil. In: Applied Catalysis B*:* Environmental [online]. 2009, 91(1–2), p. 300–307.

DŨNG, Nguyễn Anh, *et al*. Roles of ruthenium on catalytic pyrolysis of waste tire and the changes of its activity upon the rate of calcination. In: Journal of Analytical and Applied Pyrolysis [online]. 2010, 87(2), p.256–262.

GRÜN, Michael, *et al*. Novel pathways for the preparation of mesoporous MCM-41 materials: control of porosity and morphology. In: Microporous and Mesoporous Materials [online]. 1999, 27(2–3), p. 207–216.

HITA, Idoia, *et al*. Opportunities and barriers for producing high quality fuels from the pyrolysis of scrap tires. In: Renewable and Sustainable Energy Reviews [online]. 2016, 56, p. 745–759.

ISLAM Rofiqul M., *et al*. Liquid fuels and chemicals from pyrolysis of motorcycle tire waste: Product yields, compositions and related properties. In: Fuel [online]. 2008, 87(13–14), p. 3112–3122.

JI, Haiyan, *et al*. Deep oxidative desulfurization with a microporous hexagonal boron nitride confining phosphotungstic acid catalyst. In: Journal of Molecular Catalysis A: Chemical [online]. 2016, 423, p. 207–215.

KARIMI, Z. and MAHJOUB A. R. Efficient epoxidation over cyanocobalamine containing SBA-15 organic – inorganic nanohybrids. In: Applied Surface Science [online]. 2010, 256, p. 4473–4479.

KATRYNIOK, Benjamin. Nouvelle voie de synthese d'acroleine a partir de biomasse. Doctoral Thesis. Lille France: Université des Sciences et Technologies de Lille. Ecole doctoral de Science de la matière, du rayonnement et de l'environnement, 2010.

KNÖZINGER, H. and KOCHLOEFL K. Heterogeneous catalysis and solid catalysts. In: Ullmann's Encyclopedia of Industrial Chemistry [online]. 2009, 1, p. 2–110.

KRUK, M., *et al*. Characterization of the porous structure of SBA-15. In: Chemistry of Materials [online]. 2000, 12(7), p. 1961–1968.

KUMAR, G. Satish, *et al*. SBA-15 supported HPW: Effective catalytic performance in the alkylation of phenol. In: Journal of Molecular Catalysis A: Chemical [online]. 2006, 260(1–2), p. 49–55.

KYARI, Mohammed; CUNLIFFE, Adrian and WILLIAMS, Paul T. Characterization of oils, gases, and char in relation to the pyrolysis of different brands of scrap automotive tires. In: Energy and Fuels [online]. 2005, 19(3), p. 1165–1173

LI, Bing, *et al*. Ordered mesoporous Sn - SBA - 15 as support for Pt catalyst with enhanced performance in propane dehydrogenation. In: Chinese Journal of Catalysis [online]. 2017, 38(4), p. 726–734.

LI, S.Q., *et al*. Pilot-Scale Pyrolysis of scrap tires in a continuous rotary kiln reactor. In: Industrial & Engineering Chemistry Research. 2004, (1), p. 5133–5145.

LI, Wei, *et al*. Derived oil production by catalytic pyrolysis of scrap tires. In: Chinese Journal of Catalysis [online]. 2014, 35(2), p. 108–119.

MISONO, M., T. OKUHARA a N. MIZUNO. Catalysis by Heteropoly Compounds. In: Studies in Surface Science and Catalysis [online]. 1989, 44, p. 267–278.

NAMCHOT, Witsarut and JITKARNKA Sirirat. Impacts of nickel supported on different zeolites on waste tire-derived oil and formation of some petrochemicals. In: Journal of Analytical and Applied Pyrolysis [online]. 2016, 118, p. 86–97.

OLAZAR, Martín, *et al*. Effect of acid catalysts on scrap tyre pyrolysis under fast heating conditions. In: Journal of Analytical and Applied Pyrolysis [online]. 2008, 82(2), 1p. 99–204.

OLAZAR, Martin, *et al*. Catalyst effect on the composition of tire pyrolysis products. In: Energy and Fuels [online]. 2008, 22(5), p. 2909–2916.

PIREZ, Cyril, *et al*. Tunable KIT-6 Mesoporous Sulfonic Acid Catalysts for Fatty Acid Esteri fi cation. In: *ACS catalysis* [online]. 2012, p. 2–7.

PREDOEVA, Albena, *et al*. The surface and catalytic properties of titania-supported mixed PMoV heteropoly compounds for total oxidation of chlorobenzene. *Applied* In: Catalysis A: General [online]. 2007, 319, p. 14–24.

QUEK, Augustine and BALASUBRAMANIAN Rajasekhar. Liquefaction of waste tires by pyrolysis for oil and chemicals - A review.In: Journal of Analytical and Applied Pyrolysis [online]. 2013, 101, p. 1–16.

RESSLER, T., *et al*. Structure and properties of PVMo11O40 heteropolyoxomolybdate supported on silica SBA-15 as selective oxidation catalyst. *Journal of Catalysis* [online]. 2010, 275(1), p. 1–10.

RIVOIRA, Lorena, *et al*. Microporous and Mesoporous Materials Vanadium oxide supported on mesoporous SBA-15 modi fi ed with Al and Ga as a highly active catalyst in the ODS of DBT. In: Microporous and Mesoporous Materials. 2017, p. 1–18.

SAZO, Virginia, Carmen M LÓPEZ, Mireya R GOLDWASSER, Jaime FELIU a Pedro PÉREZ. Síntesis y caracterización de catalizadores HPW/AlSBA-15, y su evaluación en la reacción de esterificación del ácido benzoico con metanol. In: Avances en Ciencias e Ingeniería. 2012, 3(3), p. 1–10.

SILVA, Manuel and HENRIQUEZ, Miguel Angel. Preparación de catalizadores superácidos del tipo heteropoliacido soportados para el estudio de la reacción de alquilación de tolueno con 1-dodeceno. Thesis in Chemical Engineering. Caracas: Universidad Central de Venezuela. 2003.

SIRIWORARAT, Kritsada; DEERATTRAKUL Varisara and DITTANET Peerapan. Production of methanol from carbon dioxide using palladium-copper- zinc loaded on MCM-41 : Comparison of catalysts synthesized from fl ame spray pyrolysis and sol-gel method using silica source from rice husk ash. In: Jounal of Cleaner Production 2017, 142, p. 1234–1243.

SURESH, C., *et al*. Highly active CoMo / Al (10) KIT-6 catalysts for HDS of DBT : Role of structure and aluminum heteroatom in the support matrix. In: Catalysis Today. 2017, (January), p. 4–8.

TALEB, Abu, BHARADWAJ Saitanya K and SAIKIA Pranjal. Surfactant free synthesis of gold nanoparticles within meso-channels of non-functionalized SBA-15 for its promising catalytic activity. In: Powder Technology. 2017, 315, p. 147–156.

TAMURA, Masazumi, SHIMIZU Ken-ichi and SATSUMA Atsushi. Comprehensive IR study on acid/base properties of metal oxides. In: Applied Catalysis A: Genera*l* [online]. 2012, 433–434, p. 135–145.

TAO, Li-zhi, *et al*. Sustainable production of acrolein : Acidic binary metal oxide catalysts for gas-phase dehydration of glycerol. In: Catalysis Today [online]. 2010, 158, p. 310–316.

VISWANADHAM, Balaga, SRIKANTH Amirineni and CHARY Komandur V. R. Characterization and reactivity of 11-molybdo-1-vanadophosphoric acid catalyst supported on zirconia for dehydration of glycerol to acrolein. In: Journal of Chemical Sciences [online]. 2014, 126(2), p. 445–454.

WILLIAMS, Paul T. Pyrolysis of waste tyres: A review. In: Waste Management [online]. 2013, 33(8), p. 1714–1728.

WILLIAMS, Paul T. and BRINDLE, Alexander J. Aromatic chemicals from the catalytic pyrolysis of scrap tyres. In: Journal of Analytical and Applied Pyrolysis [online]. 2003, 67(1), p. 143–164.

WILLIAMS, Paul T. and BRINDLE, Alexander J. Catalytic pyrolysis of tyres: Influence of catalyst temperature. In: Fuel [online]. 2002, 81(18), p. 2425–2434.

Chapter 5

Study of the transformation of D,L limonene into simple aromatic compounds

Part of this chapter was summited recently in Journal Waste and Biomass valorization,

C. Tavera, P. Gauthier-Maradei, M. Capron, C. Pirez. Experimental study of the aromatics production from the pyrolysis of scrap tires rubber using heteropolyacids-based catalysts: an study of the transformation of D, L limonene into simple aromatic compounds.

5.1 INTRODUCTION

The tire rubber is composed by polymers: natural rubber, butadiene and styrene-butadiene, its pyrolysis yields products such as gas, char and oil. The oil composition includes aromatic, aliphatic, olefin and sulfur compounds. In accordance with

previous studies, it has been found that the species present in a higher proportion in the oil are aromatics and partially saturated cyclic compounds. The compound with the highest concentration in the pyrolytic oil is D, L limonene, which is obtained from the natural rubber (cis-1,4-polyisoprene) by the cracking of the allylic radicals on the double bond present in the polyisoprene chain and their intramolecular cyclization to obtain D, L Limonene [1, 2].

D, L Limonene is a partially saturated compound, which is classified within the group of monoterpenes. It has two enantiomers, D (dextro) and L (levo) limonene, which are naturally formed, and each has a different aroma: L-limonene smells like lemon, while the D smells like orange. Limonene is biosynthesized by plants and as a bio-product of the orange juice industry. Due to its pleasant fragrance, this compound is widely used as raw material in the manufacture of products for household cleaning and personal cleanliness, paints, fragrance additive and as a degreaser [3, 4].

In order to achieve the better yields of aromatic compounds, different studies have used catalysts in the scrap tire rubber (STR) pyrolysis, such as zeolites, bifunctional catalysts (metals supported on zeolites or silica), and pure silica [5–12]. Almost all of studies conclude that the catalysts need a high acidity to increase the aromatics concentration (i.e. mainly single ring aromatics) in the oil. Although this type of catalyst exhibits an improvement in the aromatic concentration, they present a disadvantage associated to the higher operating temperatures (up to 500 ºC). These temperatures also lead a high cracking activity, meaning a decrease in oil yield, an increase in gas yield and some coke formation; causing a rapid deactivation of the catalyst [13].

Several authors [6–8, 10, 14] have found that the STR pyrolysis without adding catalyst yields a higher amount of partially saturated cyclic compounds (mainly D, L limonene), 4-vinylcyclohexene and a non-negligible amount of aromatic compounds such as xylenes, toluene, ethylbenzene, trimethylbenzenes, cymenes and styrene. However, when a catalytic stage is added to the process, the concentration of aromatic compounds in the oil, mainly cymenes, increases while the D, L limonene concentration decreases with respect to pyrolysis without catalyst. These authors suggest a possible transformation of D, L limonene to aromatic compounds. According to Martín-Luengo *et al*. [15], p-cymene is produced by a reaction mechanism involving the adsorption of the extracyclic double bond of dipentene on the acid site, forming a primary carbonium ion, followed by displacement of the proton to form the more stable tertiary carbonium ion from which, terpinolenes, or terpinenes are formed. Finally, terpinolene or terpinenes are dehydrogenated to produce mainly p-cymene.

Taking into account the difficulties to understand the STR pyrolysis due mainly to a large and complex reaction mechanism associated to decomposition of its main polymers, and considering the information aforementioned, this part of the research study was focused exclusively on the transformation of D, L limonene to aromatic compounds over heteropolyacid catalysts as a way to increase their concentration in the pyrolytic oil. For that, the experimental tests were performed using D, L limonene at 98 wt% as model molecule, in a mixture 1:1 with the catalyst.

The evaluation of different series of catalysts, which consisted of different active phases deposited on different supports, was performed on a pyroprobe coupled to GC-FID. The different parameters, such as, the reaction temperature, type of the active phase and support, were evaluated to determine their influence on the selectivities and conversion.

5.2 STATE OF THE ART

In previous researches, D, L Limonene has been found as the major product of the STR pyrolysis. San Miguel *et al.*[16] studied its thermal degradation in a Py-GC/MS describing it as a process done by a radical mechanism, which comprises the progressive scission of the polymer chain. They report that the polyisoprene chains present in the tire are broken to produce 1,3 pentadiene and D, L limonene. This supports the aforementioned by Pakdel *et al.* [17] who proposed that the polyisoprene is thermally decomposed into isoprene, which is consequently, dimerized to dipentene in gas phase. A more detailed mechanism is mentioned by Danon *et al.*[1] and Mkhize *et al.*[18], they suggest that D, L limonene (dipentene) is the compound with the highest concentration in the oil of STR pyrolysis because it is obtained from the transformation of natural rubber (cis-1,4-polyisoprene) by two competitive reactions: 1) the cracking of the allylic radicals on the double bond present in the polyisoprene chain and their intramolecular cyclization to obtain D, L Limonene, and 2) the depropagation of allylic radicals to isoprene monomer (**Figure 20** in chapter 3) [1, 18].

Because D, L limonene is obtained from natural rubber, the tire composition has a strong influence on the amount of limonene obtained after pyrolysis, thus a higher amount of natural rubber allows a higher limonene concentration in the oil produced [1, 19]. These results were obtained by Islam *et al.*[20] who evaluated different types of tires founding considerable changes in the concentration of D, L limonene in the oil with each type of tire. They obtained an aromatic concentration of 10.95, 29.54 and 50.86 wt% for bicycle, motorcycle and truck tires, respectively; the latter beings the tire with the most natural rubber concentration while the bicycle tires have the least amount.

However, although the concentration of natural rubber in rubber tire plays an important role in pyrolysis process to yield the aromatic compounds, different operating conditions are also influential factors such as temperature, pressure and gas residence time. As for the influence of temperature, it has been possible to conclude for different studies that the concentration of D, L limonene decreases when the temperature increases. This trend is due to presence of secondary reactions at high temperatures that promote the limonene degradation and/or aromatization [1].

Table 19 shows a summary of the maximum concentrations of limonene reported by different authors at the operating temperature used. These studies report the maximum concentrations of D, L limonene in the temperature range between 400 - 500 °C [1, 5, 8, 18, 21–23]. The limonene concentration in the oil reported by different authors differs markedly.

Table 19. *Comparison of D, L limonene concentration reported by different authors.*

Author	**D, L limonene concentration (wt%)**	**Temperature (ºC)**
Laregoisti *et al.* [21]	5.12	500
Bajus *et al.* [24]	9.00	450
Arabiourrutia *et al.* [22]	23.93	425
Olazar *et al.*[8]	26.08	500
López *et al.* [23]	20.40	425
Wei *et al.* [25]	8.08	430

Danon *et al.* [1] mention that these variations are due to both the type of the tire used and the influential of operating conditions such as temperature, pressure and the reactor size affecting the gas residence time.

Mkhize *et al.* [18] studied the effect of the temperature and the heating rate on the production of D, L limonene. They found that the temperature and the heating rate as well as the interaction of these two variables influences D, L limonene yield. These authors also performed an optimization of these variables and found that the optimal D, L limonene yield is obtained at a temperature of 475 °C and heating rate of 20 °C/min; it is noted that this temperature is close to that reported in Table 19.

Another variable commonly studied is the pressure. The results of almost all studies report a higher production of D, L limonene with a vacuum pressure associated to a shorter gas residence time inside the reactor at these conditions and limiting the secondary reactions [1, 19, 26]. On the other hand, Danon *et al.* [1] explain that unzipping reactions are favored over internal cyclization reactions at reduced pressures, analogously to Le Chatelier's principle for chemical equilibria.

As aforementioned in Chapter 4, different catalysts have been used in the pyrolysis of tire rubber to increase the aromatic concentration in the oil. Different catalyst type had been evaluated such as zeolites, bifunctional catalysts (metals supported on zeolites or silica), and pure silica [5–12]. The results obtained with catalysts in the STR pyrolysis, show an increase of the aromatic compounds when the acid catalysts are used. Although an increase of the aromatic concentration in the oil has been found, it has also been observed that in all cases, the production of oil decreases while that increases for the gas. The authors conclude that this decrease of oil is associated to the increase of secondary reactions; mainly of cracking, which are favored by the acidity of the catalyst [1, 6–8, 19]. Moreover, many authors have observed that the addition of catalyst in STR pyrolysis promote the decrease of the

D, L limonene concentration while the concentration of simple ring aromatics increases.

When the catalysts are added, almost all studies report the presence of cymenes as the most important aromatic compounds in the pyrolytic oil. According to Martín-Luengo *et al.* [15], p-cymene are produced by a reaction mechanism involving the adsorption of the extracyclic double bond of dipentene on the acid site, forming a primary carbonium ion, followed by displacement of the proton to form the more stable tertiary carbonium ion from which terpinolenes, or terpinenes are formed. Finally, terpinolene or terpinenes formed are dehydrogenated to produce mainly p-cymene (Figure 40). Some authors have mentioned that the mechanism reaction for the transformation of limonene and other terpenes into aromatics, begins by an isomerization on acid sites followed by dehydrogenation of these intermediate terpenes, then the disproportionation of limonene and the intermediate terpenes, followed by dehydrogenation and in some cases it finish in polymerization [15, 27–29].

Figure 40. *p-cymene production from limonene.*

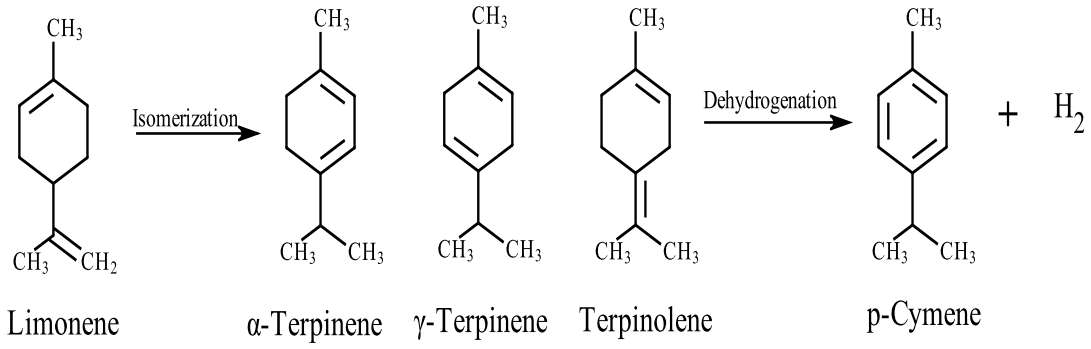

Fernandes *et al*.[28] mention that the transformation reaction of limonene carries to production of a volatile fraction and a non-volatile fraction (high-molecular weight

compounds). According with authors, the main volatile reaction products are: p-menthenes (two main isomers), alpha terpinene, gamma terpinene, p-cymene, terpinolene and isoterpinolene. Based on these results, Fernandes *et al.* propose a reaction mechanism, which is shown in Figure 41. It is based on three competitive reactions: (1) isomerization, (2) disproportionation (equimolar quantities of p-cymenes and p-menthenes) and (3) polymerization. They conclude that the primary route to p-cymene production occurred through the disproportionation of hydrogen in the dienes, in which equimolar quantities of p-cymenes and p-menthenes are obtained.

Another study about the transformation of dipentene using catalysts was performed by Du *et al.*[30]. They worked with SBA- 15 containing Al and Zn as catalysts, with different Lewis/Brønsted acid site ratios, showing that the largest amount of cymenes is obtained when the tests were performed with the catalyst having the higher number of Lewis acid sites explaining by the fact that the dehydrogenation reactions are favored in this case. However, when cracking reactions are also present, the authors observed also the presence of compounds as toluene, xylene and ethylbenzene which, the authors suppose are formed as the result of combination of cracking and dehydrogenation reactions.

Thus, the authors found differences in the p-cymene, p-menthene or aromatic compounds selectivities depending on the Lewis/Brønsted acid sites ratio and proposed a reaction pathway in which the reactions over Lewis and Brønsted sites can be explained by three steps: firstly, the reactant is isomerized to some intermediates, as reported by Martin-Luengo *et al*. [15], and subsequently, the ring is aromatized by the Lewis acid to give p-cymene. Finally, the presence of Brønsted acidity promotes the cracking reaction to produce toluene, xylenes, and ethylbenzene.

Figure 41. *Limonene isomerization/aromatization mechanisms—I: limonene, II: terpinolene, III: a-terpinene, IV: g-terpinene, V: iso-terpinolene, VI: p-cymene, VII: 1-p-menthene and VIII: 3-p-menthene, proposed by Fernandes et al.*[28].

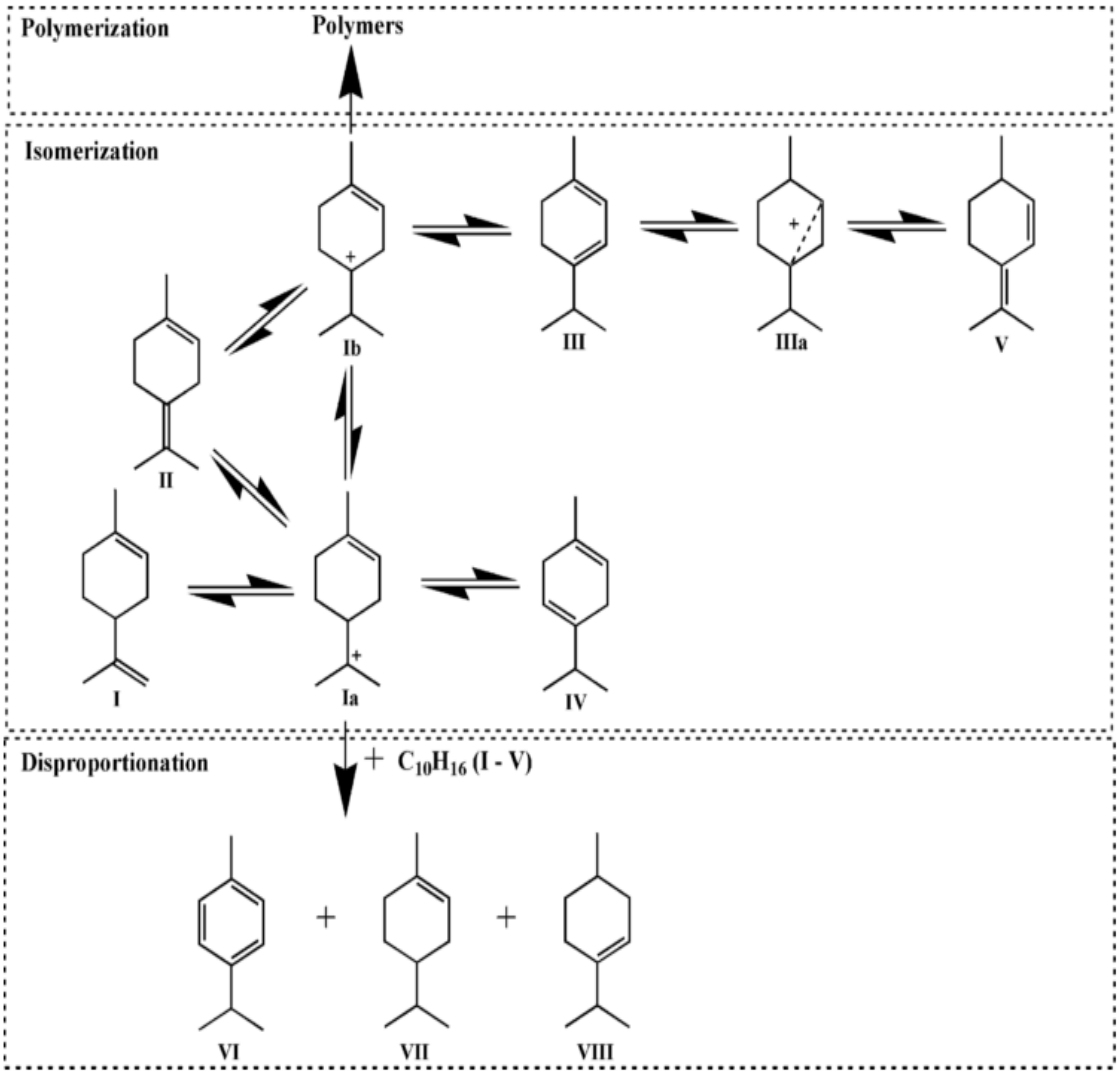

A complete pathway of the catalytic degradation of D, L limonene was presented by Ding *et al*. [31], who studied the D, L limonene transformation on a Py-GC-MS and tests three catalyst type: HY, HZ and attapulgite (PA). The authors suggest that the D, L limonene transformation into aromatic compounds is governed by a series of reactions, which are favored depending of the catalyst type. They mention that

compounds such as 1-methyl-4-(1-methyl ethyl)-1,4-cyclohexadiene (Isolimonene), 1-methyl-3-(1-methylethyl)- benzene (m-cymene) and 3-methyl- 6-(1-methyl phenyl)-cyclohexene (terpinene) are obtained in the highest concentration. They proposed a reaction pathway for each catalyst (Figure 42), which involve different kinds of reaction such as hydrogen transformation, isomerization, intramolecular diene synthesis, aromatization, demethylation and alkylation.

Figure 42. *Catalytic degradation mechanism of D, Limonene using HY, HZ and PA catalysts, proposed by Ding et al.* [31]*.*

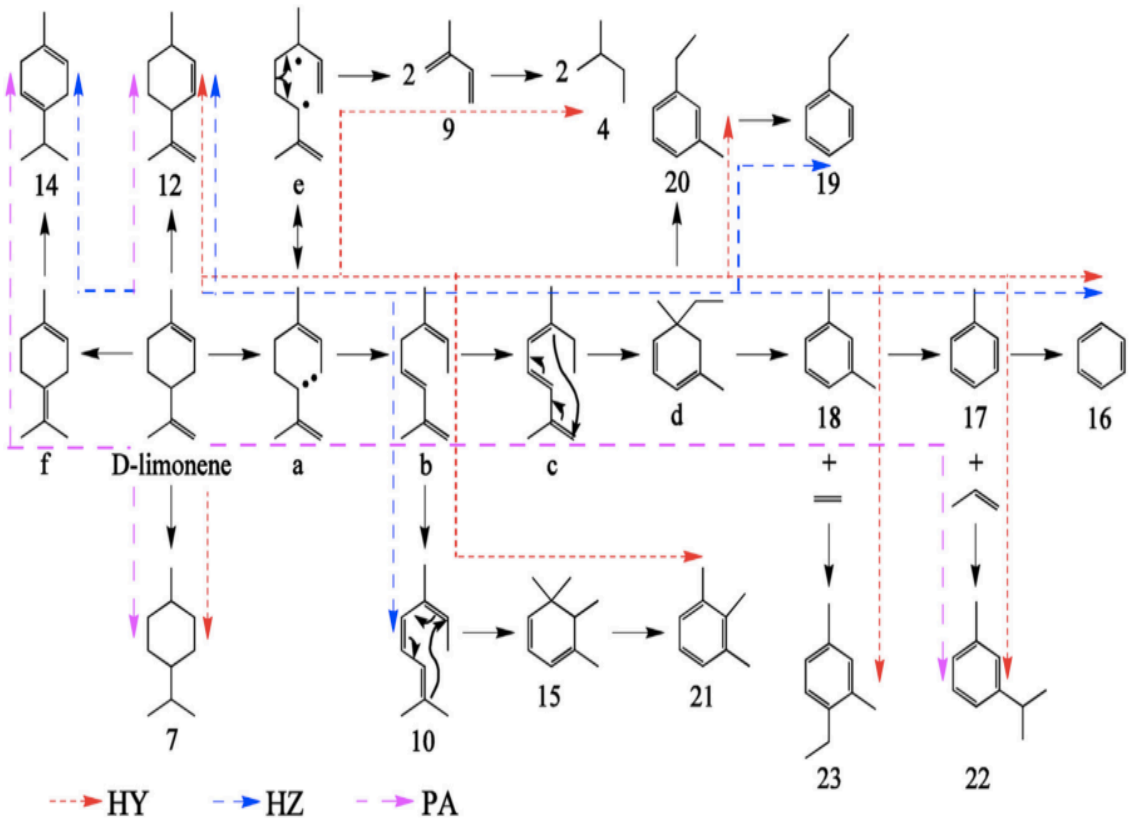

In Figure 42, it is observed that with PA catalyst, which have the lower acidity, the hydrogenation and isomerization reactions are predominates, obtaining 3-methyl-6-

(1-methylethenyl)-cyclohexene (No.12) and 1-methyl-4-(1-methylethyl)-1,4-cyclohexadiene (No. 14) and cyclohexane (No. 7). To produce aromatics, the major aromatic compound obtained with PA is m-cymene (No 22), which is produced by the alkylation reaction between toluene (No. 17) and propene meaning a decrease in xylene and toluene concentrations.

In the case of HY catalyst, only 3-methyl-6-(1-methylethenyl)-cyclohexene (No. 12) is obtained as a D, L limonene isomer, it indicates that the HY catalyst, which have the highest acidity, does not favor the isomerization reactions. On the other hand, this catalyst allows obtaining a higher aromatic concentration, it suggest that the reactions that lead to the formation of aromatics have been promoted; the single ring aromatics and polyaromatics such as indenes and naphthalenes have been obtained. Finally, HZ catalyst promotes the isomerization reactions but the isomers yield is lower than that obtained with PA catalyst. HZ catalyst also presents catalytic aromatization ability, but it is weaker than HY catalyst. Therefore, with HZ catalyst a series of ring-opening and recyclization reactions are favored, but it is weak. That is a reasonable explanation for the poor aromatization power of HZ catalyst.

Another reaction mechanism was proposed by Kamitsou *et al.*[27] They studied the use of oxide catalysts (titania) under H_2 and He atmosphere and at a temperature range between 200 and 300 °C using a fixed bed micro-reactor. They observed a complete transformation of D-limonene into p-cymene at 300 °C attributing it to high catalytic performance obtained for a good balance between the acidity and surface reducibility exhibited by the oxide catalyst. The reaction pathway proposed by Kamitsou *et al.* [27] is presented in Figure 43.

Kamitsou *et al*. (Figure 43) studied the transformation of limonene under two atmospheres: He and H_2, and they proposed a mechanism where the isomerization and disproportion take place. The limonene is initially isomerized (2), and then the

isomers undergo disproportionation (3) and finally its dehydrogenation (4). Their study shows that the yield of byproducts decreases when the reaction temperature is increased whereas the cymenes yield increases. In the presence of hydrogen, the menthenes yield are higher between 200 to 250 ° C, however at 300 °C these hydrogenated products decrease. Under He atmosphere, the yield of menthenes was decreased as the reaction temperature was increased, and the p-cymene production increased. The authors attributed this behavior to the endothermic character of dehydrogenation reactions

Figure 43. *Reaction pathways followed upon transformation of limonene to p-cymene over titania catalysts proposed by Kamitsou et al.* [27].

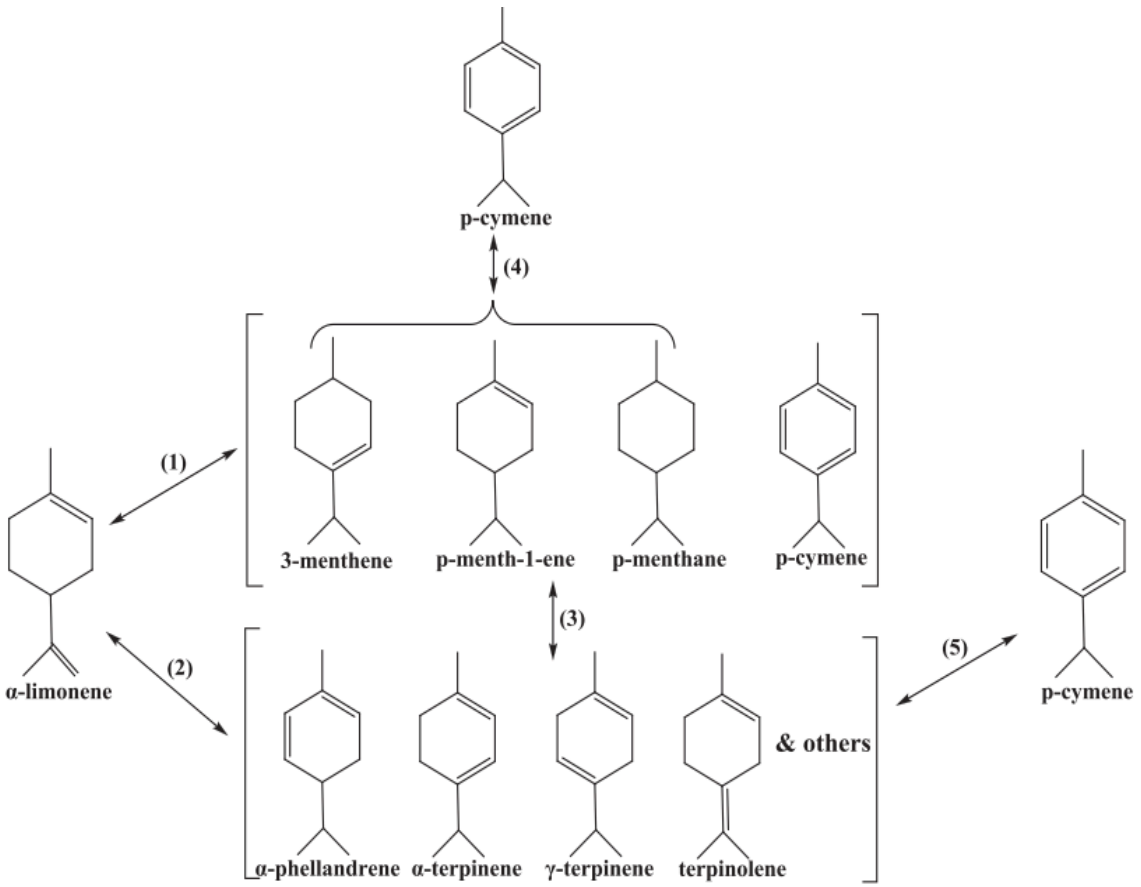

5.3 METHODOLOGY

A pyroprobe CDS 5150 coupled to a gas chromatography with flame ionization detector (Py-GC/FID) (Figure 8 in Chapter 2), and a capillary column HP-5 (30m x 0.320mm x 0.25µm) was used. The pyroprobe was programmed at initial temperature of 30°C for 0 s, until reaching a final operating temperature (see Table 20 in this chapter), at which it remains constant for 60s. The interface was programmed at initial temperature of 50 ºC, with a rate of 0ºC/min (Immediate heating), and a final temperature of 250 ºC, remaining constant during 1 min. The transfer line and the valve oven was programmed at 250 ºC. For the quantification of compounds the RRF were calculated in the same way as in chapter 3. The RRF are shown in ANNEX H.

A quartz capillary of 3 cm length and 3 mm diameter was used. The capillary was loaded as seen in the Figure 44. Approximately 5 mg of a racemix mixture 1:1 of D, L limonene (Merck-98%) were impregnated on quartz wool and placed at the bottom of the capillary. The whole sample was weighted. Subsequently, a known amount of quartz wool was added to separate the limonene and the catalyst, followed by a defined amount of this last. Finally, a new amount of quartz wool was added at the upper of the capillary. The whole sample was weighted again.

Before to begin the catalytic tests, the preliminary tests was performed in order to determine the operating conditions to guarantee no external diffusion limitations (kinetic regime). These tests were done with the catalyst HPMoV/SBA-15, at constant space-time of 1 s and at 250 ºC. According to Froment *et al*.[32] and Katryniok [33], the kinetic regime could be reached if the conversion remains constant when the flow velocity varies at a constant space-time. This last is obtained by adapting simultaneously of the catalyst weight ($W_{catalyst}$) and the initial weight of D, L limonene ($W_{limonene}$).

Referring to the internal diffusion limitations, these can be negligible using the catalysts with lower particle size. For that, the catalysts using in this study were passed through a mesh ≤ 200 µm.

Figure 44. *Loaded protocole for quartz capillary of pyroprobe coupled to GC/FID.*

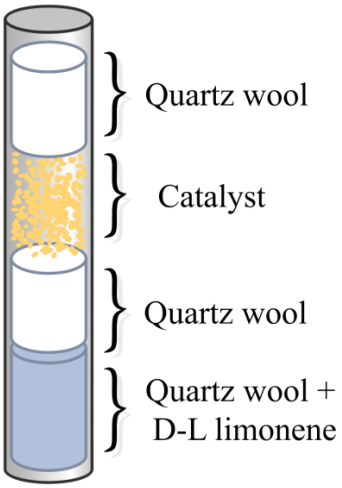

Three catalytic tests were performed to evaluate three variables: reaction temperature, active phase type and support type. The operating conditions are summarized in Table 20. In the tests Type 1, the influence of the temperature on the conversion, yield and the selectivity were evaluated with the same catalyst (HPMoV/SBA-15). In the tests Type 2, the influence of the active phase on the production of aromatic compounds was evaluated. For that, the catalysts Series 1, synthesized and characterized in Chapter 4, were used. They correspond to four active phases: HPW, HPWSi, HPMo and HPMoV, deposited at 20 wt% on the commercial support CARiACT Q-10.

In the tests Type 3, the influence of the characteristics of the support on the conversion and selectivity towards aromatics was evaluated. For that, the catalysts Series 2, which were synthesized and characterized in Section 4.3.2. of Chapter 4,

were used. They correspond to four supports: CARiACT Q-10, MCM-41, SBA-15 and KIT-6, which contained 20 wt% of the active phase that was found more selective in the tests Type 1.

Table 20. *Operating conditions and evaluated variables.*

Test	Evaluated conditions	Constant operating conditions
Type 1: Evaluation of the temperature	Four temperatures: • 180 ºC • 250 ºC • 350 ºC	• Active phase type: HPMoV • Support type: SBA-15 • Space time: 1 s • Heating rate: 20 ºC/ms
Type 2: Evaluation of the active phase type	Four active phases: • HPMo/Q-10 • HPMoV/ Q-10 • HPW/Q-10 • HSiW/Q-10	• Support type: Commercial CARiACT Q-10 • Temperature: higher conversion and aromatic yield in test Type 1 • Space time: 1 s • Heating rate: 20 ºC/ms
Type 3: Evaluation of the support characteristics	Four supports: • Q-10 • MCM-41 • SBA-15 • KIT-6	• Active phase type: More selective in test Type 1 • Temperature: 250 ºC • Space time: 1 s • Heating rate: 20 ºC/ms

5.4 RESULTS

5.4.1 Catalytic tests on pyroprobe coupled to GC-FID.

5.4.1.1 Preliminary tests for determination of kinetic regime. The results of the conversion variation at different $W_{limonene}$ at a constant space-time are shown in Figure 45. It can be seen that the conversion does not vary significantly in the range of 5-7 mg of initial limonene concluding that there are no limitations of external diffusion in this range, and indicating that the mass transfer is governed exclusively by the chemical reaction [32, 33]. On the other hand, it is necessary to clarify that due to the size of the quartz capillary, the maximum amount of catalyst is limited and thereby, it was not possible to evaluate a higher $W_{limonene}$. In addition, an amount of $W_{limonene}$ less than 5 mg was not also evaluated because the limitation of weighing equipment.

Figure 45. *Conversion of D, L limonene at different* $W_{limonene}$ *by keeping constant space-time.*

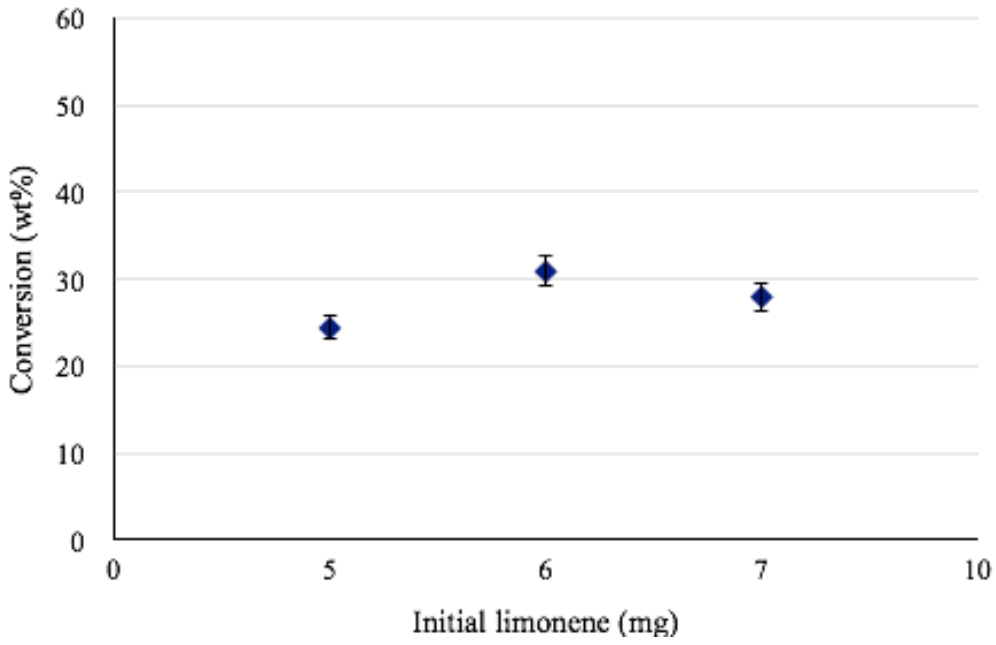

5.4.1.2 Test Type 1: Influence of temperature on the conversion of D, L limonene and the yield of products. The conversion of D, L limonene at different temperature is shown in Figure 46. It can be seen that, the conversion increases with the temperature, until reaching a maximum at 250 °C. However at 350 ºC, a decrease in conversion is observed associated probably to the decomposition of heteropolyacid, which according to Katryniok begins to decompose at 350 ºC [33].

Figure 46. *D, L limonene conversions obtained using catalyst HPMoV supported on SBA-15.*

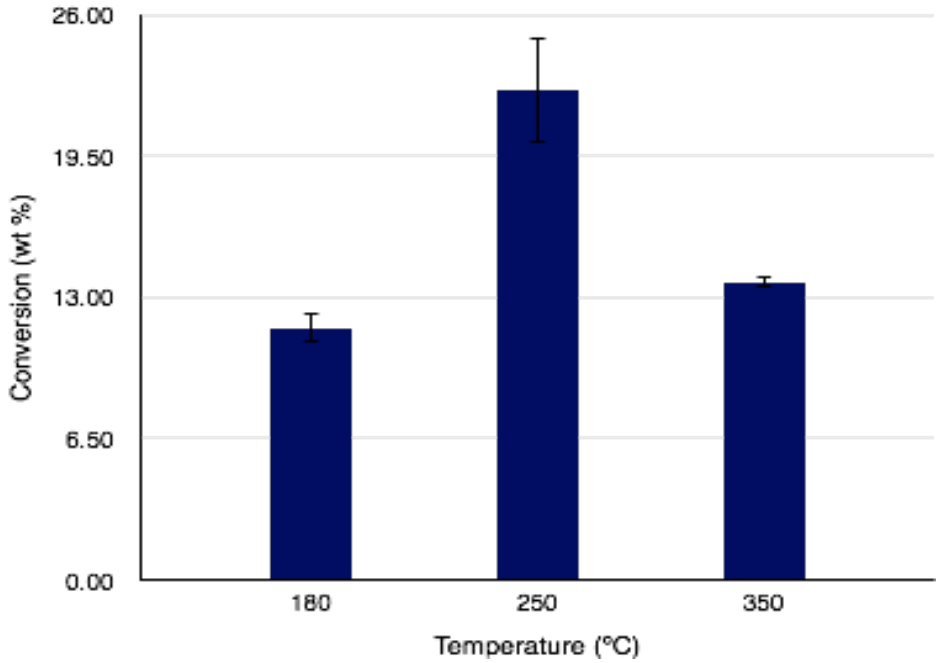

To verify the degradation temperature of the heteropolyacid (HPMoV), a TGA analysis was carried out in N_2 atmosphere, from 25 to 950 ºC (10 ºC/min). The thermogram is presented in ANNEX G. Three significant weight losses can be observed at about 70, 300 and 750 °C. The weight loss at 70 °C is attributed by several authors to crystalline water, while at 300 are related to constitutional water (protons + oxygen), which is characteristic of the beginning of the HPA

decomposition process [34–37]. It could suggest that the heteropolyacid used in this section (HPMoV) begins to be not thermally stable from 300 °C.

On other hand, according to Froment *et al.*[32] , diffusional limitations may increase as the temperature increases, seeing that they are reflected in an increase of the conversion as the temperature increases. However, although the kinetic regime in this study was evolved at 250 ºC, it can be guaranteed that at 350 ºC there are no diffusion limitations due to the fact that instead of increasing the conversion, a decrease is observed.

The yields of the products obtained from the transformation of limonene to different reaction temperatures are presented in Figure 47.

Figure 47. *Yield of products obtained by the transformation of D, L limonene using HPMoV supported on SBA-15.*

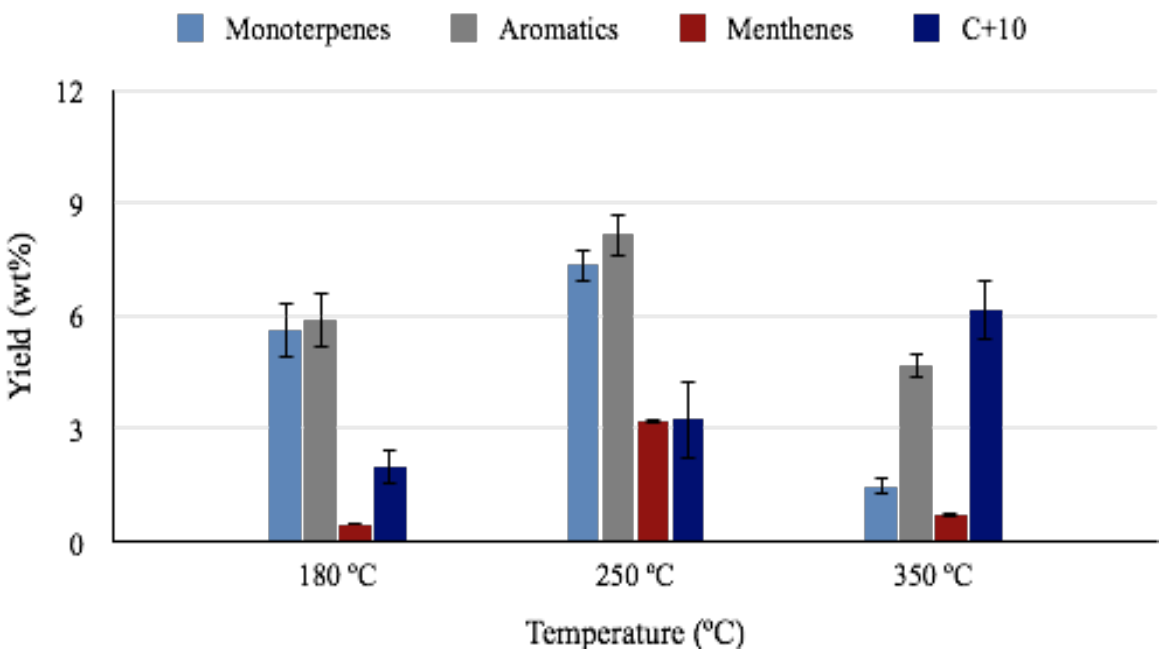

An analysis of GC-MS and GC-FID allowed to identify and quantify the compounds obtained by the transformation of limonene. The list and structure of the compounds obtained are presented in ANNEX I. The compounds with the highest concentration were classified into four groups: monoterpenes, aromatics, menthenes and C+10 (compounds with carbon numbers greater than 10). The highest yield of products is presented by aromatics and monoterpenes, and a relation 1:1 of these is obtained at 180 °C, which is maintained at 250 °C even though the yield of both increases.

Additionally, C+10 compounds have an increase as the temperature increases, this may be due to ring-opening polymerization reactions, which are favored using heteropolyzed catalysts, and which according to the results are favored when increasing the temperature.

According to the literature review, it was found that the production of aromatic compounds from limonene can follow three possible path ways (Figure 48). The route (1) is the isomerization of limonene to different monoterpenes, which are subsequently dehydrogenated, obtaining p-cymene as final product.

Route (2), involves the hydrogen transformation of limonene, followed by a diene synthesis and isomerization, and the aromatization of these isomers. With this route (2) it is possible to obtain aromatic such as trimethylbenzene, ethyl-toluene, benzene, β-cymene and xylenes as final products, and toluene as an intermediate product for the preparation of β-cymene and benzene.

Finally, route (3) involves the disproportionation of limonene to menthenes and cymene.

Figure 48. *Possible path ways for the transformation of limonene into aromatic compounds reported in the literature.*

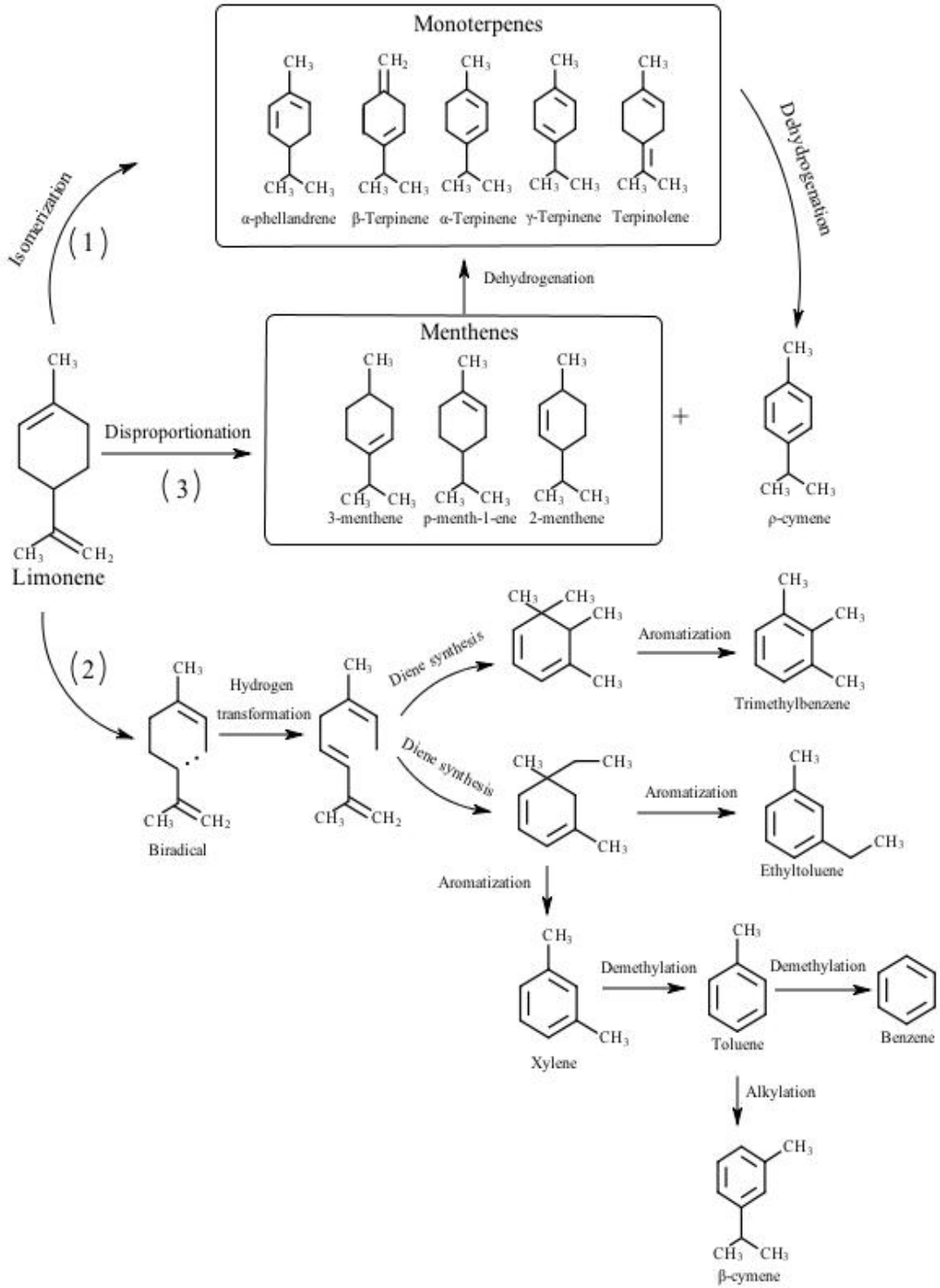

Figure 49 shows the concentration of products obtained in greater proportion and which are fundamental products to define the reaction mechanism. They were: γ-terpinene, alpha phellandrene, terpinolene, p-cymene and menthenes (3-menthene and 2-menthene). P-cymene is the predominant compound at all temperatures studied, obtaining a higher concentration at 250 ºC, and it is the only aromatic found in high concentration. Other aromatics such as ρ-α dimethyl styrene, toluene and xylenes were found in concentrations lower than 0.1% wt, while trimethylbenzene, ethyl-toluene and benzene were not found. The non-presence of these last three compounds may suggest that route (2) is not followed in its entirety since intermediate compounds of this route were not observed, only low concentrations of toluene and xylene (lower than 0.1%) that possibly do not come from this one but if not from a demethylation of the produced cymene [38].

Figure 49. *Concentration of products obtained in greater proportion using HPMoV/SBA-15.*

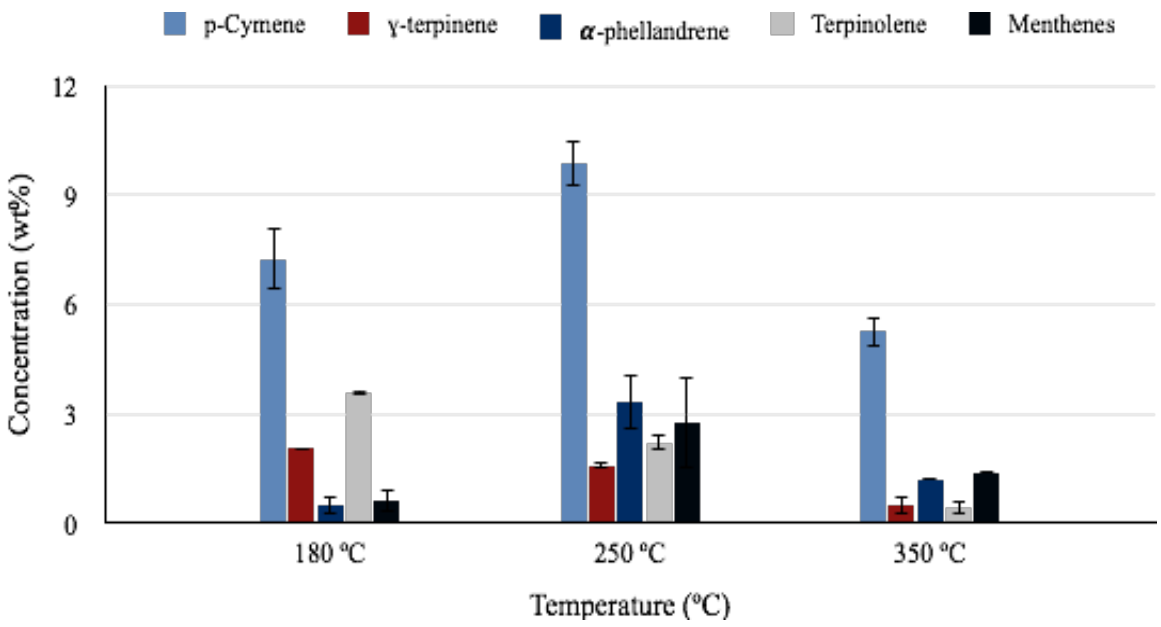

Otherwise, the presence of ρ-α dimethyl styrene, although at low concentrations, is due to the dehydrogenation of cymene [39], which proves the ability to dehydrogenation of this catalyst, leading to ρ-α dimethyl styrene as a final compound, which is not contemplated of the pathway (1) in Figure 48. This compound is obtained by isomerization of limonene and a consecutive dehydrogenation, however in this study the route is not completely fulfilled.

Regarding the obtaining of menthenes (hydrogenated compounds of terpenes), authors assigned their production by the disproportionation reaction of limonene [15, 28, 40]. However, some authors mention that when disproportionation is the dominant mechanism, the p-cymene and menthenes are formed in equal amounts, and the amount of p-cymene exceeded that of menthenes, other reactions (oxidation or hydrogenation) are taking place [28, 41].

With the results obtained in this study it is observed that at the maximum conversion temperature (250 ºC), the concentration of p-cymene exceeds approximately 4 times the concentration of menthenes, which proves that with the use of the HPMoV/SBA-15 catalyst, other paths ways different or parallel to disproportionation are carried out, as was above supposed.

The production of menthenes is possible by two routes: disproportionation or hydrogenation (in need of H_2) of either limonene or its isomers (monoterpenes). Lesage *et al*. [42] suggest that the hydrogen produced by dehydrogenation of the limonene molecule on the metallic surface could hydrogenate an adsorbed limonene molecule into p-menthane (hydrogenated compound from limonene). They tested the limonene transformation adding a hydrogen acceptor and found that it increase the yield of p-cymene (up to 92%), which according to Cui *et al*.[43] it is incompatible with the disproportionation mechanism. Cui *et al.* [43] also proposes that the hydrogenated compounds (menthane and menthenes) may be generated from the

hydrogenation with the *in situ* H_2 produced from the dehydrogenation of limonene to p-cymene. Several authors mention that with each mole of limonene that is dehydrogenated to cymene a mole of H_2 is produced [27, 42, 43].

According to the results obtained in this section we can find that at 250 ºC a p-cymene increase of 2.62% is reached while terpinolene decays 1.35% and γ-terpinene 0.43%, in addition to the non-presence of β-terpinene, which could be related to the dehydrogenation of these compounds to p-cymene. In contrast α-phellandrene increases 2.82% and menthenes 2.17%. The increase of α-phellandrene can be related to the conversion of limonene by the isomerization to this monoterpene which is favored to a higher temperature, whereas the menthenes can increase because the dehydrogenation is favored producing more amount of p-cymene and in turn of H_2, which favors hydrogenation.

As conclusion of the influence of temperature, Kamitsou *et al*. [27] suggest that the dehydrogenation reactions during the formation of cymene are endothermic and therefore, at higher temperature they are favored, which could explain the increase of p-cymene with increasing temperature. However, at 350 ºC, there is a decrease in the concentration of these compounds, which is already related to the degradation temperature of the heteropolyacid, limiting further the temperature increase to obtain higher yields of cymene. Therefore, the operating temperature most favorable is 250 °C.

Jaramillo *et al.* [40] studied the aromatization of α-pinene using HPW heteropolyacid catalyst supported on a mesoporous silica. As intermediates of this reaction, limonene is obtained, which, as already mentioned above, can be dehydrogenated to p-cymene. These authors concluded that the reaction of isomerization may be catalyzed by the acid sites, while in the dehydrogenation sites as well as the redox ones are influence. However, bearing in mind that heteropolyacid catalysts have two

types of acid sites, no reference is made to the type of acidity required for isomerization and dehydrogenation. for this reason, it is decided to evaluate different types of heteropolyacids, which will be presented in section incoming.

5.4.1.3 Test Type 2: Influence of the active phase on the conversion, yield and selectivity toward aromatics. As mentioned in the previous section, it was decided to evaluate different heteropolyacids, which according to the characterization carried out (see Table 15 in Chapter 4) have different Lewis/ Brønsted ratios, in order to determine the type of acidity required for the transformation of limonene.

The conversion obtained with the various active phases supported on the commercial support Q-10 are presented in Figure 50.

Figure 50. *Conversion of D, L limonene obtained with different active phase on commercial silica Q-10 at 250 ºC.*

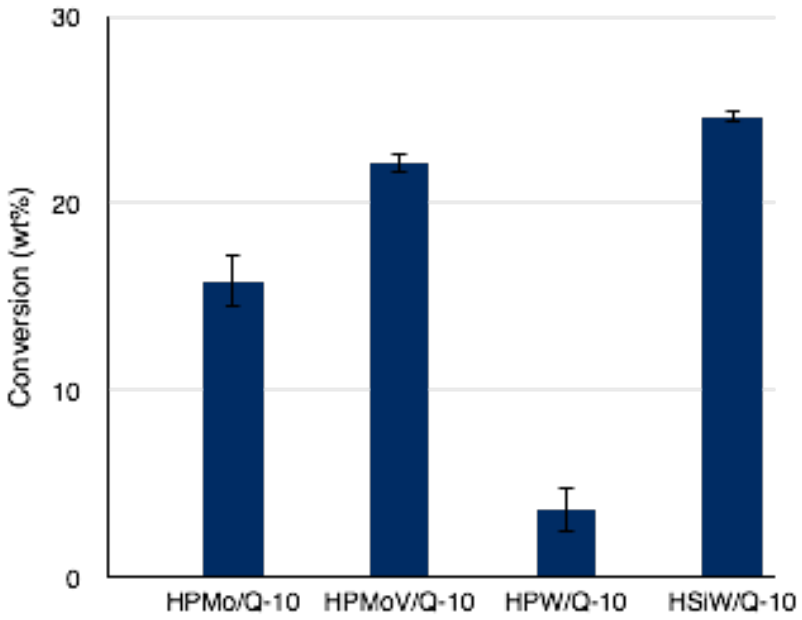

It can be seen that the highest conversion was obtained with HSiW, on the contrary, the HPW catalyst has a lower conversion compared to other active phases. In addition, conversions obtained with the active phases HPMoV and HPMo are similar, being the conversion of HPMoV / Q-10 slightly higher, being within the range of error.

Comparing the three active phases with the same central phosphorus atom (HPMoV, HPMo and HPW), a first observation can be made about the influence of the type of acidity on the conversion of D, L limonene, finding that strong acidity (Brønsted type), which is found predominantly in HPW (Table 15 in Chapter 4), does not favor conversion of D, L limonene. Now, comparing the two catalysts with similar acidic sites, it can be found that HSiW has higher conversion despite having the same acidity, which may be related to the type of central atom.

The compounds in greatest proportion found with all phases were the same presented in the previous section, therefore the yields of each will not be presented, and it is preferred to evaluate the selectivities in order to be able to determine the mechanism of reaction and the influence of acidity. The selectivity of each of the products is presented in Figure 51.

The most selective catalyst towards p-cymene was the active phase HPMo, followed by HPMoV. Moreover, although the HSiW/Q-10 catalyst showed high conversion, the selectivity of this catalyst is lower than those containing molybdenum. It was observed that the conversion of HSiW/Q-10 was mainly directed to C+10 compounds (about 12 wt% of yield), which can be obtained by ring-opening polymerization, which is due to the strong acidity of Brønsted sites, which are predominant in these catalysts (Table 15 in chapter 4).

Figure 51. *Selectivity toward the products obtained with different active phases on commercial silica Q-10 at 250 ºC.*

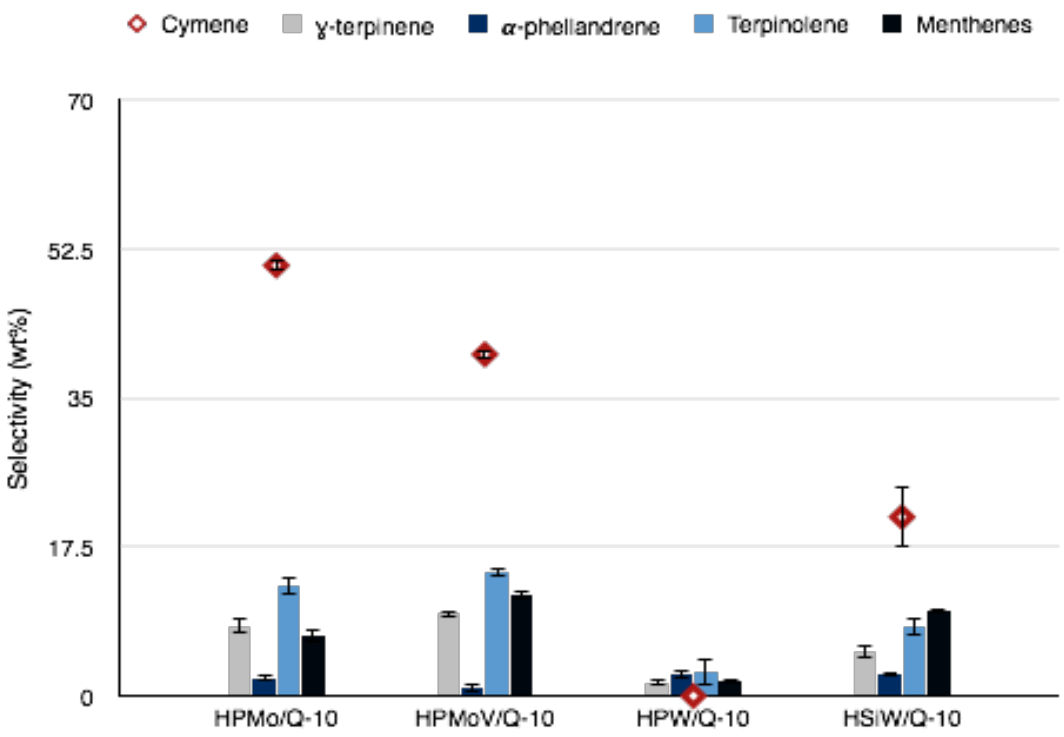

As for the selectivity toward p-cymene, which is the product of highest interest, it is observed that Lewis is required to produce p-cymene, this decreases when the isomerization products of limonene decrease (HSiW), and in the case of HPW having very low quantity of isomerization products, the amount of p-cymene obtained is zero. This may indicate that for the production of p-cymene, the presence of isomerization products is required, which corroborates the mechanism of production of p-cymene by dehydrogenation after the isomerization of monoterpenes, and which is also favored by the Lewis acidity. However, it may be noted that although the monoterpene selectivity is similar for the HPMo and HPMoV catalysts, the amount of p-cymene obtained is different. This could indicate that possibly not only the dehydrogenation of the monoterpenes is the cause of the production of p-

cymene, and/or another characteristic different to the acidity type influences the selectivity toward cymene.

As for another production route of cymene, it is observed that the only selectivity that decreases when increasing the selectivity towards p-cymene is that of menthenes (with HPMo catalyst). This could indicate that the cymene could also be obtained from menthenes by a dehydrogenation reaction. This is in accordance with the mechanism proposed by Kamitsou *et al.*[27] of the transformation of limonene over oxide catalysts.

As for a characteristic that can influence the selectivity of p-cymene, it can be found that in addition to the high Lewis acidity, a possible Lewis/Brønsted (L/B) ratio may be fundamental to favor the dehydrogenation reaction. It is found that the HPMo catalyst has a higher L/B ratio (6.64) compared to HPMoV (4.40), which may indicate that when there is a lower ratio of L/B acid sites, there is a larger number of Brønsted acid sites, which could lead to polymerization reactions for the production of C+10 compounds, in which p-cymene may be involved, which directly leads to a decrease in their yield and selectivity. Moreover, although the HSiW/Q-10 catalyst showed high conversion, the selectivity of this catalyst is lower than those containing molybdenum, and it was observed that its conversion is mainly directed to C+10 (about 12 wt%), which can be obtained by ring-opening polymerization, which is due to the strong acidity of Brønsted sites, which are predominant in these catalysts. It is also observed that with the two acid catalysts with higher acidity of Brønsted than Lewis, the selectivity towards p-cymene and monoterpenes is lower than those with higher Lewis acidity than Brønsted, which confirms the fact that for isomerization, an acidity of Lewis above that of Brønsted is required.

Besides, the poor isomerization capacity of HPW compared to HSiW is observed, indicating that the central atom has a marked influence on the isomerization capacity

and no only the acidity. This higher isomerization capacity of HSiW with respect to HPW has also been reported by different authors in reactions of isomerization of butane and n-hexane [44, 45]. According to Pinto *et al*. [44], is related to the fact that higher amount of protons in HSiW are probably compensated by a higher strength of those of HPW, and the selectivity of isomerization vs. cracking depends on the nature of the HPA engaged. Thomas *et al.* [46] compared HSiW and HPW by H MASS NMR and found that HSiW in its protonated form is stable at a higher temperature than the HPW. Legagneux *et al.* [47] explains this fact in supported HPW; three protons react with silanol groups of the support by an acid-base mechanism on impregnation, limiting the catalytic activity of HPW, while for the supported HSiW, at least some anhydrous protons remain unreacted, leading to the increase in activity. With this it can be concluded that the HSiW catalyst is also found to be more convenient for limonene isomerization reactions than the HPW catalyst.

As for the isomerization of products from limonene, it can be observed that the presence of terpinolene, followed by γ-terpinene, is mostly obtained for the three catalysts. The most selective catalysts for these products are HPMo and HPMoV, in almost the same amount, which is related to their high isomerization capacity due to their Lewis acidity, as already aforementioned. The fact of finding a higher concentration of terpinolene can be explained from carbenium ion (terpinyl carbenium), which is derived from limonene by the action of acid sites [48, 49], the hydrogen shifts easy occurs to terpinolene, and then the hydrogen is displaced by each bond inside the ring, obtaining as second isomer the γ-terpinene. A graphic explanation of this isomerization mechanism is presented in Figure 52. In the results obtained in this study, α-terpinene were obtained in low concentration (less than 0.1 wt%), whereas β-terpinene is practically zero with all catalysts. This indicates that the isomerization path followed by these catalysts, and showed in Figure 52, is route (a), while route (b) is poorly favored and hardly the hydrogen shifts reaches the α-terpinene.

Figure 52. *Mechanism proposed for limonene isomerization by hydrogen shift.*

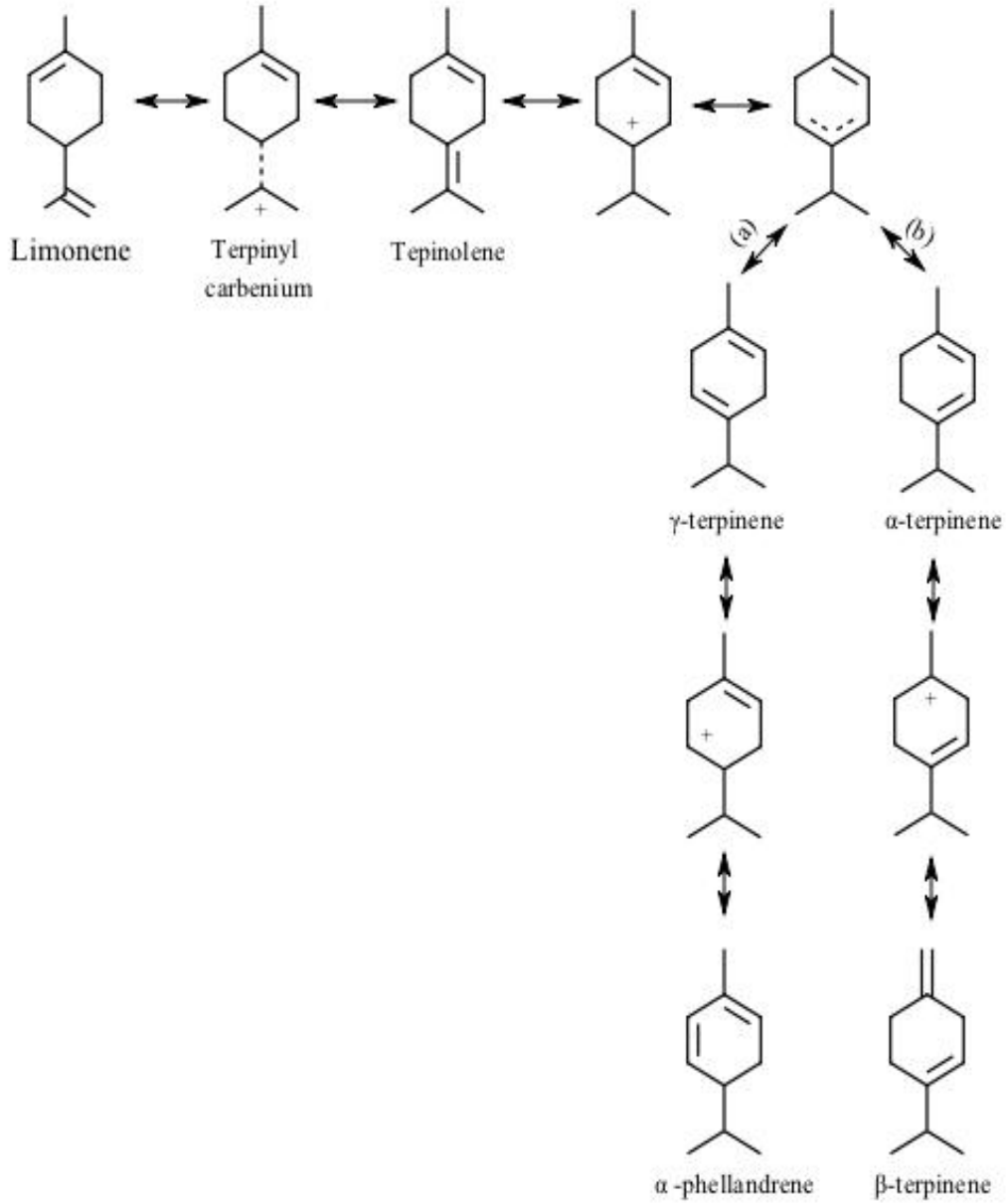

Finally, by reviewing the selectivity of menthenes it can be observed that although with the HSiW catalyst the selectivity towards p-cymene is lower than HPMo and HPMoV, the selectivity towards menthenes is relatively high, suggesting that the hypothesis given in the previous section about the production of menthenes from the

hydrogenation of p-cymene with the *in situ* H_2 produced in the dehydrogenation reaction is not completely certain or predominant. This can be verified with the HPW catalyst in which, although there is no p-cymene, which indicates that there is no H_2 production, there is a slight selectivity towards menthenes. In this way, the disproportionation reaction, reported in the literature by several authors, is verified. In this reaction, equal amounts of cymene and menthenes are obtained, which cannot be observed in this study, because the disporportionation is not only the path of obtaining p-cymene but also the dehydrogenation.

As for the influence of the acidity in disporportionation reaction, it can be found that the greater selectivity towards menthenes is found with the HPMoV catalyst followed by the HSiW catalyst. The HPMoV catalyst have a lower L/B ratio compared to the HPMo catalyst, and the HSiW catalyst has the highest Brønsted acidity compared to HPW, thereby it can be established that the reaction of disporportionation is favored by Brønsted acidity. On the other hand, although the HPMoV catalyst has lower Brønsted acidity than HSiW, a higher selectivity is present to menthene, therefore the hydrogenation pathway with H_2 *in situ* cannot be completely ruled out. Observing the selectivity of α-phellandrene, it is noted that this decreases while the selectivity of menthenes increases slightly, which may be due to a possible hydrogenation of this compound to 2-menthene.According to the observations and conclusions drawn from the results obtained in this study, we propose a reaction mechanism followed with the heteropolyacids based catalysts, which is presented in Figure 53.

Figure 53. *Mechanism proposed in this study with the heteropolyacids-based catalysts*.

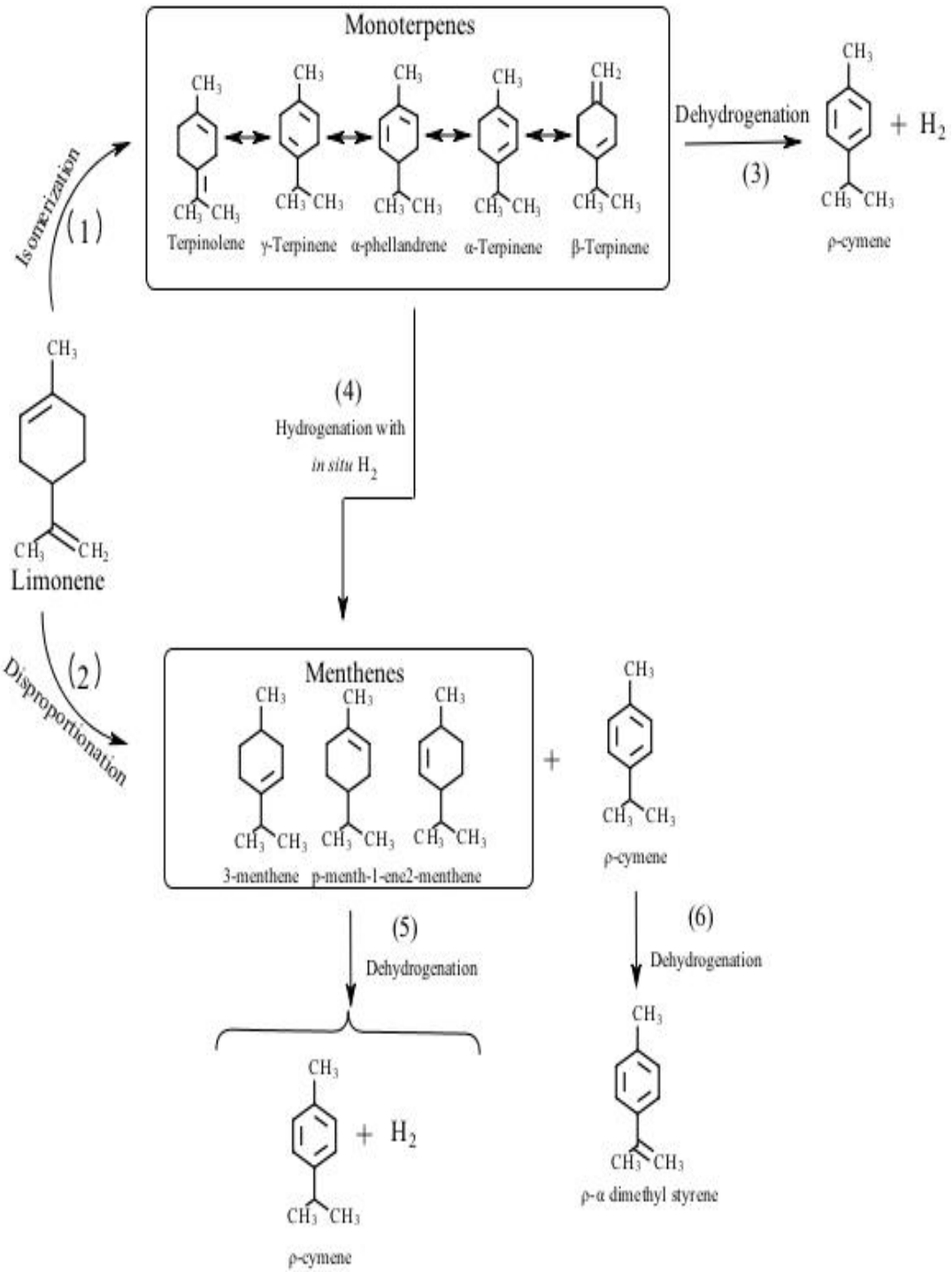

5.4.1.4 Test Type 3: Influence of the support on the conversion, yield and selectivity toward aromatics. The conversion obtained with HPMoV supported in Q-10, MCM-41, SBA-15 and KIT-6 are presented in Figure 54.

The highest conversion was obtained with the MCM-41 support, whereas with SBA-15, Q-10 and KIT-6 very similar conversions were obtained, therefore it is assumed that the conversion is directly related to the surface area, obtaining higher conversion with higher enable area for reaction. On the other hand, it is not observed influence of the other textural characteristics on the conversion, nevertheless the yield and therefore, the selectivity can be affected, by which it is decided to analyze the selectivity in order to select the most favorable supports for the obtaining p-cymene.

Figure 54. *Conversion of HPMoV supported on Q-10, SBA-15, MCM-41 and KIT-6.*

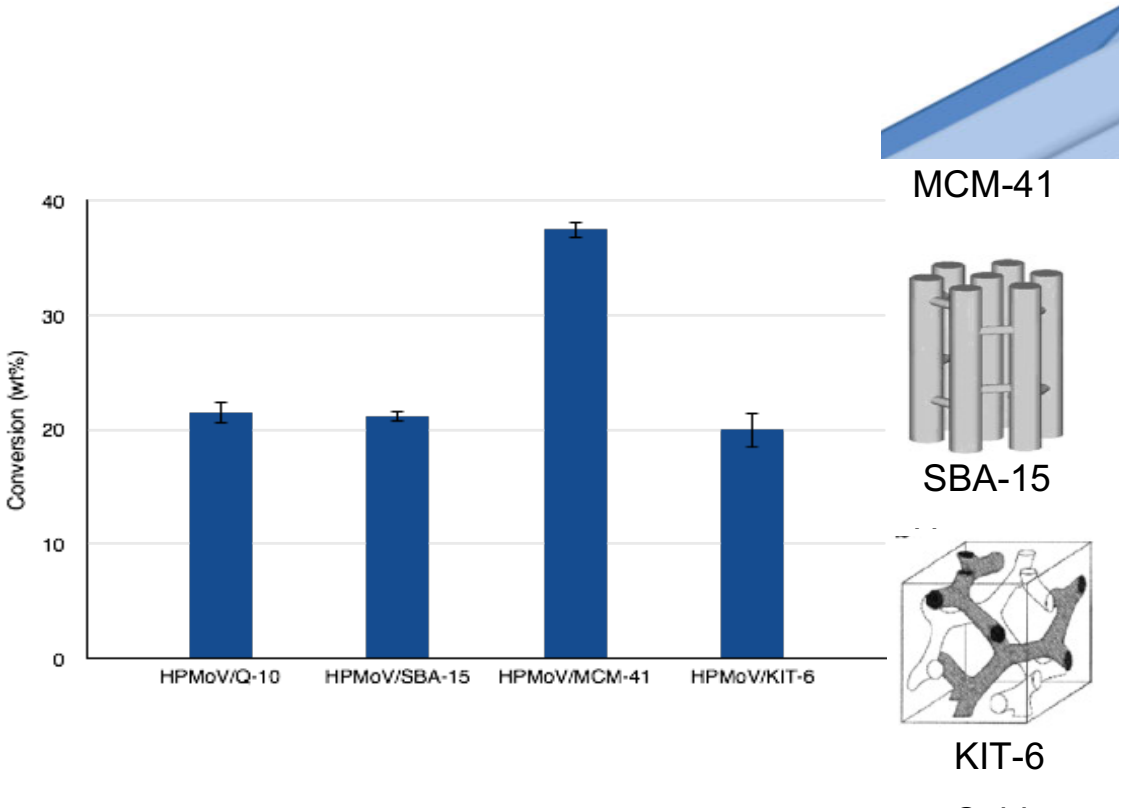

The selectivity obtained for each support is presented in Figure 55. It can be observed that MCM-41 support, although providing a greater surface area that favors the conversion, its selectivity towards p-cymene and monoterpenes is the lowest of all the supports. Comparing this support with SBA-15, which has the same ordered structure (hexagonal plane), it is found that the difference of its structures is the pore interconnectivity that the SBA-15 possesses. According to Pirez *et al.* [50] a pore interconnectivity can improve the reactant/product diffusion.

Figure 55. *Selectivity of HPMoV supported on Q-10, SBA-15, MCM-41 and KIT-6 evaluated at 250 ºC.*

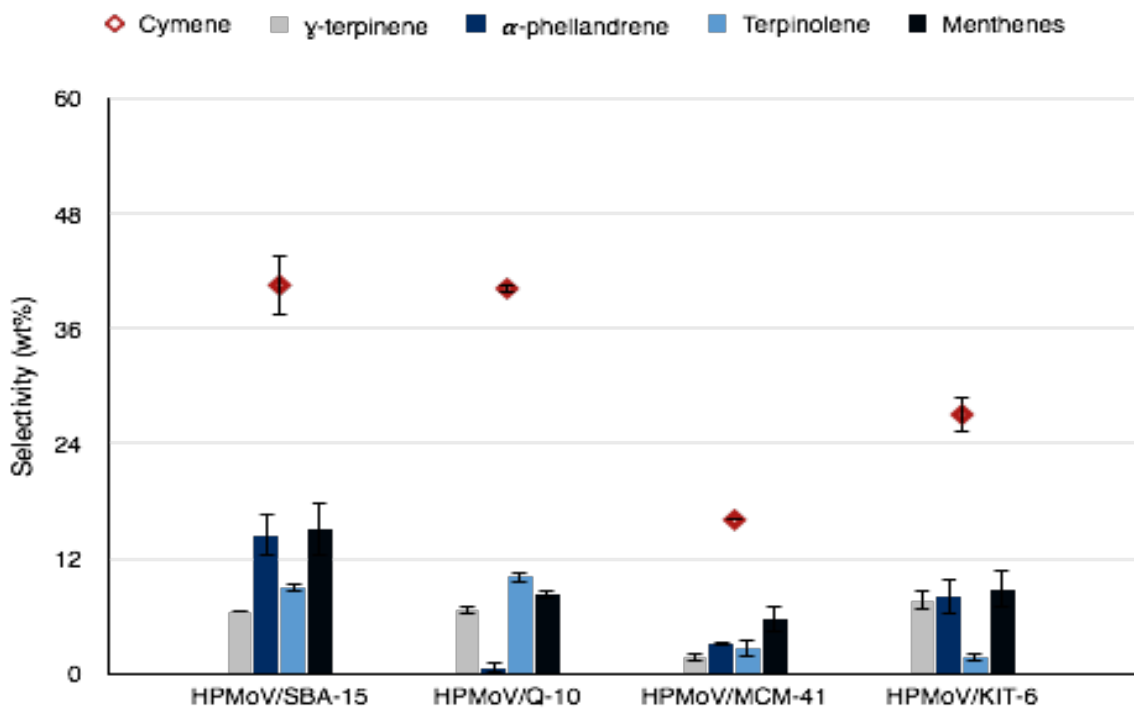

In addition to the interconnectivity, the SBA-15 has a larger pore size, approximately 2 times larger than MCM-41. This may be related to the ease of the reactants to access the active sites, and the ease of the products coming out. Considering that the conversion of MCM-41 was high, it can be assumed that the input of the reactant

is not the disadvantage, if not the output of the products, which can cause the deposition of these molecules unavailable output due to the small size on the surface of the support.

Finally, by comparing Q-10 with SBA-15, it is possible to affirm that the ordered structure as such has no effect on the transformation reaction of limonene to p-cymene, however the isomerization products are increased with the use of SBA-15. In addition, Q-10 support, despite having a very low surface area compared to the other, it has a similar conversion to that presented with SBA-15 and KIT-6 supports, in addition to a high selectivity to p-cymene. This might suggest that more than surface area, pore size and its influence on accessibility to active sites, could govern the selectivity towards p-cymene. However, it is necessary to confirm this assumption by studying different pore sizes on the same support.

5.5 CONCLUSIONS

- A mechanism was proposed, including two initial parallel reactions: (1) isomerization of limonene to monoterpenes and (2) disproportionation of limonene to p-cymene and menthenes. From the products obtained by these reactions, different reactions occur: (3) dehydrogenation of monoterpenes to p-cymene, (4) hydrogenation of alpha pellandrene to 2-menthene with hydrogen *in situ* produced in dehydrogenation reaction, and (5) a possible dehydrogenation of menthenes to p-cymene, and (6) dehydrogenation of p-cymene to p-α-dimethyl styrene.

- Lewis acidity favors isomerization and dehydrogenation reactions, whereas the reaction of disproportionation is favored by the Brønsted acidity. In addition to the need of a Lewis acidity, a high ratio of Lewis/Brønsted acid sites are required for the transformation of limonene to p-cymene, in which Lewis sites prevail over Brønsted.

- In addition to acidity, the type of central atom of the heteropolyacid also influences the activity of the catalyst. It was found that the catalyst with central silicium atom has higher isomerization capacity than that containing phosphorus, which is related to the interaction of the heteropolyacid with the support.

- As for the influence of the support, it was concluded that more than the surface area, the pore size has an influence on the selectivity towards p-cymene, which is directly related to the accessibility to the active sites and the subsequent output of the products. The ordered structure of SBA-15 favors the isomerization of terpenes, however, no differences were found in the selectivity of p-cymene compared to commercial support.

5.6 REFERENCES OF THIS CHAPTER

[1] DANON, B., *et al*. A review of dipentene (dl-limonene) production from waste tire pyrolysis. In: Journal of Analytical and Applied Pyrolysis [online]. 2015, 112, p. 1–13.

[2] ACOSTA, Rolando, *et al*. Production of Oil and Char by Intermediate Pyrolysis of Scrap Tyres: Influence on Yield and Product Characteristics. In: International Journal of Chemical Reactor Engineering [online]. 2015, 13(2), p. 189–200.

[3] KERTON, Francesca M. Alternative solvents for green chemistry Chapter 5. Renewable Solvents. Royal society of chemistry. 2009, p. 97–166. ISBN 085404163X, 9780854041633.

[4] WILLOCK, David. Molecular symmetry. John Wiley & Sons. 2009. p. 438. ISBN 0470853476, 9780470853474.

[5] CUNLIFFE, Adrian M. and WILLIAMS, Paul T. Composition of oils derived from the batch pyrolysis of tyres. In: Journal of Analytical and Applied Pyrolysis [online]. 1998, 44(2), p. 131–152.

[6] ARABIOURRUTIA, Miriam, *et al*. Efecto del uso de catalizadores ácidos sobre la distribución de productos en la pirólisis de neumáticos. In: Informacion Tecnológica [online]. 2010, 21(1), p. 33–41.

[7] OLAZAR, Martín, *et al*. Effect of acid catalysts on scrap tyre pyrolysis under fast heating conditions. In: Journal of Analytical and Applied Pyrolysis [online]. 2008, 82(2), p. 199–204.

[8] OLAZAR, Martin, *et al*. Catalyst effect on the composition of tire pyrolysis products. In: Energy and Fuels [online]. 2008, 22(5), p. 2909–2916.

[9] LI, Wei, *et al*. Derived oil production by catalytic pyrolysis of scrap tires. In: Chinese Journal of Catalysis [online]. 2014, 35(2), p. 108–119.

[10] BOXIONG, Shen, *et al*. Pyrolysis of waste tyres: The influence of USY catalyst/tyre ratio on products. In: Journal of Analytical and Applied Pyrolysis [online]. 2007, 78(2), p. 243–249.

[11] DŨNG, Nguyễn Anh, *et al*. Light olefins and light oil production from catalytic pyrolysis of waste tire. In: Journal of Analytical and Applied Pyrolysis [online]. 2009, 86(2), p. 281–286.

[12] NAMCHOT, Witsarut and JITKARNKA Sirirat. Impacts of nickel supported on different zeolites on waste tire-derived oil and formation of some

petrochemicals. In: Journal of Analytical and Applied Pyrolysis [online]. 2016, 118, p. 86–97.

[13] BOXIONG, Shen, *et al*. Pyrolysis of waste tyres with zeolite USY and ZSM-5 catalysts. In: Applied Catalysis B: Environmental [online]. 2007, 73(1–2), p. 150–157.

[14] WILLIAMS, Paul T. and BRINDLE Alexander J. Aromatic chemicals from the catalytic pyrolysis of scrap tyres. In: Journal of Analytical and Applied Pyrolysis [online]. 2003, 67(1), p. 143–164.

[15] MARTÍN-LUENGO, M. A., *et al.* Synthesis of p-cymene from limonene, a renewable feedstock. In: Applied Catalysis B: Environmental [online]. 2008, 81(3–4), p. 218–224.

[16] SAN MIGUEL, G., *et al.* Thermal and catalytic conversion of used tyre rubber and its polymeric constituents using Py-GC / MS. In: Applied Catalysis B: Environmental [online]. 2006, 64(2006), p. 209–219.

[17] PAKDEL, Hooshang, *et al.* Formation of dl-Limonene in Used Tire Vacuum Pyrolysis Oils. In: Environ. Sci. Technol. 1991, 25 (9), p. 1646–1649.

[18] MKHIZE, N. M., *et al*. Effect of temperature and heating rate on limonene production from waste tyre pyrolysis. In: Journal of Analytical and Applied Pyrolysis [online]. 2016, 120, p. 314–320.

[19] MARTÍNEZ, Juan Daniel, *et al*. Waste tyre pyrolysis - A review. In: Renewable and Sustainable Energy Reviews [online]. 2013, 23, p. 179–213.

[20] ISLAM, M. Rofiqul, *et al*. Valorization of solid tire wastes available in Bangladesh by thermal treatment. In: Proceedings of the WasteSafe 2011 – 2nd International Conference on Solid Waste Management. 2011, p. 978–984.

[21] LARESGOITI, M. F., *et al*. Characterization of the liquid products obtained in tyre pyrolysis. In: Journal of Analytical and Applied Pyrolysis [online]. 2004, 71(2), p. 917–934.

[22] ARABIOURRUTIA, M., *et al*. Product distribution obtained in the pyrolysis of tyres in a conical spouted bed reactor. In: Chemical Engineering Science [online]. 2007, 62(18–20), p. 5271–5275.

[23] LÓPEZ, Gartzen, Martin OLAZAR, Roberto AGUADO a Javier BILBAO. Continuous pyrolysis of waste tyres in a conical spouted bed reactor [online]. 2010, 89, p. 1946–1952.

[24] BAJUS, Martin and OLAHOVÁ Natália. Thermal conversion of scrap tyres. In: Petroleum and Coal. 2011, 53(2), p. 98–105.

[25] QU, Wei, *et al*. Pyrolysis of waste tire on ZSM-5 zeolite with enhanced catalytic activities. In: Polymer Degradation and Stability [online]. 2006, 91(10), p. 2389–2395.

[26] PAKDEL, Hooshang; PANTEA, Dana Magdalena and ROY, Christian. Production of dl -limonene by vacuum pyrolysis of used tires. In: Journal of Analytical and Applied Pyrolysis. 2001, 57, p. 91–107.

[27] KAMITSOU, Maria, *et al*. Transformation of D-limonene into p -cymene over oxide catalysts : A green chemistry approach. In: Applied Catalysis A: General. 2014, 474, p. 224–229.

[28] FERNANDES, C, *et al*. Catalytic conversion of limonene over acid activated Serra de Dentro (SD) bentonite. In: Applied Catalysis A: General [online]. 2007, 318, p. 108–120.

[29] OLIVEIRA, P, *et al*. Limonene oxidation over V 2 O 5 / TiO 2 catalysts [online]. 2006, 118, p. 307–314.

[30] DU, Junming, *et al*. Catalytic dehydrogenation and cracking of industrial dipentene over M/SBA-15 (M = Al, Zn) catalysts. In: Applied Catalysis A: General [online]. 2005, 296(2), p. 186–193.

[31] DING, Kuan, *et al*. Catalytic pyrolysis of waste tire to produce valuable aromatic hydrocarbons: An analytical Py-GC/MS study. In: Journal of Analytical and Applied Pyrolysis [online]. 2016, 122, p. 55–63.

[32] FROMENT, Gilbert, BISCHOFF Kenneth and DE JURAY Wilde. Chemical Reactor Analysis and Desing. 3rd Edition. John Wiley & Sons. 2011. ISBN 9780470565414.

[33] KATRYNIOK, Benjamin. Nouvelle voie de synthese d'acroleine a partir de biomasse. Doctoral Thesis. Lille France: Université des Sciences et Technologies de Lille. Ecole doctoral de Science de la matière, du rayonnement et de l'environnement, 2010.

[34] BARDIN, Billy B. and DAVIS Robert J. Characterization of copper and vanadium containing heteropolyacid catalysts for oxidative dehydrogenation of propane. In: Applied Catalysis A: General [online]. 1999, 185(2), p. 283–292.

[35] BENADJI, Siham, *et al*. Characterization of H 3+xPMo 12-xV xO 40 heteropolyacids supported on HMS mesoporous molecular sieve and their catalytic

performance in propene oxidation. In: Microporous and Mesoporous Materials [online]. 2012, 154, p. 153–163.

[36] SAZO, Virginia, *et al*. Síntesis y caracterización de catalizadores HPW/AlSBA-15, y su evaluación en la reacción de esterificación del ácido benzoico con metanol. In: Avances en Ciencias e Ingeniería. 2012, 3(3), p. 1–10.

[37] PREDOEVA, Albena, *et al*. The surface and catalytic properties of titania-supported mixed PMoV heteropoly compounds for total oxidation of chlorobenzene. In: Applied Catalysis A: General [online]. 2007, 319, p. 14–24.

[38] WEYRICH, P. A and HOLDERICH W.F. Dehydrogenation of limonene over Ce promoted, zeolite supported Pd catalysts. In: Applied Catalysis A: General. 1997, 158, p. 145–162.

[39] SANCHEZ-VAZQUEZ S.A., *et al*. The selective conversion of D-limonene to p,a- dimethylstyrene. In: RSC Advances [online]. 2014, 44(0), p. 61652–61655.

[40] JARAMILLO H.; PALACIO L.A. and SIERRA L. Characterization of a heteropolyacid supported on mesoporous silica and its application in the aromatization of pinene. In: Studies in Surface Science and Catalysis 2002, 1(20), p. 1291–1298.

[41] FRENKEL, M. Interlayer cations as reaction directors in the trnasformation of limonene on montmorillonite. In: Clay and Clays Minerals, 1983, 31(2), p. 92–96.

[42] LESAGE, P, *et al*. paracymene on silica supported palladium assisted by a-olefins as hydrogen acceptor. 1996, 169(96), p. 431-435.

[43] CUI, Huimei, *et al*. Mechanisms into dehydroaromatization of bio- derived limonene to p -cymene over Pd / HZSM-5 in the presence and absence of H 2 [online]. In: RSC Advances. 2016, p. 66695–66704.

[44] PINTO, Teresa, DUFAUD Véronique and LEFEBVRE Frédéric. Isomerization of n-hexane on heteropolyacids supported on SBA-15. 1. Monofunctional impregnated catalysts. In: Applied Catalysis A: General [online]. 2014, 483, p. 103–109.

[45] GRINENVAL, Eva, GARRON Anthony a LEFEBVRE Frédéric. Butane Isomerization over Silica-Supported Heteropolyacids : Study of Some Parameters. In: Journal of Catalysts. 2013, p. 1-8.

[46] THOMAS, Amélie, *et al*. Comparison of H3PW12O40 and H4SiW12O40 heteropolyacids supported on silica by 1H MAS NMR. In: Comptes Rendus Chimie [online]. 2005, 8(11–12), p. 1969–1974.

[47] LEGAGNEUX, Nicolas, *et al*. Characterization of silica-supported dodecatungstic heteropolyacids as a function of their dehydroxylation temperature [online]. In: Dalton Transactions. 2009, p. 2235–2240.

[48] THOMAS, A. F. and BESSIERE Y. Limonene. In: Natural product reports, 1989, p. 291-309.

[49] DE MATTOS, Marcio C.S. and BERNINI Rafael Berrelho. The Reaction of (R) -Limonene with S -Thioacids. In: Journal Braz. Chem Soc. 2007, 18(5), p. 1068–1072.

[50] PIREZ, Cyril, *et al*. Tunable KIT-6 Mesoporous Sulfonic Acid Catalysts for Fatty Acid Esteri fi cation. In: ACS catalysis [online]. 2012, p. 2–7.

5.7 BIBLIOGRAPHY OF THIS CHAPTER

ACOSTA, Rolando, *et al*. Production of Oil and Char by Intermediate Pyrolysis of Scrap Tyres: Influence on Yield and Product Characteristics. In: International Journal of Chemical Reactor Engineering [online]. 2015, 13(2), p. 189–200.

ARABIOURRUTIA, Miriam, *et al*. Efecto del uso de catalizadores ácidos sobre la distribución de productos en la pirólisis de neumáticos. In: Informacion Tecnológica [online]. 2010, 21(1), p. 33–41.

ARABIOURRUTIA, M., *et al*. Product distribution obtained in the pyrolysis of tyres in a conical spouted bed reactor. In: Chemical Engineering Science [online]. 2007, 62(18–20), p. 5271–5275.

BAJUS, Martin and OLAHOVÁ Natália. Thermal conversion of scrap tyres. In: Petroleum and Coal. 2011, 53(2), p. 98–105.

BARDIN, Billy B. and DAVIS Robert J. Characterization of copper and vanadium containing heteropolyacid catalysts for oxidative dehydrogenation of propane. In: Applied Catalysis A: General [online]. 1999, 185(2), p. 283–292.

BENADJI, Siham, *et al*. Characterization of H 3+xPMo 12-xV xO 40 heteropolyacids supported on HMS mesoporous molecular sieve and their catalytic performance in

propene oxidation. In: Microporous and Mesoporous Materials [online]. 2012, 154, p. 153–163

BOXIONG, Shen, *et al*. Pyrolysis of waste tyres: The influence of USY catalyst/tyre ratio on products. In: Journal of Analytical and Applied Pyrolysis [online]. 2007, 78(2), p. 243–249.

BOXIONG, Shen, *et al*. Pyrolysis of waste tyres with zeolite USY and ZSM-5 catalysts. In: Applied Catalysis B: Environmental [online]. 2007, 73(1–2), p. 150–157

CUI, Huimei, *et al*. Mechanisms into dehydroaromatization of bio- derived limonene to p -cymene over Pd / HZSM-5 in the presence and absence of H 2 [online]. In: RSC Advances. 2016, p. 66695–66704.

CUNLIFFE, Adrian M. and WILLIAMS, Paul T. Composition of oils derived from the batch pyrolysis of tyres. In: Journal of Analytical and Applied Pyrolysis [online]. 1998, 44(2), p. 131–152.

DANON, B., *et al*. A review of dipentene (dl-limonene) production from waste tire pyrolysis. In: Journal of Analytical and Applied Pyrolysis [online]. 2015, 112, p. 1–13.

DE MATTOS, Marcio C.S. and BERNINI Rafael Berrelho. The Reaction of (R) -Limonene with S -Thioacids. In: Journal Braz. Chem Soc. 2007, 18(5), p. 1068–1072.

DING, Kuan, *et al*. Catalytic pyrolysis of waste tire to produce valuable aromatic hydrocarbons: An analytical Py-GC/MS study. In: Journal of Analytical and Applied Pyrolysis [online]. 2016, 122, p. 55–63.

DU, Junming, *et al*. Catalytic dehydrogenation and cracking of industrial dipentene over M/SBA-15 (M = Al, Zn) catalysts. In: Applied Catalysis A: General [online]. 2005, 296(2), p. 186–193.

DŨNG, Nguyễn Anh, *et al*. Light olefins and light oil production from catalytic pyrolysis of waste tire. In: Journal of Analytical and Applied Pyrolysis [online]. 2009, 86(2), p. 281–286.

FERNANDES, C, *et al*. Catalytic conversion of limonene over acid activated Serra de Dentro (SD) bentonite. In: Applied Catalysis A: General [online]. 2007, 318, p. 108–120.

FRENKEL, M. Interlayer cations as reaction directors in the trnasformation of limonene on montmorillonite. In: Clay and Clays Minerals, 1983, 31(2), p. 92–96.

FROMENT, Gilbert, BISCHOFF Kenneth and DE JURAY Wilde. Chemical Reactor Analysis and Desing. 3rd Edition. John Wiley & Sons. 2011. ISBN 9780470565414.

GRINENVAL, Eva, GARRON Anthony a LEFEBVRE Frédéric. Butane Isomerization over Silica-Supported Heteropolyacids : Study of Some Parameters. In: Journal of Catalysts. 2013, p. 1-8.

ISLAM, M. Rofiqul, *et al*. Valorization of solid tire wastes available in Bangladesh by thermal treatment. In: Proceedings of the WasteSafe 2011 – 2nd International Conference on Solid Waste Management. 2011, p. 978–984.

JARAMILLO H.; PALACIO L.A. and SIERRA L. Characterization of a heteropolyacid supported on mesoporous silica and its application in the aromatization of pinene. In: Studies in Surface Science and Catalysis 2002, 1(20), p. 1291–1298.

KAMITSOU, Maria, *et al*. Transformation of D-limonene into p -cymene over oxide catalysts : A green chemistry approach. In: Applied Catalysis A: General. 2014, 474, p. 224–229.

KATRYNIOK, Benjamin. Nouvelle voie de synthese d'acroleine a partir de biomasse. Doctoral Thesis. Lille France: Université des Sciences et Technologies de Lille. Ecole doctoral de Science de la matière, du rayonnement et de l'environnement, 2010.

KERTON, Francesca M. Alternative solvents for green chemistry Chapter 5. Renewable Solvents. Royal society of chemistry. 2009, p. 97–166. ISBN 085404163X, 9780854041633.

LARESGOITI, M. F., *et al*. Characterization of the liquid products obtained in tyre pyrolysis. In: Journal of Analytical and Applied Pyrolysis [online]. 2004, 71(2), p. 917–934.

LEGAGNEUX, Nicolas, *et al*. Characterization of silica-supported dodecatungstic heteropolyacids as a function of their dehydroxylation temperature [online]. In: Dalton Transactions. 2009, p. 2235–2240.

LESAGE, P, *et al*. paracymene on silica supported palladium assisted by a-olefins as hydrogen acceptor. 1996, 169(96), p. 431-435.

LI, Wei, *et al*. Derived oil production by catalytic pyrolysis of scrap tires. In: Chinese Journal of Catalysis [online]. 2014, 35(2), p. 108–119.

LÓPEZ, Gartzen, Martin OLAZAR, Roberto AGUADO a Javier BILBAO. Continuous pyrolysis of waste tyres in a conical spouted bed reactor [online]. 2010, 89, p. 1946–1952.

MARTÍNEZ, Juan Daniel, *et al*. Waste tyre pyrolysis - A review. In: Renewable and Sustainable Energy Reviews [online]. 2013, 23, p. 179–213.

MARTÍN-LUENGO, M. A., *et al*. Synthesis of p-cymene from limonene, a renewable feedstock. In: Applied Catalysis B: Environmental [online]. 2008, 81(3–4), p. 218–224.

MKHIZE, N. M., *et al*. Effect of temperature and heating rate on limonene production from waste tyre pyrolysis. In: Journal of Analytical and Applied Pyrolysis [online]. 2016, 120, p. 314–320.

NAMCHOT, Witsarut and JITKARNKA Sirirat. Impacts of nickel supported on different zeolites on waste tire-derived oil and formation of some petrochemicals. In: Journal of Analytical and Applied Pyrolysis [online]. 2016, 118, p. 86–97.

OLAZAR, Martín, *et al*. Effect of acid catalysts on scrap tyre pyrolysis under fast heating conditions. In: Journal of Analytical and Applied Pyrolysis [online]. 2008, 82(2), p. 199–204.

OLAZAR, Martin, *et al*. Catalyst effect on the composition of tire pyrolysis products. In: Energy and Fuels [online]. 2008, 22(5), p. 2909–2916.

OLIVEIRA, P, *et al*. Limonene oxidation over V 2 O 5 / TiO 2 catalysts [online]. 2006, 118, p. 307–314.

PAKDEL, Hooshang, *et al*. Formation of dl-Limonene in Used Tire Vacuum Pyrolysis Oils. In: Environ. Sci. Technol. 1991, 25 (9), p. 1646–1649.

PAKDEL, Hooshang; PANTEA, Dana Magdalena and ROY, Christian. Production of dl -limonene by vacuum pyrolysis of used tires. In: Journal of Analytical and Applied Pyrolysis. 2001, 57, p. 91–107.

PINTO, Teresa, DUFAUD Véronique and LEFEBVRE Frédéric. Isomerization of n-hexane on heteropolyacids supported on SBA-15. 1. Monofunctional impregnated catalysts. In: Applied Catalysis A: General [online]. 2014, 483, p. 103–109.

PIREZ, Cyril, *et al*. Tunable KIT-6 Mesoporous Sulfonic Acid Catalysts for Fatty Acid Esteri fi cation. In: ACS catalysis [online]. 2012, p. 2–7.

PREDOEVA, Albena, *et al*. The surface and catalytic properties of titania-supported mixed PMoV heteropoly compounds for total oxidation of chlorobenzene. In: Applied Catalysis A: General [online]. 2007, 319, p. 14–24.

QU, Wei, *et al*. Pyrolysis of waste tire on ZSM-5 zeolite with enhanced catalytic activities. In: Polymer Degradation and Stability [online]. 2006, 91(10), p. 2389–2395.

SANCHEZ-VAZQUEZ S.A., *et al*. The selective conversion of D-limonene to p,a-dimethylstyrene. In: RSC Advances [online]. 2014, 44(0), p. 61652–61655.

SAN MIGUEL, G., *et al*. Thermal and catalytic conversion of used tyre rubber and its polymeric constituents using Py-GC / MS. In: Applied Catalysis B: Environmental [online]. 2006, 64(2006), p. 209–219.

SAZO, Virginia, *et al*. Síntesis y caracterización de catalizadores HPW/AlSBA-15, y su evaluación en la reacción de esterificación del ácido benzoico con metanol. In: Avances en Ciencias e Ingeniería. 2012, 3(3), p. 1–10.

THOMAS, Amélie, *et al*. Comparison of H3PW12O40 and H4SiW12O40 heteropolyacids supported on silica by 1H MAS NMR. In: Comptes Rendus Chimie [online]. 2005, 8(11–12), p. 1969–1974.

THOMAS, A. F. and BESSIERE Y. Limonene. In: Natural product reports, 1989, p. 291-309.

WEYRICH, P. A and HOLDERICH W.F. Dehydrogenation of limonene over Ce promoted, zeolite supported Pd catalysts. In: Applied Catalysis A: General. 1997, 158, p. 145–162.

WILLIAMS, Paul T. and BRINDLE Alexander J. Aromatic chemicals from the catalytic pyrolysis of scrap tyres. In: Journal of Analytical and Applied Pyrolysis [online]. 2003, 67(1), p. 143–164.

WILLOCK, David. Molecular symmetry. John Wiley & Sons. 2009. p. 438. ISBN 0470853476, 9780470853474.

Chapter 6

Experimental validation of the catalysts in the pilot pyrolysis unit

Part of this chapter was summited recently in Journal Wate and Biomass Valorization,
C. Tavera, P. Gauthier-Maradei, M. Capron, D. Ferreira, C. Palencia, O. Gardoll, J.C. Morin, B. Katryniok, F. Dumeignil. Improvement of the production of aromatic compounds obtained from the pyrolysis of scrap tires rubber using heteropolyacids-based catalysts.

6.1 INTRODUCTION

Some authors have studied the transformation of D, L limonene into aromatic compounds using a catalyst. They have proposed different mechanisms, however, there is still a lack of comprehension with the role of each acidity towards the selectivity of the aromatic compounds [27,29]. In order to reach this goal, in the previous chapter the reaction of transformation of D, L limonene was studied using heteropolyacid based catalysts, with different acidity. A mechanism was proposed, including two initial parallel reactions: (1) isomerization of limonene to monoterpenes

and (2) disproportionation of limonene to p-cymene and menthenes. From the products obtained by these reactions, consecutives reactions occur: (3) dehydrogenation of monoterpenes to p-cymene, (4) hydrogenation of alpha pellandrene to 2-menthene, (5) a possible dehydrogenation of menthenes to p-cymene, and (6) dehydrogenation of p-cymene to p-dimethyl styrene. It can be found that the aromatic compound produced in the highest concentration was the p-cymene, and as conclusion it was obtained that the acidity of Lewis favors its production, and also the ratio of Lewis/Bronsted sites has a strong incidence in the selectivity towards this compound.

Taking into account that this evaluation of catalysts was performed on a pyroprobe coupled to a chromatograph with FID detector, it was decided in this chapter to make a validation of the results obtained in the transformation of limonene, on the pilot pyrolysis unit. This part evaluated the catalysts that were more selective towards p-cymene. Additionally, once the catalysts in the transformation of D, L limonene reaction were validated, an evaluation of the most selective catalysts was conducted at the most favorable operating conditions of catalyst bed temperature, over the pyrolysis reaction of STR.

6.2 STATE OF THE ART

Pyrolysis by adding a catalytic stage has been extensively studied in order to obtain higher concentrations of value compounds such as aromatics. As for the research studies focused on the increase of aromatics, different catalysts have been used, however the zeolites have been the most studied, because these are widely used in the industry because of their size, strong acidity and strong resistance to deactivation. Several variables such as acidity, pore size of the catalyst, temperature of the catalytic bed and $\frac{W_{catalyst}}{W_{STR}}$ ratio have been the most evaluated so far.

Williams and Brindle [1] did one of the first investigations focused on the maximization of aromatic concentration. They used three types of zeolites: CBV-400 (Si/Al ratio=5.4, pore size 7.8 Å), CBV-780 (Si/Al ratio=40, pore size 7.8 Å), and ZSM-5 (Si/Al ratio=40, pore size 5.6 Å), which have different acidity and pore size. Their results show an increase in the concentration of single ring aromatic compounds when the catalyst is added, however, the oil yield decrease with all catalysts, while the gas yield increase. In addition, with the smaller pore size (ZSM-5) lower production of aromatic compounds is obtained, which is attributed by the authors to a restriction in the size of hydrocarbons entering to the pore which lead to the formation of the aromatic hydrocarbons by cracking. As for the acidity, which is measured as Si/Al ratio, they found that the catalyst CBV-400, which has the lowest Si/Al, has the highest concentration of single ring aromatics in the oil. The CBV-400 catalyst produced higher concentrations of benzene, toluene and xylenes compared to the zeolite ZSM-5 catalyst. It means that the lower silica/alumina ratio favor the increase in aromatic compounds, it is due to a high aluminium concentration increase the surface acidity of the catalyst, hence, by changing the silica/alumina ratio the number and strength of the acid sites are modified. On the other hand, these authors also evaluated the effect of the temperature of the catalyst on the production of aromatics, especially those of higher commercial value such as benzene, toluene and xylenes. Figure 56 shows the variation of the concentration of these aromatics in the temperature range of 400 to 600 ºC, which was reported by Williams and Brindle.

It can be observed in the figure that the concentration of benzene increased as the temperature increased, with a larger increase occurring after 500 °C. For toluene, which presents in higher concentration, an increase after 470 ºC is also observed, but its production remains constant after 550 ºC. In contrast, xylenes showed a decrease with temperature, with the highest decrease after 500 °C, which could suggest that xylenes may be involved in the production of toluene and benzene.

Figure 56. *Effect of catalyst bed temperature on yields of high value chemicals using CBV-400 as catalyst by Williams and Brindle [1].*

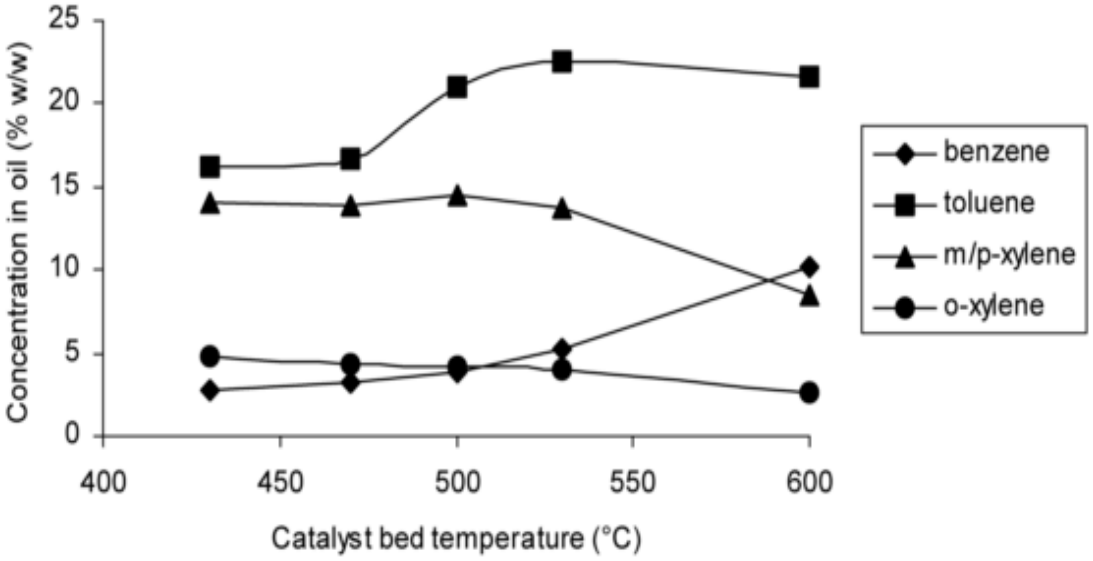

Topchiev *et al*.[2] studied the demethylation of xylenes, founding that in the catalytic treatment of a mixture of xylene, a considerable fraction of the o-xylene was demethylated to toluene, observing that the xylene fraction fell from 34.9 to 17 wt%, and the rest of the o-xylene was isomerized to m- and p-xylene. They include that, in the catalytic treatment of a mixture of xylene and benzene, the demethylation reaction is preceded by the isomerization of o-xylene to form p-xylene, and this is dealkylated with formation of toluene, suggesting that the reaction of dealkylation of xylene with associated alkylation of benzene proceeds over aluminosilicates, explaining what was found by Williams and Brindle [1].

Boxiong *et al.* [3] studied zeolites with similar characteristics to the aforementioned catalysts. They used zeolites type USY (Si/Al = 5, pore size 9) and ZSM-5 (Si/Al = 38, pore size 5.6 Å) to evaluate the influence of temperature in the catalytic bed. The results obtained by these authors show that by adding catalyst, both USY and ZSM-

5, the oil yield decrease as the gas increased, which was also found by Williams and Brindle [1]. The yield of oil, gas and char were evaluated at a catalyst temperature range of 350-500 °C, finding that beyond the addition of the catalyst, the temperature of the catalyst influences the yields of the pyrolysis products, being more severe the decrease of the oil after 400 °C for both catalysts. The concentrations of aromatics in the oil by adding catalyst, mainly toluene and m/p xylenes, is considerably higher than without catalyst, obtaining the highest concentration with USY catalyst. In addition, the values of aromatic concentration obtained by these authors confirm again the reported by Williams and Brindle [1] regarding a higher concentration of aromatics with a larger pore size and lower Si/Al ratio. The authors mention that, a large pore size allows to hydrocarbons of large size enter into the pores, thereby, the catalytic cracking is performed to formation of aromatic hydrocarbons. Additionally, Boxiong *et al*. [3] concluded that, although high aromatics concentration were obtained with lower Si/Al (USY), this catalyst presents the high cracking activity, increasing the coke formation and decreasing oil yield.

Other investigations with different zeolites were carried out by several authors such as Olazar *et al*. [4], Ding *et al.* [5] and Qu *et al.* [6], who obtained similar results to those reported by Williams and Brindle [1] and Boxiong [3] about the need for low Si/Al ratio (high acidity) and high pore size for the production of aromatics. However, different and very variable results are obtained by each author as to the concentration of simple ring aromatics. It should be noted that both the operating conditions and the equipment used in each investigation were different, which may be a possible cause of the differences found. In addition, all authors reported the high cracking capacity of the zeolites reflecting a decrease of the oil yield and an increase of that for the gas. Table 21 summarizes the zeolite catalyst used by different authors, its characteristics, the oil yield, limonene concentration, the maximum aromatic concentration (single ring) obtained and the catalyst temperature.

Table 21. *Zeolite catalysts and conditions of highest aromatic concentration obtained by different authors.*

Author	Catalyst type	Si/Al ratio	Pore size (Å)	Catalyst Temperature Catalyst/tire ratio	Single ring aromatics concentration (wt%)	Limonene concentration (wt%)
Williams and Brindle [1]	CBV-400	5.4	7.8	500 ºC 1.5	56.7 %	0 %
	CBV-780	40	7.8		44.7 %	0%
	ZSM-5	40	5.6		36.9 %	0%
Boxiong *et al.* [3]	USY	5	9	500 ºC	35.26 %	1.26 %
	ZSM-5	38	5.6	0.5	19.61 %	15.21 %
Arabiorrutia *et al.* [8]	HY	5.2	7.8	400 ºC 18.75	-	-
	HZSM-5	30	5.6		-	-
	HBeta	75	6.5		-	-
Olazar *et al.* [4]	HY			500 ºC	3.52 %	3.86 %
	HZSM-5			7.5	20.03 %	8.34 %
Qu *et al.*[6]	ZSM-5	50	-	430 ºC 0.0005	23.18 %	13.58 %

Hita *et al.* [7] mention in their review that, an increase in the $\frac{W_{catalyst}}{W_{STR}}$ ratio can lead to an increase in the cracking activity, which leads to a decrease of the oil, and a possible decrease in the aromatics production, whereas the gaseous compounds are favored. Therefore, it is possible to conclude that the production of aromatics using zeolites as catalysts, is more favorable as $\frac{W_{catalyst}}{W_{STR}}$ ratio is lower. Due to the good results obtained with zeolites, recent investigations have diverted their interest to the use of bi-functional catalysts incorporating metals on the zeolites. An example

is the research conducted by Namchot *et al.* [9] and Muenpol *et al*. [10] who incorporated Ni and Fe, respectively, to different types of zeolites.

Namchot *et al.* [9] used 5 wt% Ni loading on four type zeolites: HZSM-5, HMOR, HY, HBETA. They found that Ni loads on all zeolites, significantly increase the yield of aromatics compounds. They mention that this increase in aromatic yield does not only depend of the nickel, also the zeolite characteristics have strongly influence. It was found that, like previous investigations with zeolites without addition of metal, the pore size of the supports has a large influence on the size of the hydrocarbons produced. In addition, they studied the influence of the type of channels or structure of the zeolite, finding that the structure of the channels has a great influence on the residence time of the compounds in the pore. For instance, the Ni/HMOR catalyst (1D channel structure) produced a higher concentration of single ring aromatics than that observed with Ni/HBETA catalyst (3D channel structure). Besides, due to the shorter residence time, a lower formation of coke and polyaromatic compounds is observed while a higher production of single aromatic is obtained.

Muenpol *et al.* [10] used the zeolites HMOR, HBeta, HZSM-5, and KL with a Fe loading of 5 wt%. Figure 57 shows the yields of pyrolysis products obtained by these authors. It can be observed that, when the catalyst is added, the oil yield decreases compared to the pyrolysis without catalyst, as has been found in the investigations previously reviewed. However, it is noted that there is no significant variation in the oil when Fe is added to the zeolite, except for the Fe/HZSM-5 catalyst, while at the same time an increase in gas is observed, which confirms the high cracking activity of this catalyst. As for the coke deposit, which is produced with all the zeolites, is higher for the zeolite HBeta and Fe/HBeta, however, it is observed that when the Fe is added, the production of coke decreases.

Figure 57. *Yield of pyrolysis products obtained from using the parent zeolites and 5%Fe-promoted catalysts by Muenpol et al. [10].*

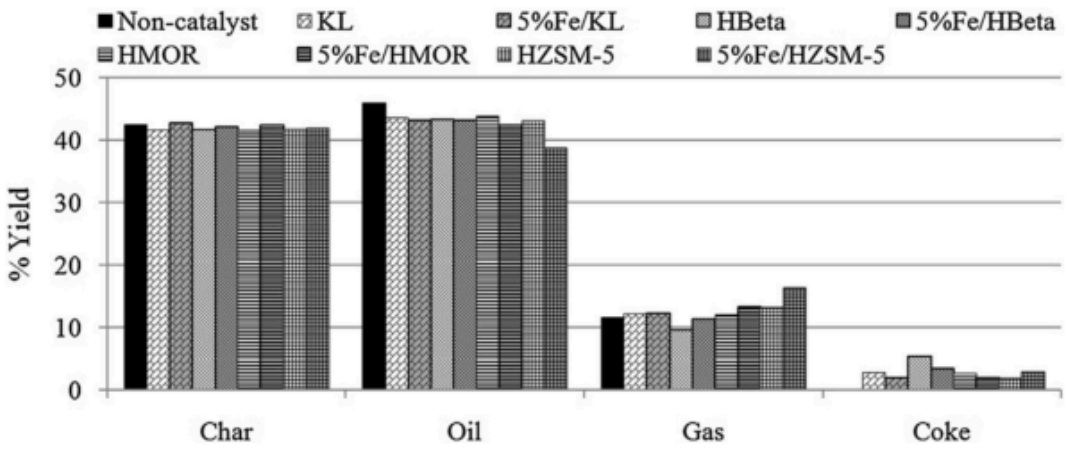

As the oil composition, the KL, HMOR and HBeta catalyst without Fe loading do not modifie the composition of the oil, whereas HZSM-5 significantly improves the formation of olefins and naphthenes and decreases the amount of total aromatics. It can be explained possibly that HZSM-5 (crystalline aluminosilicate composed of tetrahedra) to pore size and its selectivity towards compounds of greater molecular size, as explained by Boxiong *et al.* [3] and Williams and Brindle[1]. On the other hand, the addition of Fe to the zeolite, increases the concentration of naphthenes, for the catalysts Fe/HMOR and Fe/HBeta leading to a decrease of olefins and aromatics, which according to the authors indicating that these are transformed into naphthenes. Unlike, Fe loading on HZSM-5 and KL, increases the aromatic content with the suppression of olefins, possibly through cyclization and then aromatization.

In addition to the zeolites, mesoporous materials have been studied as catalysts for the increase of aromatic compounds. Dūng *et al.* [11] evaluated the use of SBA-1 finding that the use of SBA-1 does not show changes in the pyrolysis products and the oil composition (with similar concentrations of saturated hydrocarbons, mono aromatics, di-aromatics , poly-aromatics and polar-aromatics), compared to tests

without catalyst. It means that SBA-1 does not have influence and does not present catalytic activity (Figure 58).

Due to the non-catalytic activity of the SBA-1, a Ru loading of 1 wt% was supported on the SBA-1 in order to evaluate the influence of the metal loading. The results obtained by Dūng *et al.* show a decrease in oil yield and an increase in that for gas, whereas the solid remains the same with Ru/SBA-1, and confirming the cracking activity of the catalyst, which is in agreement with the previous research already mentioned.

Figure 58. *Effects of SBA-1 on the pyrolysis products: (A) product distribution, (B) liquid compositions by Dūng et al.[11]*

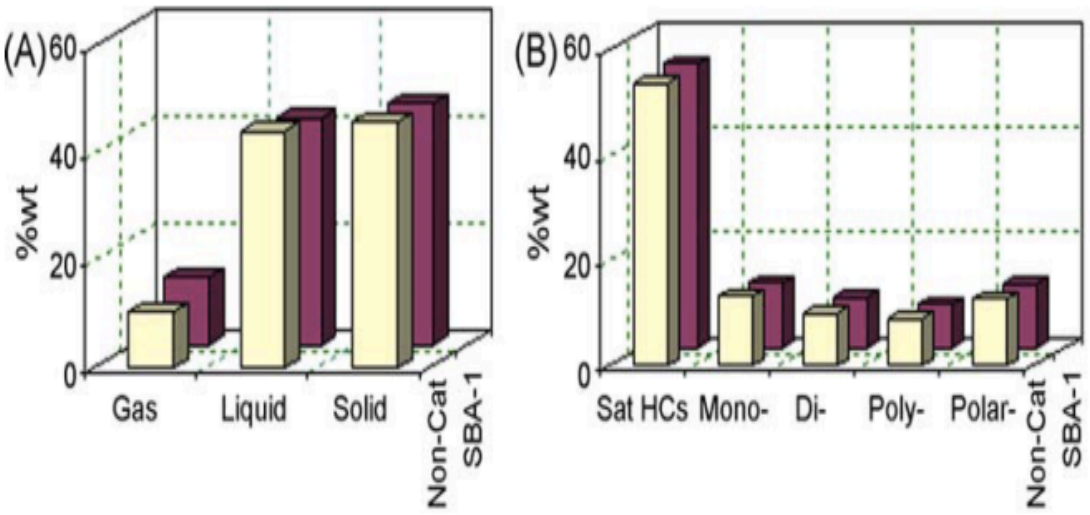

The composition of the pyrolytic oil obtained with this catalyst (Ru/SBA-1) by Dūng *et al.* [11] is shown in Figure 59. It is evidenced that with the presence of Ru, the saturated compounds, the polyaromatic and the polar aromatics decrease, whereas the simple ring aromatic (monoaromatic) and di-aromatic (alkylated) aromatics

increase.The authors attribute the decrease of aromatics to the fact that ruthenium is highly active for hydrogenation and polyaromatics are transformed to other types of molecules simpler through their hydrogenation. As for the reduction of saturated compounds, the authors attribute their transformation to the light gases, through hydrogenolysis, reducing the oil yield and increasing the gas yield.

Figure 59. *Liquid composition obtained with catalyst 1%Ru/SBA-1 by Dūng et al. [11].*

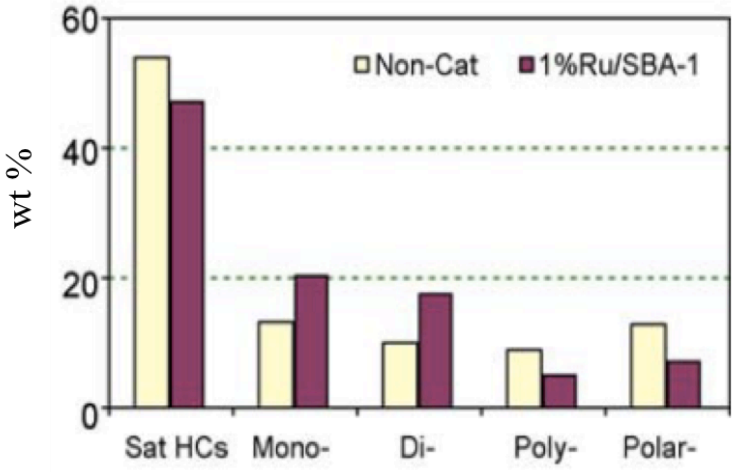

In another investigation, Dūng *et al.* [12] evaluated another mesoporous material: MCM-41. This was evaluated in the same way as the SBA-1, the pure material and with a Ru loading (2 wt%). As for the yields of pyrolysis products with MCM-41, a small change in gas and oil yield was observed with MCM-41 without Ru loading (Figure 60), unlike SBA-1 with no changes The composition of the pyrolytic oil obtained by Dūng *et al.* [12] with MCM-41 and Ru/MCM-41are shown in. As observed in the previous research works [11], a decrease in polyaromatic and polar aromatics, and an increase in simple ring aromatic was found with both MCM-41 and Ru/MCM-41, being much stronger with the presence of Ru. The authors conclude that the activity of MCM-41 is related to acidic sites on the surface, which was verified

by NH_3 TPD. On the other hand, they mention that polycyclic aromatics might be hydrogenated over ruthenium sites, and then, the hydrogenated could be rapidly transferred to the acidic sites of the undergoing cracking support and / or ring-opening reactions. It means that it is the most favorable use of support with acid sites.

Figure 60. *Compositions of pyrolysis oils obtained from non-catalytic and catalytic pyrolysis obtained by Dūng et al. [12].*

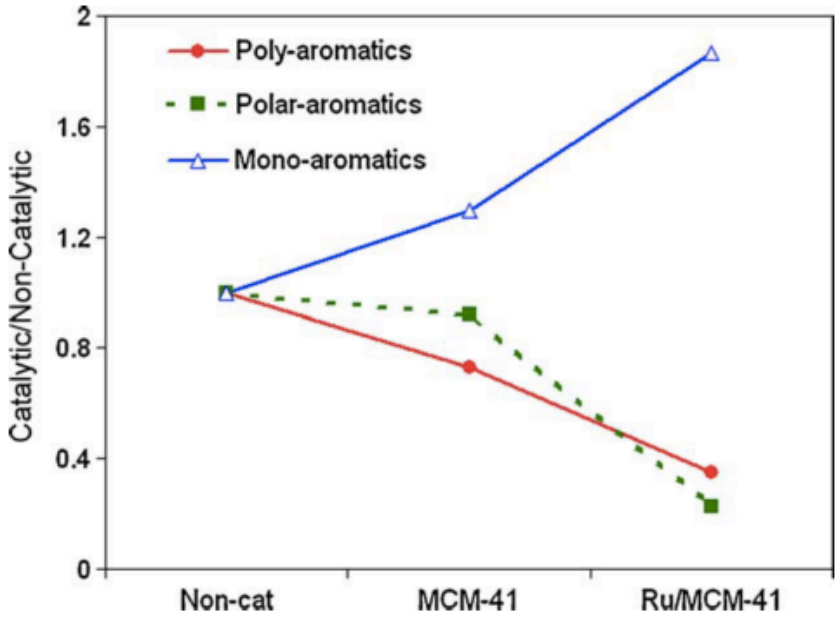

As a general conclusion, all catalysts were found to have a decrease in oil and an increase in gas yield, however the oil obtained with the more acidic catalysts are richer in simple ring aromatic compounds. A decrease in the saturated, polyaromatic and polar aromatics were observed when the concentration of simple aromatics increased, suggesting cracking reactions with acid catalysts and hydrogenation and cracking with bifunctional catalysts. On the other hand, the temperature of the catalytic bed has a great influence, however, this depends on the type of catalyst to

be used. For example, for zeolites, the working temperatures are moderately high, normally 450 ° C and 500 ° C, temperatures which may favor secondary reactions, lead to an increase in the gaseous fraction and coke, and in turn affect the yield oil and its composition, which is shown as a major disadvantage. In addition, another strongly influential variable is the catalyst/tire ratio. According to the investigations reviewed, a lower ratio favors the production of aromatics and decreases the formation of coke.

Similar results to those of Dūng *et al.*[11,12] with respect to the increase of simple aromatics and decrease of polyaromatic were found by Witpathomwong *et al*.[13], who tested the pure mesoporous MCM-48 material (structure) and with a load of 0.7 wt% of Ru on MCM-48. They explain that MCM-48, which has no acid character, can provide a mild cracking activity because the mesopores allow large molecules to enter and are cracked, thus, the amounts of polyaromatics and polar-aromatics decrease (Figure 61).

Figure 61. *Molecular compounds in oils from using synthesized MCM-48 and Ru/MCM-48 catalysts by Witpathomwong et al. [13]*

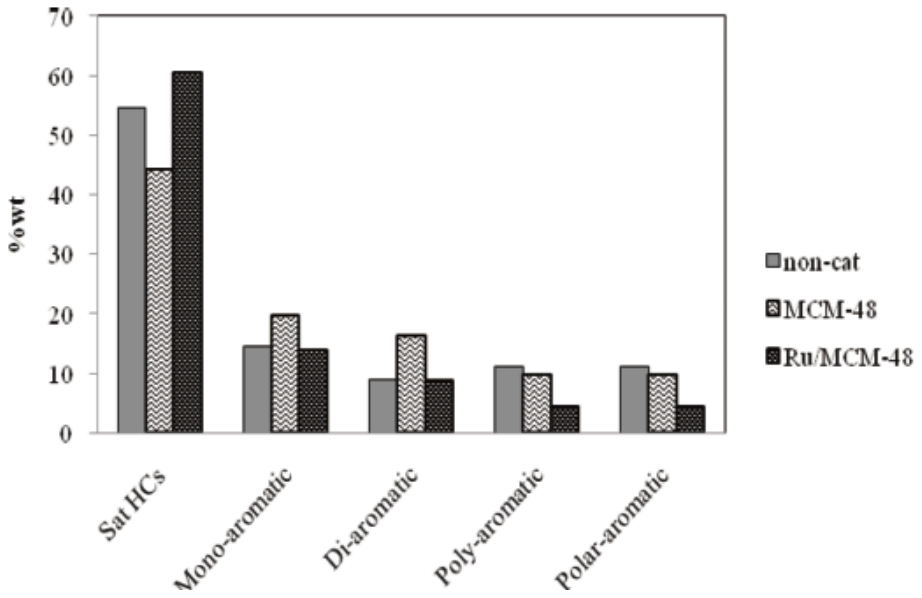

In contrast to Dūng *et al*.[11,12], Witpathomwong *et al.* [13] obtain an increase in the saturated compounds with decreasing in single aromatics when Ru is added (Figure 61), attributing this to the high hydrogenation activity of Ru metal (metal sites), as mentioned by Dūng *et al*.[11,12] previously.Finally, both the results obtained by Dūng *et al*. [11, 12] and Witpathomwong *et al.* [13]. mention that in addition to the increase of simple aromatics and the reduction of polyaromatics, it was observed that with the addition of metal (presence of metal sites) the amount of sulfur compounds in the oil is reduced, which means an improvement of the quality of the oil of pyrolysis.

6.3 METHODOLOGY

In this chapter, the most selective catalysts found in the test on Py-GC/FID were validated on the pyrolysis pilot unit. Two types of validation were performed: with D, L limonene and with STR.

6.3.1. Catalytic tests on laboratory-scale reactor using D, L limonene as raw material. The experimental unit used to carry out these tests is described in Chapter 3 (Figure 12). This unit was adapted with a system of pumping and vaporization of D, L limonene composed by a storage tank in glass with a capacity of 400 ml, a heating system, a pressure manometer, a gear pump (model 75211-10, Cole-Parmer), a rotameter to measure the D, L limonene flow previously calibrated and a heating cord (T = 200 °C) that lines the pipeline from the rotameter outlet to the reactor inlet, ensuring that limonene is fed in steam. The unit with the adaptations is shown in Figure 62.

Figure 62. *Unit Pilot used to catalytic test of D, L limonene transformation*.

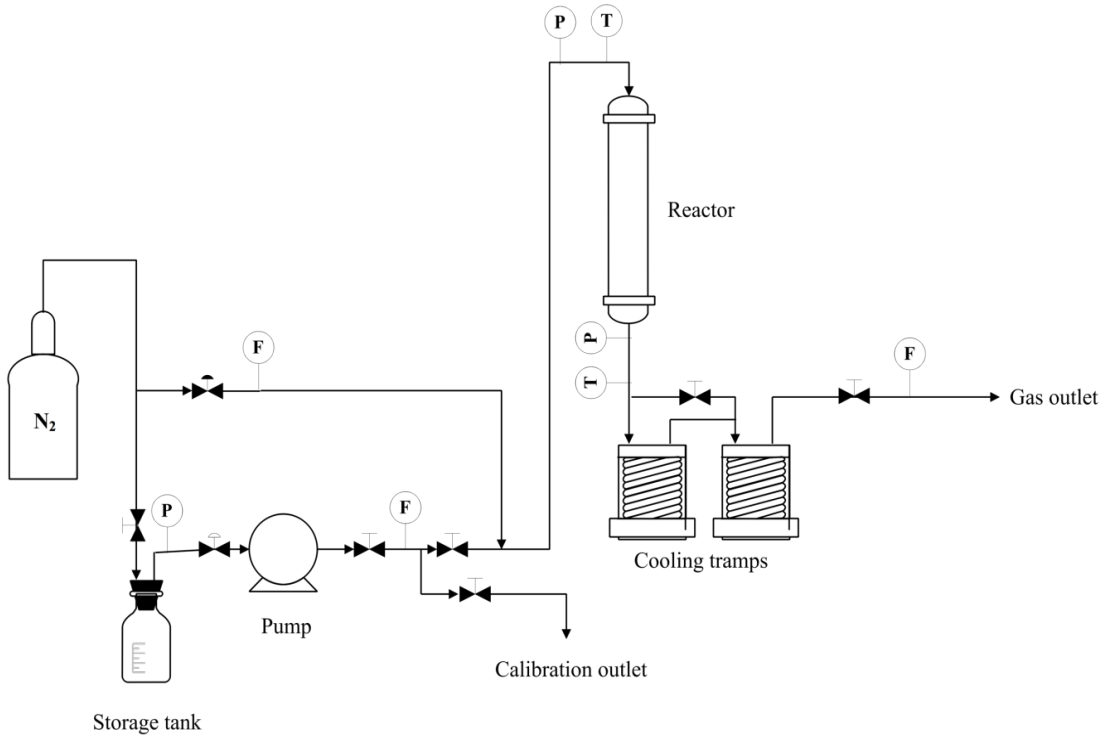

The reactor has two independent heating zones; the catalyst was loaded in the lower area on a bed of glass wool, while the upper area contained only glass wool, this in order to finish the vaporization of D, L limonene before coming in contact with the catalyst. The loaded protocol is shown in Figure 63. Once the reaction occurs, the reaction products and the unreacted reagent leave the reactor through a line heated (about 200 ºC) towards the condensation zone. This zone is composed of two cooling traps which are cooled with dry ice. Finally, non-condensable products are released into the atmosphere.

Figure 63. *Loaded protocol in the laboratory-scale reactor*.

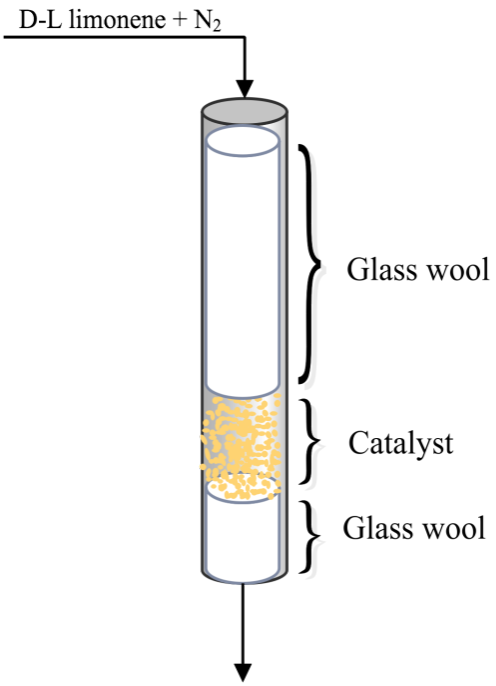

A series of preliminary tests were performed in order to verify the correct functioning of the experimental unit, the vaporization of limonene and the closure of mass balance. These preliminary tests were carried out without catalyst using the reactor loaded with glass wool. To be considered suitable for the development of the experimental tests, the closures of mass balance must be higher to 90%,

For the catalytic tests, D, L limonene liquid was fed to the heating zone with a relative pressure of 0.5 barg and a standard mass flow of 6.384 ± 0.253 g/min, during 5min. At the same time, inert gas (N_2) was fed with the same pressure and a volumetric flow rate of 155 Nml/min, being it the carrier gas for the D, L limonene vapor to the reactor. The inert gas flow was established based on the results of Chapter 3, in which it was found that 466 ºC and 155 Nml/min are the most favorable operating conditions to obtain the highest aromatic yield.

Three types of catalytic tests were performed, which are summarized in Table 22.

Table 22. *Operating conditions and evaluated variables.*

Test	Evaluated conditions	Constant operating conditions
Type 4: Evaluation of the temperature	Three temperatures: • 180 ºC • 250 ºC • 350 ºC	• Active phase type: More selective in test Type 1 • Support type: More selective in test Type 2 • Contact space-time = 0.4 s^{-1}
Type 5: Evaluation of the active phase type	The two active phases more selective on pyroprobe	• Support type: Commercial CARiACT Q-10 • Temperature: 250 ºC • Ratio Wcatalyst/Wlimonene = 1
Type 6: Evaluation of the support characteristics	The three supports more selective on pyroprobe	• Active phase type: More selective in test Type 1 • Temperature: 250 ºC • Ratio Wcatalyst/Wlimonene = 1

The test Type 4, sought to evaluate the catalysts with more selective active phase and support obtained in tests Type 1 and Type 2 (Chapter 5) at different operating temperatures to validate the results obtained on the pyroprobe. In the test Type 5,

the active phases found as more selective on the pyroprobe were evaluated (HPMo and HPMoV), on the commercial support (CARiACT Q-10). Finally, in the test Type 6, HPMoV on the supports found more selective towards aromatics on the pyroprobe tests: Q-10 and SBA-15, were evaluated.

Considering that the vaporization of D, L limonene is done at 176 °C (1 atm relative), this study was performed at temperatures of 180, 250 and 350 °C. All catalytic tests were done in duplicate, for a total of 12 tests. The conversion, selectivity towards aromatic compounds and products yield were calculated. The synthesis and characterization of these catalysts is shown in Chapter 4.

The compounds obtained were identified and quantified by gas chromatography coupled to mass detector (GC-MS) and gas chromatography coupled to a flame ionization detector (GC-FID), respectively. In both cases, an HP-5 column (30m x 0.320mm x 0.25µm) was used. Each sample was prepared at 50 wt%, and diluted in n-pentane. The samples were injected using a split 1:20 on GC-MS and a split 1: 100 on GC-FID. Similarly, for both cases, a same method was used: injection temperature of 270 ºC, detector temperature of 300 ºC and oven temperature from 50 ºC to 290 ºC with a ramp of 5 ºC/min.

Finally, in order to evaluate the amount and type of carbonaceous material deposited on the catalysts, a XPS analysis was performed. For the analysis, an excitation source of the Al Kα radiation (1486.7 eV, 15 kV) was used. Besides, a degassing before analyzes was done at 10-5 Torr. The XPS analysis was carried out at 10-9 Torr. A charge correction for all spectra: C1s (C-C bonding) at 285 eV was made.

6.3.2 Catalytic tests on laboratory-scale reactor using STR as raw material. Two different pyrolysis tests were performed in this part; with and without additional catalytic zone placed downstream of the pyrolysis zone, denoted as catalytic pyrolysis and pyrolysis, respectively. For the catalytic process, catalysts have been added in a second reaction zone after classical pyrolysis. The aim of this catalytic zone is the reforming of volatile species produced during pyrolysis to form aromatic compounds.

The pilot unit used was that used for experimental tests of Chapter 3. The reactor was loaded in pyrolysis tests as shown in Figure 64 (a), using glass wool in the lower zone, and STR in the highest zone. This configuration was chosen to minimize the residence time of volatile compounds produced during the reaction in the hot zone and ensure their condensation only in the cooling trap. The mass of STR sample was calculated according to bulk density, allowing a fixed bed with a length of 11 cm. For a particle size in the range between 0,85 and 1 mm, the real and bulk densities measured were 511.9 and 347.7 kg/m^3, respectively.

Figure 64. Loading scheme to fill the reactor on: (a) pyrolysis, (b) pyrolysis with catalytic bed.

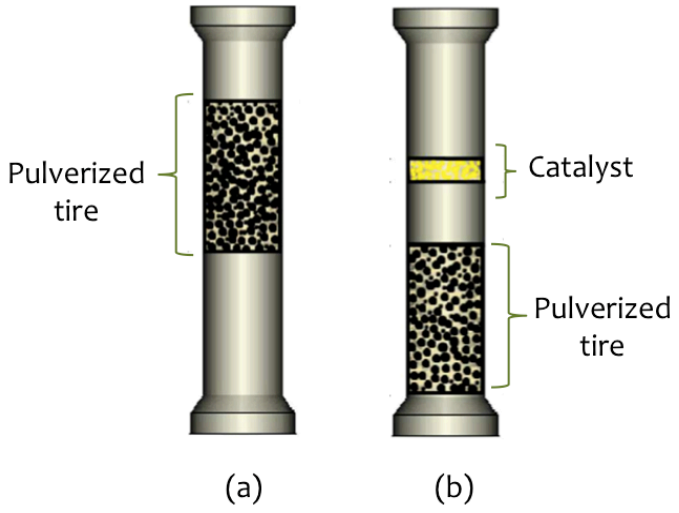

For the catalytic pyrolysis tests, the reactor was charged with the catalyst supported on glass wool in the higher zone and STR in the lower zone (Figure 64- b). The mass of STR sample was calculated as explained for the pyrolysis test. The catalyst/tire ratio was arbitrarily fixed at 0.2. The operating temperature for the lower zone (STR bed) was 466 ºC, according to Acosta *et al.* [14] to maximize the aromatics yields in the pyrolytic oil, and 350 ºC for the higher zone (catalytic bed) a temperature lower than the stability limit of the catalysts [15]. The reaction time for all tests was 1 h.

All tests were performed by duplicate, which allow us to provide accurate data. The oil and char yields in each experimental test are determined by gravimetry, whereas the gas yield was calculated by mass balance once the possible leaks in the unit were minimized. Therefore, a leak test was performed before each experimental test. In the leak test, the unit was isolated using Nitrogen at 300 kPa (relative) for 10 h approximately, in which the pressure loss was monitored. The leaks were considered negligible and the experimental test could start up only if the pressure loss during the leak test time was lower than 10%.

The pyrolytic oil obtained in each test was recollected and stored at 5°C. The chemical identification and quantification of compounds present in each sample was performed by GC-MS (Agilent Technologies, HP-5 column) and GC-FID (Agilent Technologies, HP-5 column, 29.5 m × 250 µm × 0.25 µm), respectively. The compounds that could not be identified by GC-MS were identified by GC-FID using standards (e.g. toluene, limonene, xylene, naphthalene and styrene). For the quantification, an external standard technique was used, employing n-heptane.

The relative response factors (RRF) of the aromatic compounds (ANNEX E) were taken from Katrizky et al. [16]. In the case of limonene, the RRF was calculated according to the method and expression reported by this author obtaining an RRF of 0.97. The GC oven temperature was programmed from 50°C (2 min) to 290°C at 5 °C/min, maintaining the temperature at 290°C for 2 min. The injector and detector

temperatures were equal to 250 and 280°C, respectively. For the analysis, the oil samples were filtered and diluted to 50 wt% in hexane. The yield of each product (*i.e.* char, oil and gas) was calculated as the mass of each product versus the mass of STR sample charged in the reactor (Equation 1).

The determination of carbonaceous material deposited in the catalyst was performed in the same way as in the catalysts used in the transformation of D, L limonene (previous section).

6.4 RESULTS

6.4.1. Catalytic tests on laboratory-scale reactor using D, L limonene as raw material.

6.4.1.1 Study of the influence of the active phase on the conversion and production of p-cymene. According to the results obtained in the previous chapter, it was concluded that the active phases more selective towards aromatics are HPMo and HPMoV. Therefore, these active phases supported on commercial support Q-10 were evaluated in these catalytic tests. The conversion of the D, L-limonene obtained with the HPMo/Q-10 and HPMoV/Q-10 catalysts are presented in Figure 65. The higher conversion is obtained with the catalyst HPMoV/Q10, which agrees with the results obtained on the pyroprobe.

Figure 65. *Conversion of D, L limonene obtained using HPMo and HPMoV supported on commercial Q-10.*

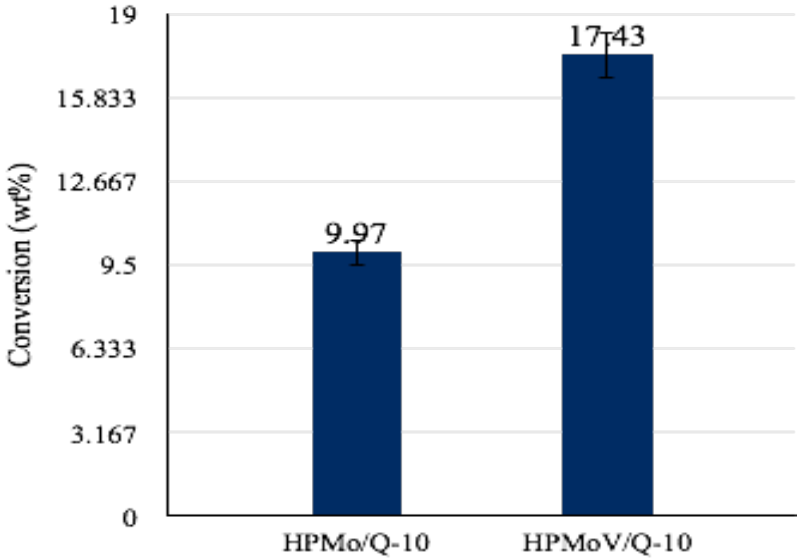

An analysis of the characterization performed on the products, allows to define that the compounds obtained in higher concentration correspond to the same ones found in the pyroprobe: p-cymene, α-phellandrene, α and γ-terpinene, terpinolene, 2-menthene, and 3-menthene. The selectivity was evaluated by grouping the monoterpenes and menthenes, and it is presented in Figure 66. It should be mentioned that the sum of selectivities in this study does not give a total of 100% due to two reasons: the first because the reaction products are divided into three fractions (solid, liquid and gas) and for quantification only the liquid fraction was analyzed; The second one, the selectivities shown only correspond to the compounds of interest, those as C + 10 compounds, and some unidentified ones are not presented.

The same trend found on pyroprobe, as the selectivity towards p-cymene, was observed on the reactor, in which the active phase HPMo presents better selectivity than HPMoV for families of compounds evaluated. As was concluded and explained

in the previous chapter, this is related to the Lewis/Bronsted ratio, seeing the selectivity favored by a higher L/B ratio.

Figure 66. *Selectivity towards p-cymene, monoterpenes and menthenes obtained from D, L limonene with HPMo/Q-10 and HPMoV/Q-10 catalysts at 250 ºC.*

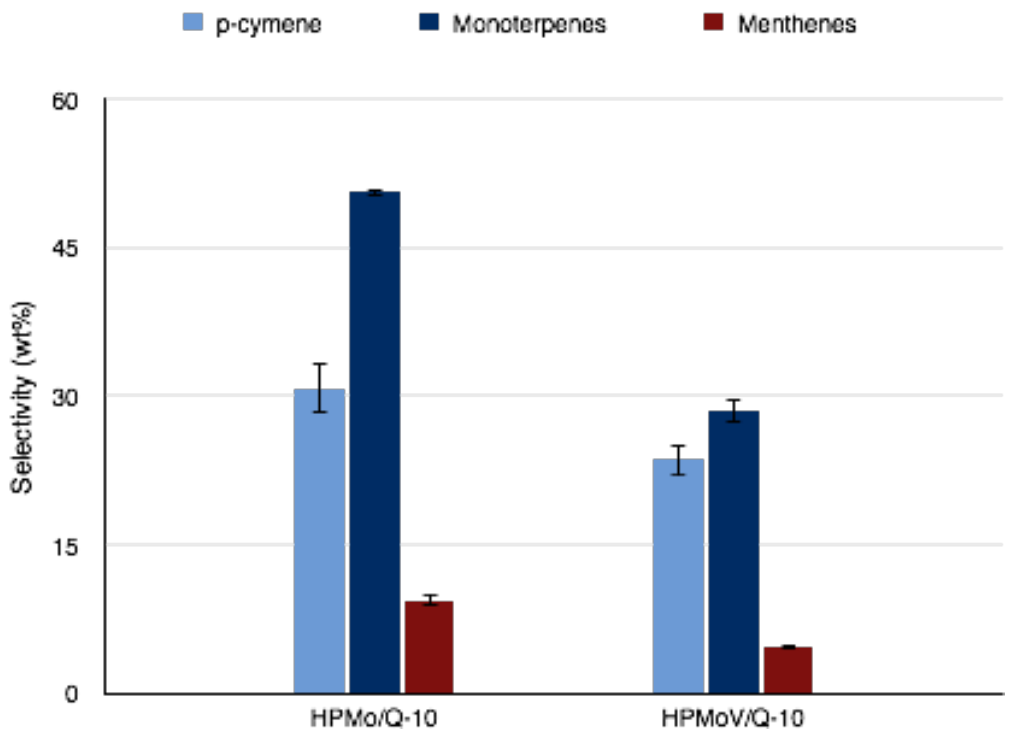

6.4.1.2 Study of the influence of support on the aromatic production. Based on what was found in the previous chapter, in which the Q-10 and SBA-15 support presented the same selectivities, the reactor was validated on the pyroprobe with the catalysts HPMoV/Q-10 and HPMoV/SBA-15. The variation of the D, L limonene conversion for the two supports is shown in Figure 67. A slight decrease in the conversion of HPMoV/Q-10 is found, compared to that obtained in the pyroprobe, whereas the conversion of HPMoV/SBA-15 is similar. The fact that the conversion

is lower is related to a possible non-constant flux of limonene, which is more difficult to control over the reactor than over the quartz capillary.

Figure 67. *Conversion of D, L limonene at 250 °C with HPMoV supported on Q-10 and SBA-15 supports.*

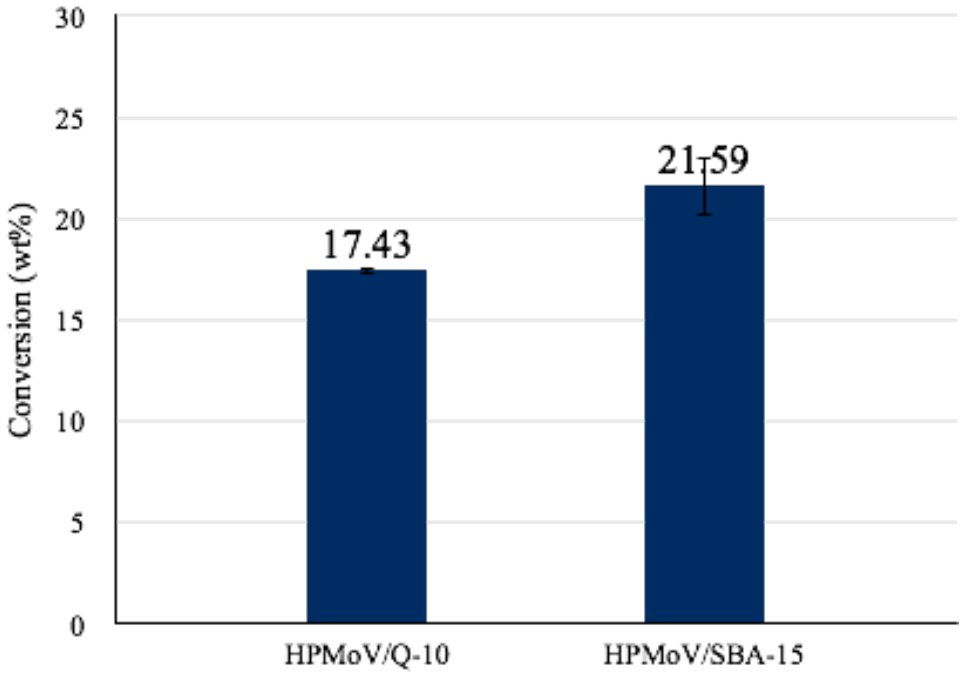

The selectivity obtained with the two supports is shown in Figure 68. It can be evidenced and verified again that there is no significant influence of the support (between Q-10 and SBA-15) on the selectivity towards p-cymene, monoterpenes and menthenes.

Figure 68. *Selectivity to p-cymene, monoterpenes and menthenes obtained with HPMoV supported in Q-10 and SBA-15 at 250 ° C.*

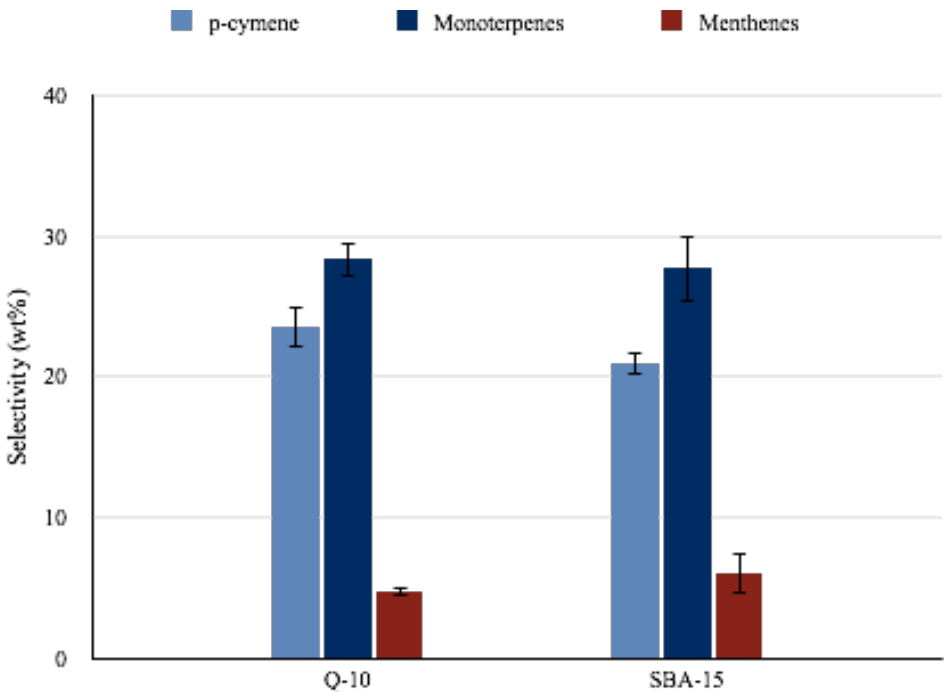

6.4.1.3 Influence of the temperature on the conversion and production of p-cymene. The catalyst HPMoV/SBA-15 was evaluated at three temperatures. The conversion of D, L limonene at different temperatures are presented in Figure 69. Comparing with the results obtained in Py-GC/FID, it is possible to find that the conversion in the reactor test follows the same trend, an increase with the temperature until reaching the maximum at 250 °C, and a decrease at 350 °C. At 180 °C an increase in conversion was observed compared to pyroprobe, which may be related to the difficulty of temperature control of the reactor furnace at low temperatures.

Figure 69. *Influence of temperature on the conversion of DL-limonene using HPMoV supported in SBA-15.*

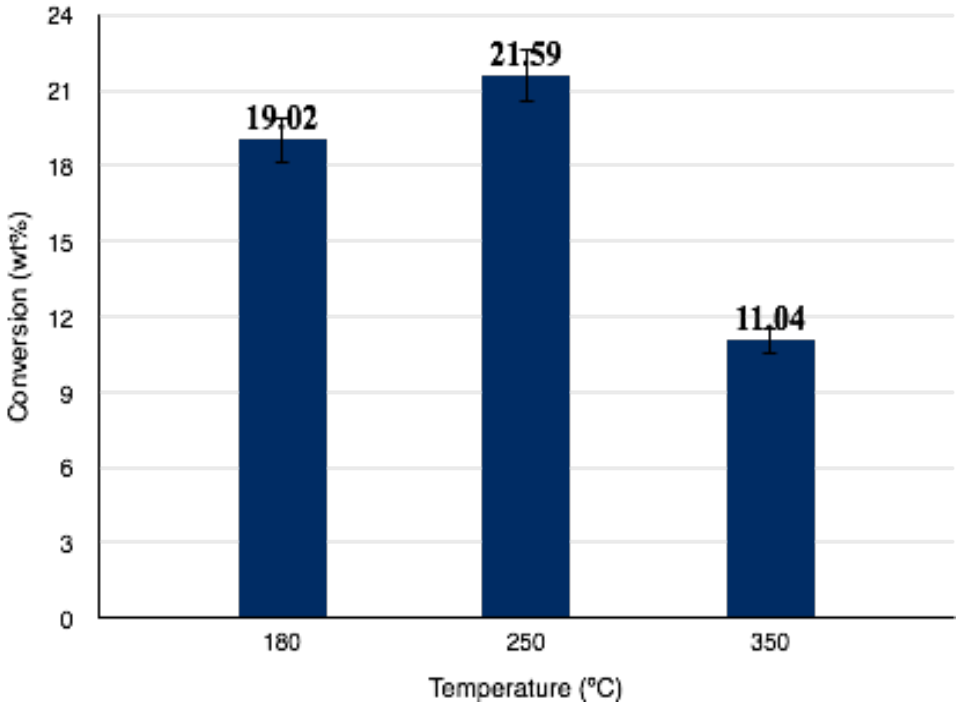

The yield of the most interesting products: p-cymene, monoterpenes and menthenes are presented in Figure 70. It can be observed that there is a difference in the results obtained in the pyroprobe, the yield of p-cymene does not vary significantly with temperature, obtaining lower yields on the reactor. On the other hand, the monoterpenes in the reactor present a higher yield than on pyroprobe, which suggests that the isomerization reaction may be predominant to the dehydrogenation reaction. The low concentration of p-cymene may be related to the possibility of secondary reactions which on the reactor may be more favored due to the longer residence time than the reaction products within the hot zone.

Figure 70. *Yield of p-cymene, monoterpenes and menthenes with HPMoV/SBA-15 catalyst at 250 ºC.*

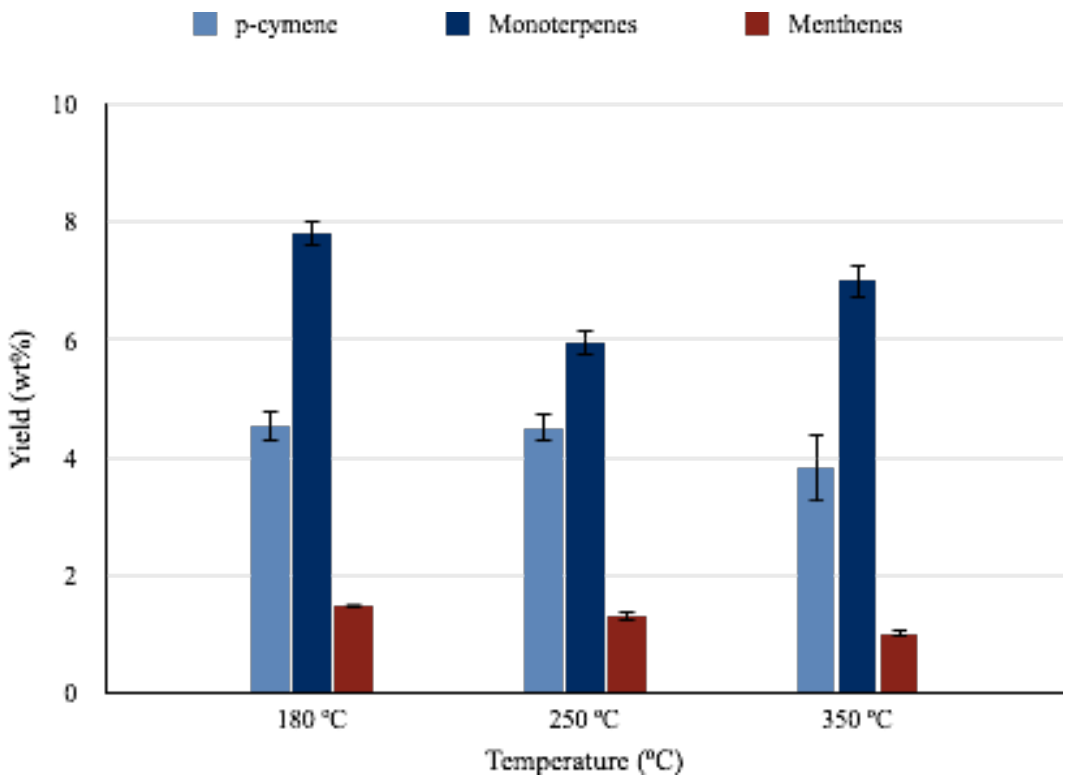

Taking into account that the yields of p-cymene don't vary with temperature, it is decided to evaluate the selectivity towards p-cymene at each temperature. The selectivity is shown in Figure 71. It is observed that at 350 ºC the selectivity towards p-cymene is greater, as well as the selectivity towards monoterpenes, which indicates that although at 350 ºC the conversion is smaller, it is oriented towards the compounds of interest: p-cymene and monoterpenes.

Figure 71. *Selectivity towards p-cymene, monoterpenes and menthenes with HPMoV/SBA-15 catalyst at 250 ºC.*

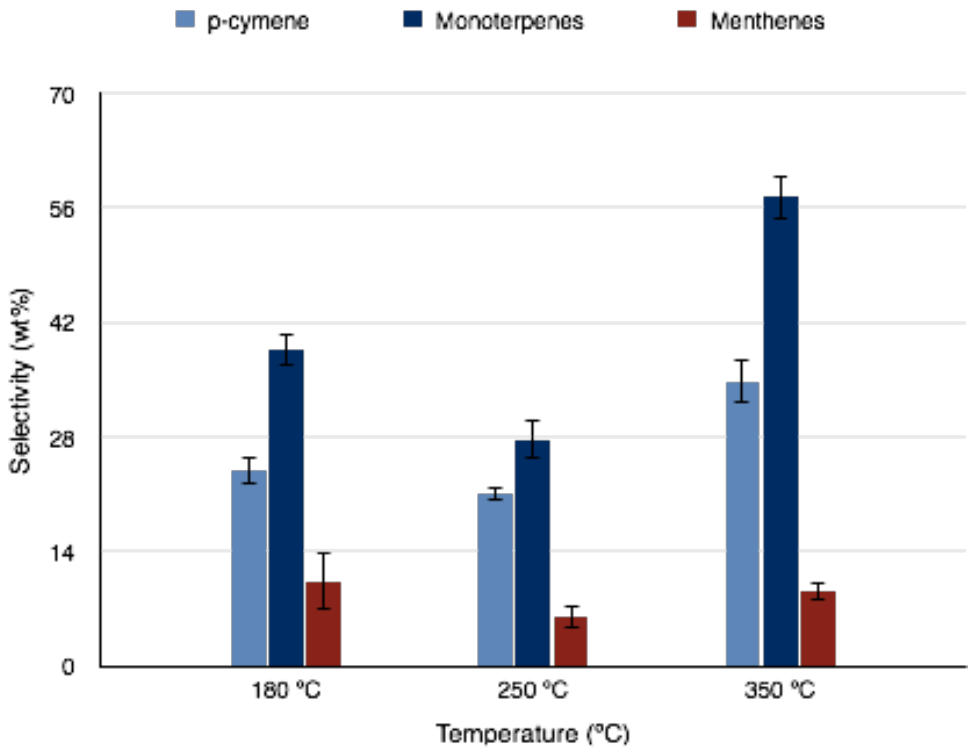

6.4.1.4 Identification and quantification of the carbonaceous material deposited on the catalyst surface. The spectra obtained from C1s for the catalysts HPMo/Q-10, HPMoV/Q-10 after reaction at 250 °C are presented in ANNEX J. The decomposition of C 1s spectra allows observing the existence of different carbon species at 285, 286.5 and 289 eV for all catalyst. According to literature [17–20], the peak at 285 eV are associated with C-C bonds of graphite. The peaks in 285.7-286.5 eV are assigned to hydrogenated carbon species in aliphatic polymers CxHy, and the peaks in 287.3-288.1 eV are due to oxidized carbon in ketone groups C = O [17–20].

Table 23 shows the concentration of carbonaceous material, expressed as percentage of area for each catalyst after reaction at 250 ºC (temperature of maximum conversion). It can be concluded that for all cases, the deposition of carbonaceous material mainly corresponds to graphite.

Table 23. *Carbonaceous material content determinated by XPS analysis.*

Catalyst	Graphite	Aliphatic polymers CxHy	Oxidized carbon in ketone groups	Total carbonaceous material content (wt%)
HPMo/Q-10	27.59	5.22	3.77	36.58
HPMoV/Q-10	28.49	3.83	1.55	33.87

6.4.2 Catalytic tests on laboratory-scale reactor using STR as raw material. The product yields obtained in the pyrolysis and catalytic pyrolysis tests and the composition of pyrolytic oil are given in Table 24. The pyrolysis leads mainly to oil (yield > 50%), but by adding a catalyst decrease in the quantity of oil and increase in the yield of char and gas. This is in agreement with other studies where acid catalysts like HZSM-5 zeolite ($T_{pyrolysis}$ = 450°C; $T_{catalyst\ zone}$ = 400°C; flash pyrolysis) [21] or mesoporous silica MCM-41 zeolite ($T_{pyrolysis}$ = 500°C; $T_{catalyst\ zone}$ = 350°C; heating rate = 10°C/min) [11] have been used and exhibit the same results. According to authors, this could be linked to the strength of acid sites present in these catalysts that promote the cracking reactions favoring the gas yield. The comparison between both studies shows that the lowest oil yield was obtained with HZSM-5 zeolite that, according to NH_3 TPD, has a weak and medium acidity compared with mesoporous silica MCM-41 that presents only weak acidity.

Table 24. *Products yields obtained with the pyrolysis with and without catalytic step and mass percentage in pyrolytic oil of aromatic and partially saturated cyclic compounds.*

TEST	Yield [wt%]					Composition of pyrolytic oil [wt%]	
	Oil	Char	Gas	Aromatic compounds	Partially saturated cyclic compounds	Aromatic compounds concentration	Partially saturated cyclic compounds concentration
Pyrolysis	51.41	36.72	5.62	8.06	10.79	15.67	21.00
HPW/Q-10	30.18	50.10	8.90	8.95	1.00	29.66	3.33
HPMo/Q-10	40.01	44.22	8.07	15.06	1.65	37.66	4.13
HPMoV/Q-10	37.69	47.26	7.95	14.02	2.06	37.22	5.46

HPAs have two main chemical properties: acidity and redox character which give its catalytic performances [22]. Therefore, the decrease of oil yield observed in this study when supported HPA based catalysts are used is due to first property (Table 15). Regarding the pyridine adsorption experiments, the number of strong and medium acid sites is directly linked with the quantity of oil (i.e. the more the number of strong and medium acid site is, the less the oil quantity is). The strength of acid sites is not the only parameter explaining the evolution of oil yield. Xu *et al.* [23] showed that a carbonium ion could be formed on Brønsted sites once the reactants are physisorbed in the pores of support and activated through proton transfer. This carbonium ion formed may thus undergo cracking to produce alkanes and alkenes leading to the increase of the gas product yield. The lowest oil yield was given for the catalyst that has the higher number of Brønsted sites, i.e. HPW/Q10. According to catalyst characterization (Table 15, Chapter 4), the oil yield decreases when the number of strong Brønsted sites increases.

Zeolite catalysts are known to have mainly Brønsted acid sites; the acid strength per site could be modified with the relation between Si and the trivalent T-atom in the framework or by the last type. Many studies have been performed using zeolite catalysts with a trivalent Al atom to improve the production of aromatics from pyrolysis of TR; this is the case of Olazar *et al.* [21] that used a pyroprobe to compare experimentally the performance of three zeolites catalysts (HY, HZSM-5 and HBeta) on in-situ pyrolysis of TR. Their results show that even if the HY zeolite has the highest total acidity measured by NH_3 TPD, its performance to produce oil is the best. On the contrary, HBeta zeolite with the least total acidity shows the most cracking activity that promotes the production of gas compounds. This highest cracking activity must be, therefore, linked to its acidity strength. The similar results were obtained and published by Ding *et al.* [5] for the same zeolite catalysts. Unfortunately, these studies do not perform an analysis based on the type of acid sites that could promote the reforming reactions of volatile compounds formed during pyrolysis.

Figure 72 and Table 24 show that the composition of the pyrolytic oil is also affected by the acidity of the catalyst. Without this additional catalytic step (pyrolysis test), a higher amount of partially saturated cyclic compounds is produced by pyrolysis process, mainly limonene (dipentene), 4-vinylcyclohexene and a non-negligible amount of aromatic compounds such as xylenes, toluene, ethylbenzene, trimethylbenzenes, cymenes and styrene.

The yield of pyrolytic oil and aromatic compounds in the pyrolysis test are in agreement with those obtained by Ucar *et al.* [24] for a STR sample of truck tires. Dipentene, 4-vinylcyclohexene and styrene are the main products from degradation of NR, BR and SBR, respectively. [5,23] According to Ucar *et al.* [24], other compounds are present in pyrolytic oil, but they were not analyzed in this paper, for example, the paraffins. Danon *et al.* [25] published a review of different studies to explain the reaction mechanism of degradation and/or depolymerization of NR. The

most acceptable theory is based on radical reactions beginning by scission of the β bond on the double bonds of the main polymer chain to form different allylic radicals that could undergo an intramolecular cyclization followed by scission and to produce dipentene, among others.

Figure 72. *Concentration of the aromatics and the partially saturated cyclic compounds in the pyrolytic oil produced by pyrolysis with and without catalytic stage*.

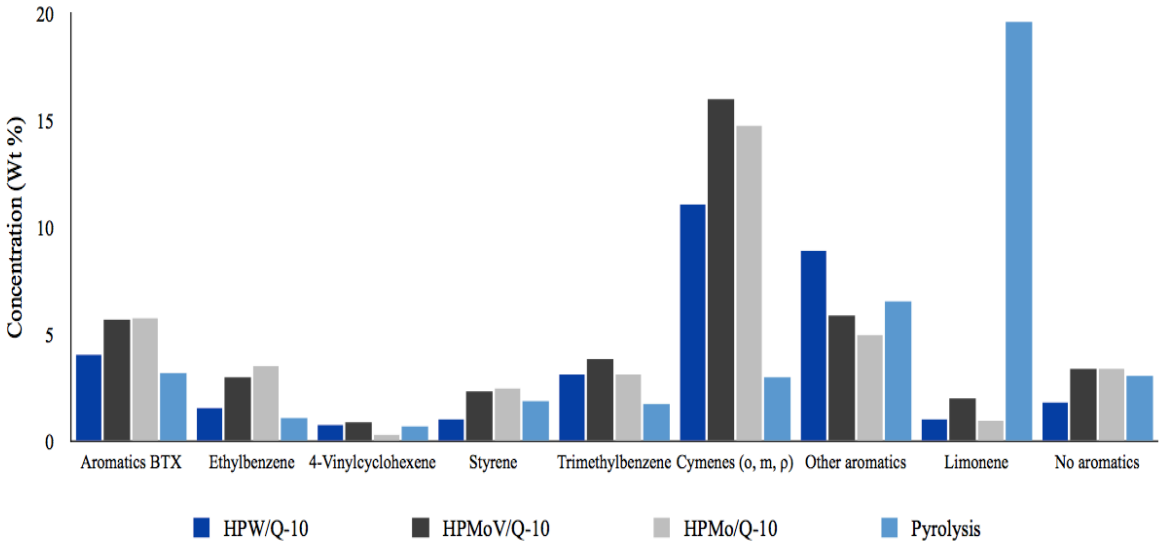

In the case of catalytic pyrolysis tests, cymenes are the most important aromatic compounds present in the pyrolytic oil, which is in accordance with what was found and concluded in chapter 5. According to Boxiong *et al.* [26], two reasons could explain the increase of aromatics concentration in catalytic tires pyrolysis. The first one (1) is the transformation of dipentene via diallyl diradical followed by intramolecular hydrogen transfer, isomerization, intramolecular diene synthesis, dehydrogenation and demethylation [5], in which isomerization step could favor two ways to produce BTX compounds or trimethylbenzene (Figure 73). The second one (2) is based on reactions involving alkenes and alkanes to form single aromatic compounds via Diels-Alder reactions (Figure 73) [27]. Moreover, the authors pointed

out that the first way cannot explain the production of whole aromatic compounds entirely.

Figure 73. *BTX aromatics production from two pathways: (1) Decomposition of dipentene - (2) Diels Alder reaction*

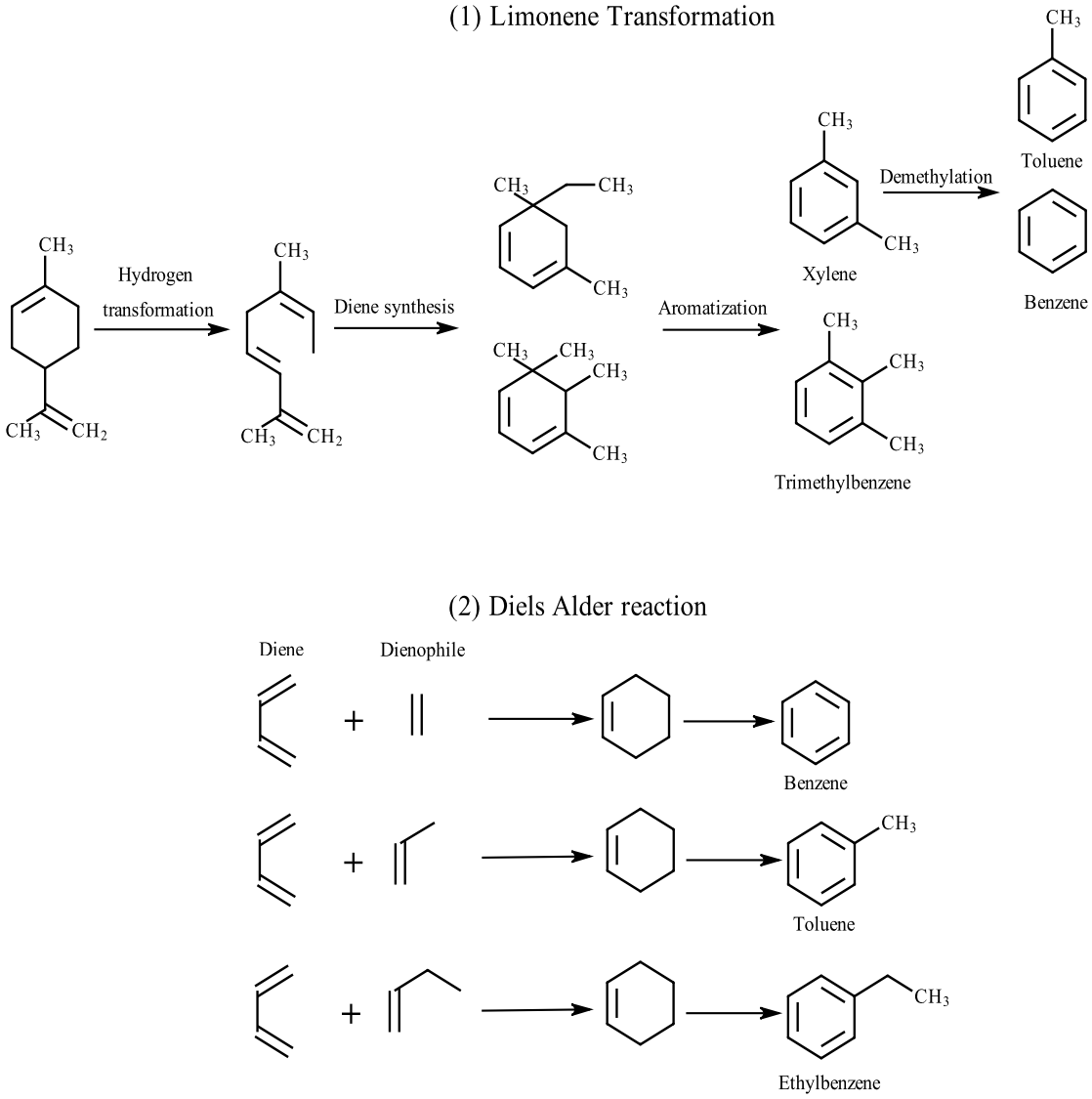

Du *et al*. [28] found differences in the p-cymene, menthene or aromatic compounds (mainly toluene, xylenes and ethylbenzene) selectivities depending on the

Lewis/Brønsted acid sites ratios. This indicates that there are competitive reactions to produce aromatic compounds, in agreement with Boxiong *et al.* and Ding *et al.* [3,5,26]. In this study, for almost all compounds, the lowest yields and concentrations are obtained when HPW/Q10 catalyst is used. This behavior is linked to its higher number of Brønsted acid sites and its strong acidity (chapter 4) that, as aforementioned, allow facilitating the cracking reactions to yield both light gases (alkanes and alkenes) and aromatic compounds of higher molecular weight (denoted in Figure 72 as “other aromatics”). On the other hand, the highest amounts of trimethylbenzene and BTX compounds are obtained with HPA catalyst containing more Lewis acid sites than Brønsted ones. However, for the HPA based catalysts with similar strength acid sites and total acidity, i.e. HPMo/Q10 and HPMoV/Q10, no difference on the composition of BTX compounds is observed. It has to be noted that the catalyst containing a higher Lewis/Brønsted ratio, i.e. HPMo/Q10, favors the trimethylbenzene production. It should also be remarked that, in contrast to BTX compounds that could participate in alkylation reactions with alkenes, trimethylbenzene is a final product in the reaction mechanism proposed by Ding *et al.* [5]. Therefore, its production can be increased by methanation reaction of dimethyl ethylbenzene given on Brønsted acid sites.

Table 25 gives a comparison of gases and aromatic compounds yields presented in this paper and those reported in the literature using zeolite catalysts. The use of HPA based catalysts allows production of fewer gases, indicating less activity towards cracking reactions. A difference of 17 and 6 wt% between pyrolytic and catalytic tests was reported by Olazar *et al.* [21] and Williams and Brindle [1] , respectively, whereas in this study, this difference is close at 3.5 wt% (Table 25). On the other hand, the table shows a significant difference between the yields of aromatic compounds obtained using zeolite based catalysts or HPA based catalysts; the first allows producing BTX compounds, mainly, whereas the second promotes the formation of cymenes. As aforementioned, the difference between the selectivities could be explained by differences between the types of acid sites in the catalysts.

Unfortunately, these studies do not perform an analysis based on the type of acid hindering the comparison with the data presented in this paper.

Table 25. *Concentration of aromatic compounds as a function of the HPA catalysts and operating conditions in a fixed bed reactor.*

Catalyst [Ref]	Catalyst/tire ratio Temperature of catalytic zone, temperature of pyrolysis zone and Heating rate	Yield [wt %]							
		Gases	Benzene	Toluene	Xylene (o,m,p)	Ethylbenzene	Styrene	TMB	Cymene (o,m,p)
Y CBV – 400*	0.25 500 ºC	12	-	3.4	3.8	0.5	-	1.9	-
Y CBV - 780*	500 ºC 10 °C/min	12	-	2.4	3.5	0.5	-	2.1	-
HZSM – 5**	18.75 400 °C 450 ºC 20 °C/ms	20	2.6	4.9	3.2	0.1	-	0.7	-
HPW/Q-10	0.2 350 ° C 466 °C 30°C/min	8.90	-	0.5	0.7	0.5	0.3	0.9	3.3
HPMoV/Q-10		8.07	-	0.8	1.5	1.1	0.9	1.44	6.0
HPMo/Q-10		7.95	-	1.9	1.9	1.4	1.0	1.2	5.9

* Data of Williams and Brindle [1]. Aromatic yield calculated from oil yield and its composition in wt%.

** Data of Olazar *et al*. [21].

The spectra obtained from C1s for the catalysts HPMo/Q-10, HPMoV/Q-10 and HPW/Q-10 after reaction with STR at 350 °C are presented in ANNEX J. The decomposition of C 1s spectra allows to see the existence of different carbon species. The peaks in 285.7-286.5 eV are assigned to hydrogenated carbon species in aliphatic polymers CxHy, and the peaks in 287.3-288.1 eV are due to oxidized carbon in ketone groups C = O[17–20].

Table 26 shows the concentration of carbonaceous material, expressed as percentage of area for each catalyst after reaction at 250 ºC (temperature of maximum conversion).

Table 26. *Carbonaceous material content determinated by XPS analysis*.

Catalyst	Graphite	Aliphatic polymers CxHy	Oxidized carbon in ketone groups	Total carbonaceous material content (wt%)
HPMo/Q-10	36.35	3.59	4.98	44.92
HPMoV/Q-10	40.56	6.93	4.42	51.91
HPW/Q-10	22.75	3.02	2.61	28.34

It can be concluded that in all cases the deposition of carbonaceous material, mainly, is the type of graphite. It is possible to observe that the catalyst with the highest deposition is presents on HPMoV/Q10). The catalyst with the lowest amount of carbonaceous matter is HPW/Q-10, which has the lowest total acidity, the strongest acid sites, and lower L/B ratio than other two catalysts (Chapter 4). It can be concluded that the amount of carbonaceous matter is lower with respect to the lower L/B ratio, therefore to reduce the carbon deposit and subsequent deactivation of the catalyst, a low L/B ratio and strong acid sites are necessary. This could be associated to the possible high acidity (Bronsted acidity) favoring the cracking reactions and helping that large molecules that can be deposited on the surface are cracked, facilitating their exit. This may be related to the higher concentration of other aromatic compounds (Figure 72) and gases (Table 24) which are higher for HPW/Q-10 than for other catalysts.

6.5 CONCLUSIONS

- The results obtained in Py-GC / FID of the transformation of D, L limonene were validated on the reactor. It was found that the HPMo catalyst which has the highest L/B ratio exhibits the highest aromatic selectivity in both the pyroprobe and reactor.

- The reforming of volatile produced during STR pyrolysis using HPA based catalysts allowed improving the concentration of aromatic compounds in pyrolytic oil (until approx. 37 wt% in the pyrolytic oil) in comparison with the value obtained without catalysts.

- Cymenes compounds are the most important aromatics in pyrolytic oil produced by reforming reaction of dipentene. The selectivity of catalysts to produce p-cymene, menthene or aromatic compound as BTX depend on the Lewis/Brönted acid sites ratio. This study has found that the highest amount of BTX compounds are obtained with HPA catalysts contained more Lewis acid sites than Brönsted ones, i.e. Molybdenum-based catalysts.

- No difference in the concentration of BTX compounds was observed for catalysts with similar strength acid sites and total acidity. On the other hand, the highest amounts of cymenes compounds were obtained with the Molybdenum-based catalysts with the highest number of Lewis sites.

- Higher number of Brönsted acid sites and its strong acidity allow facilitating the cracking reactions to yield both light gases and aromatic compounds of higher molecular weight and decreasing the amount of carbonaceous material deposited in the catalyst. This one corresponding to a graphite type.

6.6 REFERENCES OF THIS CHAPTER

[1] WILLIAMS, Paul T. and BRINDLE Alexander J.. Aromatic chemicals from the catalytic pyrolysis of scrap tyres. In: Journal of Analytical and Applied Pyrolysis [online]. 2003, 67(1), 143–164.

[2] TOPCHIEV, A. V.; MAMEDALIEV G. M. and MAMEDALIEV Yu. G.. Demethylation and isomerization of o-Xylene over aluminosilicates. Institute of Petroleum of the Academy of Sciences of the USSR. 1955, p 1421-1429.

[3] BOXIONG, Shen, *et al*. Pyrolysis of waste tyres with zeolite USY and ZSM-5 catalysts. In: Applied Catalysis B: Environmental [online]. 2007, 73(1–2), p. 150–157.

[4] OLAZAR, Martin, *et al*. Catalyst effect on the composition of tire pyrolysis products. In: Energy and Fuels [online]. 2008, 22(5), p. 2909–2916.

[5] DING, Kuan, *et al*. Catalytic pyrolysis of waste tire to produce valuable aromatic hydrocarbons: An analytical Py-GC/MS study. In: Journal of Analytical and Applied Pyrolysis [online]. 2016, p. 122, 55–63.

[6] QU, Wei, *et al*. Pyrolysis of waste tire on ZSM-5 zeolite with enhanced catalytic activities. In: Polymer Degradation and Stability [online]. 2006, 91(10), p. 2389–2395.

[7] ARABIOURRUTIA, Miriam, *et al*. Efecto del uso de catalizadores ácidos sobre la distribución de productos en la pirólisis de neumáticos. In: Informacion Tecnológica [online]. 2010, 21(1), p. 33–41.

[8] HITA, Idoia, *et al*. Opportunities and barriers for producing high quality fuels from the pyrolysis of scrap tires. In: Renewable and Sustainable Energy Reviews [online]. 2016, 56, p. 745–759.

[9] NAMCHOT, Witsarut and JITKARNKA Sirirat. Impacts of nickel supported on different zeolites on waste tire-derived oil and formation of some petrochemicals. In: Journal of Analytical and Applied Pyrolysis [online]. 2016, 118, p. 86–97.

[10] MUENPOL, Suttipong and JITKARNKA Sirirat. Effects of Fe supported on zeolites on structures of hydrocarbon compounds and petrochemicals in waste tire-derived pyrolysis oils. In: Journal of Analytical and Applied Pyrolysis. 2016, 117, p. 147–156.

[11] DŨNG, Nguyễn Anh, *et al*. Roles of ruthenium on catalytic pyrolysis of waste tire and the changes of its activity upon the rate of calcination. In: Journal of Analytical and Applied Pyrolysis [online]. 2010, 87(2), p. 256–262.

[12] DŨNG, Nguyễn Anh,*et al*. Light olefins and light oil production from catalytic pyrolysis of waste tire. In: Journal of Analytical and Applied Pyrolysis [online]. 2009, 86(2), p. 281–286.

[13] WITPATHOMWONG, Chaiyaporn, *et al*. Improving light olefins and light oil production using Ru/MCM-48 in catalytic pyrolysis of waste tire. In: Energy Procedia [online]. 2011, 9, p. 245–251.

[14] ACOSTA, Rolando, *et al*. Production of Oil and Char by Intermediate Pyrolysis of Scrap Tyres: Influence on Yield and Product Characteristics. In: International Journal of Chemical Reactor Engineering [online]. 2015, 13(2), p. 189–200.

[15] MISONO, M., OKUHARA T. and MIZUNO N. Catalysis by Heteropoly Compounds. In: Studies in Surface Science and Catalysis [online]. 1989, 44, p. 267–278.

[16] KATRITZKY, Alan R, *et al*. Prediction of gas chromatographic retention times and response factors using a general quantitative structure-property relationship treatment. In: Anal. Chem. 1994, 6(11), p. 1799–1807.

[17] BAI, Ting, *et al*. Coking behaviors and kinetics on HZSM-5/SAPO-34 catalysts for conversion of ethanol to propylene. In: Journal of Energy Chemistry [online]. 2016, 25(3), p. 545–552.

[18] WANG, Zhiyuan and BAO Binbin. Investigation on Coking Performance with Sulfur / Phosphorous-Containing Additive and Anti-coking SiO2/S Coating during Thermal Cracking of Light Naphtha [online]. In: Energy Procedia. 2017, 105, p. 5122–5127.

[19] LI, Yu, *et al*. Coke formation on the surface of Ni/HZSM-5 and Ni-Cu/HZSM-5 catalysts during bio-oil hydrodeoxygenation. In: Fuel [online]. 2017, 189, p. 23–31.

[20] LIU, B. S., *et al*, and TG/DTA characterization of deposited carbon in methane dehydroaromatization over Ga-Mo/ZSM-5 catalyst. In: Applied Surface Science [online]. 2007, 253(11), p. 5092–5100.

[21] OLAZAR, Martín, *et al*. Effect of acid catalysts on scrap tyre pyrolysis under fast heating conditions. In: Journal of Analytical and Applied Pyrolysis [online]. 2008, 82(2), p. 199–204.

[22] AHMAD, M. Irfan, ZAIDI S. M. Javaid and AHMED Shakeel. Proton conducting composites of heteropolyacids loaded onto MCM-41. In: Journal of Power Sources [online]. 2006, 157(1), p. 35–44.

[23] XU, Bin, *et al*. Catalytic activity of Brønsted acid sites in zeolites: Intrinsic activity, rate-limiting step, and influence of the local structure of the acid sites. In: Journal of Catalysis [online]. 2006, 244(2), p. 163–168.

[24] UCAR, Suat, *et al*. Evaluation of two different scrap tires as hydrocarbon source by pyrolysis. In: Fuel [online]. 2005, 84(14–15), p.1884–1892.

[25] DANON, B., *et al*. A review of dipentene (dl-limonene) production from waste tire pyrolysis. In: Journal of Analytical and Applied Pyrolysis [online]. 2015, 112, p. 1–13.

[26] BOXIONG, Shen, *et al*. Pyrolysis of waste tyres: The influence of USY catalyst/tyre ratio on products. In: Journal of Analytical and Applied Pyrolysis [online]. 2007, 78(2), p. 243–249.

[27] CYPRES, R. Aromatics hydrocarbons formation during coal pyrolysis. In: Fuel Processing Technology. 1987, 15, p. 1–15.

[28] DU, Junming, *et al*. Catalytic dehydrogenation and cracking of industrial dipentene over M/SBA-15 (M = Al, Zn) catalysts. In: Applied Catalysis A: General [online]. 2005, 296(2), p. 186–193.

6.7 BIBLIOGRAPHY OF THIS CHAPTER

ACOSTA, Rolando, *et al*. Production of Oil and Char by Intermediate Pyrolysis of Scrap Tyres: Influence on Yield and Product Characteristics. In: International Journal of Chemical Reactor Engineering [online]. 2015, 13(2), p. 189–200.

AHMAD, M. Irfan, ZAIDI S. M. Javaid and AHMED Shakeel. Proton conducting composites of heteropolyacids loaded onto MCM-41. In: Journal of Power Sources [online]. 2006, 157(1), p. 35–44.

ARABIOURRUTIA, Miriam, *et al*. Efecto del uso de catalizadores ácidos sobre la distribución de productos en la pirólisis de neumáticos. In: Informacion Tecnológica [online]. 2010, 21(1), p. 33–41.

BAI, Ting, *et al*. Coking behaviors and kinetics on HZSM-5/SAPO-34 catalysts for conversion of ethanol to propylene. In: Journal of Energy Chemistry [online]. 2016, 25(3), p. 545–552.

BOXIONG, Shen, *et al*. Pyrolysis of waste tyres with zeolite USY and ZSM-5 catalysts. In: Applied Catalysis B: Environmental [online]. 2007, 73(1–2), p. 150–157.

BOXIONG, Shen, *et al*. Pyrolysis of waste tyres: The influence of USY catalyst/tyre ratio on products. In: Journal of Analytical and Applied Pyrolysis [online]. 2007, 78(2), p. 243–249.

CYPRES, R. Aromatics hydrocarbons formation during coal pyrolysis. In: Fuel Processing Technology. 1987, 15, p. 1–15.

DANON, B., *et al*. A review of dipentene (dl-limonene) production from waste tire pyrolysis. In: Journal of Analytical and Applied Pyrolysis [online]. 2015, 112, p. 1–13.

DING, Kuan, *et al*. Catalytic pyrolysis of waste tire to produce valuable aromatic hydrocarbons: An analytical Py-GC/MS study. In: Journal of Analytical and Applied Pyrolysis [online]. 2016, p. 122, 55–63.

DU, Junming, *et al*. Catalytic dehydrogenation and cracking of industrial dipentene over M/SBA-15 (M = Al, Zn) catalysts. In: Applied Catalysis A: General [online]. 2005, 296(2), p. 186–193.

DŨNG, Nguyễn Anh, *et al*. Roles of ruthenium on catalytic pyrolysis of waste tire and the changes of its activity upon the rate of calcination. In: Journal of Analytical and Applied Pyrolysis [online]. 2010, 87(2), p. 256–262.

DŨNG, Nguyễn Anh,*et al*. Light olefins and light oil production from catalytic pyrolysis of waste tire. In: Journal of Analytical and Applied Pyrolysis [online]. 2009, 86(2), p. 281–286.

HITA, Idoia, *et al*. Opportunities and barriers for producing high quality fuels from the pyrolysis of scrap tires. In: Renewable and Sustainable Energy Reviews [online]. 2016, 56, p. 745–759.

KATRITZKY, Alan R, *et al*. Prediction of gas chromatographic retention times and response factors using a general quantitative structure-property relationship treatment. In: Anal. Chem. 1994, 6(11), p. 1799–1807.

LI, Yu, *et al*. Coke formation on the surface of Ni/HZSM-5 and Ni-Cu/HZSM-5 catalysts during bio-oil hydrodeoxygenation. In: Fuel [online]. 2017, 189, p. 23–31.

LIU, B. S., *et al*, and TG/DTA characterization of deposited carbon in methane dehydroaromatization over Ga-Mo/ZSM-5 catalyst. In: Applied Surface Science [online]. 2007, 253(11), p. 5092–5100.

MISONO, M., OKUHARA T. and MIZUNO N. Catalysis by Heteropoly Compounds. In: Studies in Surface Science and Catalysis [online]. 1989, 44, p. 267–278.

MUENPOL, Suttipong and JITKARNKA Sirirat. Effects of Fe supported on zeolites on structures of hydrocarbon compounds and petrochemicals in waste tire-derived pyrolysis oils. In: Journal of Analytical and Applied Pyrolysis. 2016, 117, p. 147–156.

NAMCHOT, Witsarut and JITKARNKA Sirirat. Impacts of nickel supported on different zeolites on waste tire-derived oil and formation of some petrochemicals. In: Journal of Analytical and Applied Pyrolysis [online]. 2016, 118, p. 86–97.

OLAZAR, Martin, *et al*. Catalyst effect on the composition of tire pyrolysis products. In: Energy and Fuels [online]. 2008, 22(5), p. 2909–2916.

OLAZAR, Martín, *et al*. Effect of acid catalysts on scrap tyre pyrolysis under fast heating conditions. In: Journal of Analytical and Applied Pyrolysis [online]. 2008, 82(2), p. 199–204.

QU, Wei, *et al*. Pyrolysis of waste tire on ZSM-5 zeolite with enhanced catalytic activities. In: Polymer Degradation and Stability [online]. 2006, 91(10), p. 2389–2395.

TOPCHIEV, A. V.; MAMEDALIEV G. M. and MAMEDALIEV Yu. G.. Demethylation and isomerization of o-Xylene over aluminosilicates. Institute of Petroleum of the Academy of Sciences of the USSR. 1955, p 1421-1429.

UCAR, Suat, *et al*. Evaluation of two different scrap tires as hydrocarbon source by pyrolysis. In: Fuel [online]. 2005, 84(14–15), p.1884–1892.

XU, Bin, *et al*. Catalytic activity of Brønsted acid sites in zeolites: Intrinsic activity, rate-limiting step, and influence of the local structure of the acid sites. In: Journal of Catalysis [online]. 2006, 244(2), p. 163–168.

WANG, Zhiyuan and BAO Binbin. Investigation on Coking Performance with Sulfur / Phosphorous-Containing Additive and Anti-coking SiO2/S Coating during Thermal Cracking of Light Naphtha [online]. In: Energy Procedia. 2017, 105, p. 5122–5127.

WILLIAMS, Paul T. and BRINDLE Alexander J.. Aromatic chemicals from the catalytic pyrolysis of scrap tyres. In: Journal of Analytical and Applied Pyrolysis [online]. 2003, 67(1), 143–164.

WITPATHOMWONG, Chaiyaporn, *et al*. Improving light olefins and light oil production using Ru/MCM-48 in catalytic pyrolysis of waste tire. In: Energy Procedia [online]. 2011, 9, p. 245–251.

General Conclusions

The pyrolysis of STR for the production of single ring aromatics was evaluated experimentally by optimizing the thermal decomposition process of the rubber and subsequent catalytic reforming of the vapors produced using supported heteropolyacid catalysts.

In the first stage, an evaluation of influential variables in the thermal pyrolysis (without catalyst) by a statistical analysis was performed, in which the temperature was the most influential variable, and also its interaction with nitrogen flow. The pyrolytic oil obtained in each test was characterized and it was observed that both: nitrogen volumetric flow and operating temperature do not affect the density or HHV. However, it noted that the acidity varies, it is because the acidity depends mainly on the composition of the pyrolytic oil. The lowest acidity is obtained at the operating conditions of maximum yield of total aromatics (466 °C and 155 Nml/min).

In addition to temperature and nitrogen flow, the influence of other variables such as the residence time of the volatiles in the reactor and the reaction time were evaluated. It was determined that the residence time is an influential variable in the pyrolytic oil yield and the production of aromatic compounds of interest. The higher BTX concentration was produced at low residence time.

As a conclusion of this stage of thermal pyrolysis, models to predict the variability of the pyrolytic oil and aromatics yield as a function of temperature and nitrogen flow were established. In addition, the operating conditions were determinated to obtain

the maximum yield of aromatics, within the range studied for each variable. From the results found in first stage, where the limonene concentration (compound in highest concentration in the oil) decreases when the aromatic concentration increases, suggesting the possible transformation of this to simple ring aromatics, in second stage was icnluded to study the transformation of D-L limonene into aromatics using different heteropolyacid/support combinations, under different conditions.

For the synthesis of catalysts, four different active phases (*i.e.* $H_3PW_{12}O_{40}$, $H_3PMo_{12}O_{40}$, $H_4SiW_{12}O_{40}$ and $H_3PMo_{11}VO_{40}$) were used, which were deposited on different supports (*i.e.* CARiACT Q-10, SBA-15, MCM-41 and KIT-6). The catalysts (HPA based on support) were characterized by N_2 adsorption - desorption, XRD, NH_3 TPD, FTIR, pyridine adsorption - FTIR. These characterizations allowed to check the correct catalysts synthesis and to determine of the textural and structural properties, the types of acid sites (i.e. Brönsted, Lewis), their strength and their number for each catalyst.

The results in this stage showed a conversion of limonene to p-cymene, monoterpenes and menthenes, mainly. A mechanism was proposed, in which p-cymene can be obtained by two types of reactions: isomerization/dehydrogenation and disproportionation. It was found that Lewis acidity favors isomerization and dehydrogenation reactions, whereas the reaction of disproportionation is favored by the Brønsted acidity. In addition to the need for Lewis acidity, the high ratio of Lewis/Brønsted acid sites are required for the transformation of limonene to p-cymene, in which Lewis sites prevail over Brønsted.

On the other hand, the pore size of the support has an influence on the selectivity towards p-cymene, which is directly related to the accessibility to the active sites and the subsequent output of the products. The ordered structure of SBA-15 favors the

isomerization of terpenes, however, no differences were found in the selectivity of p-cymene compared to commercial support.

Once the mechanism of transformation of limonene to single ring aromatics was defined, in the third stage, the catalysts more selective were evaluated on the STR pyrolysis reaction. It was found that the reforming of volatile produced during STR pyrolysis using HPA based catalysts allowed to improve the concentration of aromatic compounds in pyrolytic oil, until approx. 37 wt% in the pyrolytic oil) in comparison with the value obtained without catalysts. Cymenes compounds, mainly p- cymene, are the most important aromatics in pyrolytic oil produced by transformation reactions of limonene, and was proved and validated that the selectivity of catalysts to produce p-cymene, menthene or aromatic compound as BTX, depend on the Lewis/Brønsted acid sites ratio. This study has found that the highest amount of BTX compounds are obtained with HPA catalysts contained more Lewis acid sites than Brønsted ones, i.e. Molybdenum-based catalysts. Besides, no difference in the concentration of BTX compounds was observed for catalysts with similar strength acid sites and total acidity.

The highest amounts of cymenes compounds were obtained with the Molybdenum-based catalysts with the highest number of Lewis sites. On the contrary, the lowest yields and concentration are obtained when the Tungsten-based catalyst was used, linked to its higher number of Brønsted acid sites and its strong acidity that allow facilitating the cracking reactions to yield both, light gases and aromatic compounds of higher molecular weight.

Publications

- Production of oil and char by intermediate pyrolysis of scrap tyres: Influence on yield and product characteristics". R. Acosta, C. Tavera, P. Gauthier-Maradei, D. Nabarlatz. International journal of chemical reactor engineering, (Int. J. Chem. React. Eng.) *ISSN:* 1542-6580, *v.*13 *fasc.* p.189 - 200 ,2015.

- Experimental study of the aromatics production from the pyrolysis of scrap tires rubber using heteropolyacids-based catalysts: an study of the transformation of D, L limonene into simple aromatic compoundsC. Tavera, P. Gauthier-Maradei, M. Capron, C. Pirez.. Recently submitted to journal Waste and Biomass Valorization.

- Improvement of the production of aromatics compounds obtained from the pyrolysis of scrap tires rubber using heteropolyacids-based catalysts C. Tavera, P. Gauthier-Maradei, M. Capron, D. Ferreira, C. Palencia, O. Gardoll, J.C. Morin, B. Katryniok, F. Dumeignil. Recently submitted to journal Waste and Biomass Valorization.

Communications

- Oral communication: Improvement of aromatics compounds production from pyrolysis of scraps tyres rubber using heteropolyacids based catalysts, in 21 International Symposium on analytical and applied pyrolysis Pyro 2016, May 9-12, 2016, Nancy-France.

- Oral communication: Improvement of aromatics compounds production from pyrolysis of scraps tires rubber using heteropolyacids based catalysts: Study of D,L limonene transformation to aromatic compounds, in Fourth Bilateral Indo-French Symposium, June 27-30, 2016, -Villeneuve D'Asqc-France.

- Poster communication: D,L limonene transformation to aromatic compounds of industrial value using heteropolyacids based catalyst, in French conference on catalysis FCCAT, May 23-27,2016, Frejús - France.

- Poster communication: Improvement of the production of aromatic compounds obtained from the pyrolysis of scrap tires rubber using heteropolyacids-based catalysts, in Summer School: Catalysis Fundamentals and Practice, July 17-21, 2017, Liverpool - UK.

ANNEXES

ANNEX A THE PROXIMATE ANALYSIS IN DRY BASIS

Annex A. 1 *The proximate analysis of natural rubber.*

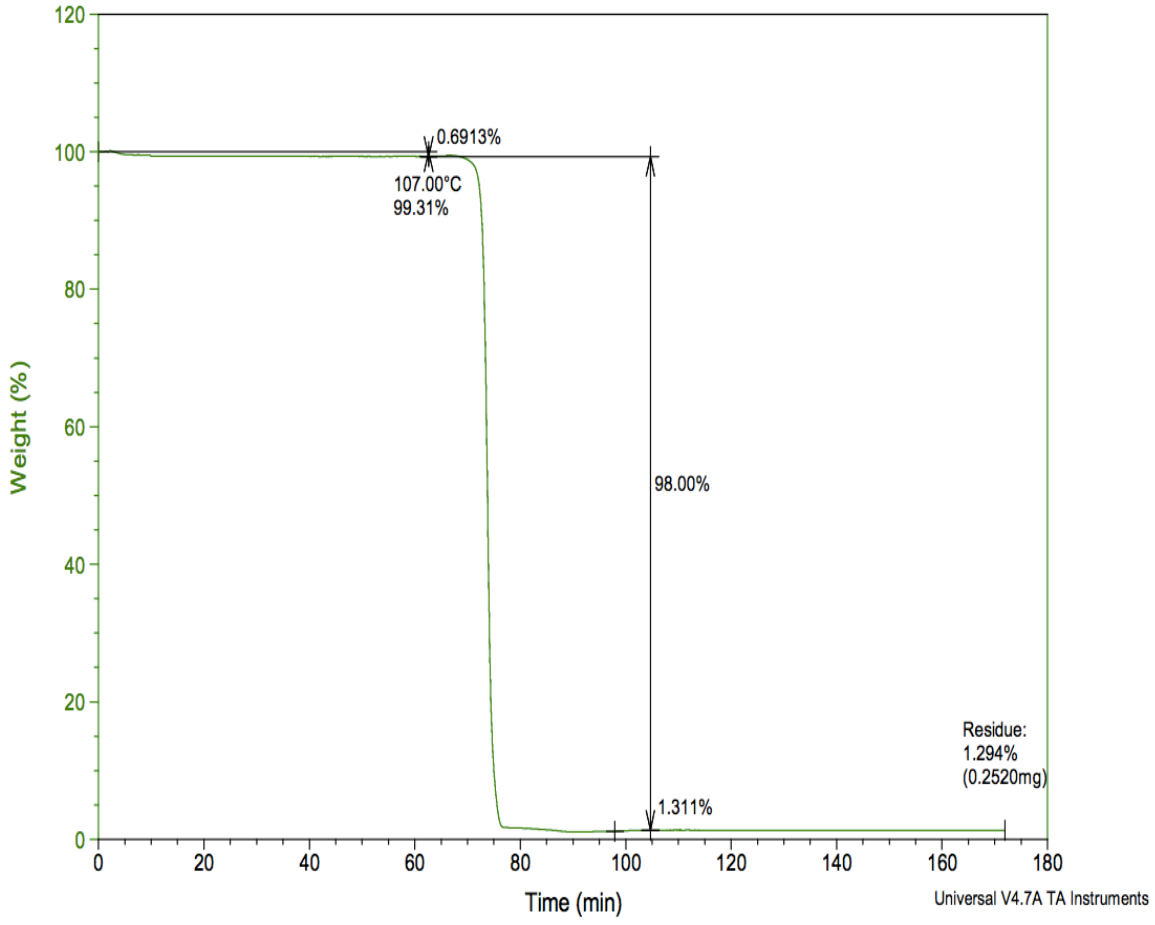

	Wt%
Moisture	0.69
Volatile matter	98
Fixed carbon	0.01
Ash	1.29

Annex A. 2 ***The proximate analysis of polybutadiene rubber.***

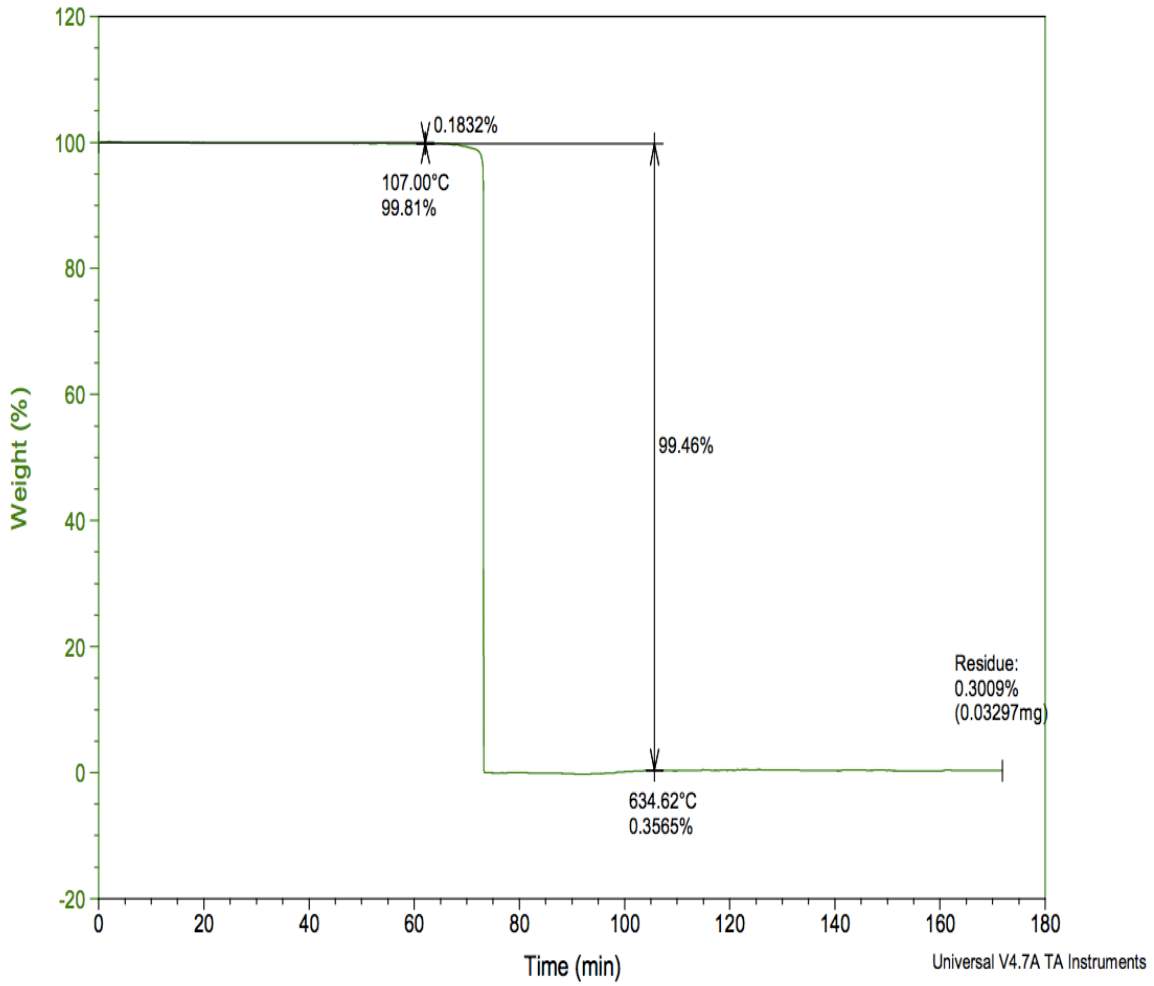

	Wt%
Moisture	0.18
Volatile matter	99.5
Fixed carbon	0.02
Ash	0.30

Annex A. 3 ***The proximate analysis of styrene rubber.***

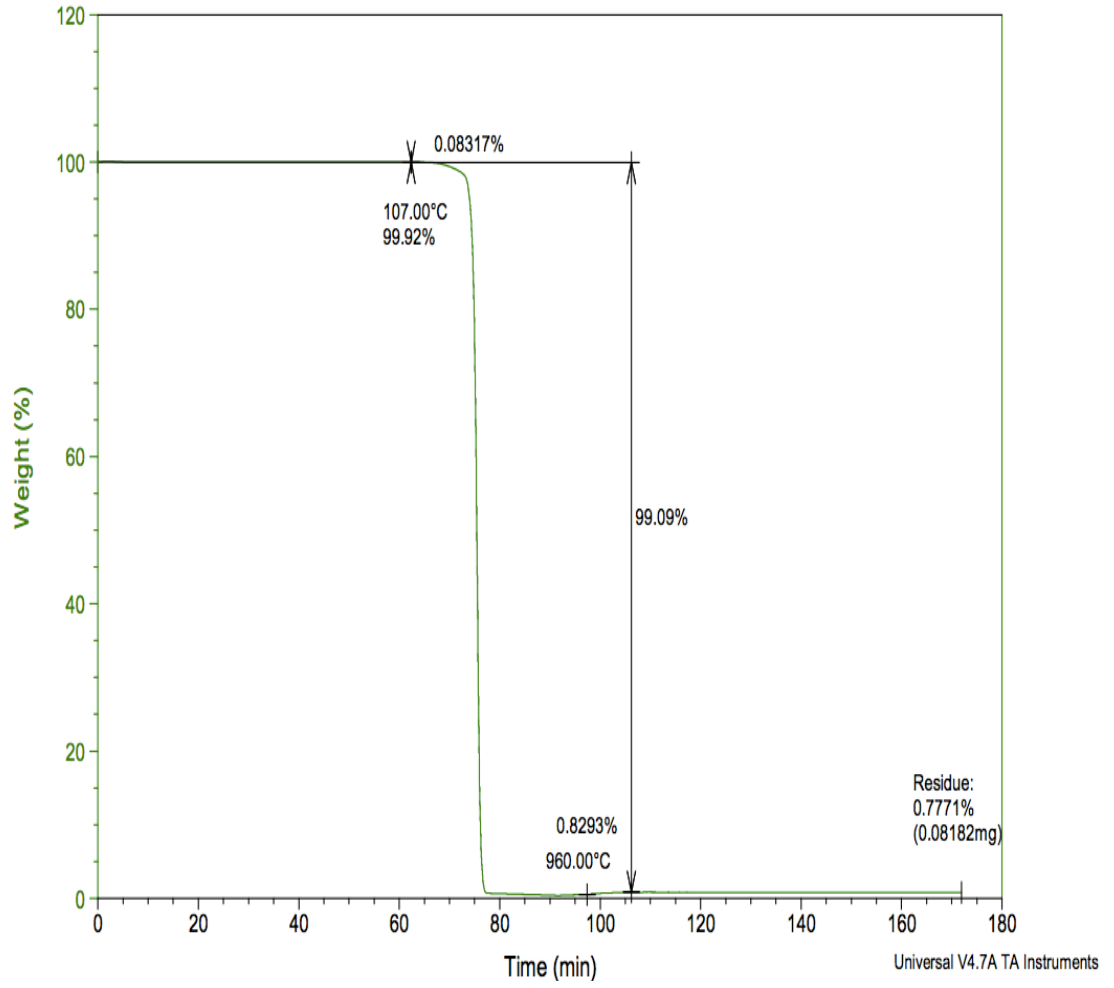

	Wt%
Moisture	0.08
Volatile matter	99.09
Fixed carbon	0.05
Ash	0.78

ANNEX A. 4 ***The proximate analysis of styrene butadiene rubber***

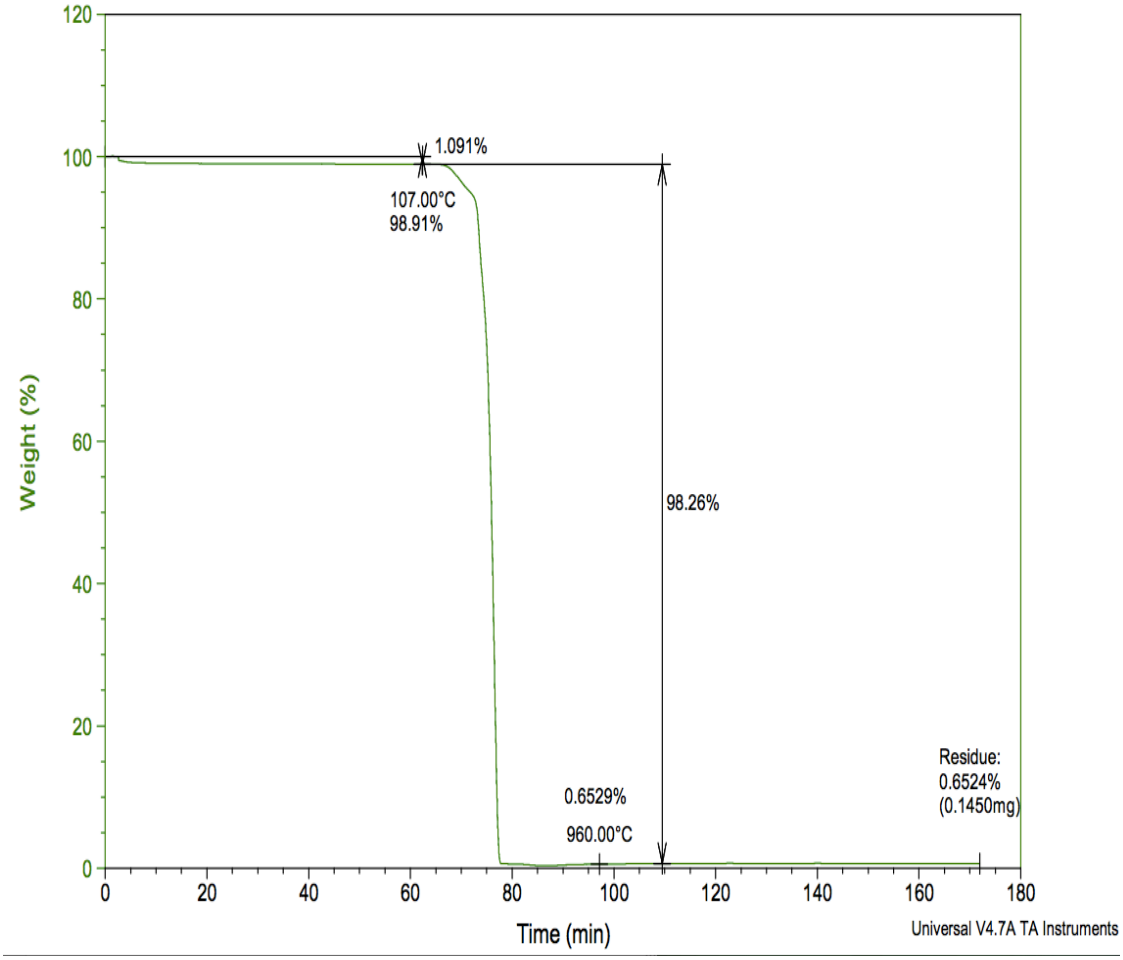

	Wt%
Moisture	1.09
Volatile matter	98.26
Fixed carbon	0.00
Ash	0.65

ANNEX B. METHOD USED FOR QUANTIFICATION OF THE POLYMERS IN THE TIRE.

For the calculation of NR concentration, isoprene was taken as the main monomer, and a calibration curve for this compound, which is shown in Figure A- 1. The curve adjusted is a cubic polynomial con un R-square= 0.9976.

Figure A- 1. *Calibration curve of Isoprene.*

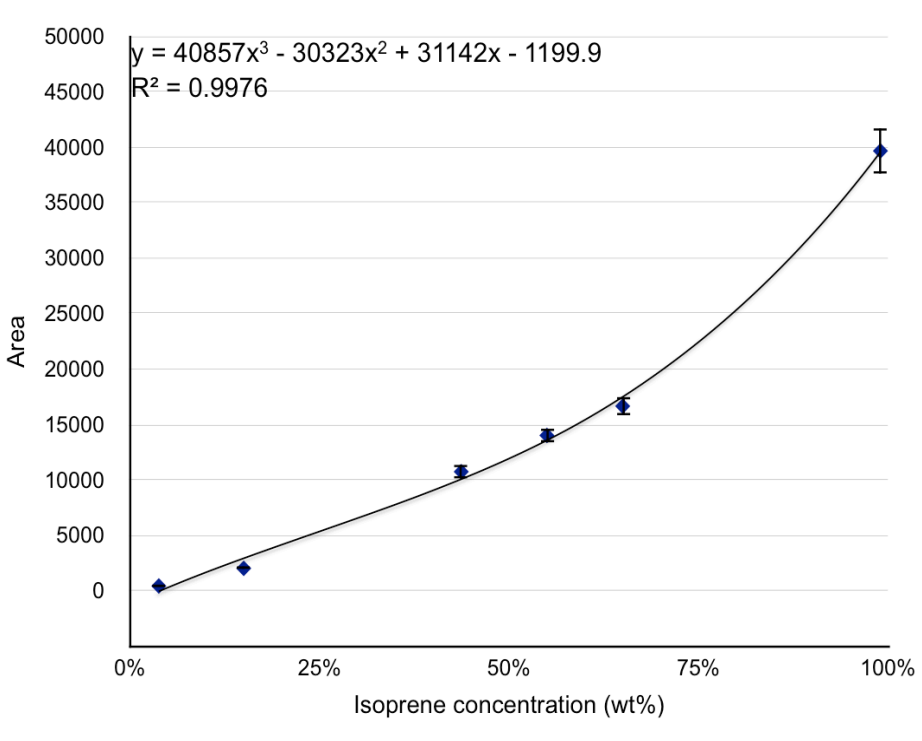

After obtaining the calibration curve for the isoprene, the NR was pyrolyzed and the peak corresponding to the isoprene was identified in the chromatogram (Figure A-2). According to the chromatogram, the isoprene (retention time =2.615) of the NR has an area of 16401.8 pA*s. Using the polynomial equation of the calibration curve, the concentration of isoprene in NR volatiles is obtained. Solving the cubic equation

for the area of 16401.8 pA*s was obtained that the concentration of Isoprene in the NR volatiles is 62.52 wt% (Equation A).

$$C_{\text{Isoprene in volatiles NR}} = \frac{Wt_{\text{isoprene}}}{Wt_{\text{NR volatiles}}} * 100 = 62.52 \text{ wt\%} \qquad \text{Equation (A)}$$

Figure A- 2. *Chromatogram of the NR.*

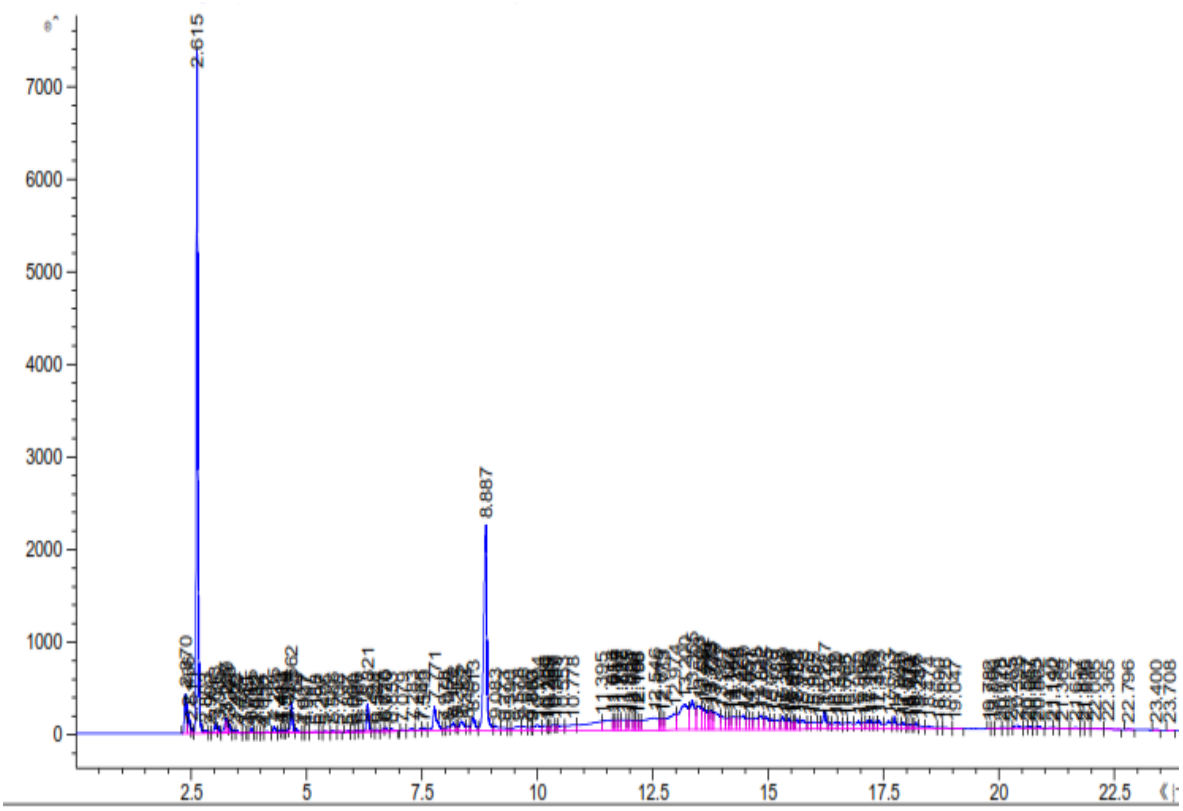

The tire sample was then pyrolyzed and the peak of Isoprene (retention time=2.723) was identified in the chromatogram (
Figure A- *3*). According to the chromatogram of the tire sample, the Isoprene peak has an area of 10779.2 pA*s. Using again the equation of the calibration curve of Isoprene (Figure A- 1) it is also possible to obtain the Isoprene concentration in the

volatiles of the tire. From the equation of the curve we obtain that the concentration of Isoprene in the volatiles of the tire is 46.33 wt% (Equation B).

$$\text{Concentration}_{\substack{\text{Isoprene} \\ \text{in volatiles tire}}} = \frac{\text{Wt}_{\text{Isoprene}}}{\text{Wt}_{\text{Tire volatiles}}} * 100 = 46.33\ \text{wt\%} \qquad \text{Equation (B)}$$

Figure A- 3. *Chromatogram of the tire sample.*

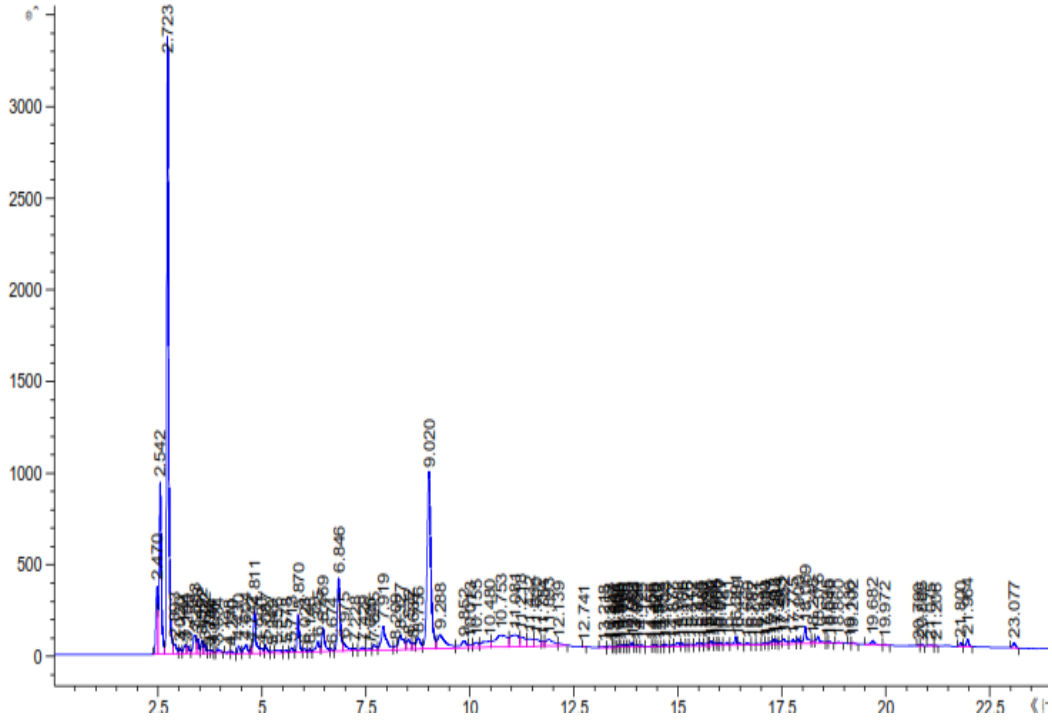

With the concentration of isoprene in the volatiles of NR, the isoprene concentration in the NR is obtained according to equation (C).

$$\text{Concentration}_{\text{Isoprene in NR}} = \left(\frac{\text{Wt}_{\text{Isoprene}}}{\text{Wt}_{\text{Volatiles NR}}}\right) * \left(\frac{\text{Wt}_{\text{volatiles NR}}}{\text{Wt}_{\text{NR}}}\right) \qquad \text{Equation (C)}$$

The expression $\left(\frac{\text{Wt}_{\text{Isoprene}}}{\text{Wt}_{\text{Volatiles NR}}}\right)$ is obtained from equation A. The expression $\left(\frac{\text{Wt}_{\text{volatiles NR}}}{\text{Wt}_{\text{NR}}}\right)$ corresponds to the volatile matter of the NR, which was taken from the

TGA analyzes (ANNEX A), and this is equal to 98%. By replacing these values in the equation D it was obtained that the concentration of Isoprene in NR is 61.26%.

In the same way, the calculation of the isoprene concentration in the tire was done, using equation D.

$$\text{Concentration}_{\text{Isoprene in tire}} = \left(\frac{\text{Wt}_{\text{Isoprene}}}{\text{Wt}_{\text{Volatiles tire}}}\right) * \left(\frac{\text{Wt}_{\text{volatiles tire}}}{\text{Wt}_{\text{tire}}}\right) \qquad \text{Equation (D)}$$

The expression $\left(\frac{\text{Wt}_{\text{Isoprene}}}{\text{Wt}_{\text{Volatiles tire}}}\right)$ is obtained from equation B. The expression $\left(\frac{\text{Wt}_{\text{volatiles tire}}}{\text{Wt}_{\text{tire}}}\right)$ corresponds to the volatile matter of the tire, which was taken from the proximate analysis (Annex A), and this is equal to 65.41%. By replacing these values in the equation it was obtained that the concentration of Isoprene in tire is 30.30%. Finally, with the concentration of Isoprene in NR and Isoprene in the tire, the concentration of NR in the tire can be obtained, according to equation E.

$$\text{Concentration}_{\text{NR in tire}} = \left(\frac{\text{W}_{\text{Isoprene}}}{\text{W}_{\text{tire}}}\right) * \frac{1}{\left(\frac{\text{W}_{\text{Isoprene}}}{\text{W}_{\text{NR}}}\right)} \qquad \text{Equation (E)}$$

Therefore, replacing the values the NR concentration in the tire is obtained, which is equal to 49.46 wt%.

For the determination of the SBR concentration in the tire, styrene was taken as the main monomer. A calibration curve for the styrene was performed, which is shown in Figure B.2.4. The curve adjusted is a cubic polynomial con un R-square= 0.9999.

According to the chromatogram of the pyrolyzed tire (Figure A- 4), the peak corresponding to styrene (retention time = 6.846 min) has an area of 342.43 pA*s. Using the equation of the calibration curve it is obtained that the styrene concentration in the tire volatiles is 0.5444 wt%.

Figure A- 4. *Calibration curve of Styrene.*

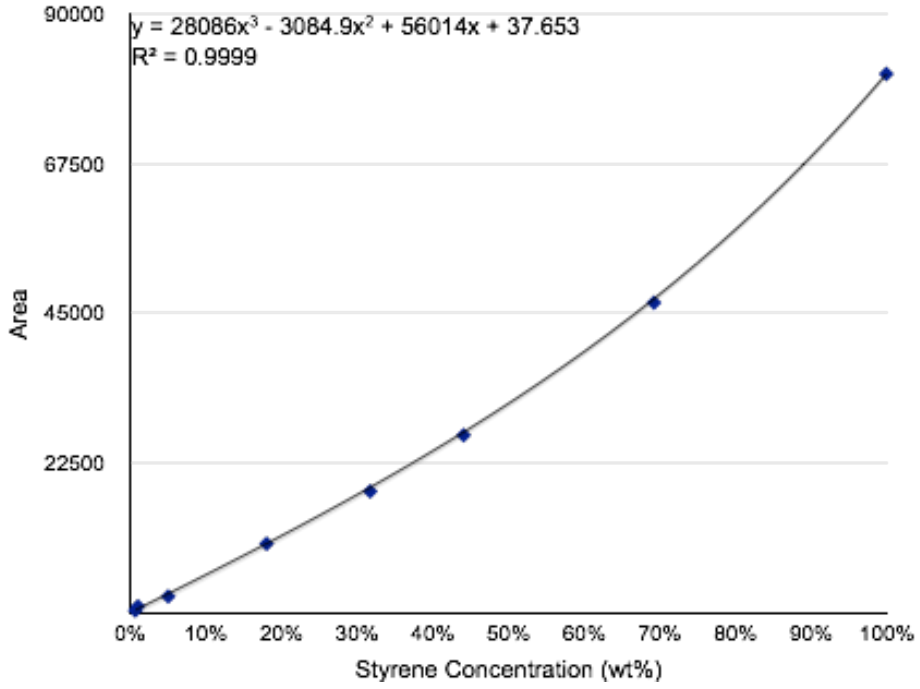

The styrene concentration in the tire is determined by according to equation F.

$$\text{Concentration}_{\text{Styrene in tire}} = \left(\frac{\text{Wt}_{\text{Styrene}}}{\text{Wt}_{\text{Volatiles tire}}}\right) * \left(\frac{\text{Wt}_{\text{volatiles tire}}}{\text{Wt}_{\text{tire}}}\right) \qquad \text{Equation (F)}$$

As mentioned earlier, the volatile matter of the tire was taken from the TGA analyzes, and it is equal to 65.41%. By replacing these values, the result is that the styrene concentration in the tire is 0.3560 wt%.

To determine the SBR concentration in the tire, equation G was used.

$$\text{Concentration}_{\text{SBR in tire}} = \left(\frac{\text{W}_{\text{Styrene}}}{\text{W}_{\text{tire}}}\right) * \frac{1}{\left(\frac{\text{W}_{\text{Styrene}}}{\text{W}_{\text{SBR}}}\right)} \qquad \text{Equation (G)}$$

The expression $\left(\frac{W_{Styrene}}{W_{SBR}}\right)$ corresponds to the styrene concentration in the polymer mixture SBR, which is 25 wt% according to the literature [23–25]. Finally it is obtained that the SBR concentration in the tire is 1.424 wt%.

ANNEX C. TGA CURVE OF THE TIRE SAMPLE.

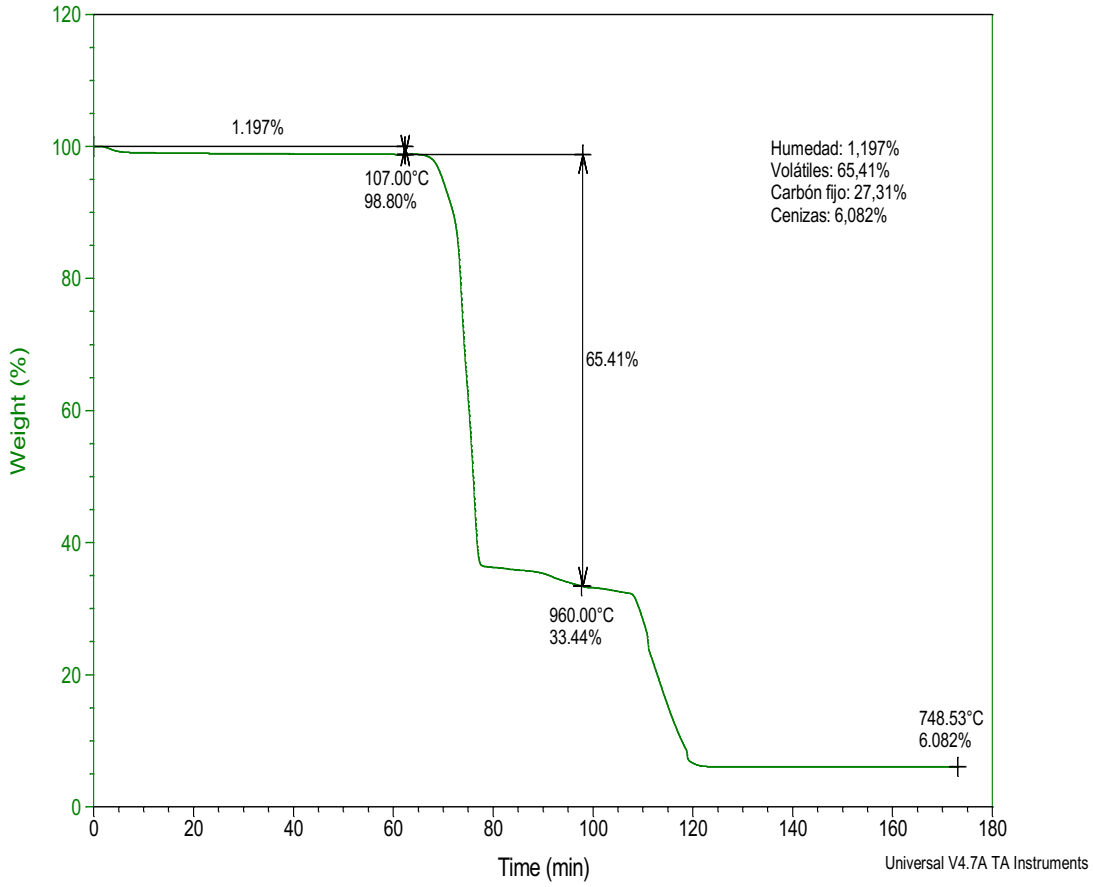

ANNEX D OPERATING PROTOCOLS

Annex C. 1. Load Protocol

The batch of tires used has a particle size of less than 1 mm and has an apparent density of 347.7 kg/m^3 (chapter 2). From these data, the amount of raw material required will be the same for all tests, according to the following expression:

$$m = \rho_{apa} * \pi * r^2 * h$$

Where ρ_{apa} is the bulk density, r it is the radius of the reactor which is equal to 0.9 cm and h is the height of the bed which corresponds to 11 cm.

The amount of glass wool or alumina employed as the support for the rim bed and catalyst depends on the type of test to be performed.
For thermal pyrolysis the reactor is divided into three sections of the following form: lower support, in this case alumina (12 cm), rim bed (11 cm) and upper support, which is glass wool (7.5 cm). The reactor must be charged as shown in
For catalytic pyrolysis the reactor must be divided into five sections which are divided as follows: the lower support (2.5 cm), the rim bed (11 cm), the intermediate support (5 cm), the catalyst bed (1 cm) and the top support (11 cm).
The upper, intermediate and lower supports for catalytic pyrolysis are always glass wool.

After having the necessary quantities of the materials and compounds to be used, proceed to charge the reactor as follows:

1. Insert the lower wool support, then carefully insert the lower cover until it fits with the reactor and tighten with the clamps as tightly as possible to seal as tightly as possible to avoid leakage.

2. After verifying that the bottom of the reactor is completely closed, the pre-weighed raw material is added with a funnel.

3. If thermal pyrolysis is to be carried out, the reactor is charged with 7.5 cm glass wool and the upper part of the reactor is closed in the same way as the lower one. If the test to be carried out is a catalytic pyrolysis, the 5 cm glass wool corresponding to the intermediate support is introduced.

4. The catalyst is added with the aid of a funnel after the intermediate support. To finish the loading the wool of the upper support of 11 cm is introduced and the closing of the reactor is verified in the same way as in the lower part.

Once the reactor is correctly charged, it is closed and placed in the furnace supports and connected to the inlet and outlet pipes. Tramps 1 and 2 must be weighed, since with these initial weights the amount of oil obtained in the test can be determined. To finalize the loading protocol, the traps must be adjusted with the clamps, placing in the middle an available rubber to make the closure as airtight as possible.

Annex C. 2 Leak test protocol

In order to guarantee the efficiency of the process and to avoid pressure losses, a system-wide leak test must be carried out before the pyrolysis is started, so after the reactor is charged, the leakage procedure is as follows:

1. Open all valves in the system except the vent valve (v8).

2. Allow the pipes to fill with inert gas (N2) at a pressure equal to twice the working pressure, ie 2 barg. Check the pressure in the digital gas flowmeter and in the N2 bottle; When the pressure is stable, proceed to close the manual flowmeter that regulates the inlet of the inert gas.

3. Check the pressure of the digital flowmeter and the pressure gauge. If the pressure gauge begins to decrease, a solution of water-soap should be applied to the pipe joints and to the reactor. In the place where bubbles form is the leak that causes the decrease in pressure of the system.

4. After correcting leaks that are obvious, the pressure that marks the system and note a period of 2 hours should be noted. If, at the end of the leakage time, the pressure drop is less than 10% of the initial pressure, the system is guaranteed to be leak-free.

Annex C. 3 Start-up and stop protocol

To start the test the following steps must be taken:

1. The exhaust valve must be opened to the atmosphere (v8) to depressurize the system.

2. Set the system pressure to 1 barg with the bottle of N2.

3. Set the necessary flow of the inert gas (N2) with the manual flowmeter and wait for it to stabilize.

4. Close valves v4 and v6, which are safety valves only open if there is any obstruction in the pipe or damage to the filter.
5. Load the condensation traps, trap 1 with dry ice and trap 2 with normal ice. When the inert gas flow is stabilized, the position that is marked on the feed flowmeter must be referenced to ensure that the same flow is maintained throughout the test.

6. Connect the heating cord that is located in the pipe connecting the reactor outlet to the condensation traps and wait until it has a temperature of 180 ° C or greater.

7. Connect the oven, raise the blocks and set the temperature set point for the process. When all of the above has been done, proceed to start the oven by turning the heating knob from 0 to 1 and pressing the heating button which is green and becomes orange. From this moment the data is started in the log every two minutes for one hour. The data to be taken are temperatures, pressure and gas outflow.

Once the test operation time is finished, the reactor is shut down, the steps to follow for this are:

8. Verify that the gas outflow is equal to the one initially set to ensure that the thermal decomposition reactions are complete.

9. Turn off the oven heating by pressing the orange button to warm it up and confirm that it will turn green again, turn the heating knob from 1 to 0 and wait for the oven temperature to begin to decrease. When the oven controller registers a temperature of 250 °C, the oven jacket is opened to accelerate the cooling process of the oven.

10. Finally, when the temperature is equal to or less than 50 °C, the oven plugs are lowered and switched off, as well as closing the nitrogen flow step and disconnecting the heating cord.

Annex C. 4 Discharge protocol

In order to carry out the download protocol, the following steps must be carried out:
1. Using asbestos gloves, the reactor must be removed from the oven supports and wait until it is at room temperature.

2. Remove ice from the cooling traps, open the joints of the inlet and outlet pipes to the traps and remove them. Put plugs in the pipes and pour water to more than 70ºC

inside the traps, then have compressed air transferred under pressure of 2 barg in order to extract the remains of oil that remain attached to the pipe. Remove the water from the traps and dry them and then open them and weigh the oil collection plates.

3. Locate the reactor in a universal holder and open the top of the reactor.

4. The top wool is removed and weighed to calculate the amount of oil retained in it. If it is a catalytic pyrolysis, the catalyst and the wool must be extracted and weighed, which is used as an intermediate support.

5. Remove the char from the reactor by collecting it in aluminum foil and to ensure that all the char comes out and then weigh it.

6. Open the bottom of the reactor and remove the remaining wool, weigh it and register its weight to reduce mass losses in the balance.

ANNEX E. RESPONSE FACTORS CALCULATED AND USED FOR THE QUANTIFICATION OF COMPOUNDS IN THE TESTS OF CHAPTER 3.

COMPUESTO	RRF

HEPTANE	1
TOLUENE	0.92
4-ETHENYL CYCLOHEXENE	0.97
ETYLBENZENE	0.93
o,m,p- XYLENES	0.93
STYRENE	0.92
CUMENE	0.93
1-METHYL-6-(1-METHYLETHYL)LIDENE	0.96
LIMONENE	0.97
1-ETHYL-4-METHYLBENZENE	0.93
TRIMETHYLBENZENE	0.93
1-METHYLETHENYLBENZENE	0.92
1-*p*-MENTHENE	0.98
1-METHYL-4-(1-METHYLETHYL)LIDENE	0.96
o,m,p- CYMENES	0.94
1-METHYL-3-PROPYLBENZENE	0.94
4-ETHYL-(1,2-DIMETHYL)BENZENE	0.94
1-METHYL-2-(2-PROPENYL) BENZENE	0.93
1-ETHYL-(2,4-DIMETHYL)BENZENE	0.94
TETRAMETHYLBENZENE	0.94
5-METHYLINDANE	0.92
1-METHYL-2-PROPENYLBENZENE	0.93
1,6-DIMETILINDANO	0.93
NAPHTHALENE	0.90

ANNEX F. STATISTICAL ANALYSIS OF THE PYROLYTIC OIL YIELD

In order to determine the significance and influence of each variable in the oil yield an analysis of variance ANOVA was performed using Statgraphics Centurion software. Table A- 1 presents the summary of the ANOVA results.

Table A- 1. *Analysis of variance ANOVA Sum of squares type III for oil yield with all factors.*

Source	Sum of squares	*DF*	*Middle Square*	*F-Value*	*P-Value*
MAIN EFFECTS					
A:Temperature	2511.4	3	837.132	101.34	0.0000
B:Nitrogen Flow	46.5235	2	23.2618	2.82	0.0863
RESIDUES	148.687	18	8.26036		
TOTAL (Corrected)	2706.61	23			

In the ANOVA analysis, a level of significance of 5% and the sum of squares type III were chosen, therefore, the individual contribution of each variable was measured by eliminating the effects of the others. Analyzing the ANOVA results, it shows that the only variable with p-value less than 0.05 is the temperature, indicating that this variable satisfies the 95% confidence level and rejects the null hypothesis. Following this, is found the nitrogen flow with a p-value of 0.0813. This variable does not satisfy the 95% confidence level and does not reject the null hypothesis, therefore, this variable does not have a statistically significant effect on the oil yield at the confidence level chosen. Although the nitrogen flow at a 95% confidence level has not significance, it has significance at a level of 90% as can be observed in the ANOVA.

As a conclusion we have that temperature is the most influential variable in the oil yield, as can be observed in Figure_, however the nitrogen flow can have an effect that still can not be discarded in whole. From this, it is decided to perform a new analysis of variance considering the two variables and their possible interactions, in order to establish the model that can predict the oil yield. Table A- 2 shows the results of the analysis of variance with all the interactions of the variables.

Table A- 2. *Analysis of variance ANOVA Sum of squares type III for oil yield with all factors and their interactions.*

Source	Sum of squares	*DF*	*Middle Square*	*F-Value*	*P-Value*
A:Temperature	90.0938	1	90.0938	7.04	0.0162
B:Nitrogen Flow	13.2439	1	13.2439	1.03	0.3226
A*B	24.2664	1	24.2664	1.90	0.1855
A*A	33.5121	1	33.5121	2.62	0.1231
B*B	0.828008	1	0.828008	0.06	0.8021
Residue	230.455	18	12.8031		
Total (corrected)	2706.61	23			

R-Square = 91.4855 %
R-Square (ajusted by DF) = 89.1203 %
Standar Error of estimate = 3.57814
Absolute mean error = 2.28756
Durbin-Watson statistic = 2.71009 (P=0.8823)

The R-Squared statistic indicates that the model, thus adjusted, explains 91.4855% of the variability in the Oil yield. The adjusted R-Squared statistic, which is more adequate to compare models with different number of independent variables, is

89.1203%. The standard error of the estimate shows that the standard deviation of the residues is 3.57814, value can be used to construct prediction limits for new observations. The absolute mean error (MAE) of 2.28756 is the average value of the residuals. The Durbin-Watson (DW) statistic tests the residuals to determine if there is any significant correlation. Note that the highest P-value is 0.8021, which corresponds to B*B. Since the P-value is greater than or equal to 0.05, that term is not statistically significant at a confidence level of 95.0%, and the software recommends eliminating this interaction from the model.

Table A- 3 shows the estimates for each effect and their interactions. The standard error of each one is also shown, which measures its sampling error. The largest variance inflation factor (V.I.F.) is equal to 1.03704. The variance inflation factors are quite satisfactory because for a perfectly orthogonal design, all factors are equal to 1. [74]

Table A- 3. *Estimated effects for Oil yield (wt%/wt%).*

Efect	Estimate	Standard Error	V.I.F.
Average	31.9547	1.77381	
A:Temperature	26.3145	2.03033	1.01786
B:Nitrogen Flow	3.405	1.8371	1.03704
A*A	-5.31749	3.37496	1.0
A*B	-3.24498	2.42031	1.01786
B*B	-0.902813	3.64538	1.03704
Block	-0.4	1.49998	1.0

The effects in decreasing order of importance are shown in a Pareto diagram in Figure A- 5.

Figure A- 5. *Pareto diagram of the standardized effect for oil yield.*

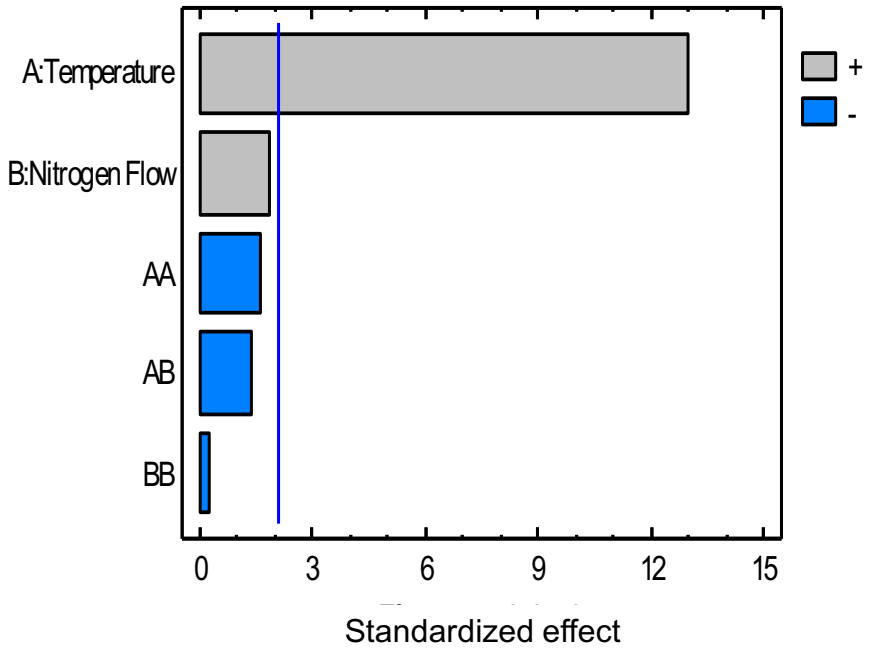

It can be observed that the interaction between variables is not significant in the 95% confidence interval, and it can be corroborated that most significant variable is the temperature and the least influential is in this confidence interval. For this reason it is decided to do a new analysis of variance by eliminating the interaction B* B, which is presented in Table A- 4.

In this analysis of variance we find that the highest P-value is 0.0802, which corresponds to variable B. Since the P-value is greater than or equal to 0.05, that term is not statistically significant with a confidence level Of 95.0%, therefore it is considered to eliminate B from the model. In this case the R-Square of this analysis (93.2477%) is greater than the analysis of Table A- 2 indicating that the removal of B * B adjusted the model by approximately 3%.

Table A- 4. *Analysis of variance ANOVA Sum of squares type III for oil yield eliminating B*B of the model.*

Source	**Sum of squares**	*DF*	*Middle Square*	*F-Value*	*P-Value*
A:Temperature	222.364	1	222.364	19.85	0.0003
B:Nitrogen Flow	38.5143	1	38.5143	3.44	0.0802
A*B	76.6612	1	76.6612	6.84	0.0175
A*A	109.352	1	109.352	9.76	0.0059
Residue	201.687	18	11.2048		
Total (corrected)	2986.95	23			

R-Squared = 93.2477 %
R-Squared (ajusted by DF) = 91.3721 %
Standar Error of estimate = 3.34736
Absolute mean error = 2.2381
Durbin-Watson Statistic= 2.53107 (P=0.7739)

With this analysis the effect of variable B can be definitively discarded, which was doubted in the first analysis performed (Table A- 1), Although this variable does not have a significant individual effect, it can have an effect when it interacts with the other variable, for thus a new analysis of variance by eliminating B is performed to discarded this possible interaction.

The new analysis is presented in Table A- 5.

Table A- 5. *Analysis of variance ANOVA Sum of squares type III for oil yield eliminating B of the model.*

Source	**Sum of squares**	*DF*	*Middle Square*	*F-Value*	*P-Value*
A:Temperature	222.364	1	222.364	19.85	0.0003
A*B	76.6613	1	76.6613	6.84	0.0175
A*A	109.352	1	109.352	9.76	0.0059
Residue	2.43469	1	2.43469		
Total (corrected)	201.687	18	11.2048		

R-Squared = 93.2477 %
R-Squared (ajusted by DF= 91.3721 %
Standar Error of estimate = 3.34736
Absolute mean error = 2.2381
Durbin-Watson Statistic = 2.53107 (P=0.7739)
The mean error (ME)
The mean error rate (MPE)

In order to know if the model is properly adjusted, a residue analysis was done, which allows to evaluate the performance of the model to adjust the data, and to predict any value retained outside the adjustment process. The results are shown in Table A- 6, each one of the statistics presented in the table is based on residues. The first three statistics measure the magnitude of errors. The best model will be the one with the smallest value. For the model 2 and the model 3 the values are the same, and these are smaller than the model with all interactions.

Table A- 6. *Residues Analysis of each analysis of variance.*

	Estimate		
	Model 1 (with all interactions)	*Model 2 (without B*B)*	*Model 3 (without B*B and B)*
The average error square (AES)	12.8031	11.2048	11.2048
The absolute mean error (AME)	2.28756	2.2381	2.2381
The absolute mean error rate (AMER)	7.82675	2.98586	2.98586
The mean error (ME)	1.68014E-14	-8.11203E-14	5.00341E-14
The mean error rate (MER)	-1.0203	-0.157173	-0.157173

The last two statisticians measure bias. The best model will give a value close to 0. Comparing every model we can see that for the model 1 the ME is the smallest and the closest to zero, but the MPE is the largest one. Now reviewing the models 2 and 3 it is found that although the two have equal values for AES, AME and AMER, they differ in the ME and MER, being the closest to zero the ME of the model 3, so confirming that it is the model more adjusted.

Once the model is obtained, the predictive and experimental results are compared to check how predictive the model is. The experimental value plot Vs predictive values are presented in Figure A- 6. ***Experimental values Vs Predictive values.***. The graph shows a good linearity with a R^2 = 0.9273, which means that the model represents and predicts the oil yield with a reliability of 92%. It can also be observed that there are two points in approximately 20 and 40% that do not follow the linearity and are a little dispersed and far from the trend, in addition the predicted value is below the experimental value. These points coincide with those with the highest

standard deviation, therefore there is a high possibility of experimental error, and no prediction error of the model.

Figure A- 6. *Experimental values Vs Predictive values.*

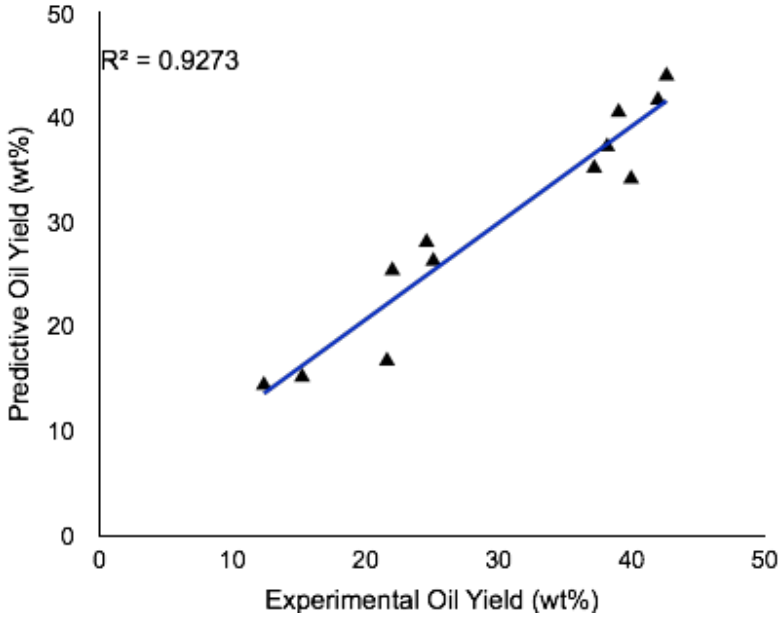

ANNEX G. TGA PROFILE OF HPMOV HETEROPOLYACID UNDER N_2 ATMOSPHERE.

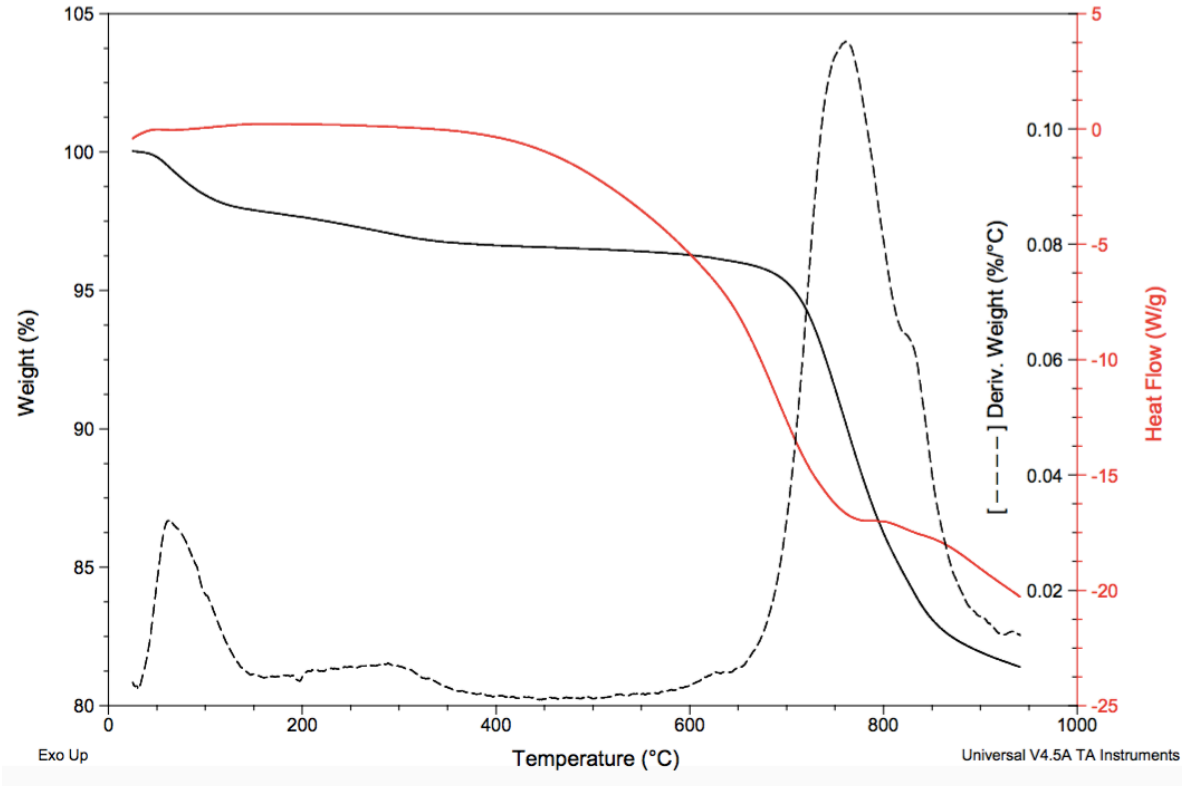

ANNEX H. RESPONSE FACTORS CALCULATED AND USED FOR THE QUANTIFICATION OF COMPOUNDS IN THE TESTS OF CHAPTER 5.

COMPOUND	RRF
Heptane	1
Benzene	0.91
Toluene	0.92
2-methyl-2,4 hexadiene	0.96
4-etheyilcyclohexene	0.945
4-vinyl-cyclohexeny	0.945
Xylenes	0.928
Styrene	0.91
Alpha pinene	0.952
Cumene	0.933
Neo-allo cimene	0.952
Carene	0.952
3-menthene	0.966
2-menthene	0.966
Alpha phellandrene	0.952
p-cymene	0.938
D-L Limonene	0.952
Beta Terpinene	0.952
Gama Terpinene	0.952
3,8 - Mentadienoe	0.952
alpha dimethyl styrene	0.924
1,4,8-terpadiene	0.952

ANNEX I. LIST OF COMPOUNDS OBTAINED FROM THE TRANSFORMATION OF D,L LIMONENE.

Compound	Structure
Benzene	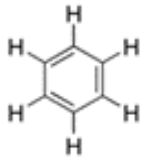
Toluene	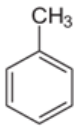
2-methyl-2,4 hexadiene	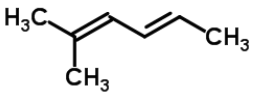
4-vynil cyclohexene	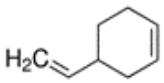
Xylenes	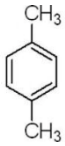
Styrene	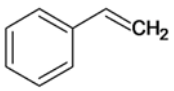
3-ethyl-2-methyl-1,3 hexadiene	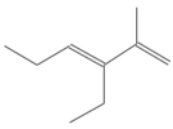

Alpha pinene	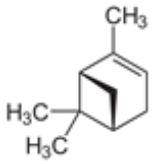
Cumene	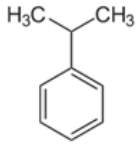
Neo-allo cimene	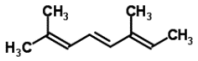
5,5-dimethyl-1-propyl-1-1,3-cyclopentadiene	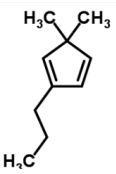
Carene	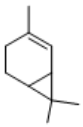
1-isopropenyl-4-methyl-cyclohexene	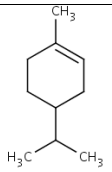
3-menthene	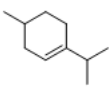
2-menthene	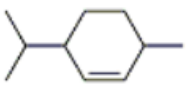

Alpha pellandrene	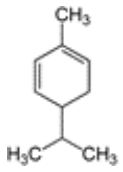
p-cimene	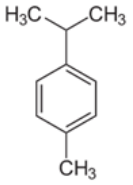
Beta terpinene β	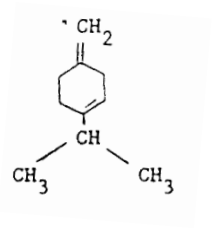
Gamma terpinene	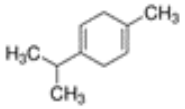
3,8 menthadiene	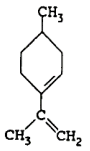
p,α-dymethylstyrene	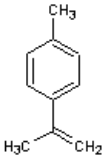
1,4,8-terpadiene	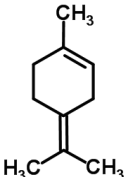

ANNEX J. XPS SPECTRA OF C1S FOR IDENTIFICATION AND QUANTIFICATION OF THE CARBONACEOUS MATERIAL DEPOSITED ON THE CATALYST SURFACE.

Annex I. 1 XPS spectra of C1s for HPMo/Q-10 after reaction of transformation of D, L limonene.

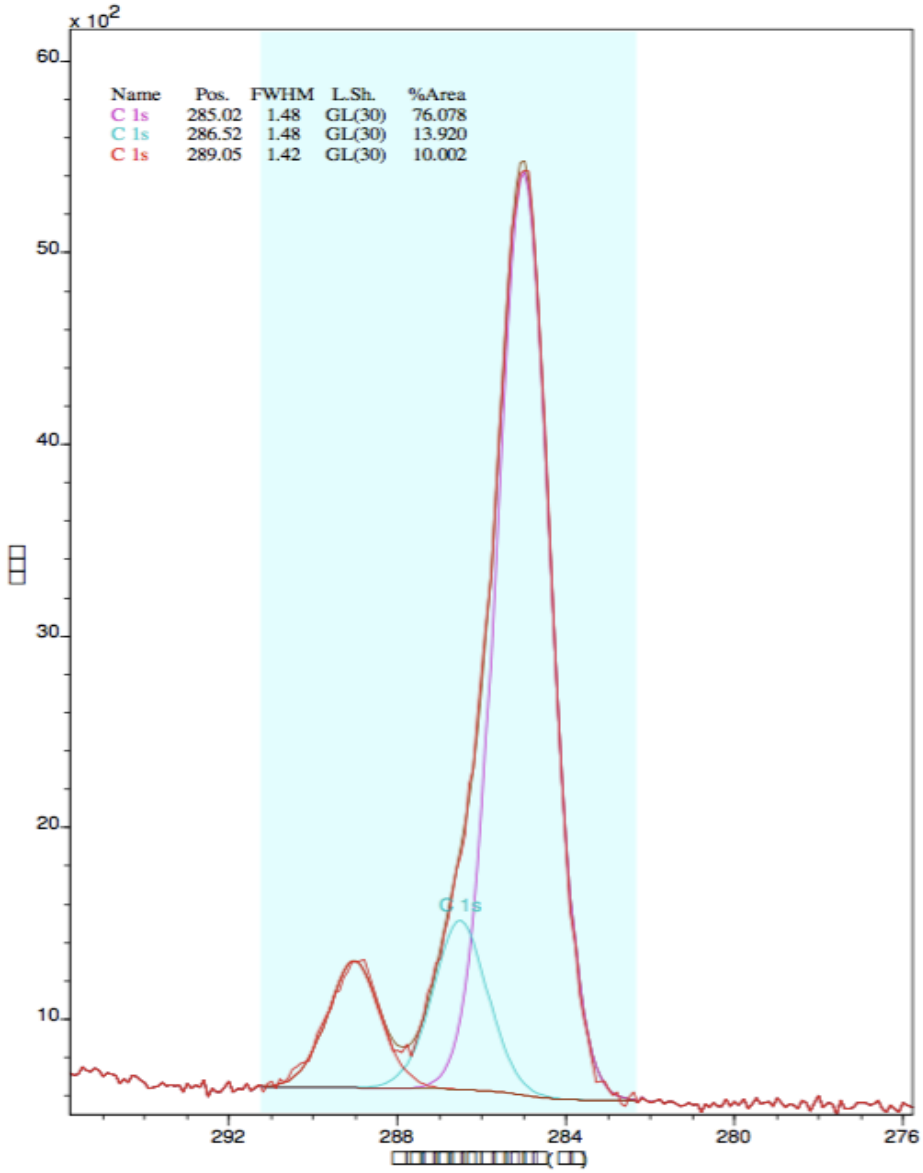

Annex I. 2 XPS spectra of C1s for HPMoV/Q-10 after reaction of transformation of D, L limonene.

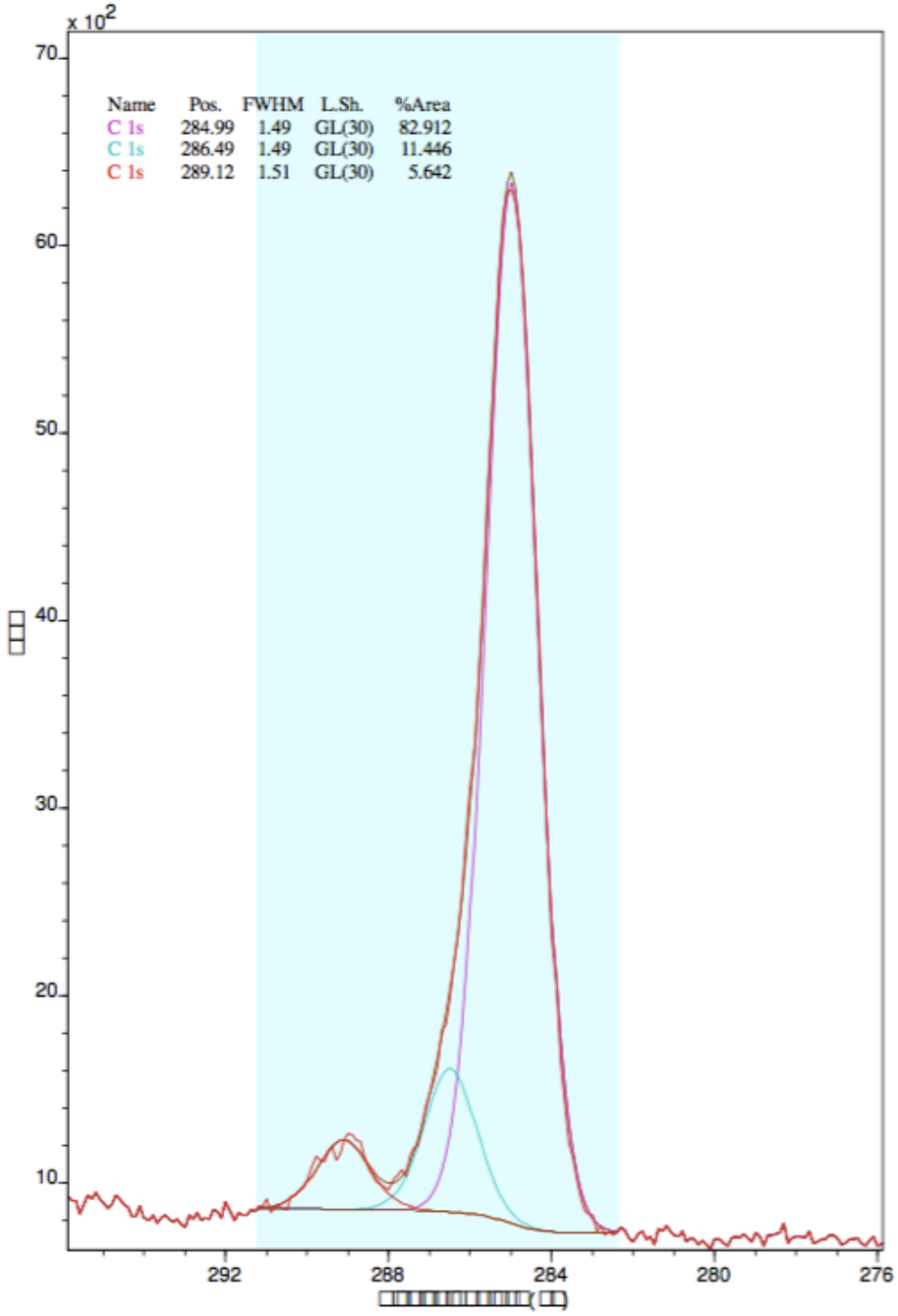

Annex I. 3 XPS spectra of C1s for HPMo/Q-10 after reaction of STR pyrolysis

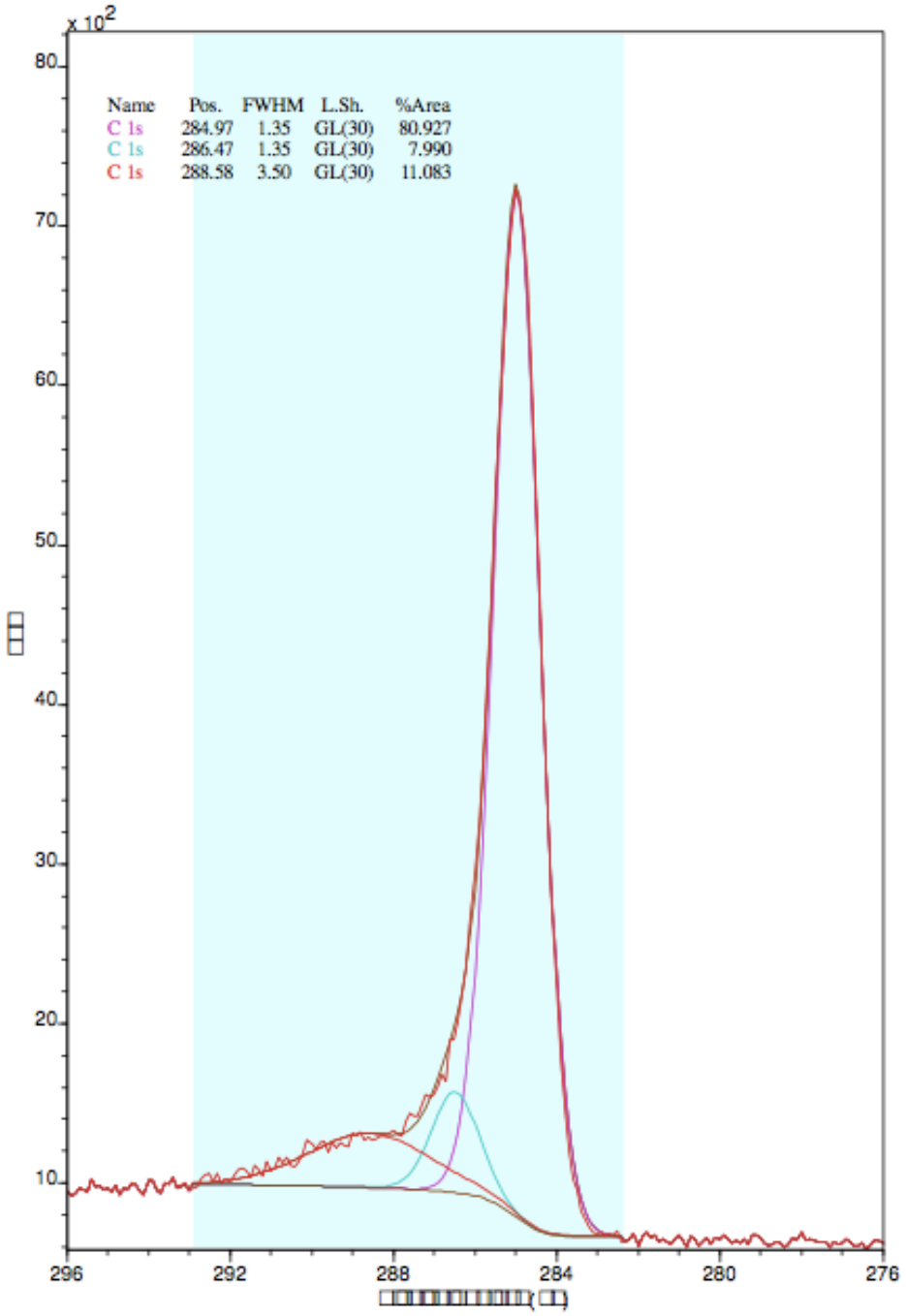

Annex I. 4 XPS spectra of C1s for HPMoV/Q-10 after reaction of STR pyrolysis

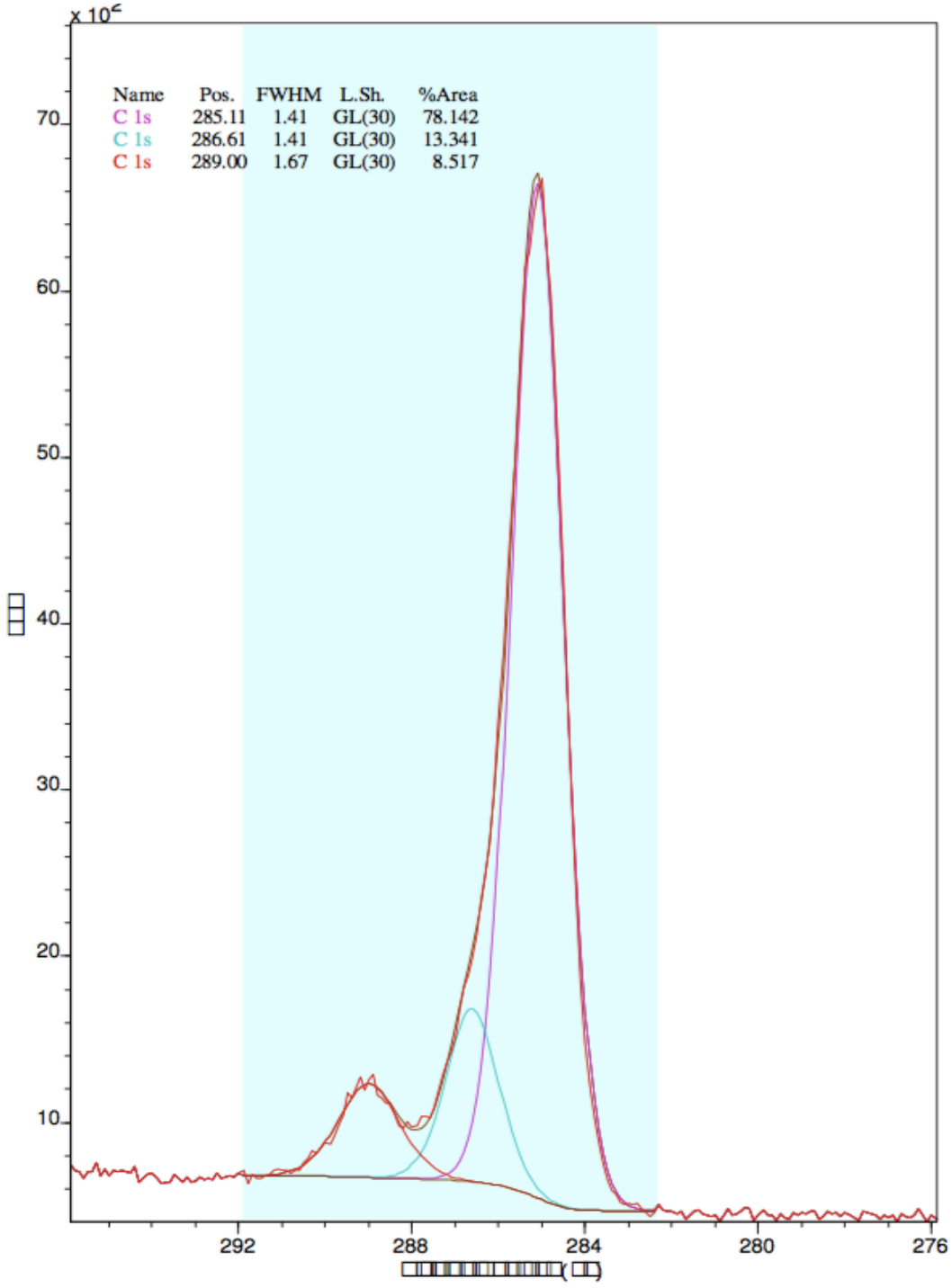

Annex I. 5 XPS spectra of C1s for HPW/Q-10 after reaction of STR pyrolysis